

**STUDIES IN CATALYSIS AND REACTION  
ENGINEERING ASPECTS OF MULTIPHASE CATALYTIC  
REACTIONS**

**KALPENDRA B. RAJURKAR**

**FOR THE DEGREE OF  
DOCTOR OF PHILOSOPHY  
IN  
CHEMICAL ENGINEERING**

**RESEARCH GUIDE  
Dr. R. V. CHAUDHARI**

**CHEMICAL ENGINEERING AND PROCESS DEVELOPMENT DIVISION  
NATIONAL CHEMICAL LABORATORY  
PUNE-411008, INDIA  
November 2008**

**STUDIES IN CATALYSIS AND REACTION  
ENGINEERING ASPECTS OF MULTIPHASE  
CATALYTIC REACTIONS**

**A THESIS  
SUBMITTED TO  
THE UNIVERSITY OF PUNE  
FOR THE DEGREE OF  
DOCTOR OF PHILOSOPHY  
IN  
CHEMICAL ENGINEERING**

**BY  
KALPENDRA B. RAJURKAR**

**AT  
CHEMICAL ENGINEERING AND PROCESS  
DEVELOPMENT DIVISION  
NATIONAL CHEMICAL LABORATORY  
PUNE 411 008  
INDIA**

**NOVEMBER 2008**



राष्ट्रीय रासायनिक प्रयोगशाला  
(वैज्ञानिक तथा औद्योगिक अनुसंधान परिषद)  
डॉ. होमी भाभा मार्ग पुणे - 411 008. भारत  
**NATIONAL CHEMICAL LABORATORY**  
(Council of Scientific & Industrial Research)  
Dr. Homi Bhabha Road, Pune - 411 008. India.



**FORM 'A'**

Certified that the work incorporated in the thesis entitled: “**Studies in Catalysis and Reaction Engineering Aspects of Multiphase Catalytic Reaction**” submitted by **Mr. Kalpendra B. Rajurkar** was carried out under my supervision. Such material as has been obtained from other sources has been duly acknowledged in the thesis.

October, 2008

Pune

**Dr. R. V. Chaudhari**

(Supervisor/Research Guide)

## **Declaration**

I hereby declare that the thesis entitled “**Studies in Catalysis and Reaction Engineering Aspects of Multiphase Catalytic Reactions**”, submitted for the Degree of Doctor of Philosophy to the University of Pune, has been carried out by me at the National Chemical Laboratory, Pune under the supervision of Dr. R. V. Chaudhari. The work is original and has not been submitted in part or full by me for any other degree or diploma to this or any other University.

Date:

(Kalpendra B. Rajurkar)

Place:

---

*Dedicated to*

*My Beloved Parents*

*&*

*My Teachers*

*Dr.R.V.Chaudhari*

*&*

*Dr.B.V.Babu*

---

## ACKNOWLEDGEMENT

I wish to express my sincere gratitude to my research supervisor, Prof. R.V. Chaudhari. I feel deeply indebted to his immense contribution in the making of this thesis. I wish to acknowledge his ceaseless inspiration, thoughtful guidance, constructive criticism, patience and friendship to shape up the researcher in me. I take this opportunity to salute his supporting attitude that has always led me to think and work independently, and follow them in the proper perspectives. My deepest regards for the patience he has kept and given me enough time for learning and so this piece of work is dedicated to him.

I would like to thank the Council of Scientific and Industrial Research for awarding of research fellowship. I am thankful to Dr. S. Sivaram, Director, NCL, Dr. B.D. Kulkarni, Deputy Director, National Chemical Laboratory to carry out my research work and extending all possible infrastructural facilities for completion of my research work.

I take this opportunity to express my sincere gratitude to Dr. B. V. Babu for inspiring me to do research at NCL. Needless to say that it was his blessings, which transformed into thesis today.

I would like to acknowledge Dr. R. Jaganathan and Dr. V. H. Rane, C.E. and P.D. Division, NCL, for their help, support and encouragement particularly at my final stage of research.

I would like to gratefully acknowledge Mr. S.S. Joshi for his support and valuable help through out my research at NCL.

I would like to acknowledge Dr. V. V. Ranade, Dr. A.A. Kelkar, Dr. S. P. Gupte, Dr. C. V. Rode, Mr. P. B. Jadkar, and Mr. Raheja for their valuable help and encouragement during my research work.

I sincerely acknowledge the invaluable interactions with my senior Dr. R.M. Deshpande and also for their valuable help and co-operation during my research work in NCL.

My research journey has started with my friends Mahesh and Abhijit. I would like to acknowledge their help, support encouragement through out my research work at NCL. It is needless to say that the completion of my thesis without these friends was impossible task.

I sincerely acknowledge my friend Dr. S.S. Tonde (Kaka) and Nilesh Kulkarni, who stood behind me in sun and shadows during my research work in NCL.

I would like to acknowledge my friends Makarand, Pradip, Gopal, Sunil and Girish who has been always my strength and support. Special thanks to Prakash, Ratnakar, Rahul, Anuj, Ashish Gujrathi, Manish Mundada and my BITS-2001 batch for the support.

I would like to thank all my colleagues and labmates (past and present) for their helpful hand and cheerful attitude that had made my working very easy and enjoyable. I should mention my labmates Aditi, Charu, Swapanali, Swapana, Umesh, Satish, Sanjay, Atul, Sandeep, Ravi, Raj, Samadhan, Dinesh and many more in NCL, who made my stay more colorful

I also wish to thank my seniors Avinash, Vivek, Nitin, Abhishek, Bibhas for their helpful hand and sympathetic ear. I would like to express my deep felt gratitude to my colleagues and friends, Makarand, Ajay, Vivek, Anand, Amit, Nandu, Shweta, Lalita, Piplad, Vikas, Deepak, Jayaprakash, Atul, Amit, and many in NCL who are not named in person, for their valuable suggestions and helping hand.

I would like to acknowledge Yogi, Debu, Sangeeta, Savita, Shashi, Nitin and Abhishek for the help and support during my Ph.D.

I am also thankful to Library, administrative and other supporting staff of NCL for their co-operation. I wish to thank Mr. Borkar, Mr. Narawade, Dure kaka, Shinde kaka, Wanjale, Radha, Subbu, Patane, Kamble, Kedari and Durai for their help in my research work in NCL.

I sincerely acknowledge support of my brothers and sisters Nikhu, Meghu, Sanket, Akka, Manjiri and Aman.

No thanks can be enough to acknowledge for the encouragement and support of Aai, Baba and my dear most sisters Renu, Meghu, and Deven dada, Siddhant. They have been my constant source of strength.

Kalpendra B. Rajurkar

---

## List of Contents

---

| Description   | Page Number |
|---|-------------|
| Chapter Index   | i           |
| List of Tables  | viii        |
| List of Figures   | x           |
| List of Schemes   | xv          |
| Abstract of the Thesis                                  | xiv         |
| Appendix I - Confirmation of the product formed by GCMS | xxiii       |
| Appendix II - List of abbreviations                     | xliii       |
| List of Publication / Conference / symposium            | xliv        |

---

### CHAPTER 1: Introduction and Literature Survey

---

|  |    |
|--|----|
| 1. Introduction  | 1  |
| 1.2. Multiphase Catalytic Reactions  | 3  |
| 1.3. Oxidation reaction  | 7  |
| 1.3.1. Hydrocarbon oxidation   | 9  |
| 1.3.1.1. Selective liquid phase oxidation of toluenes to benzaldehydes     | 16 |
| 1.3.1.2. Selective liquid phase oxidation of side chain alkyl benzenes     | 20 |
| 1.3.2. Selective liquid phase oxidation of aldehydes                       | 23 |
| 1.3.3. Kinetics of Catalytic reactions                                     | 27 |
| 1.3.3.1. Kinetics of Liquid phase Oxidation                                | 27 |
| 1.3.4. Mechanism of oxidation reactions                                    | 29 |
| 1.3.4.1. One-electron oxidations with oxygen/ air as oxidant               | 29 |
| 1.3.4.2. Oxidations with H <sub>2</sub> O <sub>2</sub> / organic peroxides | 30 |
| 1.4. Literature Survey on Hydroformylation                                 | 33 |



|   |    |
|---|----|
| 1.4.1. Hydroformylation of functionalized olefins: VAM hydroformylation | 40 |
| 1.4.2. Hydroformylation of vinylarenes: Synthesis of NSAIDs             | 43 |
| 1.4.3. Hydroformylation in tandem and sequential synthesis              | 51 |
| 1.4.4. Mechanism of hydroformylation                                    | 54 |
| 1.4.5. Kinetics of Hydroformylation Reaction                            | 57 |
| 1.5. Scope and Objective of the Thesis                                  | 59 |
| References  | 61 |

---

## **CHAPTER 2: Selective Liquid Phase Oxidation of Toluenes to Benzaldehydes**

---

|  |    |
|--|----|
| 2.1. Introduction                                    | 71 |
| 2.2. Experimental Section                            | 72 |
| 2.2.1. Materials                                     | 72 |
| 2.2.2. Experimental Procedure                        | 73 |
| 2.2.3. Catalyst Recycle Procedure                    | 74 |
| 2.2.4. Work up Procedure for Isolation of Product    | 75 |
| 2.2.5. Analytical Methods                            | 75 |
| 2.3. Results and Discussion                          | 76 |
| 2.3.1. Liquid Phase Oxidation Experiments            | 77 |
| 2.3.1.1. Preliminary Experiments                     | 77 |
| 2.3.1.2. Screening of Co-catalysts                   | 80 |
| 2.3.1.3. Selection of Catalyst System                | 81 |
| 2.3.1.4. Effect of solvents                          | 83 |
| 2.3.1.5. Effect of Temperature                       | 84 |
| 2.3.1.6. Effect of Pressure                          | 85 |
| 2.3.1.7. Effect of substrates (substituted toluenes) | 86 |
| 2.3.1.8. Catalyst Recycle                            | 87 |
| 2.3.1.9. Solubility of Oxygen in Solvent             | 88 |
| 2.4. Kinetics of Liquid Phase Oxidation of Toluene   | 90 |
| 2.4.1. Mass Transfer Effects                         | 92 |
| 2.4.1.1. Gas-liquid Mass Transfer Effect             | 92 |

|  |     |
|--|-----|
| 2.4.2. Parametric Effects  | 93  |
| 2.4.2.1. Effect of Mn (OAc) <sub>2</sub> Concentration           | 94  |
| 2.4.2.2. Effect of FeCl <sub>3</sub> Concentration               | 97  |
| 2.4.2.3. Effect of NaBr Concentration                            | 100 |
| 2.4.2.4. Effect of Toluene Concentration                         | 102 |
| 2.4.2.5. Effect of Oxygen Partial Pressure                       | 105 |
| 2.4.3. Kinetic Model   | 107 |
| 2.4.4. Estimation of Kinetic Parameters and Model Discrimination | 108 |
| 2.5. Reaction Pathway  | 113 |
| 2.6. Conclusions   | 116 |
| Nomenclature   | 118 |
| References   | 119 |

### **CHAPTER 3: Selective Oxidation of Ethylbenzene using Hydrotalcite like Compounds as Catalyst**

|   |     |
|---|-----|
| 3.1. Introduction                                 | 121 |
| 3.2. Experimental                                 | 123 |
| 3.2.1. Chemicals                                  | 123 |
| 3.2.2. Synthesis of HTlcs                         | 123 |
| 3.2.3. Experimental Procedure                     | 124 |
| 3.2.4. Catalyst Recycle Procedure                 | 126 |
| 3.2.5. Analytical Methods                         | 126 |
| 3.2.5.1 Analysis of TBHP consumption              | 127 |
| 3.3. Results and Discussion                       | 127 |
| 3.3.1. Characterizations of the Solid Catalysts   | 128 |
| 3.3.1.1. Powder X-Ray Diffraction                 | 129 |
| 3.3.1.2. Scanning Electron Microscopy             | 131 |
| 3.3.1.3. X-Ray Photoelectron Spectroscopy         | 131 |
| 3.3.1.4. Fourier Transform Infra Red Spectroscopy | 133 |
| 3.3.1.5. TGA-DTA                                  | 134 |

|   |     |
|---|-----|
| 3.3.1.6. Surface Area Measurement                             | 135 |
| 3.3.2. Catalysis Using HTlcs                                  | 136 |
| 3.3.2.1. Screening of HTlcs                                   | 137 |
| 3.3.2.2. Optimization of Reaction Parameters                  | 138 |
| 3.3.2.3. Effect of Co:Al Ratio on Ethylbenzene Oxidation      | 139 |
| 3.3.2.4. Effect of Solvents                                   | 140 |
| 3.3.2.5. Effect of Temperature                                | 141 |
| 3.3.2.6. Screening of Ethylbenzenes                           | 142 |
| 3.3.2.7. Catalyst Recycle Study                               | 143 |
| 3.3.3. Kinetics of Liquid Phase Oxidation of Ethylbenzene     | 146 |
| 3.3.3.1. Preliminary Experiments                              | 146 |
| 3.3.3.1.1. Evaluation of Kinetic Regime                       | 147 |
| 3.3.3.1.2. Effect of Agitation Speed                          | 147 |
| 3.3.3.2. Analysis of Initial Rate Data with HTlcs as Catalyst | 148 |
| 3.3.3.2.1. Effect of Co-Al HTlc Concentration                 | 149 |
| 3.3.3.2.2. Effect of Ethylbenzene Concentration               | 151 |
| 3.3.3.2.3. Effect of TBHP Concentration                       | 152 |
| 3.3.4. Kinetic Model  | 154 |
| 3.4. Conclusions  | 162 |
| Nomenclature  | 163 |
| References  | 164 |

**CHAPTER 4: Hydroformylation of 6-methoxy-2-vinylnaphthalene as a Potential Route  
for the Synthesis of Naproxen**

|                                     |     |
|-------------------------------------|-----|
| 4.1. Introduction                   | 166 |
| 4.2. Experimental Section           | 168 |
| 4.2.1. Materials                    | 168 |
| 4.2.2. Hydroformylation Experiments | 168 |
| 4.2.3. Oxidation Experiments        | 169 |
| 4.2.4. Analytical Methods           | 170 |

|   |     |
|---|-----|
| 4.2.5. Synthesis of Complexes                                   | 171 |
| 4.2.5.1. Preparation of Rh(CO) <sub>2</sub> (acac)              | 171 |
| 4.2.5.2. Synthesis of [Rh(COD)Cl] <sub>2</sub>                  | 172 |
| 4.2.5.3. Preparation of HRh(CO)(PPh <sub>3</sub> ) <sub>3</sub> | 173 |
| 4.3. Results and Discussions                                    | 175 |
| 4.3.1. Hydroformylation of MVN: Preliminary Experiments         | 176 |
| 4.3.1.1. Screening of Catalysts Precursor                       | 176 |
| 4.3.1.2. Ligand Screening and Concentration Effect              | 177 |
| 4.3.1.3. Screening of Solvents                                  | 179 |
| 4.3.1.4. Effect of Temperature                                  | 180 |
| 4.3.1.5. Effect of Total Pressure                               | 181 |
| 4.4. Kinetics of Hydroformylation of MVN                        | 181 |
| 4.4.1. Agitation Effect   | 183 |
| 4.3.2. Solubility of H <sub>2</sub> and CO in Solvent           | 183 |
| 4.4.3. Gas-liquid Mass Transfer Effect                          | 184 |
| 4.4.4. Initial Rate Data  | 186 |
| 4.4.5. Effect of Catalyst Concentration                         | 187 |
| 4.4.6. Effect of MVN Concentration                              | 188 |
| 4.4.7. Effect of Partial Pressure of Carbon Monoxide            | 190 |
| 4.4.8. Effect of Partial Pressure of Hydrogen                   | 191 |
| 4.5. Kinetic Model  | 193 |
| 4.6. Semibatch Reactor Model                                    | 196 |
| 4.7. Reaction Pathway   | 198 |
| 4.8. Liquid Phase Oxidation of 2-MNP                            | 200 |
| 4.8.1. Preliminary Studies                                      | 201 |
| 4.8.2. Sodium Tungstate Concentration Effect                    | 202 |
| 4.8.3. TBAHS Concentration Effect                               | 203 |
| 4.8.4. H <sub>2</sub> O <sub>2</sub> Concentration Effect       | 204 |
| 4.8.5. 2-MNP Concentration Effect                               | 204 |
| 4.8.6. Effect of Temperature                                    | 205 |
| 4.9. Conclusions  | 205 |
| Nomenclature  | 207 |
| References  | 208 |

---

**CHAPTER 5: Hydroformylation of Vinyl Acetate Monomer as a Potential Route for the  
Synthesis of Hydroxy Propionic Acid**

---

|   |     |
|---|-----|
| 5.1. Introduction   | 210 |
| 5.2. Experimental   | 212 |
| 5.2.1. Materials  | 212 |
| 5.2.2. General Experimental Procedure                         | 213 |
| 5.2.3. Catalyst Recycle Procedure                             | 214 |
| 5.2.4. Synthesis of $\text{Co}_2(\text{CO})_8$                | 214 |
| 5.2.5. Preparation of 3-acetoxy Propanal (3-ACPAL)            | 216 |
| 5.2.6. Preparation of 2-acetoxy Propanal (2-ACPAL)            | 216 |
| 5.2.7. Oxidation Experiments                                  | 217 |
| 5.2.8. Hydrolysis Experiments                                 | 218 |
| 5.2.9. Analytical Methods                                     | 218 |
| 5.3. Results and Discussion                                   | 219 |
| 5.3.1 Hydroformylation Experiments                            | 220 |
| 5.3.1.1 Preliminary Experiments                               | 220 |
| 5.3.1.1.1 Effect of Synthesis Gas Pressure                    | 221 |
| 5.3.1.1.2 Effect of Temperature                               | 222 |
| 5.3.1.1.3 Screening of Solvents                               | 223 |
| 5.3.1.1.4 Catalyst Recycle Study                              | 225 |
| 5.4 Kinetics of Hydroformylation of VAM                       | 226 |
| 5.4.1 Evaluation of Kinetic Regime                            | 226 |
| 5.4.1.1 Effect of Agitation Speed                             | 226 |
| 5.4.1.2 Solubility of $\text{H}_2$ and $\text{CO}$ in Solvent | 227 |
| 5.4.1.3 Mass Transfer Effects                                 | 228 |
| 5.4.1.3.1 Gas-liquid Mass Transfer Effect                     | 229 |
| 5.4.2 Initial Rate Data                                       | 230 |
| 5.4.2.1 Effect of $\text{Co}_2(\text{CO})_8$ Concentration    | 231 |
| 5.4.2.2 Effect of VAM Concentration                           | 232 |
| 5.4.2.3 Effect of Partial Pressure of Hydrogen                | 233 |

|   |     |
|---|-----|
| 5.4.2.4 Effect of Partial Pressure of Carbon monoxide | 234 |
| 5.4.3 Kinetic Models                                  | 235 |
| 5.5 Mechanism of Hydroformylation of VAM              | 238 |
| 5.6 Liquid Phase Oxidation of Acetoxy Propanals       | 240 |
| 5.6.1 Oxidation of ACPALs: Screening of Catalysts     | 242 |
| 5.6.2 Screening of Solvents                           | 242 |
| 5.7 Liquid Phase Oxidation of 2-ACPAL                 | 243 |
| 5.7.1. Kinetics of Liquid Phase Oxidation of 2-ACPAL  | 244 |
| 5.7.2 Evaluation of Kinetic Regime                    | 245 |
| 5.7.2.1 Effect of Agitation Speed                     | 245 |
| 5.7.2.2 Effect of Oxygen Flow Rate                    | 246 |
| 5.7.3 Initial Rate Data                               | 247 |
| 5.7.3.1 Effect of Catalyst Concentration              | 248 |
| 5.7.3.2 Effect of 2-ACPAL Concentration               | 249 |
| 5.7.3.3 Effect of Oxygen Partial Pressure             | 249 |
| 5.7.4 Kinetic Models                                  | 250 |
| 5.8 Hydrolysis of Acetoxy Propionic Acids             | 253 |
| 5.9 Conclusion  | 255 |
| Nomenclature  | 257 |
| References  | 258 |

## List of Tables

| Description   | Page Number |
|---|-------------|
| Table 1.1. Applications of multiphase catalytic reactions                                 | 5           |
| Table 1.2. Major Chemical Processes Utilizing Hydrocarbon Oxidation                       | 13          |
| Table 1.3. Some Important Process Parameters in the Commercially Important Oxidations     | 15          |
| Table 1.4. Liquid phase oxidation of toluenes   | 19          |
| Table 1.5. Liquid phase oxidation of ethylbenzene   | 22          |
| Table 1.6. Liquid phase oxidation of aldehydes  | 25          |
| Table 1.7. Comparison of various industrial oxo processes                                 | 34          |
| Table 1.8. Survey of commercial application of Rh catalyzed hydroformylation              | 37          |
| Table 1.9. Hydroformylation of vinyl aromatic compounds                                   | 50          |
| Table 1.10. Examples of tandem or sequential synthesis                                    | 53          |
| <br>  |             |
| Table 2.1. Screening of catalyst  | 79          |
| Table 2.2. Screening of co-catalysts  | 80          |
| Table 2.3. Effect of catalyst and promoter concentrations                                 | 82          |
| Table 2.4. Results with substituted toluene substrates                                    | 87          |
| Table 2.5. Henry's law constant   | 89          |
| Table 2.6. Range of operating conditions  | 90          |
| Table 2.7. Parameters used for $k_{LAB}$ calculations                                     | 93          |
| Table 2.8. Model discrimination   | 111         |
| <br>  |             |
| Table 3.1. Surface area of HTlcs  | 136         |
| Table 3.2. Screening of hydrotalcite for liquid phase oxidation of ethylbenzene           | 138         |
| Table 3.3. Optimization of reaction parameters for liquid phase oxidation of ethylbenzene | 139         |
| Table 3.4. Effect of Co-Al ratio on ethyl benzene oxidation                               | 140         |
| Table 3.5. Properties of Co-Al HTlc   | 140         |
| Table 3.6. Screening of solvents for liquid phase oxidation of ethylbenzene               | 141         |
| Table 3.7. Screening of alkylbenzene for liquid phase oxidation                           | 143         |

|             |  |     |
|-------------|--|-----|
| Table 3.8.  | Range of operating conditions for liquid phase oxidation of ethylbenzene | 149 |
| Table 3.9.  | Model Discrimination   | 161 |
| Table 4.1.  | MVN hydroformylation: screening of catalysts                             | 177 |
| Table 4.2.  | MVN hydroformylation: screening of ligands                               | 178 |
| Table 4.3.  | MVN hydroformylation: Solvent screening                                  | 180 |
| Table 4.4.  | Henry's law Constant   | 184 |
| Table 4.5.  | Parameters used for $k_{L,AB}$ calculations                              | 185 |
| Table 4.6.  | Range of operating conditions  | 186 |
| Table 4.7.  | Rate models examine to fit the data on MVN hydroformylation              | 196 |
| Table 4.8.  | Screening of catalysts   | 202 |
| Table 4.9.  | Effect of sodium tungstate concentration                                 | 203 |
| Table 4.10. | Oxidation of 2-MNP: effect of TBAHS concentration                        | 203 |
| Table 4.11. | Oxidation of 2-MNP: effect of $H_2O_2$ concentration                     | 204 |
| Table 4.12. | Oxidation of 2-MNP: effect of MNP concentration                          | 204 |
| Table 4.13. | Oxidation of 2-MNP : Effect of temperature                               | 205 |
| Table 5.1.  | Hydroformylation of VAM: Effect of Temperature                           | 223 |
| Table 5.2.  | Screening of solvents  | 224 |
| Table 5.3.  | Henry's law constant   | 228 |
| Table 5.5.  | Parameters used for $k_{L,AB}$ calculations                              | 230 |
| Table 5.6.  | Range of conditions used for the kinetic studies                         | 231 |
| Table 5.7.  | Rate models examine to fit the data on VAM hydroformylation              | 236 |
| Table 5.8.  | Liquid phase oxidation ACPALs: Screening of catalyst                     | 242 |
| Table 5.9.  | Liquid phase oxidation ACPALs: Screening of solvents                     | 243 |
| Table 5.10. | Liquid phase oxidation 2-ACPAL: Preliminary experiments                  | 244 |
| Table 5.11. | Range of conditions used for the kinetic studies                         | 247 |
| Table 5.12. | Rate models examine to fit the data on liquid phase oxidation of 2-ACPAL | 251 |
| Table 5.13. | Hydrolysis of ACPAs  | 255 |



## List of Figures

| Description   | Page Number |
|---|-------------|
| Figure 1.1. Process options in oxidation reaction   | 9           |
| Figure 1.2. Oxometal vs peroxometal pathway   | 31          |
| Figure 1.3. Hydridometal pathways for alcohol oxidation   | 32          |
| Figure 1.4. Classification of hydroformylation based on the substrates employed.  | 39          |
| Figure 1.5. Hydroformylation of styrene   |             |
| Figure 1.6. Substitution of (PPh <sub>2</sub> Py) to RhH(CO)(PPh <sub>3</sub> ) <sub>3</sub> at a variable ligand to metal ratio. |             |
| Figure 1.5. Anti-inflammatory compounds   | 44          |
| Figure 1.6. Synthesis of ibuprofen from p-isobutyl styrene.   | 47          |
| Figure 1.7. Scheme for the asymmetric hydroformylation of MVN for direct sythnehsis of (S)-naproxen                               | 48          |
| Figure 1.8. The most active catalyst for asymmetric hydroformylation of MVN   | 49          |
| Figure 1.9. Catalytic cycle of hydroformylation with unmodified cobalt catalysts.   | 54          |
| Figure 1.10. Mechanism for hydroformylation using modified rhodium catalysts (L=PPh <sub>3</sub> )                                | 56          |
| Figure 2.1. A schematic of the reactor setup for batch oxidation reactions  | 74          |
| Figure 2.2. Effect of solvents  | 84          |
| Figure 2.3. Effect of temperature in Mn (OAc) <sub>2</sub> / FeCl <sub>3</sub> / NaBr catalyzed oxidation of toluene              | 85          |
| Figure 2.4. Effect of O <sub>2</sub> Partial pressure   | 86          |
| Figure 2.5. Effect of catalyst recycle  | 88          |
| Figure 2.6. Concentration time profile at 393K  | 91          |
| Figure 2.7. Effect of agitation speed   | 94          |
| Figure 2.8a. Effect of Mn(OAc) <sub>2</sub> concentration on rate of formation of benzyl alcohol                                  | 95          |
| Figure 2.8b. Effect of Mn(OAc) <sub>2</sub> concentration on rate of formation of benzyl acetate                                  | 96          |

|               |  |     |
|---------------|--|-----|
| Figure 2.8c.  | Effect of $\text{Mn}(\text{OAc})_2$ concentration on rate of formation of benzaldehyde | 96  |
| Figure 2.8d.  | Effect of $\text{Mn}(\text{OAc})_2$ concentration on rate of formation of benzoic acid | 97  |
| Figure 2.8.   | Effect of $\text{Mn}(\text{OAc})_2$ concentration on liquid phase toluene oxidation    | 97  |
| Figure 2.9a.  | Effect of $\text{FeCl}_3$ concentration on rate of formation of benzyl alcohol         | 98  |
| Figure 2.9b.  | Effect of $\text{FeCl}_3$ concentration on rate of formation of benzyl acetate         | 98  |
| Figure 2.9c.  | Effect of $\text{FeCl}_3$ concentration on rate of formation of benzaldehyde           | 99  |
| Figure 2.9d.  | Effect of $\text{FeCl}_3$ concentration on rate of formation of benzoic acid           | 99  |
| Figure 2.9.   | Effect of $\text{FeCl}_3$ concentration on liquid phase toluene oxidation              | 99  |
| Figure 2.10a. | Effect of $\text{NaBr}$ concentration on rate of formation of benzyl alcohol           | 100 |
| Figure 2.10b. | Effect of $\text{NaBr}$ concentration on rate of formation of benzyl acetate           | 101 |
| Figure 2.10c. | Effect of $\text{NaBr}$ concentration on rate of formation of benzaldehyde             | 101 |
| Figure 2.10d. | Effect of $\text{NaBr}$ concentration on rate of formation of benzoic acid             | 102 |
| Figure 2.10.  | Effect of $\text{NaBr}$ concentration on liquid phase toluene oxidation                | 102 |
| Figure 2.11a. | Effect of toluene concentration on rate of formation of benzyl alcohol                 | 103 |
| Figure 2.11b. | Effect of toluene concentration on rate of formation of benzyl acetate                 | 103 |
| Figure 2.11c. | Effect of toluene concentration on rate of formation of benzaldehyde                   | 104 |
| Figure 2.11d. | Effect of toluene concentration on rate of formation of benzoic acid                   | 104 |
| Figure 2.11.  | Effect of toluene concentration on liquid phase toluene oxidation                      | 104 |
| Figure 2.12a. | Effect of oxygen partial pressure on rate of formation of benzyl alcohol               | 105 |
| Figure 2.12b. | Effect of oxygen partial pressure on rate of formation of benzyl acetate               | 106 |
| Figure 2.12c. | Effect of oxygen partial pressure on rate of formation of benzaldehyde                 | 106 |
| Figure 2.12d. | Effect of oxygen partial pressure on rate of formation of benzoic acid                 | 107 |
| Figure 2.12.  | Effect of oxygen partial pressure on liquid phase toluene oxidation                    | 107 |
| Figure 2.13.  | Arrhenius Plot   | 109 |
| Figure 2.14.  | Experimental Vs predicted concentration time profile at 393K                           | 112 |
| Figure 2.15.  | Experimental Vs predicted concentration time profile at 403K                           | 112 |
| Figure 2.16.  | Experimental Vs predicted concentration time profile at 383K                           | 113 |
| Figure 2.17.  | Spectroscopic analysis   | 115 |
|               |  |     |
| Figure 3.1.   | Hydrotalcite synthesis set up  | 124 |
| Figure 3.2.   | Liquid phase oxidation reactor set up  | 125 |

|               |   |     |
|---------------|---|-----|
| Figure 3.3.   | Powder XRD patterns for unused and recovered Co-Al-HT catalyst  | 130 |
| Figure 3.4.   | Scanning Electron Microscopy patterns of for unused and recovered Co-Al-HT catalyst                     | 131 |
| Figure 3.5.   | Full-range XPS spectrum of Co-Al-HTlc   | 132 |
| Figure 3.6.   | XPS spectra of unused and recovered Co-Al-HT catalyst   | 133 |
| Figure 3.7.   | FTIR spectra of Co-Al-HT catalyst   | 134 |
| Figure 3.8.   | TGA and DTA patterns of Co-Al-HT catalyst   | 135 |
| Figure 3.9.   | Effect of temperature on ethylbenzene oxidation   | 142 |
| Figure 3.10.  | Recycle study of Co-Al-HTlc for ethylbenzene oxidation  | 144 |
| Figure 3.11.  | Hot filtration experiment for confirming the reusability of the catalyst Co-Al-HT                       | 145 |
| Figure 3.12.  | Concentration - time profile of liquid phase oxidation of ethylbenzene.                                 | 147 |
| Figure 3.13.  | A plot of rate of liquid phase oxidation of ethylbenzene vs. agitation speed.                           | 148 |
| Figure 3.14a. | Effect of Co-Al HTlc concentration on rate of formation of Acph   | 150 |
| Figure 3.14b. | Effect of Co-Al HTlc concentration on rate of formation of PE   | 150 |
| Figure 3.15a. | Effect of ethylbenzene concentration on rate of formation of Acph                                       | 151 |
| Figure 3.15b. | Effect of ethylbenzene concentration on rate of formation of PE   | 152 |
| Figure 3.16a. | Effect of TBHP concentration on rate of formation of Acph.  | 153 |
| Figure 3.16b. | Effect of TBHP concentration on rate of formation of PE.  | 153 |
| Figure 3.17.  | Experimental Vs predicted concentration time profile for liquid phase oxidation of ethylbenzene at 333K | 158 |
| Figure 3.18.  | Experimental Vs predicted concentration time profile for liquid phase oxidation of ethylbenzene at 323K | 159 |
| Figure 3.19.  | Experimental Vs predicted concentration time profile for liquid phase oxidation of ethylbenzene at 313K | 160 |
| Figure 4.1    | A schematic of the reactor setup for hydroformylation of MVN  | 169 |
| Figure 4.2    | A schematic of the reactor setup for oxidation reactions  | 170 |
| Figure 4.3:   | FTIR spectrum of Rh(CO) <sub>2</sub> (acac)   | 172 |
| Figure 4.4.   | FTIR spectra of [Rh (COD)Cl] <sub>2</sub>   | 173 |
| Figure 4.5.   | FTIR spectra of Rh(CO)Cl(PPh <sub>3</sub> ) <sub>2</sub>  | 174 |
| Figure 4.6    | FTIR spectra of HRhCO (PPh <sub>3</sub> ) <sub>3</sub>  | 175 |
| Figure 4.7(a) | Effect of ligand concentration on the rate of hydroformylation  | 178 |

|                  |  |     |
|------------------|--|-----|
| Figure 4.7(b)    | Effect of ligand concentration on n/iso ratio                                      | 179 |
| Figure 4.8.      | Effect of temperature on hydroformylation of MVN                                   | 180 |
| Figure 4.9       | Effect of total pressure on hydroformylation of MVN                                | 181 |
| Figure 4.10.     | Hydroformylation of MVN: concentration time profile                                | 182 |
| Figure 4.11.     | Hydroformylation of MVN: Effect of agitation speed                                 | 183 |
| Figure 4.12 (a). | Effect of catalyst concentration on rate of hydroformylation of MVN                | 187 |
| Figure 4.12 (b). | Effect of catalyst concentration on rate n/iso ratio                               | 188 |
| Figure 4.13 (a). | Effect of MVN concentration on rate of hydroformylation of MVN                     | 189 |
| Figure 4.13 (b). | Effect of MVN concentration n/iso ratio  | 189 |
| Figure 4.14 (a). | Effect of $P_{CO}$ on rate of hydroformylation of MVN                              | 190 |
| Figure 4.14 (b). | Effect of $P_{CO}$ n/iso ratio   | 191 |
| Figure 4.15 (a). | Effect of $P_{H_2}$ on rate of hydroformylation of MVN                             | 192 |
| Figure 4.15 (b). | Effect of $P_{H_2}$ on n/iso ratio   | 192 |
| Figure 4.16.     | MVN hydroformylation: Experimental rates vs Predicted rates                        | 194 |
| Figure 4.17.     | Hydroformylation of MVN: Arrhenius plot  | 195 |
| Figure 4.18.     | Hydroformylation of MVN: experimental Vs predicted concentration time profile      | 198 |
| Figure 4.19.     | Concentration time profile of oxidation of 2-MNP                                   | 201 |
|                  |  |     |
| Figure 5.1.      | A schematic of the reactor setup for hydroformylation of VAM                       | 214 |
| Figure 5.2.      | FTIR spectra of $Co_2(CO)_8$   | 216 |
| Figure 5.3.      | A schematic of reaction set-up for oxidation experiments                           | 217 |
| Figure 5.4.      | A schematic of reaction set-up for hydrolysis experiments                          | 218 |
| Figure 5.5.      | Concentration time profile of hydroformylation of VAM                              | 221 |
| Figure 5.6.      | Effect synthesis gas pressure on conversion of VAM and selectivity to aldehydes    | 222 |
| Figure 5.7.      | Hydroformylation of VAM: Study of catalyst recycle                                 | 225 |
| Figure 5.8.      | A plot of rate of hydroformylation of VAM vs. agitation speed                      | 227 |
| Figure 5.9.      | A plot of Initial rate vs. catalyst concentration in hydroformylation of VAM       | 232 |
| Figure 5.10.     | A plot of Initial rate vs. VAM concentration effect in the hydroformylation of VAM | 233 |
| Figure 5.11.     | A plot of rate vs. $P_{H_2}$ for the hydroformylation of VAM                       | 234 |
| Figure 5.12.     | A plot of rate vs. $P_{CO}$ for the hydroformylation of VAM.                       | 235 |

|              |  |     |
|--------------|--|-----|
| Figure 5.13. | Comparison of experimental rates and rates predicted using model I | 238 |
| Figure 5.14. | Temperature dependence of rate constant                            | 238 |
| Figure 5.15. | Concentration time profile for oxidation of 2-ACPAL                | 245 |
| Figure 5.16. | Effect of agitation speed on the rate of oxidation of 2-ACPAL      | 246 |
| Figure 5.17. | Effect Oxygen Flowrate on rate of 2-ACPAL oxidation                | 247 |
| Figure 5.18. | Effect of catalyst concentration on rate of 2-ACPAL oxidation      | 248 |
| Figure 5.19. | Effect of 2-ACPAL concentration on rate of 2-ACPAL oxidation       | 249 |
| Figure 5.20. | Effect of $P_{O_2}$ on rate of 2-ACPAL oxidation                   | 250 |
| Figure 5.21. | Comparison of experimental rates and rates predicted using model I | 252 |
| Figure 5.22. | Temperature dependence of rate constant                            | 253 |

## List of Schemes

|             | <b>Description</b>  | <b>Page Number</b> |
|-------------|---|--------------------|
| Scheme 1.1. | General hydroformylation reaction.  | 33                 |
| Scheme 1.2. | Hydroformylation of Styrene   | 43                 |
| Scheme 2.1. | Schematic of liquid phase oxidation of toluene                                      | 77                 |
| Scheme 2.2. | Liquid phase oxidation of substituted toluenes to benzaldehyde derivatives          | 87                 |
| Scheme 2.3. | Simplified reaction scheme for Liquid phase oxidation of toluene                    | 91                 |
| Scheme 2.4. | Mechanism of liquid phase oxidation of toluene                                      | 116                |
| Scheme 3.1. | Schematic of liquid phase oxidation of ethylbenzene                                 | 128                |
| Scheme 3.2. | Simplified reaction scheme for liquid phase oxidation of ethylbenzene               | 154                |
| Scheme 4.1. | Synthesis of dl-naproxen by hydroformylation-oxidation route                        | 175                |
| Scheme 4.2. | A plausible mechanism for rhodium catalyzed MVN hydroformylation to 2-MNP and 3-MNP | 199                |
| Scheme 5.1. | Synthesis of hydroxy propionic acid   | 220                |
| Scheme 5.2. | Mechanism of hydroformylation of VAM  | 240                |
| Scheme 5.3. | General scheme for hydrolysis of acetoxy propionic acids                            | 254                |

## Abstract of the Thesis

Multiphase catalytic reactions have significant impact on the development of new synthetic routes and their scope has been expanding into diverse areas of applications for making value added products. Catalytic reactions in multiphase systems are prevalent in production of fuels, bulk and specialty chemicals, pharmaceuticals, food etc. The success of catalytic processing of multiphase systems has resulted from a synergetic approach to the problem by chemists and chemical engineers<sup>1</sup>. Making useful products, at economical yields and selectivities, from the diverse chemistries in such a broad range of applications requires the ability to quantify the interplay of transport phenomena and kinetics<sup>1,2</sup>. Hydroformylation, oxidation, epoxidation, hydrogenation, carbonylation, oxidative carbonylation and amination are some of most important examples of multiphase catalytic reactions.

Liquid Phase Oxidation (LPO) and hydroformylation are two of the most prominent examples of multiphase catalytic reactions in industry. LPO has been employed for synthesis of a variety of industrial products such as aldehydes, ketones, alcohols, carboxylic acids etc. The conventional LPO processes have relied on classical stoichiometric oxidants, which are not acceptable from environmental considerations, as they generate large quantities of mineral wastes and employ toxic reagents. Oxidation of hydrocarbon and aldehydes using metal complex catalysts has emerged as an important tool for synthesis of a variety of drug intermediates and specialty products like aldehydes, alcohols and carboxylic acids. In case of liquid phase oxidation of hydrocarbons like alkyl benzenes, the products of commercial interest are the aldehydes or ketones, which are prone to over oxidation, lowering selectivity to desired product<sup>3</sup>. In this respect, selection of catalysts, solvents and reaction conditions is very important to achieve high yield and selectivity.

Hydroformylation is a well-known synthetic tool for the preparation of a wide range of organic molecules of high commercial value through aldehyde or alcohol products. It manifests the largest application of homogeneous catalysis in industry for the manufacture of oxo-alcohols. The process, now conventionally known as the oxo-

process, may be applied to linear as well as substituted olefins. Hydroformylation technology for linear olefins has advanced considerably in the last few decades with development of novel catalysts and ligands as well as better understanding of reaction mechanism<sup>4</sup>. However, literature shows limited information on hydroformylation of substituted olefins with respect to kinetics and mechanism.

Tandem as well as sequential syntheses using cheaper feedstocks as starting materials have gained a lot of interest in an attempt to avoid the old generation multi-step syntheses and development of cleaner and cheaper alternatives. In this context, the sequential synthesis of important pharmaceutical products like dl-naproxen via 6-methoxy-2-vinyl naphthalene (MVN) hydroformylation–oxidation route and hydroxy propionic acids (HPAs) via vinyl acetate monomer (VAM) hydroformylation-oxidation-hydrolysis investigated in the present thesis may contribute to some extent.

Considering the status of developments discussed above, the following problems were chosen for detailed study in this thesis.

- ✓ Selective liquid phase oxidation of toluenes to benzaldehydes
- ✓ Selective oxidation of ethylbenzene using hydrotalcite like compounds as catalyst
- ✓ Hydroformylation of 6-methoxy-2-vinylnaphthalene as a potential route for the synthesis of naproxen
- ✓ Hydroformylation of vinyl acetate monomer as potential route for the synthesis of hydroxy propionic acids

The thesis will be presented in five distinguished chapters, the brief details of which are presented below.

Chapter 1, a detailed survey of the literature on catalysis and kinetics of multiphase catalytic reactions involving oxidation and hydroformylation is presented as well as the conventional, stoichiometric or catalytic processes for synthesis of aromatic aldehydes, ketones, arylpropionic acids and hydroxypropionic acids (HPAs).

The oxidation product of aromatic hydrocarbons like aromatic aldehydes and ketones are important intermediates in various synthetic procedures. Benzaldehyde, for example, is used in flavors, fragrances, as intermediates in manufacture of dyes, perfumes, pharmaceuticals and pesticides<sup>5</sup>. Aromatic ketones like acetophenone are important



chemical intermediates in perfumery, drugs and pharmaceuticals<sup>6</sup>. The conventional modes of manufacturing industrially important aldehydes or ketones involve reagent-based synthesis like vapor phase catalytic hydrolysis of benzyl chloride to benzaldehyde<sup>3</sup>; and Friedel-Craft's acylation of aromatics<sup>7</sup>. These procedures yield low selectivity and generate large amounts of wastes. The oxidation of hydrocarbons in liquid phase (LPO) is better alternatives considering cleaner synthesis and atom economy.

Several transition metal catalysts like iron, cobalt, manganese, copper, molybdenum or nickel as monometallic or their combinations as multimetallic catalysts promoted by bromides have been successfully investigated for LPO of toluene<sup>8,9</sup>. Comparatively much lesser literature is available on selective acetophenone synthesis via ethylbenzene oxidation. The latter is reported in many instances for the synthesis of either ethylbenzene hydroperoxide or phenyl ethanol. The few reported catalyst systems for acetophenone synthesis include salts of cobalt, manganese etc in acidic solvents which report formation of byproducts like phenyl ethanol, benzaldehyde and benzoic acid<sup>10</sup>. Provided that an economically viable, easily recoverable and reusable catalyst is designed, LPO offers better alternatives for the synthesis of such aldehydes and ketones.

Naproxen has been manufactured via multistep syntheses, e.g. acylation, ketalization, bromination, hydrolysis and reductive cleavage starting from nerolin; bromination, methylation and alkylmetal coupling reactions starting from naphthol and chiral syntheses involving chiral catalysts and ligands like (*S*)-BINAP<sup>11</sup>. The multistep synthesis suffer from the lower yield of naproxen 50-60%. These routes suffer from use of hazardous chemicals, generation of wastes and high costs.

The industrial synthesis procedure for hydroxypropionic acids, 2-HPA and 3-HPA is achieved via fermentation of molasses, which employs high dilutions, mineral acids for work-up, and has lower reaction rates. The commercial synthesis of 2-HPA is also practiced by hydrocyanation of acetaldehydes followed by hydrolysis of cyanohydrin produced. This route produces cyanohydrin upon hydrocyanation of acetaldehyde using toxic HCN. The cyanohydrin produced is hydrolyzed with corrosive sulfuric acid, leading to waste salt generation<sup>12</sup>. Attempts have been made for the synthesis of 2-HPA by hydroformylation of VAM in acidic solvents, followed by oxidation of corresponding 2

acetoxy propanal to 2 acetoxy propionic acid (2-APA) and the hydrolysis of 2-APA, yields 2-HPA. This route suffers from the lower yield of aldehydes in hydroformylation step<sup>13</sup>. Moreover there is no literature on synthesis of 3-HPA, by synthetic route.

**Chapter 2**, a study on liquid phase oxidation of toluenes has been presented with the aim of achieving high selectivity to the aldehydes at optimum conversion of toluenes. Cobalt based catalyst systems are the most extensively explored for the oxidation of toluene to benzaldehyde. It was reported that the incorporation of Mn-acetate as an initiator in cobalt-catalyzed oxidation of toluene increases the activity and selectivity to benzaldehyde. In this study, Mn (OAc)<sub>2</sub> was chosen as the main catalyst along with FeCl<sub>3</sub> as a co-catalyst for liquid phase oxidation of toluene. It was found that the benzaldehyde selectivity (60.2%) is significantly improved at good conversion of toluene (18.4%) due to addition of FeCl<sub>3</sub>, which is a Lewis acid as a co-catalyst to Mn(OAc)<sub>2</sub>, catalyst. Moreover, the observed selectivity to benzaldehyde, benzyl alcohol and benzyl acetate with the Mn based catalyst system is higher than that reported in the literature. Screening of various Lewis acids like FeCl<sub>3</sub>, SnCl<sub>2</sub>, CuCl<sub>2</sub>, NiCl<sub>2</sub>, SbCl<sub>3</sub> etc was therefore carried out to investigate their effect on activity and selectivity in the oxidation of toluene.

The kinetics of liquid phase oxidation of toluene using Mn (II) acetate- FeCl<sub>3</sub>-NaBr catalyst was investigated in the temperature range of 383 to 403 K and pressure range of 2 to 5 MPa in acetic acid as solvent. Based on the data several empirical rate equations were evaluated and the best model was found to predict the concentration time profile in good agreement with the experimental data.

**Chapter 3**, selective synthesis of acetophenone *via* liquid phase oxidation of ethyl benzene was investigated using hydrotalcite-like compounds (HTlcs). Very few literature references are available on ethyl benzene oxidation using TBHP as oxidant, among which supported cobalt and copper are the best catalysts, giving > 80% selectivity to acetophenone at a conversion of 36-50%, along with byproducts like benzaldehyde and benzoic acid, which lower the selectivity. In the present study, Layered Double Hydroxides with various M(II) + M(III) combinations were screened for their catalytic activity for the liquid phase oxidation of ethylbenzene, using *tert*-butyl hydroperoxide

(TBHP) as the oxidant. Excellent selectivity (> 95%) for acetophenone with good ethylbenzene conversion (>50%) was obtained using Co-containing hydrotalcites. The hydrotalcites are shown to be highly active and reusable catalysts for oxidation of ethylbenzene. The component balance was first established for TBHP oxidation of ethylbenzene using the best catalyst i.e. Co-Al –HTlc.

The heterogeneous nature and reusability of the hydrotalcite catalysts was confirmed by carrying out the recycle experiments. The activity of the hydrotalcites remained unchanged upon three recycles. Negligible loss of metal in the reaction was observed by AAS studies of fresh and recovered catalyst (less than 0.1%). The hydrotalcite were fully characterized using XRD, IR, XPS, BET, AAS and SEM. The catalysts vary widely in their surface and bulk properties, depending on the divalent and trivalent metals used for their synthesis. The kinetics of liquid phase oxidation of ethylbenzene using hydrotalcite like compounds and TBHP as oxidant was investigated in the temperature range of 323 to 343 K. A model proposed was found to predict the concentrations in good agreement with the experimental data.

**Chapter 4,** A two-step route consisting of hydroformylation-oxidation was investigated for the synthesis of naproxen. The present synthesis of naproxen involves stoichiometric synthesis, which is non-ecofriendly in terms of waste generation. The alternative catalytic routes proposed employ chiral catalysts and reagents, which are costly and sensitive to reaction conditions. In the hydroformylation of substituted styrene using Rh catalyst, high selectivity to branched aldehydes (>95%) has been reported with quantitative conversions. The separation of enantiomers used to be the cost-centre in the past, which has evolved in recent years considerably, and the cost of resolution of optical isomers is drastically reduced. With this background, the catalytic synthesis of racemic naproxen holds immense significance. Accordingly, in this chapter, the hydroformylation of 6-ethoxy-2-vinylnaphthalene (MVN) to 2-(6-methoxy-2-naphthyl) propanal (2-MNP) using homogeneous  $\text{Rh}(\text{CO})_2(\text{acac})$  as the catalyst with 1,2-bis-(diphenylphosphino) ethane (dppe) as a ligand was investigated to achieve high selectivity to the branched isomer, i.e. 2-MNP; followed by its oxidation to achieve high yields of the corresponding acid was studied as an alternative route for the synthesis of *dl*-naproxen.

A detailed study on the key MVN hydroformylation step was carried out and its feasibility was demonstrated. The roles of the catalyst, ligands, and solvents, and the effect of reaction conditions on the reaction rate and regioselectivity of the product 2-MNP was investigated. By using  $\text{Rh}(\text{CO})_2(\text{acac})$  as a catalyst and dppe as a ligand, >98% selectivity to 2-MNP (an important precursor to *dl*-naproxen) was achieved and this catalyst and ligand combination has been used for the further studies on the hydroformylation step. A detailed kinetic analysis was carried out using initial rate data of hydroformylation of MVN using NMP as solvents in a temperature range of 383-403 K.

In, the second step in the proposed route for Naproxen, oxidation of 2-MNP to the racemic 2-(6-methoxynaphthyl) propanoic acid (*dl*-naproxen) was studied using  $\text{Na}_2\text{WO}_4$  as a catalyst and an acidic phase transfer catalyst with  $\text{H}_2\text{O}_2$  as the oxidant. Screening of early transition metals like salts of tungsten, vanadium and molybdenum showed that  $\text{Na}_2\text{WO}_4$  gives the best performance for the oxidation step with >80% selectivity to 2-(6-methoxynaphthyl) propanoic acid (naproxen). Optimization of reaction parameters and condition was carried out for the synthesis of naproxen.

**Chapter 5**, a three step route involving of hydroformylation-oxidation-hydrolysis was investigated for the synthesis of hydroxy propionic acids. Conventionally 2- and 3-hydroxy propionic acids are synthesized by enzymatic route. Tinkar and co-workers have reported hydroformylation-oxidation-hydrolysis route for 2-hydroxy propionic acid, but the overall yields are very poor due to use of acidic solvents and also, the reaction conditions are harsh. Moreover, there is no synthetic route for exclusive synthesis of 3-hydroxy propionic acid. In this chapter, hydroformylation of VAM was studied as key step with  $\text{Co}_2(\text{CO})_8$  as catalyst to give 2-acetoxy propanal (52%) and 3-acetoxy propanal (48%). The results show that this catalyst gives ~ 100 % conversion of VAM and more than 94% selectivity to aldehydes. The detailed investigations of the liquid phase oxidation of these aldehydes were carried in a glass reactor. The screening of different supported transition metal catalysts was carried out and Co/C was found to be the best catalyst. The mixture of 2 and 3-acetoxy propanal was oxidized with a high selectivity (>98%) to 2- and 3-acetoxy propionic acids respectively; with high conversion (>95%) of the aldehydes, using molecular oxygen as oxidant and Co/C as catalyst. Hydrolysis

experiments were carried out using different acid catalysts and Amberlite IR 120 resin was found to be the best catalyst. The latter was found to give >90% conversion of 2 and 3-acetoxy propionic acids with high selectivity to the corresponding hydroxy propionic acids. The kinetics of the key hydroformylation step was investigated with  $\text{Co}_2(\text{CO})_8$  as catalyst. Various empirical rate models were considered to explain the trends observed. It was observed that rates predicted by the model were in excellent agreement with experimental rates.

Further, the liquid phase oxidation of 2-acetoxypropanal was investigated in detail to understand catalysis and kinetics involved, using Co/C catalyst and air as the oxidant, in the temperature range of 303 to 343 K.

## Reference

---

- 1 Dudukovic, M.P.; *Catalysis Today* **1999**, 48, 5
- 2 Mills, P.L.; Chaudhari, R.V.; *Catalysis Today* **1999**, 48, 17
- 3 Kantam, M.L.; Choudhory, B.M. ; Sreekanth, P; Rao, K.K.; Naik, K.; Kumar, T. P.; Khan, A.; *Catalysis Letters* **2002**, 81 223
- 4 Haas, T. ; Jaeger, B.; Weber, R.; Mitchell, S.F.; King C.F.; *Applied Catalysis A: General* **2005**, 280, 83
- 5 Borgaonkar, H.V.; Raverkar, S R.; Chandalla, S.B.; *Ind. Eng. Chem.. Prod. Res. Dev.* **1984**, 23, 455
- 6 Chaudhari, V. R.; Indurkar, J.R.; Narkhede, V.S.; Jha R; *Journal of Catalysis* **2004**, 227, 257
- 7 Jana, S.K.; Wu, P. and Tatsumi, T.; *Journal of Catalysis.* **2006**, 240. 268.
- 8 Suresh, A.K.; Sharma,M.M.; Shridhar, T; *Ind. Eng. Chem.* **2000**, 39,3958
- 9 Sheldon, R.A.; Kochi, J.K.; *Metal catalyzed oxidation of organic compounds academic press*, New york **1881**
- 10 Sanders, H.J.; Keag, H.F.; McCollough, H.S. ; *Ind. Eng. Chem.* **1953**, 45,2
- 11 Harrington, P.J. ; Lodewijk, E.; *Org. Process Res. Dev.* **1997**, 1, 72
- 12 Nangeroni, J. F.; Hartmann, M. H.; Iwen, M. L.; Ryan, C. M.; Kolstad, J. J.; McCarthy, K. T.; *WO Pat.* 9853141, **1998**
- 13 Tinkar, H.B.; *US* 4072709 **1978**

# **Chapter 1**

## **Introduction and Literature Survey**

This chapter presents a survey of the literature on multiphase catalytic reactions and its importance to chemical process industry and hence the mankind. For development of cleaner energy efficient and atom economical processes. The gradual build-up of the problems around certain issues of current economic and environmental concern for the present day technology of oxidation and hydroformylation reactions has been presented. Moreover, applications of multiphase catalytic reaction for the respective reactions from literature have been reviewed to identify & choose the most effective one for the studies. The thorough discussion of the different aspects of the existing state-of-the-art, and the understanding gained from this review has evolved into a well-defined objective to work with.

## 1.1. Introduction

Multiphase catalytic reactions have significant impact on the development of new synthetic routes and their scope has been expanding into diverse areas of applications for making value added products. Catalytic reactions in multiphase systems are prevalent in production of fuels, bulk and specialty chemicals, pharmaceuticals, food etc. The success of catalytic processing of multiphase systems has resulted from a synergetic approach to the problem by chemists and chemical engineers<sup>1,2</sup>. Making useful products, at economical yields and selectivities, from the diverse chemistries in such a broad range of applications requires the ability to quantify the interplay of transport phenomena and kinetics<sup>3,4</sup>.

The importance of catalysis to society is based on its great economic impact in the production of broad range of commodity products that improve our standards of living and quality of life. Most of the industrial reactions are catalytic and the number of chemical compounds produced world wide at the present time are roughly in the range of 20,000 to 30,000<sup>5</sup>. Catalysis plays a key role not only in the production of a wide variety of products, which are having applications in food, clothing, drugs, plastics, agrochemicals, detergents, fuels etc<sup>6</sup>, but also offers significant contribution in the balance of ecology and environment by providing cleaner alternative routes for stoichiometric technologies<sup>7,8</sup> by conversion of polluting emissions to harmless streams.

Catalysis has been in broader terms classified in two different types as homogeneous and heterogeneous catalysis depending on the physical nature of the catalyst employed. In homogeneous catalysis, the catalyst is soluble in the reaction medium making a single phase whereas in heterogeneous catalysis the catalyst is present as a separate phase (a solid or an immiscible liquid phase). Though, both the types of catalysts have contributed significantly to the industry, homogeneous catalysts have distinct advantages like high activity at milder operating conditions, selectivity control, feasibility to understand detailed mechanistic aspects at microscopic level to tailor it further and negligible diffusion limitations. These advantages of homogeneous catalysts have been used in industry for several years for a number of processes involving carbonylation, hydroformylation, hydrogenation, oligomerization, isomerization, polymerization and

oxidation reactions<sup>9,10</sup>. Industrial significance of homogeneous catalysis was realized several decades ago after the development of oxo process<sup>11</sup> (hydroformylation technology), Wacker process (olefin oxidation)<sup>3</sup>, Acetic Acid manufacture by BASF<sup>12,13</sup>, Monsanto<sup>14,15</sup> and BP<sup>16,17</sup> processes (methanol carbonylation technology), ethylene polymerization by Zeigler-Natta catalysts<sup>18</sup> and *p*-xylene oxidation to terephthalic acid<sup>19,20</sup>. Initially, the application of homogeneous catalysts was limited to Lewis and Brønsted acids, bases, simple metal salts and simple organic molecules. As the need for more specialized products increased, transition metals with tailored co-ordination environment were preferred as catalysts to achieve selectivity control at milder reaction conditions. Selectivity control is the main advantage of homogeneous catalysts, which is achieved by ligand design utilizing the knowledge of organometallic, coordination and theoretical chemistry. Chemistry of chiral synthesis via asymmetric catalysis is mainly based on homogeneous catalysis. Despite these advantages, about 80% of the industrial catalytic processes employ heterogeneous catalysts for easier catalyst-product separation, which is often a tedious job in homogeneous catalysis. On the other hand, recent development in synthesis of new metal complex catalysts, novel ligands, new designs for tandem reactions and asymmetric catalysis indicates a strong potential of homogeneous catalysis for the synthesis of a wide variety of bulk, specialty and pharmaceutical products.

The multiphase reactions pose several challenges from a reaction-engineering viewpoint, such as complexities of process chemistry, kinetics, transport effects, energy management and mixing of fluid phases. Detailed analysis of reaction engineering aspects is therefore necessary in identification of critical design factors. Traditionally, the focus of the chemists has been on the catalyst, its preparation, active form, activity, active centers, turnover numbers, kinetics and poisons that might damage it. Engineers were mainly concerned with how to bring the reactants effectively in contact with the chosen catalyst form, and how to provide or remove the heat associated with the progress of reaction. They also concerned themselves with scale-up issues, as how to reproduce the selectivity and rates reached in the laboratory on large process scale. Catalytic reaction engineering (CRE) emerged as a powerful methodology that quantifies the interplay between transport phenomena and kinetics on a variety of scales and allows formulation



of quantitative models for various measures of reactor performance such as reaction rate, conversion and selectivity. The ability to establish such quantitative links between measures of reactor performance and input and operating variables is essential in optimizing the operating conditions in manufacturing, for proper reactor selection in design and scale-up, and in correct interpretation of data.

The aim of this thesis was to investigate in detail the catalysis, mechanism, kinetics and reaction engineering aspects of complex multiphase reactions like liquid phase oxidation and hydroformylation. Hence the focus of this chapter is a detailed survey of the relevant literature of multiphase catalytic reactions with reference to catalysis and kinetics of the reported homogeneous and heterogeneous catalysts for these two industrially important chemical reactions.

## **1.2. Multiphase Catalytic Reactions**

Multiphase catalytic reactions have played an important role in the development of new processes for pharmaceuticals, fine chemicals and specialties. Multiphase catalytic processes have been expanding into diverse areas of applications and continue to make a significant impact on the development of new synthetic routes and high-value products. Conventional technologies for pharmaceuticals and fine chemicals were largely chemistry intensive with a focus on quality assurance and overall productivity. Due to the high cost of these products, the processes were commercially feasible even with lower yields so that issues related to reactor design and environmental needs were considered in low priority. However, the stoichiometric synthetic routes used in pharmaceuticals have several drawbacks, such as generation of waste products consisting of inorganic salts, and use of toxic and corrosive reagents or raw materials with significant safety issues. In recent years, increasingly stringent environmental regulations and societal awareness of safety aspects, coupled with increasing competition, have led to innovations in new processes that are largely based on multiphase catalysis. Therefore, analysis of reactor systems for fine chemicals and pharmaceuticals has gained considerable attention in the recent years. For example, catalytic reactions involving hydrogenation, oxidation, carbonylation, hydroformylation, epoxidation, and amination are extensively used in defining novel synthetic routes with significant economic advantages for pharmaceutical

products<sup>21,22</sup>. Classification of multiphase reaction processes for pharmaceuticals, specialty and fine chemicals can generally be done using two methods: (1) classification based upon the mode of utility of the reactants and the type of phases involved, such as gas-liquid, gas-liquid-solid, liquid-solid, gas-liquid-liquid and gas-liquid-liquid-solid reactions and (2) classification depending on the process chemistry or type of catalysis involved. The first method is more convenient for analysis of reactor design issues, while the second method is more useful for describing the process routes, since each of the examples will belong to one of the categories in (1). In either case, the final applications of these multiphase processes occur in the manufacturing of products for agrochemicals, pharmaceuticals, detergents, dyestuffs, perfumery and fragrances, feed additives, flavors and food products, polymers, textiles and synthetic fibers. Hydroformylation, oxidation, epoxidation, hydrogenation, carbonylation, oxidative carbonylation and amination are some of the most important examples of multiphase catalytic reactions (Table 1.1).

**Table 1.1.** Applications of multiphase catalytic reactions

| Sr. | Reaction   | Catalyst                 | Product  | Type  | Reference |
|-----|--|--------------------------|--|-------|-----------|
| 1   | Oxidation of <i>p</i> - <i>t</i> -butyl toluene  | Co complex - Br promoted | <i>p</i> - <i>t</i> -Butylbenzaldehyde (fine chemicals and perfumery)        | G-L   | 23        |
| 2   | Hydrogenation of adiponitrile                    | Raney Ni                 | Hexamethylene diamine (HMDA) intermediate for Nylon 6,6(specialty chemicals) | G-L-S | 24,25     |
| 3   | Epoxidation of styrene followed by isomerization | Ti-silicate (TS-1)       | Phenylacetaldehyde (fine chemicals)  | L-S   | 26        |
| 4   | Oxidation of glucose                             | Pd-Bi/C                  | Gluconic acid (food, detergents and pharmaceuticals)                         | G-L-S | 27,28     |
| 5   | Oxidation of indole to indigo                    | Cumyl hydroperoxide      | Indigo - a dye stuff   | G-L   | 29        |
| 6   | Hydrogenation of 2,4-dinitrotoluene              | Pd/alumina or Raney Ni   | Toluenediamine - an intermediate for TDI (free chemicals)                    | G-L-S | 30        |
| 7   | Reductive amination of 4-chloroacetylcatechol    | Pd/support               | Adrenaline - a drug (pharmaceuticals)  | G-L-S | 31        |

|    |   |  |   |       |    |
|----|---|--|---|-------|----|
| 8  | Hydrogenation of glucose  | Raney Ni                                     | Sorbitol (pharmaceuticals)  | G-L-S | 32 |
| 9  | Hydroformylation of higher olefins  | $\text{HCo}(\text{CO})_3\text{PBu}_3$        | Oxo alcohols  | G-L   | 33 |
| 10 | Acylation of substituted benzenes with carboxylic acids                                       | Ce-Y or HZSM-5                               | Aromatic ketones (substituted) (fine chemicals)   | L-S   | 34 |
| 11 | Hydroformylation of Ethylene oxide  | $\text{Co}_2(\text{CO})_8$                   | 2-hydroxy propanal  |       | 35 |
| 12 | Condensation of isophytol with 2,3,5-trimethyl hydroquinone                                   | Heteropolyacids PW/SiW                       | $\alpha$ -Tocopherol (vitamin E) (pharmaceuticals)  | G-L-S | 36 |
| 13 | Hydrocyanation of bicyclo(2,2,1)-5-heptene-2-carboniwile followed by hydrogenation            | $\text{Ni}(\text{OPh})_4\text{-ZnClE-OPh}_3$ | Diaminomethylnorbonone (NBDA) - hardener for epoxy resin (fine chemicals)                                   | G-L   | 37 |
| 14 | Oxidation of ethylene   | $\text{PdCl}_2/\text{CuCl}_2$                | Acetaldehyde  | G-L   | 38 |
| 15 | Oxidation of p-xylene   | Co/Mn-salts                                  | Terephthalic acid/ester   | G-L   | 39 |
| 16 | Hydrodesulfurization of o-aminobenzyl sulfides, 2-methyl (trimethyl-6-trifluoromethylaniline) | Co-molybdate on $\text{Al}_2\text{O}_3$      | 2-Methyl-6-trifluoromethyl aniline (MTMA) - a pre-emergent herbicide intermediate (specialty agrochemicals) | G-L-S | 40 |

Multiphase catalytic reactions would always involve reaction engineering issues, such as complexities of chemistry, kinetics, transport effects, energy management, mixing of fluid phases, and modes of operation. Although, it is not always feasible to develop a predictive reactor performance model in each case, a detailed analysis of reaction engineering aspects would certainly be useful in identification of critical design factors. The new design for gas–liquid–liquid reactors and the relevant mass transfer and hydrodynamic data is most essential to understand the design and scale-up of these emerging technologies in chemical process industries.

The need of catalytic technologies, for conversion of cheaper feedstock to industrially important products is the need of future. New routes for fine chemicals, pharmaceuticals and specialties, removal of pollutants, waste minimization and global supply and preservation of energy are the most important requirements. These objectives can be achieved by catalytic routes. Liquid Phase Oxidation (LPO) and hydroformylation are the most prominent examples of multiphase catalytic reactions in industry. These reactions have been employed for the synthesis of a variety of industrial products such as aldehydes, ketones, alcohols, carboxylic acids etc, few of which having industrial and academic importance are studied in detail for their catalytic and engineering aspects in this thesis.

### **1.3. Oxidation Reaction**

Catalytic oxidation is the single most important technology for the conversion of hydrocarbon feedstocks (olefins, alkanes and aromatics) to industrially important oxygenated derivatives<sup>41</sup>. The success of catalytic oxidation depends on metal catalysts to promote rates of reaction and selectivity to partial oxidation products. Liquid phase and gas phase oxidations, using homogeneous and heterogeneous catalyst are practiced in industry. Some of the well-known examples of liquid phase oxidation in industry are oxidation of *p*-xylene to terephthalic acid, cyclohexane to adipic acid, *n*-butane to acetic acid and higher homologues and ethylene to acetaldehyde, oxidation of butadiene to 2,4-diacetoxybutene, epoxidation of propylene to propylene oxide, and hydroxylation of phenol to hydroquinone and catechol using H<sub>2</sub>O<sub>2</sub> as oxygen donor<sup>42</sup>. Traditionally, in fine chemicals industry, the use of stoichiometric quantities of classical inorganic oxidants

such as potassium dichromate and potassium permanganate were more, which are not acceptable from environmental view point. Because much smaller production volumes are involved, there was much less pressure in the past to replace such environmentally unacceptable technologies. Nevertheless, the amount of by-products (largely inorganic salts) per kilogram of product is generally much larger in fine chemicals and specialties<sup>43</sup>. The substantial increase in waste generation is partly due to the fact that the production of fine chemicals and specialties generally involve multi-step synthesis and partly to the widespread use of stoichiometric rather than catalytic technologies. Consequently, the fine chemical industry is being subjected to increasing environmental pressure. One motivation in developing liquid phase catalytic oxidation processes is also due to increasingly stringent government regulations concerning emission of organic and inorganic wastes and related environmental problems. The older generation of oxidation processes was based on classical stoichiometric oxidants such as dichromate, permanganate, manganese dioxide and nitric acid, which are not accepted from environmental considerations as they produce large quantities of waste materials and employ toxic reagents. Catalytic liquid phase oxidation has played a vital role in providing alternative to these stoichiometric reagent based processes with minimal amount of undesired by-products.

In choosing suitable methodology for oxidation of particular organic substrate<sup>44</sup>, there are various options as shown in the Figure 1.1. Each methodology has its advantages and disadvantages. In these, liquid phase oxidation expands the scope of catalytic oxidation to non volatile and thermally sensitive substrates and products. Higher heat capacity of the liquid phase facilitates temperature control of the exothermic reaction and avoids the formation of hot spots and temperature run away. Liquid phase oxidation requires less temperature and hence advantageous for energy saving and safe operations. Also, oxidants like  $H_2O_2$  and hydroperoxide can be safely used in liquid phase oxidation. So depending on requirement, there is a choice of oxidants.

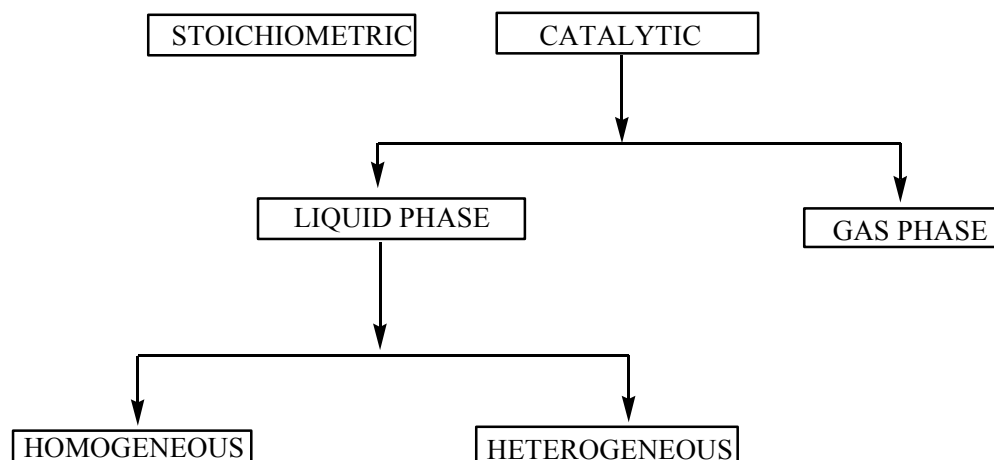


**Figure 1.1.** Process options in oxidation reaction

### 1.3.1. Hydrocarbon Oxidation

Liquid-phase air oxidation of hydrocarbons, notably oxidation of *p*-xylene to terephthalic acid and dimethyl terephthalate, cyclohexane to cyclohexyl hydroperoxide and cyclohexanol/cyclohexanone, cumene to cumene hydroperoxide, toluene to benzaldehyde, ethylbenzene to acetophenone, iso-butane to *tert*-butyl hydroperoxide and *tert*-butyl alcohol, is of great scientific, technological, and commercial importance<sup>45</sup>. Oxidative transformations of functional groups are basic to organic chemistry and are used extensively in the laboratory and industrial synthesis of a variety of fine organic chemicals. Some of the major inefficiencies in the production of such chemicals can often be traced to the operation of the reactor. The study also lacks in the detailed understanding of the mechanism, kinetics and reaction engineering aspects of such important class of reaction. It is therefore not surprising that this class of reactions has spawned much study and research.

The major developments in hydrocarbon oxidations have most often been motivated by the need for appropriate feedstocks for the evergrowing polymer industry. From early days, the functionalization of naturally occurring petroleum components through reaction with air was naturally seen as the simplest way to derive useful

chemicals. Industrial practice also developed alongside with vapour phase oxidation being the prime focus.

Liquid phase oxidation processes began from the 1950s. The Wacker process for the conversion of terminal olefins to carbonyl compounds and the Hock process for the production of phenol from cumene (via the hydroperoxide) were commercialized during this period. The cumene-phenol process was developed, by Distillers Co. in the U.K. and Hercules Powder Co. in the U.S., from a reaction discovered by Hock and Lang during the war<sup>46,47</sup>. At that time, the free-radical chemistry of such reactions was establishing. Several major contributions to that field, such as the concept of activation of a tertiary C atom by a phenyl ring (which leads to the specificity of oxidation in this process) and an understanding of the role of impurities, came during the process development effort. Several developments of an engineering nature also played a part in the final commercialization, such as the improvement in rate and selectivity through staging of reactors and the imposition of a temperature profile (with the temperature decreasing as the hydroperoxide concentration increases) on the reactor cascade.

The discovery of the “Mid-Century” catalysts and the subsequent development of the Mid-Century (MC) process for the oxidation of *p*-xylene to terephthalic acid belong to this period. The impetus for the discovery of the Mid-Century catalyst was provided by the need for a cheap source of aromatic acids for the industrial production of aromatic polyesters, in particular, poly(ethylene terephthalate) (PET)<sup>48</sup>. In searching for an alternative to esterification (Witten process of 1951) for overcoming the inhibiting effect of the first carboxyl group on further oxidation, Landau and co-workers at Scientific design discovered the promoting effect of the bromide anion<sup>13</sup> and immediately obtained qualitative improvements in yield over the norm using cobalt catalyst alone and then further and proceeded to develop the oxidation technology<sup>49</sup>. Landau has recently given a fascinating account of this development. In the subsequent decades, many aspects of the action of Mid-Century catalysts have been clarified, and the principle has been extended to over 200 other aromatic, alkylaromatic, and other systems. In particular, improvements in the technology for purification have today put Pure Terephthalic Acid (PTA) in a dominant position in the world market as the preferred raw material for PET fiber.



A broad survey of the commercially important processes employing liquid-phase hydrocarbon oxidation is presented in Table 1.2. The production volumes of the chemicals listed is high, and reflects the importance of liquid-phase oxidation in industry. It is interesting to note the different roles of the oxidation step in these processes. In some of the processes, such as the Amoco process for the manufacture of PTA, the oxidation step leads directly to the product of interest<sup>49</sup>. There are others, such as the process for caprolactam, in which oxidation is the step that produces a key intermediate that is then further processed to the product of interest. In the oxirane process, hydrocarbon oxidation provides a convenient carrier of oxygen for the selective oxidation of propylene to propylene oxide<sup>50</sup>. A choice of hydrocarbons is therefore available<sup>51</sup>, and the market for the coproduct determines which hydrocarbon is chosen in a given context. Although treatises on hydrocarbon oxidations underline the similarities that exist in the mechanisms that govern various organic oxidations, from an engineering point of view, it is the differences that exist between hydrocarbons that are often of interest; these differences call for innovative technological developments. In the manufacturing of terephthalic acid, the product of interest forms fairly late in the reaction sequence, and, considering its resistance to oxidation, it may in fact be considered as the end product. In a majority of situations however, the desired product is an intermediate; susceptible to further oxidation, and selectivity considerations become extremely important like in toluenes oxidation, benzaldehydes overoxidizes to carboxylic acid. Synthesis of benzaldehyde selectively is the major challenge involved.

In many hydrocarbon oxidations, the desired intermediates have a tendency to undergo further reactions in the oxidizing medium. The limitation imposed by the chemistry on the selectivity to the desired intermediates that is achieved has often meant that conversions are kept low to minimize the formation of unwanted products. The need to achieve better selectivity at reasonable conversions has naturally been a major driving force for research. In reactions of complex molecules, the concepts of chemoselectivity (competing reactions at different functional groups), regioselectivity (e.g. *ortho* vs. *para* substitution in aromatics) and stereoselectivity (enantio- or diastereoselectivity ) are commonly used. However, one category of selectivity is completely ignored by organic

chemists i.e. atom selectivity or atom utilization. The atom utilization concept is a useful tool for quickly evaluating the amount of waste produced by alternative processes.

Appropriate choice of reaction conditions for higher conversion and selectivity is a major problem area and a lot of scope exists for technology development. The reaction conditions are very harsh with respect to temperature, pressure etc which needs detailed experimntaion and understanding. Some of the process parameters of the existing industrial process are given in Table 1.3. The thesis investigates some of the important aspects of this problem and validates the results on a laboratory scale reactor for few important oxidation reactions like liquid phase catalytic oxidation of toluene and ethylbenzene. Below, a detailed literature survey for these reactions is presented.

**Table 1.2.** Major Chemical Processes Utilizing Hydrocarbon Oxidation <sup>52,49,53</sup>

| <b>Product</b>                   | <b>Capacity<br/>10<sup>6</sup> tpy</b> | <b>Oxidation step</b>  | <b>Important<br/>Processes</b>                                 | <b>Main<br/>Application</b>              | <b>Remarks</b>  |
|----------------------------------|--|--|--|--|---|
| Purified terephthalic Acid (PTA) | 11.38                                  | <i>p</i> -xylene to terephthalic acid  | Amoco<br>Mid-Century   | PET<br>(fiber, film,<br>resin)           | Applies also to other alkylaromatics such as <i>m</i> -xylene, pseudocumene, 2,6-dimethylnaphthalene  |
| Dimethyl terephthalate (DMT)     | 4.06                                   | <i>p</i> -xylene to <i>p</i> -toluic acid and monomethyl ester of pTA to DMT | Witten, BASF,<br>DuPont  | PET<br>(fiber, film,<br>resin)           | Two-step process or one-step process  |
| Benzoic acid                     | 0.28                                   | Toluene to benzoic acid  | DSM, Dow   | Phenol and salts, esters of benzoic acid | Coproduct: acetone also applies to cresols, resorcinol/hydroquinone from cymenes, diisopropylbenzenes |
| Caprolactam                      | 3.7                                    | cyclohexane to KA  | BASF, Bayer,<br>DuPont, DSM,<br>Stamicarbon<br>Scientific Des. | Nylon-6<br>(Perlon)                      | Also employed in the Snia-Viscosa route to caprolactam and Henkl route to TA                          |

|                    |              |   |   |  |  |
|--------------------|--------------|---|---|--|--|
| Adipic acid        | 2.2          | Cyclohexane to cyclohexanone/<br>cyclohexanol (KA)<br>and KA to adipic acid | BASF, Bayer,<br>Dupont,<br>Stamicarbon<br>Scientific Des. | nylon-6,6  | K:A ratio depends on<br>use of boric acid  |
| Propylene<br>oxide | 4            | <i>iso</i> -butane to TBHP  | Oxirane   | propylene<br>glycol,<br>polyols<br>styrene               | Coproduct: <i>tert</i> -butyl<br>alcohol<br>(gasoline additive)<br>phenyl methyl carbinol<br>(dehydrated to styrene) |
| Acetic acid        | 6.0 <i>b</i> | Ethylbenzene to<br>hydroperoxide<br>butane/naphtha                          | Celanese,<br>BP, UCC                                      | Vinyl acetate,<br>cellulose<br>acetate,<br>PTA, solvent. | Main route is via<br>carbonylation<br>of methanol  |

**Table 1.3.** Some Important Process Parameters in the Commercially Important Oxidations

| Sr. | Hydrocarbon                     | Desired Product                   | Reaction Conditions |              |                            |            |            | Process  |
|-----|---------------------------------|-----------------------------------|---------------------|--------------|----------------------------|------------|------------|--|
|     |                                 |                                   | Temp., °C           | Pressure bar | Catalyst                   | Conv., %   | Sele., %   |  |
| 1   | <i>p</i> -xylene                | PTA                               | 190-205             | 15-30        | MC Catalyst                | 95%        | >90%       | Amoco process                                  |
| 2   | <i>p</i> -xylene                | <i>p</i> -toluic acid <i>p</i> TA | 140-170             | 4-8          | Co and Mn salts            |            |            | Witten process                                 |
| 3   | Monomethyl ester of <i>p</i> TA | DMT                               | 140-240             | 40           | <i>p</i> TSA or other acid |            | 85%        | Witten process                                 |
| 8   | <i>iso</i> -butane              | TBHP                              | 120-140             | 35           | initiator                  | 25%        | 60%        | Oxirane  |
| 9   | Ethylbenzene                    | EBHP                              | 120-140<br>110-120  | 35<br>2-3    | initiator<br>Co salts      | 15-17%     | 87%<br>90% | Oxirane<br>Dow                                 |
| 10  | Toluene                         | benzoic acid                      | 165                 | 9            | Co acetate<br>MC cata      | 99%<br>99% | 90%<br>96% | Snia iscosa<br>caprolactam<br>process<br>Amoco |

### 1.3.1.1. Selective Liquid Phase Oxidation of Toluenes to Benzaldehydes

In the modern chemical industry, the liquid-phase oxidation of aromatic hydrocarbons by molecular oxygen is a very attractive process from an economic and environmental point of view<sup>54</sup>. A range of valuable oxygenated compounds can be produced by this process. For example, benzaldehyde and benzoic acid can be produced from toluene and *p*-toluic acid and terephthalic acid from *p*-xylene. Aromatic aldehydes like benzaldehyde, chlorobenzaldehyde, fluorobenzaldehyde etc. are FDA approved synthetic flavoring substances and have extensive applications in food, pharmaceutical, dye, agricultural and perfumery industries<sup>55</sup>. Particularly, benzaldehyde is the most important aromatic aldehyde concerning industrial applications, and has a wide range of application from food and pharmaceuticals to perfumery industry<sup>56,57</sup>. Conventionally benzaldehydes have been synthesized by chlorination of toluenes to give benzyl chloride, which after hydrolysis gives benzaldehydes. From an industrial viewpoint, chlorination method suffers from disadvantages like high production cost, large amount of polluting residues, formation of byproducts, and troublesome product purification; besides the use of toxic chlorine and associated corrosion problems. However, for the production of benzaldehydes, particularly for the grade conforming to perfumery and pharmaceutical applications that require chlorine free products, the vapour phase oxidation of toluenes is an obvious alternative route. However, in the vapour phase oxidation of toluenes, the lower value carboxylic acids are formed as major products and benzaldehyde is only a minor product.<sup>58,59</sup> From the literature, it is also evident that, in vapour phase oxidation, the reaction conditions are too stringent; with temperatures in the range of >773K and pressures in the range of 0.5-2.5 MPa, to achieve an optimum selectivity (~25) to benzaldehyde<sup>60,61</sup>. The major disadvantage is the recovery of the toluene from toluene-air mixture, owing to low concentration of toluene in the toluene-air feed<sup>62,63</sup>. The major challenge is to avoid the formation of benzoic acid and the loss of carbon in the form of gaseous products such as CO and CO<sub>2</sub><sup>64,65,66</sup> which is highly undesirable and adversely affects atom economy. The liquid phase oxidation of toluene with homogeneous metal salt catalysts was industrially realized in the Rhodia<sup>67</sup>, Dow<sup>68</sup> and Snia-Viscosa<sup>69</sup> processes using oxygen or peroxides as oxidants. For example, the Snia-Viscosa process operates at 165<sup>0</sup>C and under 10 atm of air in the presence of a homogeneous cobalt

catalyst in acetic acid. At the optimal conditions, benzoic acid as the target product is produced with 90% selectivity, and benzaldehyde as a minor byproduct is obtained in 3% selectivity at 15% conversion of toluene. In these processes, however, halogen ions and acidic solvents are unavoidable, and they easily cause erosion. The formation of benzoic acid via toluene oxidation was also reported in supercritical CO<sub>2</sub> and ionic liquids as solvents<sup>70,71</sup>. In the latter report, the maximum conversion of toluene was only 4.7% after 48 h. Hence, the recent interests are increasing in the development of an efficient and selective catalytic system for the liquid phase air oxidation of toluenes to benzaldehydes at milder reaction conditions.

The liquid phase catalytic oxidation of toluene to benzaldehyde has major advantages in avoiding the use of hazardous and toxic chlorine, mineral acids and improving the overall process economics as well as the product quality. In most of the reported literature,<sup>72,73,74</sup> the catalyst systems used for this reaction contain mainly cobalt catalyst. Extensive work has been done on cobalt based catalyst system along with different co-catalyst and promoter. Recently Can-Cheng Guo *et al*<sup>75</sup> have reported toluene oxidation by the use of cobalt tetraphenylporphyrin as catalyst has also reported but the reaction conditions are harsh (temperature ~170<sup>0</sup>C) and also selectivity to benzaldehyde ~ 30 for ~ 8% conversion of toluene. Few other catalysts like Mo, Cu, Mn, Zn etc are also reported for the liquid phase oxidation of toluenes<sup>76,77</sup>. Salts of cobalt along with bromide are highly active catalysts for oxidation of methyl benzenes in acetic acid media, which yield the corresponding carboxylic acids as the major product e.g. toluene to benzoic acid<sup>78,79</sup>. Moreover, as the conversion increases, selectivity to aldehydes is further lowered. In MC-type catalyst systems with acidic solvents like acetic acid, benzoic acid and propionic acid, the aldehyde formed is usually over-oxidized to the aromatic acid, thus reducing the aldehyde selectivity<sup>80,81</sup>. Formation of benzyl alcohol and a side reaction of equilibrium esterification of benzyl alcohol to benzyl acetate in presence of acetic acid solvent was observed, which reduces the selectivity to benzaldehyde. Thus, during liquid phase oxidation of toluene, benzyl acetate, and benzoic acid were formed as byproducts along with benzyl alcohol and benzaldehyde. Recent developments show significant improvement in benzaldehyde selectively with the incorporation of metal salts like Mn, Cr, Ni, Mo etc, which are weaker than cobalt.

As temperature of the reaction is a critical factor in oxidation reaction, at higher temperature the formation of byproducts increases due to over oxidation and the formation of CO and CO<sub>2</sub> is observed, thus reducing the selectivity and atom economy. Few attempts have been made for low temperature liquid phase oxidation of toluene using Zn, Cu, Al-layered double hydroxide with hydrogen peroxide as the oxidant<sup>82</sup> using different radical generator, marginal increase in the selectivity of aldehyde was observed.

The use of promoters in the oxidation can increase the reaction rate and improve selectivity to the aldehyde product. Borgaonkar *et al*<sup>62</sup>. have reported paraldehyde as a promoter which, however, results in higher benzoic acid formation<sup>74</sup>. In conventional homogeneous oxidation cobalt, manganese, and bromine ions serve as promoters. Co/Mn/Br is highly active and selective catalyst system for liquid phase oxidation of toluene. Synergistic of addition of salts of Mn to benzaldehyde selectivity and conversion of toluene has been reported by Kantam *et al*<sup>81</sup>. Recently, MnCO<sub>3</sub> catalyzed liquid phase oxidation of toluene has been reported, however the conversion (6%) is poor with moderate selectivity (41.7%) to benzaldehyde.<sup>83</sup> Some of the important literature reports are tabulated in Table 1.4. Also, heterogeneous promoters containing Mn for the oxidation of aromatics have attracted increasing attention due to their practicability and relatively high activity. For example, amorphous, microporous Mn/Si mixed oxide, Mn (III) complexes of Salen, and Mn-layered double hydroxides (LDHs) have been used in the oxidation of aromatic hydrocarbons. However, these promoters were generally prepared in a multi-step process and combined with a particular oxidant, e.g. H<sub>2</sub>O<sub>2</sub> or TBHP. Therefore, it is necessary to develop an active, reusable, and easily prepared active Mn promoter for the oxidation of aromatic hydrocarbons with molecular oxygen as oxidant, which is one of the motivation of investigating in the thesis.



**Table 1.4.** Liquid phase oxidation of toluenes

| Sr. | Catalyst   | Temp.,<br>K | Activity |                 | Reference |
|-----|--|-------------|----------|-----------------|-----------|
|     |  |             | Conv.,%  | Ald. Sel.,<br>% |           |
| 1   | Co-Mn-Br   | 100-140     | 12-16    | 25-35           | 81        |
| 2   | Co-Br  | 100-140     | 13-20    | 35-42           | 84        |
| 3   | MnCO <sub>3</sub>  | 190         | 17-26    | 8-28.3          | 85        |
| 4   | Fe,Cu,Mn zn, supported on Al <sub>2</sub> O <sub>3</sub> | 190         | 5-26     | 12-74           | 86        |
| 5   | Co(Oac) <sub>2</sub> /NaBr/AIBN                          | 110-150     | 30-36    | 5-10            | 87        |
| 6   | cobalt tetraphenylporphyrin                              | 150-180     | 6-15     | 28-35           | 88        |
| 7   | Co/MTiO <sub>2</sub>                                     | 90-110      | 20-45    | 78-99           | 89        |
| 8   | Co(OAc) <sub>2</sub> /MnSO                               | 70-106      | 10-25    | 45-75           | 90        |
| 9   | Cu/APO-5   | 60          | 10-27    | 25-30           | 91        |
| 10  | Co-Br  | 100-130     | 12-30    | 70-90           | 62        |
| 11  | Co-Mn-Br   | 80-160      | 10-30    | 25-40           | 80        |
| 12  | bromide  | 110-130     | 10-36    | 10-27           | 92        |
| 13  | vanadium(V) polyoxometalates                             | 25          | 6-32     | 12-38           | 76        |
| 14  | vanadium containing catalyst                             | 70-150      | 13-45    | 60-80           | 93        |
| 15  | Mn-Lewsi acid-Br   | 90-130      | 9-30     | 55-76           | 94        |

### 1.3.1.2. Selective Liquid Phase Oxidation of Side Chain Alkyl benzenes

Aromatic ketones are of significant importance in synthetic chemistry. For example, acetophenone (Acph) is an important intermediate in perfumery, drug and pharmaceutical industry. The industrial synthesis of aromatic ketones involves the Friedel-Craft's acylation of aromatic compounds by acid halide or acid anhydride, using stoichiometric amounts of anhydrous aluminium chloride or homogeneous acid catalysts, leading to formation of large volumes of highly toxic and corrosive wastes.<sup>95,96</sup> In the past extensive work has been done to synthesize the aromatic ketones by oxidizing the methyl group attached to an aromatic ring using stoichiometric amount of oxidizing agents like  $\text{KMnO}_4$ . A few illustrations of this kind of oxidations are the oxidation of diphenylmethane to benzophenone by  $\text{KMnO}_4$ ,  $\text{SeO}_2$  or  $\text{CrO}_3\text{-SiO}_2$ <sup>97,98</sup> and the oxidation of alkylarenes by  $\text{KMnO}_4$  supported on Mont-K<sup>99</sup>. These reactions produce large amounts of salt waste, and also, the separation and isolation of the products and unconverted substrate from the reaction mixture is difficult. Recently, there has been an increased interest in developing cleaner, economical catalytic processes for synthesizing value-added products like ketones by benzylic oxidation of alkylaromatics<sup>100</sup>

Acetophenone can also be produced by liquid phase air oxidation of ethylbenzene using soluble salts of Co, Mn, Cu or Fe as catalysts and using acetic acid as solvent<sup>101</sup>. Although the metal compounds used in these processes are in catalytic amounts, the reaction conditions are harsh; the ketone selectivity is poor, corrosive promoters like bromide ions are required along with the catalyst. Also the recovery and recycle of the catalyst is tedious and costly which becomes complicated due to formation of tarry compounds<sup>102</sup>. In industrial processes, the cost centre is obviously the metal catalyst used, which implies that the reactions to be carried out in a manner that simplifies the separation, isolation and reuse of the catalyst. Due to this fact, extensive research has been done in heterogenization and recovery of the catalyst, catalyst poisoning etc.

There has been an increased interest in developing eco-friendly catalyst systems for the oxidation of alkylaromatics. The oxidation of many organic substrates using  $\text{H}_2\text{O}_2$  as oxidant over  $\text{Ti}^{4+}$  analogues of ZSM-5 (TS-1) and ZSM-11 (TS-2) has been well-documented.<sup>103,104,105</sup> Titanium substituted silicates have been thought to catalyze ring hydroxylation of arenes with  $\text{H}_2\text{O}_2$ , but vanadium<sup>106</sup>, tin<sup>107</sup> and chromium<sup>108,109</sup>

substitution into a variety of zeolites and aluminophosphate molecular sieves has led to favored oxidation at the side-chain. The presence of molecular oxygen or single oxygen atom donors such as *tert*-butyl hydroperoxide (TBHP) for the oxidation of alkanes to alcohols and ketones are shown to be important<sup>110,111,112</sup>.

Oxidation using hydroperoxides is attracting great interest because of the fact that they yield the desired oxidation product with high selectivity under mild reaction conditions and generate easily separable co-products like water or aliphatic alcohols<sup>113</sup>. Among the various transition metal catalyst systems reported for ethylbenzene oxidation, the most effective ones are the heterogenized cobalt catalysts like cobalt-containing hexagonal mesoporous materials (Co-HMS) and cobalt-substituted silicate xerogels. Chromium substituted aluminophosphate catalysts are found to yield ketones with high selectivity from alkyl arenes with TBHP as oxidant<sup>114</sup>. Manganese analogues of these systems have also been shown to catalyze oxidation of alkanes using TBHP<sup>115</sup>. Scanty literature is available on kinetics and mechanistic studies in liquid phase oxidation of ethylbenzene using TBHP as oxidant. Most of the work has been done on the homogeneous and supported Co, Cu, Ni, V, Sn etc as catalyst using TBHP as oxidant for liquid phase oxidation of ethylbenzene (Table 1.5).

Layered double hydroxides (hydrotalcites) have received much attention because of their potential as bulk catalysts, catalyst supports, and ion exchangers. This is due to their ability to accommodate a large variety of bivalent and trivalent cations, the homogeneous mixture of the cations on an atomic scale, and the formation of thermo stable mixed oxides with a high surface area<sup>116</sup>. Transition metals, that are known to act as active catalysts can also be introduced in the brucite layer. Hydrotalcites containing metals like Ni, Cu, Co, Pd etc., have already been reported in the literature. Hydrotalcites with zirconium incorporated into the layers have been used for the selective oxidation of alcohols etc. The structural studies of hydrotalcites have shown that they are laminar structures consisting of positively charged brucite-type metal hydroxide layers with balancing anions and water molecules in the interlayer space, the most common and representative of this category being the Mg-Al hydrotalcite having the molecular formula  $Mg_3Al(OH)_8(CO_3)_{0.5} \cdot 2H_2O$ . Cavani *et al*<sup>116</sup>. have taken a detailed account of the catalytic activity of hydrotalcites (HT) and hydrotalcite like compounds (HTLcs) for

several chemical reactions<sup>116</sup>. Hydrotalcites are effective catalysts for isomerization, Aldol, Knoevengel and related condensations that are widely used in fine chemical synthesis. There few reports of oxidation of methylbenzenes using hydrotalcite like compounds using air as oxidant, where the rates of the reaction are very low. Literature lacks the detail study of oxidation of hydrotalcite using oxidants like TBHP, which is one of the motivations behind this study.

**Table 1.5.** Liquid phase oxidation of ethylbenzene

| Sr. | Catalyst                                       | Temp.,<br>K | Activity |   | Reference |
|-----|--|-------------|----------|---|-----------|
|     |  |             | Conv.,%  | Sel., %                                       |           |
| 1   | Mn-MCM-41                                      | 333         | 29.1     | PE =81.5, Acph=16.9,<br>Bzald=1.1, Other= 0.5 | 117       |
| 2   | Co-MCM 41                                      | 353         | 36.1     | Acph= 71, Bzald=18.2,<br>Bzacid= 9.5          | 118       |
| 3   | Cu(tacn) (ClO <sub>4</sub> ) <sub>2</sub>      | 333         | 49.6     | Acph= 91, Other= 5.9                          | 119       |
| 4   | Mn/Co/Ni                                       | 343         | 29.4     | PE =39.6, Acph=52.3,<br>Other= 6              | 120       |
| 5   | Cr-MCM-41                                      | 353         | 88       | Acph=85.3, Other= 13.5                        | 121       |
| 6   | Co-HMS   | 353         | 49.5     | Acph= 60, Bzald=25,<br>Bzacid= 15             | 122       |
| 7   | Mn complexes                                   | 313         | 13       | Acph= 51, PE=25.7, others=<br>25              | 123       |
| 8   | Mn(tacn) (ClO <sub>4</sub> ) <sub>2</sub>      | 313         | 27       | Acph= 57, PE=15.7, others=<br>28              | 124       |
| 9   | Zeolite encapsulated<br>Co(II), Ni(II), Cu(II) | 323         | 24       | Acph= 74, Others= 26                          | 125       |
| 10  | Iron complexes                                 | 303         | 16.8     | Acph= 70, PE=10.7,<br>Bzald=8, Bzacid= 9      | 126       |
| 11  | Cr exchanges ZSM-5                             | 353         | 21       | Acph= 85, PE=2.3,<br>Bzald=4.6, Bzacid= 2     | 127       |

### 1.3.2. Selective Liquid Phase Oxidation of Aldehydes

The oxidation of aldehydes to their corresponding carboxylic acids is one of the most common organic reactions in organic chemistry<sup>128</sup>. The oxidation products of aldehydes have wide range of applications in food, pharmaceuticals and fine chemical industries. Particularly oxidation of substituted aldehydes to carboxylic acid is of increasing interest due to its importance in pharmaceutical industry. In addition to numerous versatile methods for the oxidation of aldehydes, more convenient methods such as Baeyer–Villiger oxidation<sup>129</sup>, Cannizzaro reaction<sup>130</sup>, and metal catalyzed oxidation have been reported. Aldehydes are prone to oxidation; they oxidize very easily with the oxidants like chromic acid, potassium dichromate, vanadium oxide etc. The conventional methods for the oxidation of aldehydes employ a) Chemical oxidation involving oxidants like chromic acid b) biochemical oxidation using enzymes. c) Electrochemical oxidation. d) Non-catalytic oxidation by using molecular oxygen e) Catalytic oxidation using homogeneous and heterogeneous catalyst<sup>131</sup>.

Despite the growing awareness of the need for ‘green chemistry’, many chemists still use environmentally unacceptable reagents or unnecessarily sophisticated conditions for the oxidation of aldehydes<sup>132,133,134</sup>. Several literature references quote oxidation of aldehydes to carboxylic acids using molecular oxygen as oxidant in acidic solvents like acetic acid, peracetic acid, butyric acid etc.<sup>135,136</sup> Majority of the available literature on aldehyde oxidation is on reagent-assisted oxidation of aldehydes. From the literature it appears that non noble metal catalysts have been studied for the liquid phase oxidation of aldehydes. Oxidation of aromatic and aliphatic aldehydes to corresponding acids have been studied by Bhatia *et al.* by using cobalt chloride as a catalyst in presence of acetic anhydride and yields in the range of 41% to 80%. Choi *et al.*<sup>140</sup> have reported benzeneseleninic acid catalyzed oxidation of aldehydes to corresponding acids with 80% to 98 % yield at room temperature, using hydrogen peroxide as an oxidant<sup>137</sup>. Springer and Dinslaken have reported non-catalytic oxidation of aliphatic aldehydes with oxygen in pure or mixture forms with excellent yields of corresponding carboxylic acid. From the literature it is observed that transition metal catalysts like Mn, Co, Cu, Fe etc have been used for the oxidation of aldehydes to corresponding acids with conversions in the range of 85% to 95% and the selectivity more than 90% to corresponding carboxylic

acid<sup>138,139,132</sup>. Major work has been done on the homogeneous catalyst i.e. salts of transition metals, which are soluble in reaction phase and acidic solvents. Few authors have reported metal-based catalyst system and inorganic or organic promoters for the efficient oxidation of aldehydes using the more acceptable 'green' oxidants like H<sub>2</sub>O<sub>2</sub>, TBHP etc in acidic solvents<sup>140</sup>. The use of such acidic solvents implies corrosion and safety hazards, besides the generation of salts, which usually have to be land filled. Some of the prominent literature report are given in Table 1.6.

The use of soluble catalysts, which leads to separation problems, and the corrosive acidic solvents, are major shortcomings of this process. Besides this, the isolation and purification of the products are the major issues, mainly because of the applications of the products are in food and pharmaceutical industry. While a number of catalytic systems need to investigate, a detailed study on the role of promoters, catalyst preparation methods, and supports has not been investigated. Similarly the information of kinetic modeling and reactor performance study has been very rare. So to understand the catalysis and reaction engineering aspects of aldehydes oxidation of 2-acetoxy propionaldehyde has been investigated in details using 2-acetoxypropanal, 3 acetoxy propanal and 2-MNP as substarte.

**Table 1.6.** Liquid phase oxidation of aldehydes

| Sr. | Catalyst  | Temperature, °C | Other details (Solvent / Substrate)  | Conversion/ Yield | Selectivity, % | Reference |
|-----|---|-----------------|--|-------------------|----------------|-----------|
| 1   | Cobalt acetate  | 130             | Acetic acid as solvent veratraldehyde  | 100               | 99             | 141       |
| 2   | CeO <sub>2</sub> -Ru  | 140-160         | Toluene as solvent,<br>Benzaldehyde, octaldehyde                                       | 60-70             | 83 – 95        | 142       |
| 3   | Cobalt H-form resin   | 20-22           | Heptaldehyde in bubble column<br>reactor   | 50-70             | 82-90          | 143       |
| 4   | Cobalt (II) chloride  | 25              | Acetic unhydride used, benzaldehyde,<br>octaldehyde, propionaldehyde,<br>butyraldehyde | 40-60             | 80- 93         | 144       |
| 5   | Au/C, Pt/C  | 90              | Water as solvent,<br>Propanal  | 85-93             | 86-92          | 145       |
|     | Co(II) heteropolyacid   | 30              | 2-Phenyl acetaldehyde,<br>isobutyraldehyde   | 54                | 76             | 146       |
| 6   | CoTBCOPP  | 30              | Acetic acid/ acetone as solvent <i>p</i> -<br>chlorobenzaldehyde, benzaldehyde         | 85-93             | 92-95          | 147       |
| 7   | NaC102-HzOzn  | 60              | furan-2-carboxaldehyde<br>15 thiophene- 2-carboxaldehyde                               | 93-96             | -              | 148       |
| 8   | ebsele  | 75              | H <sub>2</sub> O <sub>2</sub> , Aromatic aldehydes                                     | 95-100            | 95-98          | 149       |
| 9   | [CH <sub>3</sub> ( <i>n</i> -<br>C <sub>8</sub> H <sub>17</sub> ) <sub>3</sub> N]HSO <sub>4</sub> |                 | H <sub>2</sub> O <sub>2</sub> , Aromatic aldehydes                                     | 80-90             | 95-98          | 150       |

|    |  |    |   |       |       |     |
|----|--|----|---|-------|-------|-----|
| 10 | Pd/C and NaBH <sub>4</sub> ,<br>KOH                  | 30 | Methanol as solvent, Aromatic<br>aldehyde         | 86-90 | 93-97 | 151 |
| 11 | TBA <sub>4</sub> HPW <sub>11</sub> CoO <sub>39</sub> | 20 | Acetonitrile as solvent,<br>isobutyraldehyde      | 92    | 78-82 | 152 |
| 12 | Cu, Ni and iPrCHO                                    | 25 | Alcohol as solvent, methoxy aromatic<br>aldehydes | 92    | 85-94 | 153 |



### 1.3.3. Kinetics of Catalytic Reactions

The basic objective of the chemical reaction engineering is to model the reaction/process occurring in the chemical reactor as accurately as possible. It is generally divided into two sub groups i.e. reaction kinetics and heat and mass transport. Catalytic reactions are complex, involving reactions in series and parallel which, in most reaction engineering models are taken into account in complex rate equations.

Kinetic modeling of catalytic reactions is one of the key aspects investigated in order to understand the rate behavior of catalytic reactions as well as reaction mechanism. Knowledge of intrinsic reaction kinetics (a scale independent property) and development of rate equations is most essential for reactor design. While the subject of kinetic modeling has been well investigated for heterogeneous catalysis, only limited information is available on this aspect in homogeneous catalysis especially for kinetics of hydrocarbon oxidation reactions.

#### 1.3.3.1. Kinetics of Liquid Phase Oxidation

The determination of kinetics of liquid-phase organic oxidation presents a nontrivial problem. Over the years, reactor and process design aspects have received considerable attention. The models used in the early attempts were rather crude and did not pay adequate attention to the influence of mass transfer, and hence, process development usually involved extensive experimentation at different scales. The first attempt to explicitly acknowledge the role of mass transfer in organic oxidations was the work of Hobbs *et al.*<sup>154</sup>, in which the possibility of the reaction becoming mass transfer limited and the bulk becoming starved of oxygen was recognized. These authors made an attempt to explain certain experimental observations that could not be explained on the basis of considerations of chemistry alone by maintaining the role of mass transfer, even though in a qualitative manner.

Development of kinetic models for liquid phase oxidation systems using homogeneous catalyst has not received much attention from a reaction engineering perspective. However, reviews on the kinetics and mechanism from a chemical perspective are available in the literature<sup>155,156,157</sup>. Oxidation reaction generally involves

several products in reaction system, the quantitative analysis of which is a challenge. Considering the complex chemistry and mechanism of these reactions the detailed kinetic is usually not feasible<sup>158</sup>. An engineering and industrial approach to kinetics involving lump is usually followed which postulates the series and parallel network depending on the nature and requirement of the reaction. The possible influence of mass transfer on the observed behavior is considered carefully in the interpretation of the rate data because oxidation reactions are generally conducted using air or oxygen containing gas as oxidant. The theory of gas liquid reactions had made significant impact, starting with the work of Higbie in 1935, and hydrocarbon oxidations had been recognized as a major class of reactions of industrial significance falling within the scope of the theory applied to complex reactions with kinetics of the type encountered in organic oxidations. These attempts to bring hydrocarbon oxidations within the domain of the theories of mass transfer with chemical reaction, but could not get much success. In the last two or three decades, several studies have attempted to address these gaps, but much remains to be done.

The lack of data on the important mass transfer parameters in systems and under the conditions of temperature and pressure, where the industrial processes operate. Given the complexity of the chemistry involved in hydrocarbon oxidation, and the fact that one often must estimate the kinetics from rate data in heterogeneous (gas-liquid) systems, the planning and execution of laboratory studies to establish true kinetics is usually a demanding task. A growing appreciation for the interaction between physical transport phenomena and chemical kinetics in organic oxidations has led to an examination of the possibility of using oxygen-rich gases for oxidation. The issues of safe design and operation of oxidation reactors, always at the forefront due to the use of oxygen and oxygen containing gases, which needs innovative reactor design.

A recent trend in kinetic modeling involves a molecular level approach to the development of rate models. Evidence suggests that there is a close analogy between reaction mechanisms based upon adsorption and those based on molecular species through organometallic intermediate species. This aspect can allow better understanding of the kinetic trends in complex reactions, which are otherwise modeled using empirical approaches. A recent review on this subject is by Waugh<sup>159</sup>, though examples of the

molecular level approach for industrially important selective oxidation reactions are rare. This approach needs an independent study on the nature of catalytic sites and molecular species formed as intermediates. This might lead to a reaction scheme that can form the basis for deriving rate equations.

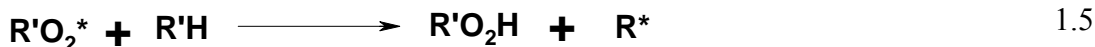
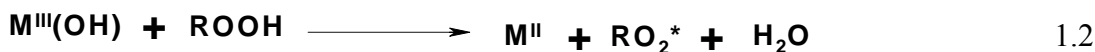
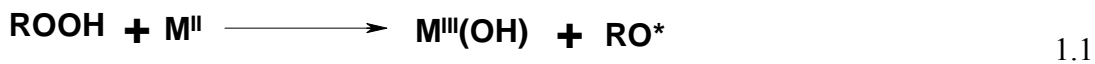
For many liquid-phase oxidation processes, detailed kinetic models that account for the formation of the various byproducts are still poorly understood. Moreover, the engineer must decide the level of detail at which he needs to investigate the kinetics of particular reaction to understand the particular phenomenon. Thus, the engineer is often forced to depend on the empirical approach to establish kinetics, with some basis from the known mechanisms.

#### **1.3.4. The Mechanism of Oxidation Reactions**

The chemistry of liquid-phase autoxidation of hydrocarbons, both catalyzed and uncatalyzed, has been the subject of several monographs and reviews<sup>160,161,162,163,164</sup>. According to Sheldon *et al*<sup>165</sup>, a detailed insight of the mechanism of oxidation reactions suggests that the mode of catalytic cycle depends on the 1) the metal catalyst employed, and 2) the oxidant used. MC type catalysts have been extensively investigated for their catalytic activity as well as mechanistic features in the oxidation of hydrocarbons in liquid phase. The mechanism of oxidation reaction, though complex, can be accounted in terms of two modes- one with molecular oxygen, as oxygen gas diluted with a neutral counterpart like nitrogen or as air; and the other with hydrogen peroxides or organic peroxides, both in aqueous or non-aqueous media.

##### **1.3.4.1. One-electron Oxidations with Oxygen/ Air as Oxidant**

One-electron oxidants, e.g. Co(III), Mn(III), Ce(IV), Fe(III), Cu(II), etc. catalyze free radical autoxidation processes by promoting the decomposition of alkyl hydroperoxides into chain initiating alkoxy and alkyl peroxy radicals in one electron transfer processes (reactions 1 and 2). Strictly speaking the metal ion acts as an initiator of free radical autoxidation, which proceeds via reactions, rather than a catalyst.



As evident from the literature, catalysts used in hydrocarbon oxidations mostly involve transition metals. Cobalt has been the most prominent among the transition metals used. According to Partenheimer<sup>166</sup>, cobalt performs at least three functions in the oxidation medium: (a) It quickly reacts with the primary peroxides via the Haber-Weiss cycle as in steps 1 and 2. (b) It acts as a radical initiating species when in the higher (+3) oxidation state (i.e., it generates R'· radicals from RH), thereby enhancing the rate by participating in the initiation step (see eq 11). (c) It reacts rapidly and selectively with peracids, which are formed in the oxidation of aldehydes, and thus facilitates intermediate product conversion at advanced stages of oxidation. The first two mechanisms can operate in all cobalt catalyzed reactions. The ease of reactions 1 and 2 depends on the redox potential of the Co(III)/Co(II) couple; the nature of the ligand (acetate or bromide, etc.) and the solvent also have some influence on this. The reason for the effectiveness of cobalt (and manganese) is the fact that the two-oxidation states in its case are of comparable stability, so that reactions 6 and 7 can occur concurrently, and a catalytic process results<sup>167</sup>. With other metals (such as copper), alternative routes for reducing the metal, such as hydrogen transfer by the solvent, sometimes operate to close the catalytic cycle. The possibilities are discussed by Sheldon and Kochi<sup>167</sup>.

#### 1.3.4.2. Oxidations with H<sub>2</sub>O<sub>2</sub>/ Organic Peroxides

Metal ions which catalyze oxygen transfer reactions with H<sub>2</sub>O<sub>2</sub> or RO<sub>2</sub>H can be divided into two types based on the active intermediate: a peroxometal or an oxometal complex<sup>168</sup>. This is illustrated for alcohol oxidations in Figure 1.2<sup>169</sup>. In the peroxometal

pathway the metal ion does not undergo any change in oxidation state during the catalytic cycle and no stoichiometric oxidation is observed in the absence of  $\text{H}_2\text{O}_2$ . In contrast, oxometal pathways involve a two electron change in oxidation state of the metal ion and a stoichiometric oxidation is observed, with the oxidized state of the catalyst, in the absence of  $\text{H}_2\text{O}_2$ . Indeed, this is a test for distinguishing between the two pathways. Peroxometal pathways are typically observed with early transition metal ions with a  $d(0)$  configuration, e.g.,  $\text{Mo(VI)}$ ,  $\text{W(VI)}$ ,  $\text{Ti(IV)}$ ,  $\text{Re(VII)}$ , that are relatively weak oxidants. Oxometal pathways are characteristic of late transition elements and first row transition elements, e.g.,  $\text{Cr(VI)}$ ,  $\text{Mn(V)}$ ,  $\text{Os(VIII)}$ ,  $\text{Ru(VI)}$  and  $\text{Ru(VIII)}$ , that are strong oxidants in their highest oxidation states. Some metals can operate via both pathways depending, *inter alia*, on the substrate, e.g., vanadium(V) operates via a peroxometal pathway in olefin epoxidations and via an oxometal pathway in alcohol oxidations<sup>161</sup>.

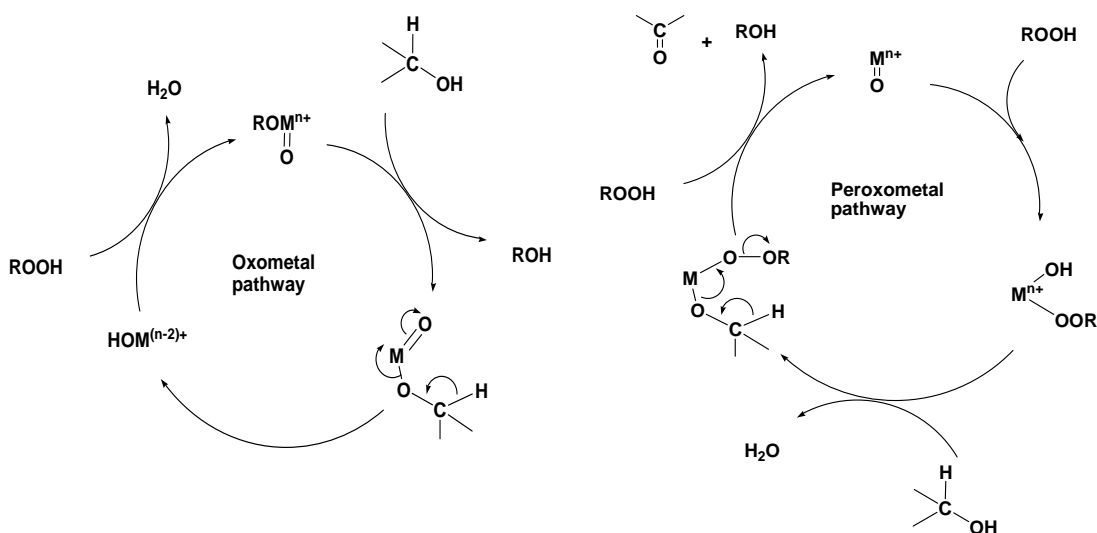


**Figure 1.2.** Oxometal vs peroxometal pathway

In aerobic oxidations of alcohols a third pathway is possible with late transition metal ions, particularly those of Group VIII elements. The key step involves dehydrogenation of the alcohol, via  $\beta$ -hydride elimination from the metal alkoxide to form a metal hydride (Figure 1.3). This constitutes a commonly employed method for the synthesis of such metal hydrides. The reaction is often base-catalyzed which explains the use of bases as cocatalysts in these systems. In the catalytic cycle the hydridometal species is reoxidized by  $\text{O}_2$ , possibly via insertion into the  $\text{M-H}$  bond and formation of

$\text{H}_2\text{O}_2$ . Alternatively, an alkoxymetal species can afford a proton and the reduced form of the catalyst, either directly or via the intermediacy of a hydridometal species (Figure 1.2). Examples of metal ions that operate via this pathway are Pd(II), Ru(II) and Rh(III). We note the close similarity of the  $\beta$ -hydride elimination step in this pathway to the analogous step in the oxometal pathway (Figure 1.2).

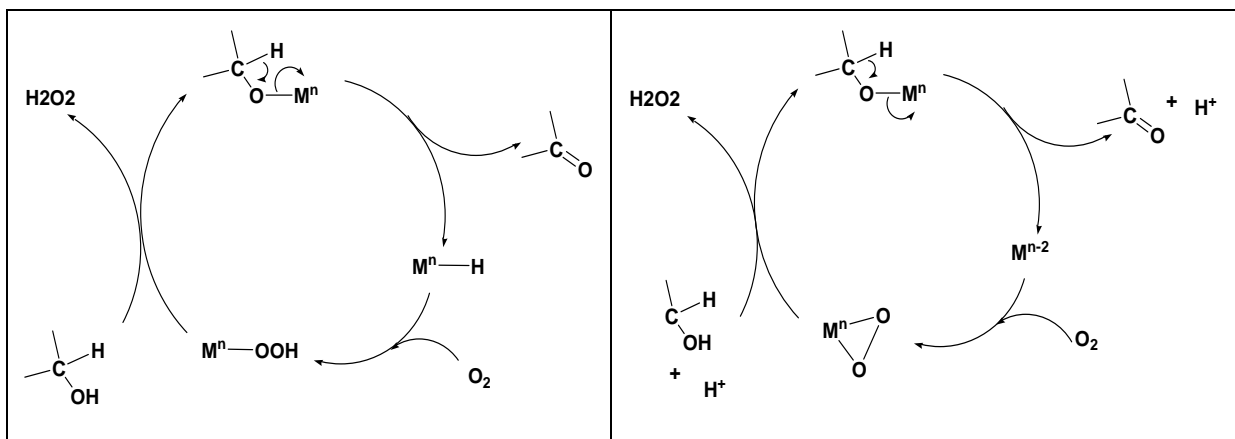


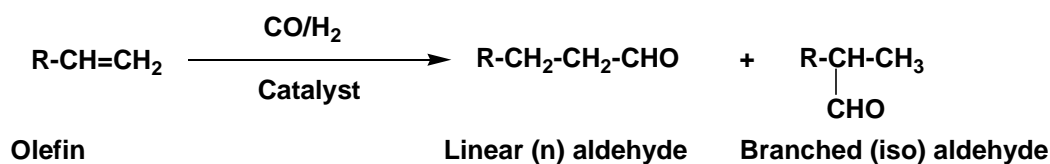
**Figure 1.3.** Hydridometal pathways for alcohol oxidation

Some metals, e.g. ruthenium, can operate via both pathways and it is often difficult to distinguish between the two. A further variation on the hydridometal pathway is observed with supported noble metal catalysts, e.g., palladium or platinum on activated charcoal. In this case the zerovalent metal dehydrogenates the alcohol to form surface metal hydrides that subsequently react with  $\text{O}_2$  to regenerate the metal. Some elements, e.g. vanadium, can employ oxometal or peroxometal pathways depending on the substrate. Reactions that typically involve peroxometal pathways are olefin epoxidation and heteroatom oxidations. Oxometal species, on the other hand, display a broader range of activities, including benzylic and allylic oxidations. An important difference is that peroxometal pathways do not involve any change in oxidation state of the metal, i.e. the metal acts as a Lewis acid and activity is not restricted to variable valence elements. An oxometal pathway, in contrast, involves two-electron redox reactions of the metal ion. Furthermore, most metals which catalyze oxygen transfer processes, via peroxometal or oxometal pathways, are also capable of catalyzing one-electron transfer processes with peroxides. Consequently, competition from free radical processes is often observed, to a greater or lesser extent, in oxygen transfer processes. When alkyl hydroperoxides are

used as oxidants homolytic versus heterolytic processes can be distinguished by the use of suitable probe molecules<sup>170,171</sup>. We also note that immobilization of a redox-active element in a solid matrix will probably not influence the oxidation mechanism, e.g. one-electron oxidants such as Co(III) will still catalyze free radical processes when incorporated in the framework of a molecular sieve.

#### 1.4. Literature Survey on Hydroformylation

Hydroformylation is one of the most flexible and important tools for the functionalisation of carbon-carbon double and triple bonds. The evolution of catalytic systems, especially ligands, has enabled control of the regio- and stereoselectivity in the hydroformylation reaction<sup>172</sup>. Hydroformylation is essentially the addition of H and the formyl group to an olefin or alkyne. It is a prototype of an efficient atom economic transformation as defined by B. Trost<sup>173</sup>, since all the atoms of the starting materials are incorporated in the product. It also is one of the important and largest scale applications of homogeneous catalysis. It is used in the industry for the manufacture of aldehydes and alcohols from olefins. About 5.9 million TPA aldehydes [C<sub>4</sub> to C<sub>20+</sub> range] are produced by this process all over the world<sup>3a</sup>. These are further hydrogenated to alcohols for different applications. The aldehydes act as intermediates for a variety of bulk and fine chemicals, whereas alcohols find applications as solvents, surfactants, detergents and plasticizers. Hydroformylation involves the reaction of alkenes with carbon monoxide and hydrogen in the presence of a catalyst to form linear and branched aldehydes. The stoichiometric reaction is as shown in scheme 1.1.



**Scheme 1.1:** General hydroformylation reaction

Discovered by Otto Roelen in 1938<sup>174</sup>, the hydroformylation reaction was first named as “Oxo” reaction, with oxo being a short form of oxonation, i.e. addition of oxygen to double bond. Later on, the reaction was renamed as “Hydroformylation” since there is

addition of hydrogen and formyl group across the double bond. Linear and branched aldehydes are the major products in the hydroformylation reaction along with some side products like alcohols and saturated hydrocarbons by hydrogenation of olefins and aldol derivatives by condensation of aldehydes. Selectivity to the *n*-isomer is an important consideration in the catalyst development, since the normal products are generally more useful in commercial practice.

Extensive work has been done on the hydroformylation reaction, which is very well documented in the literature<sup>175</sup>. The role of different catalysts and promoters on product distribution and selectivity towards desired product and the kinetics and reaction mechanism has been studied in detail using cobalt and rhodium catalysts. These are incidentally the two metals around which the hydroformylation processes are built. Table 1.7 shows the comparison of various industrial oxo processes.

**Table 1.7.** Comparison of various industrial oxo processes

| Particulars | Cobalt                                  |  | Rhodium                |  |                                    |
|-------------|---|--|------------------------|--|------------------------------------|
|             | Classical <sup>a</sup>                  | Modified <sup>b</sup>                        | Classical <sup>c</sup> | Modified <sup>d</sup><br>(LPO)                 | Water-soluble <sup>e</sup>         |
| Catalyst    | HCo (CO) <sub>4</sub>                   | [HCo (CO) <sub>3</sub><br>PBU <sub>3</sub> ] | HRh(CO) <sub>4</sub>   | [HRh(CO)<br>(PPh <sub>3</sub> ) <sub>3</sub> ] | [HRh(CO)<br>(TPPTS) <sub>3</sub> ] |
| T (°C)      | 110-180                                 | 160-200                                      | 100-140                | 60-120   | 110-130                            |
| P (bar)     | 200-350                                 | 50-100                                       | 200-300                | 1-50   | 40-60                              |
| Product     | aldehyde                                | alcohol                                      | aldehyde               | aldehyde                                       | aldehyde                           |
| n:iso ratio | 80:20                                   | 88:12  | 50:50                  | 92:8   | 97:3                               |
| By-product  | alcohols,<br>acetals and<br>heavy ends. | paraffins                                    | isomeric<br>aldehydes  | condensation<br>products                       | n-butanol<br>isobutanol            |

a = BASF, Ruhrchemie; b= Shell; c= Ruhrchemie; d= Union Carbide; (LPO); e= Ruhrchemie/Rhone-Poulenc, Hoechst.



The Table 1.7 reveals the immense potential of hydroformylation reaction in chemical industry, which has been realized in the past few decades. Hydroformylation therefore, has been one of the most studied catalytic reactions, the evolution of which can be explained into three phases or generations.

The *first generation* hydroformylation processes were exclusively based on cobalt catalyst<sup>176</sup>. The reaction conditions needed for this catalyst were relatively harsh (200-350 bar pressure and 150-180°C temperature). Later on, researchers<sup>177</sup> at Shell discovered that phosphines (or arsines) were able to replace carbon monoxide as electron donating ligand to produce a modified cobalt catalyst, which shows improved regioselectivity towards the *n*-isomer, due to the electronic and steric properties of the phosphine ligand. The Shell process reduced the operating pressure to 50-100 bar and temperature to 80°C to 200°C. The major drawback of this process was the side reaction of hydrogenation of olefins to paraffins. The *second generation processes* combined the advantages of ligand modification with a changeover from cobalt to rhodium as the catalyst. The rhodium-phosphine catalysts achieved very high chemoselectivity and regioselectivity towards *n*-aldehydes, at milder reaction conditions (60-120°C and 1-50 bars) and hence this process is termed as the Low Pressure Oxo Process (LPO process)<sup>178</sup>. Owing to this advantage of LPO, most of the cobalt-based hydroformylation processes were shifted to LPO, especially for hydroformylation of propylene. The catalyst employed in LPO process is  $\text{HRh}(\text{CO})(\text{PPh}_3)_3$ , also popularly known as Wilkinson's catalyst. The *third generation process* using aqueous biphasic catalysis was developed by Kuntz<sup>179</sup> of Rhone-Poulenc in 1984, which addressed the catalyst product separation issue to some extent. The basic idea was to immobilize the catalyst in to an immiscible *liquid*. The necessity of this variation was to convert the organic soluble ligand to its water-soluble counterpart. Aqueous biphasic catalysis particularly gained importance because of the many advantages of water as the reaction solvent. The best example of the aqueous-biphasic catalysis is the hydroformylation of propylene using  $[\text{Rh}(\text{COD})\text{Cl}]_2\text{-TPPTS}$  (triphenyl phosphine trisulfonate trisodium), which has been commercialized by Ruhrchemie-Rhone Poluenc at a 300 MTPA scale.

Apart from cobalt and rhodium catalysts, the hydroformylation reaction has also been explored with a few other transition metal complexes of Ni, Pd, Se, Cu, Fe, Ru, Ir,

Pt, Ag or Mn, though for academic interest<sup>30a</sup>. Tin (II) chloride modified platinum catalysts have significantly gained importance in the field of asymmetric hydroformylation. The order of hydroformylation activity with regard to the central metal atom follows the trend Rh>Co>Ir,Ru>Os>Pt>Pd>Fe>Ni. The Rh catalyzed hydroformylation has been applied for a variety of olefins from linear  $\alpha$ -olefins to higher olefins as well as functionalized olefins, with numerous applications of the aldehyde products. A list of the rhodium catalyzed commercial hydroformylation processes is given in Table 1.8.

Similarly, a large variety of ligands have been screened for the cobalt and rhodium catalyst systems to improve activity/selectivity of hydroformylation. Phosphines are the most widely studied ligands in hydroformylation chemistry. Nitrogen containing ligands like amines, amides or isonitriles<sup>180</sup> though active, show lower reaction rates in the oxo reaction due to their stronger co-ordination to the metal center. The order of reactivity of ligands according to the donor atom:  $\text{Ph}_3\text{P} > \text{Ph}_3\text{N} > \text{Ph}_3\text{As}, \text{Ph}_3\text{Sb} > \text{Ph}_3\text{Bi}$  proves the superiority of phosphine ligands<sup>181</sup>. Polydentate phosphines have also been used for hydroformylation reaction but their uses are limited, as they show much lower activities than their monodentate counterparts. In addition, the regioselectivities are not as high as expected for these bulky ligands<sup>182</sup>. Due to the extensive use of phosphines in catalysis, their co-ordination chemistry has been studied in more detail<sup>183</sup>. Carbene ligands obtained from imidazolium salts also show good activity and selectivity for hydroformylation of 1-hexene<sup>184</sup>.

**Table1.8.** Survey of commercial application of Rh catalyzed hydroformylation<sup>185</sup>

| <b>Sr.</b> | <b>Alkene</b>                                | <b>Products</b>                                | <b>Developed by</b>                             | <b>Year</b> | <b>Ligand</b> | <b>Capacity<br/>kTPA</b> |
|------------|--|--|---|-------------|---------------|--------------------------|
| 1          | C <sub>6</sub> -C <sub>14</sub><br>1-alkenes | higher alcohols                                | Mitsubishi                                      | 1970        | none          | 23                       |
| 2          | ethene                                       | propanal                                       | Celanese, Union Carbide                         | 1974        | TPP           | 400                      |
| 3          | propene                                      | butanol , isobutanol<br>2-EH, neopentyl glycol | BASF, Celanese,<br>Union Carbide,<br>Mitsubishi | 1974        | TPP           | 4000                     |
|            |  |  | RCH-RP  | 1984        | TPPTS         | 600                      |
| 4          | 1,2-diacetoxy<br>3-butene                    | vitamin-A                                      | BASF  | 1970        | none          | 3                        |
| 5          | 1,4-diacetoxy<br>2-butene                    | vitamin-A                                      | Hoffmann-LaRoche                                | 1970        | TPP           | 3                        |
| 6          | 1-hexene,<br>1-octene                        | carboxylic acids                               | Celanese  | 1980        | TPP           | 18                       |
| 7          | branched<br>internal<br>octenes              | isononanol                                     | Mitsubishi                                      | 1987        | TPPO          | 30                       |

|    |                       |                          |                            |      |                       |     |
|----|-----------------------|--------------------------|----------------------------|------|-----------------------|-----|
| 8  | 3-methyl 3-butene1-ol | 3-methyl-1,5-pentanediol | Kuraray                    | 1988 | bulky mono- phosphite | 3   |
| 9  | allyl alcohol         | 1,4-butanediol           | Kuraray                    | 1990 | TPP + dppb            | 180 |
| 10 | 7-octenal             | 1,9-nonanediol           | Kuraray                    | 1993 | TPPMS                 | 2-3 |
|    |                       |                          |                            |      | bulky mono- phosphite |     |
| 11 | 1-butene              | 2-propyl-1-heptanol      | Hoechst                    | 1995 | TPPTS                 | 40  |
| 12 | 1-butene/ 2-butenes   | 2-propyl-1-heptanol      | Union Carbide              | 1995 | diphosphites          | 80  |
| 13 | higher 1-alkenes      | detergent alcohols       | Kvaerner,<br>Union Carbide | 2001 | DPBS                  | 120 |

Even though majority of the hydroformylation applications utilize linear hydrocarbon olefins (especially  $\alpha$  - olefins), there are many reports on hydroformylation of functionalized olefins *e. g.* acetates, alcohols, halides, ethers *etc.*, and substrates other than olefins *e. g.* epoxides, alcohols, halides *etc.*, as shown in Figure 1.2. Most of the lower olefins feedstock for hydroformylation is made available from the mineral oil processing units such as cracking processes, especially thermal cracking<sup>186</sup> whereas higher olefins are mostly produced either by ethylene oligomerization, paraffins dehydrogenation, or SHOP process.<sup>186</sup> In the past few decades, hydroformylation of diacetoxy butenes, allyl alcohol and ethylene oxide have found industrial applications. Thus, functionalized olefins, as substrates are useful, especially for the fine chemicals and pharmaceutical industries (Figure 1.4).

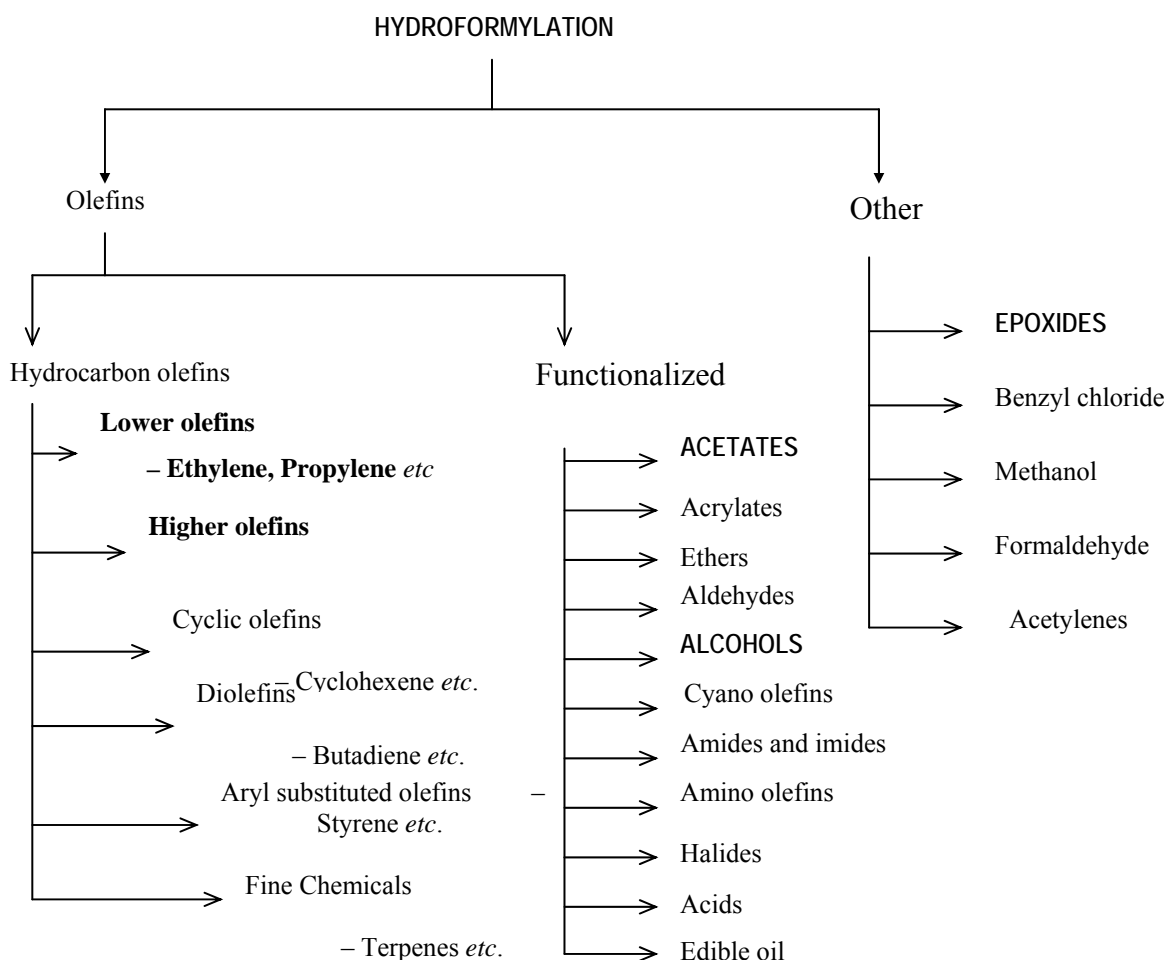


**Figure 1.4.** Classification of hydroformylation based on the substrates employed.

The work presented in this thesis, in part, deals with the application of hydroformylation reaction for the synthesis of (i) hydroxypropionic acids by the hydroformylation of vinyl acetate monomer (VAM), a functionalized lower olefin; and (ii) arylpropionic acids by the hydroformylation of 6-methoxy vinyl naphthalene (MVN), which is an aryl olefin. Hydroxypropionic acids are useful in dyeing wool and to make plasticizers for resin food industry as preservatives etc., while the arylpropionic acids are important non-steroidal anti-inflammatory agents (NSAIDs). Hence, a more detailed account of the literature on lower olefins and styrenes is taken in this chapter.

#### **1.4.1. Hydroformylation of Functionalized Lower Olefins: VAM Hydroformylation**

Functionalized olefins are important substrates for hydroformylation as they produce dual functional organic compounds, which are very useful fine chemicals for organic synthesis. The commercial utility of functionalized olefins category is very well demonstrated by various processes like, Ajinomoto process for acrylonitrile hydroformylation to L-glutamic acid (Na-salt)<sup>187</sup>, Vit. A synthesis from diacetoxy butenes, Shell process for 1,3-propanediol from ethylene oxide *etc.* In spite of the importance, functionalized olefins are somewhat ignored by the hydroformylation researchers mainly because of the following limitations,

1. Because of two functional groups, chemoselectivities/ regioselectivities are often low.
2. Substrates sometimes are unstable under hydroformylation conditions.
3. Products formed, sometimes acts as a catalyst poison.
4. In general reaction rates are lower than those found for hydrocarbon olefins.

VAM is an important substrate for hydroformylation because of the possibility of obtaining propanediols through VAM hydroformylation followed by hydrogenation and hydrolysis (adjacent Scheme). Both 1,3- and 1,2-propanediols (1,3-PDO and 1,2-PDO) are commercially important products, 1,3-PDO has many applications in polymer industry and 1,2-PDO is mainly used as an antifreeze agent.

Prochiral nature is yet another reason for the continued interest of researchers in VAM hydroformylation. Most of the reports on VAM hydroformylation consist of

asymmetric synthesis to obtain optically pure 2-acetoxypropanal and 1,2-propanediol. Majority of the reports uses Rhodium complexes as catalysts and like  $\alpha$ -esterification dominance in VAM carbonylation, in VAM hydroformylation  $\alpha$ -formylation is predominant, thus always giving 2-acetoxy propanal (branched isomer) as a major product.

2-acetoxy propanal and also other 2-alkoxypropanals, are important intermediates for a novel one step synthesis of furan carboxylic acid derivatives, which are of great industrial importance in seed-disinfection<sup>188</sup> and in wood preservation<sup>189</sup>. Reaction of with acetoacetamides or acetoacetates leads to 2,5-dimethyl-3-furancarboxamides or the corresponding esters in high selectivity. Adkins *et al*<sup>248</sup>. reported VAM hydroformylation for the first time in their survey of usefulness and limitations of the hydroformylation. The authors have studied dicobalt-octacarbonyl catalyzed hydroformylation of many olefinic substrates and in that they have reported one reaction with VAM. With 31.5 MPa syngas pressure, at 398 K they obtained 70 % conversion of VAM. The selectivity to 2-acetoxypropanal (branched isomer) was 65 % whereas 3-acetoxy propanal (normal isomer) selectivity was 35 %. The VAM hydroformylation was not explored further by Ajinomoto Co. Inc. have prepared 2-acetoxy propanal by VAM hydroformylation with rhodium tricarbonyl as a catalyst. With 16.4 MPa, 1:1 syngas pressure at 353 K, they obtained 96 % conversion with 72 % selectivity to 2-acetoxypropanal and < 2 % selectivity to 3-acetoxypropanal. Watanabe *et al*<sup>186</sup> studied hydrido cobalt carbonyl catalyzed hydroformylation of VAM in some detail with temperature and carbon monoxide and hydrogen partial pressure effects. They could obtain 100 % conversion of VAM in 1 h at 393 K and 12.3 MPa 1:1 syngas pressure. Watanabe *et al*<sup>186</sup>. observed that with 1:3 = CO:H<sub>2</sub> at 373 K, the VAM conversion stops at 18 %. Tinkar *et al*<sup>190</sup>. have studied VAM hydroformylation as a potential route for lactic acid production. In acetic acid solvent they have taken Rh-phosphine complexes and hydroformylation is carried out at 398 K with 3.7 MPa, 1:1 syngas pressure. The products were subjected to oxidation with 0.2 MPa air and 298 K temperature. After oxidation, hydrolysis was carried out with water at 423 K for 2 hours. 60 % yield of lactic acid yield (based on VAM reacted) was obtained along with 22 % propionic acid. No  $\beta$ -hydroxy propionic acid was observed indicating that 3-acetoxypropanal was not formed during VAM hydroformylation.

Different rhodium precursors and phosphine ligands for VAM hydroformylation were tested by the authors and observed that 3-acetoxypropanal doesn't form during Rh catalyzed VAM hydroformylation.

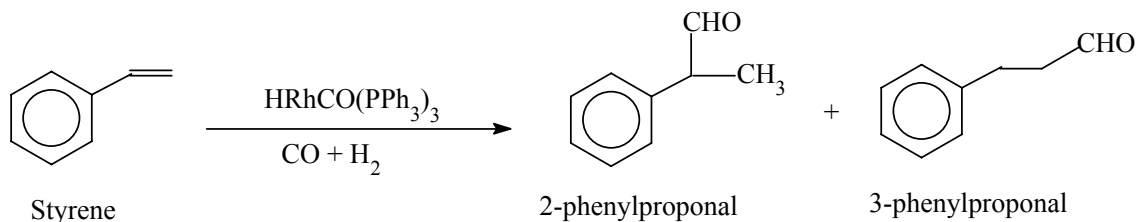
Detailed study on rhodium catalyzed VAM hydroformylation was carried out *and* the effect of different phosphines at various temperatures on the decomposition of 3-acetoxypropanal and found that in presence of triphenyl phosphine or tri-*n*-butyl phosphine all the 3-acetoxypropanal is decomposed to acetic acid and acrolein at 333 K within an hour. Effect of different phosphines on the regioselectivity of rhodium catalyzed VAM hydroformylation is also studied but none of the phosphine ligand could improve the selectivity of 3-acetoxypropanal beyond 20 %. A side reaction of catalytic decomposition of vinyl acetate with  $\text{HRh}(\text{CO})(\text{PPh}_3)_3$  to yield ethylene and  $\text{Rh}(\text{CO})(\text{OCOCH}_3)(\text{PPh}_3)_2$  was observed and this rhodium complex was isolated and characterized by elemental analysis. Different vinyl carboxylates other than VAM were also hydroformylated but 3-acetoxypropanal formed was always < 10 %. Presence of acetic acid was found to retard the hydroformylation of vinyl acetate. The speculated formation of species responsible for higher selectivity to 2-acetoxypropanal (branched isomer) and lower selectivity to 3-acetoxypropanal (*n*-isomer). Two alkyl species formed after the hydride additions differ in their stability and five-member ring chelate predominates thus giving more branched aldehyde.

Two reports on kinetics of VAM hydroformylation catalyzed by  $\text{HRh}(\text{CO})(\text{PPh}_3)_3$  and  $[\text{Rh}(\text{CO})\text{Cl}]_2$  catalyst complexes are available in the literature (Deshpande *et al*<sup>250</sup>). With  $\text{HRh}(\text{CO})(\text{PPh}_3)_3$  the kinetics of hydroformylation of vinyl acetate has been investigated in the temperature range 323 – 343 K. It was observed that certain minima of concentration of and  $\text{H}_2$  partial pressure are necessary for the reaction to proceed. Beyond such critical concentrations, the rate was found to be first order with  $\text{H}_2$  and catalyst. With increasing CO and vinyl acetate concentrations, the rates passed through maxima, indicating substrate inhibition at higher concentrations. The observed kinetics has been discussed on reaction mechanism. Several rate equations were examined and the activation energy was found to be 17.86 kcal / mol.



### 1.4.2. Hydroformylation of Vinylarenes: Synthesis of NSAIDs

Hydroformylation of styrene is a convenient model reaction to study the catalysis and kinetic modeling. Several different catalyst systems have been employed in the hydroformylation of styrene and a summary of literature on styrene hydroformylation are discussed in this section. The stoichiometry of the reaction is as shown below scheme 1.2.



**Scheme 1.2.** Hydroformylation of styrene

The reaction has been attempted by using ruthenium<sup>191</sup>, Cobalt<sup>192</sup>, rhodium<sup>193</sup>, Takeda and coworkers<sup>194</sup>, Iridium<sup>195</sup> and Pt catalysts<sup>196</sup>, but high activities and selectivities to the branched aldehydes were achieved with rhodium-phosphine systems only. The rhodium-triphenylphosphine-catalyzed hydroformylation of styrene proceeds under mild conditions (298 K, 0.1 MPa) and selectivities to 2-phenyl propanal up to 94% can be achieved. Neibecker *et al.*<sup>197</sup> have reported that rhodium-phosphole and rhodium-phosphanorboranadiene systems show even better activity than triphenylphosphine systems (Four times more active than triphenylphosphine) with very high selectivity towards branched aldehyde and without any hydrogenation or other side reaction under mild reaction conditions. It was also found that 1,2,5- triphenylphosphole as a ligand is independent of 1,2,5- triphenylphosphole/Rh ratio above 2, unlike PPh<sub>3</sub>, where the activity decreases with increase in P/Rh ratio<sup>198</sup>. Rhodium catalysts with bulky phosphite ligands are more active for sterically hindered less reactive alkenes. For example phosphite-modified rhodium catalysts with tris (o-t-butylphenyl) phosphite and tris(hexafluoroisopropyl) phosphite are thirty times higher active than that of triphenylphosphine towards unreactive olefins such as 2-methyl-1-hexene, limonene, cyclohexene and methylene cyclohexene. The high rates observed are attributed to the steric and electronic properties of these phosphite ligands and their ability to stabilize unsaturated rhodium species<sup>199</sup>.

Non-steroidal anti-inflammatory (NSAI) agents are one of the largest classes of drugs both due to their high number and to their therapeutic interest. All these compounds have a similar mode of action: by cyclooxygenase inhibition they stop the arachidonic acid cascade to prostaglandins and thromboxane A<sub>2</sub>, which are responsible for the inflammation mechanism. Non-steroidal anti-inflammatory agents can be classified according to their chemical structure.

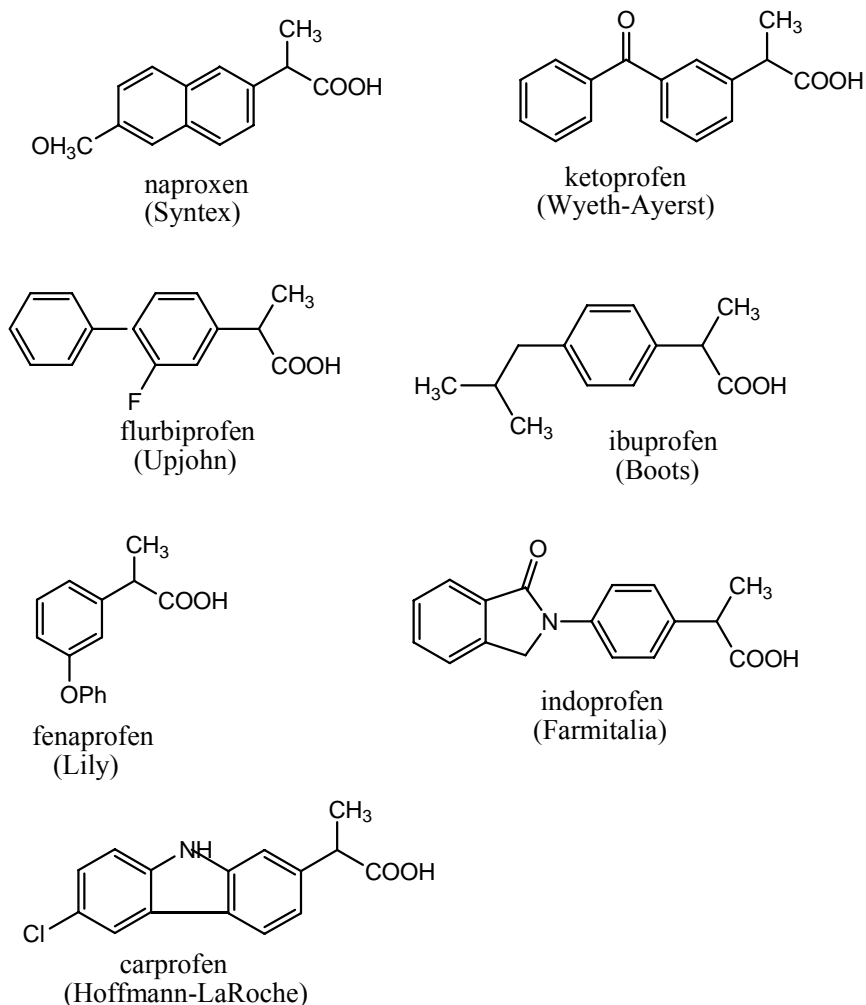


**Figure 1.5.** Anti-inflammatory compounds

Except for the latest class of oxicams with piroxicam and isoxicam, most of the more thoroughly studied NSAID agents can be categorized into three main classes.

(1) Benzoic derivatives with salicylic group where aspirin is often the highlight and with the new diflunisal compound; anthranilic compounds with mefenamic and niflumic acids.

(2) Aryl acetic acid compounds among which the most representative ones are indomethacin, sulindac, ibufenac and diclofenac.

(3)  $\alpha$ -Aryl propionic acids with ibuprofen as the first representative.

The structures of seven nonsteroidal anti-inflammatories are presented in Figure 1.5, of these seven, only naproxen is currently marketed exclusively in an optically pure form. The major manufacturers of the respective drug are given in the parentheses with each of the structure.

The synthesis of the optically active NSAIDs is possible through three general approaches (1) synthesis of the racemic mixture followed by separation of racemates (classical resolution, direct crystallization, kinetic resolution using an enzyme), (2) use of the chiral pool (R-amino acids, R-hydroxy acids, etc.), and (3) asymmetric synthesis (noncatalytic, catalytic, enzyme mediated). There is precedent for large-scale manufacturing of pharmaceutically important, optically active compounds using each of these approaches. The large list of examples of manufacturing using chiral pool technology includes nafarelin acetate, ampicillin, and three ACE inhibitors. The decapeptide nafarelin acetate, effective in the treatment of endometriosis, is manufactured at Syntex using D-naphthylalanine. D-Phenylglycine is a key component of the antibiotic ampicillin. The top-selling ACE inhibitors, enalapril, captopril, and lisinopril, are all derived from L-proline. There is an even longer list of manufacturing processes incorporating a resolution. D-Biotin is resolved using ephedrine. Technology for resolution of (S)-naproxen using an N-alkylglucamine was already in place in the 1980s. There is considerable interest in optically pure (S)-ibuprofen, which is accessible by resolution with R-ethylbenzylamine. The least precedented manufacturing processes to obtain optically active targets employ asymmetric synthetic methods. The list of examples is small but compelling.

Synthesis of NSAIDs has experienced continuous evolution. Ibuprofen is the most commonly used NSAID, and a survey of the literature on the synthesis processes for the same shows continuous improvements with regard to the number of steps involved, the atom economy, operating conditions for the synthesis and overall process cost. Boots process, which utilized isobutyl benzene as the starting material, was the first route

employed commercially for large-scale synthesis of ibuprofen. It is a multi-step, complex synthesis involving several reagents. This was later replaced by the BHC process, which involved lesser number of steps, and was more atom-economical<sup>200</sup>.

The BHC process, a three step catalytic route for ibuprofen using catalytic acylation, hydrogenation and carbonylation represents one of the best examples of the use of catalysis for cleaner processes in pharmaceuticals. Similarly, naproxen- the second most important member of the NSAIDs is another important drug in this category, which is currently manufactured by multistep stoichiometric synthetic routes: (a) Syntex Process starting with  $\beta$ -naphthol and involving stoichiometric bromination, methylation and alkylmetal coupling reactions to yield naproxen, (b) Zambon Process involving acylation of nerolin (2-methoxynaphthalene), ketalization, bromination, hydrolysis and reductive cleavage as the key steps and (c) asymmetric hydrogenation of 6-methoxy naphthacrylic acid using Ru-(S) BINAP catalyst<sup>201</sup>.

The attempts towards direct synthesis of chiral naproxen via chiral pool using (S)-lactate, and asymmetric hydroformylation followed by oxidation were also made. These routes suffer from the drawbacks like use of hazardous reagents and generation of undesired waste consisting of inorganic salts. Therefore, it is most desirable to develop an environmentally benign catalytic route for the synthesis of naproxen. Hydroformylation of vinylarenes to 2-arylpropanals under mild conditions is of great significance, since these aldehydes can be easily oxidized to corresponding acids, which are used as the largest selling anti-inflammatory class of drugs<sup>202,203</sup>. In the conventional process, 2-arylpropionic acids are synthesized using Friedel Crafts reaction, which generate large amount of waste and expensive raw materials such as 2-chloropropionic acid<sup>204</sup>. The preparation of 2-arylpropionaldehydes by hydroformylation of easily available corresponding vinylarenes is a simple and environmentally attractive process. A typical example of this type is the synthesis of Ibuprofen from *p*-isobutyl styrene as shown in Figure 1.6.

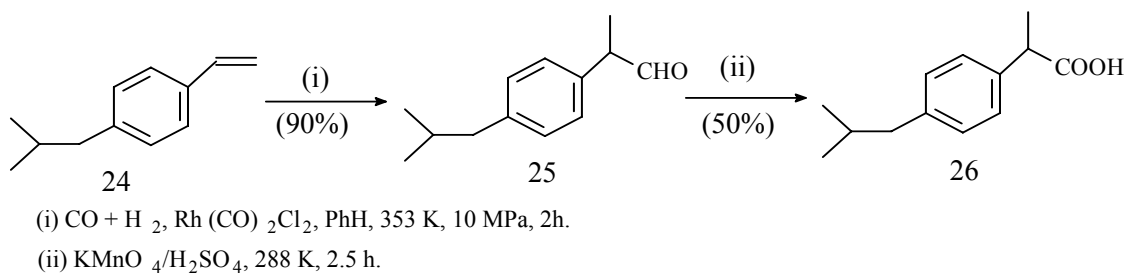


**Figure 1.6.** Synthesis of ibuprofen from *p*-isobutyl styrene.

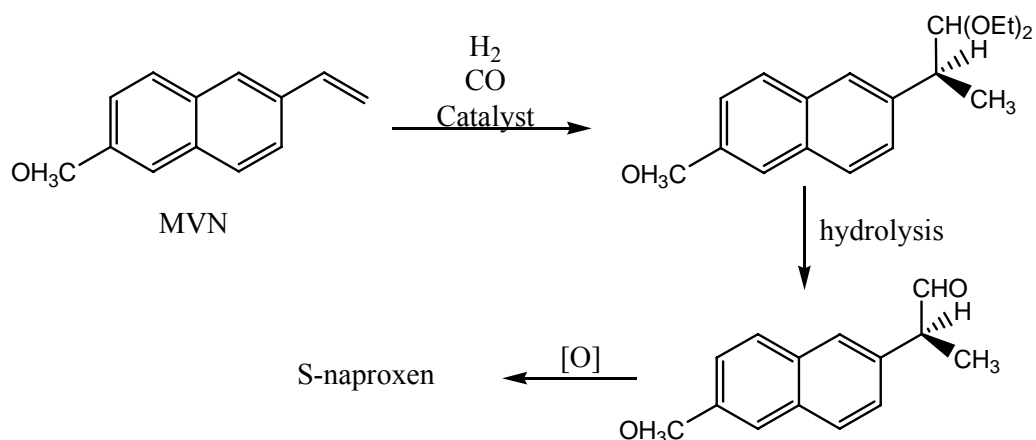
*p*-isobutyl styrene is hydroformylated in presence of  $\text{Rh}(\text{CO})_2\text{Cl}_2$  at 353 K and  $\text{CO}/\text{H}_2$  pressure of 10 MPa in benzene for two hours to yield *p*-isobutyl-2-phenylpropionaldehyde, which upon subsequent oxidation with  $\text{KMnO}_4/\text{H}_2\text{SO}_4$  mixture at 288 K for 2.5 hours yields Ibuprofen. [Arakawa (1977)]. Riley and co-workers (1987) have reported an efficient method for the oxidation 2-arylpropionaldehydes using manganese stearate as catalyst and *m*-chloro-peroxybenzoic acid as oxidizer.

Several approaches for industrial synthesis of naproxen have also been evaluated. There are several asymmetric technologies specifically designed for naproxen manufacture<sup>205</sup>. The Zambon process is well known, which utilizes 2-Methoxy-6-propionynaphthalene (MPN) prepared by Friedel-Crafts acylation of nerolin, as the starting material. The synthesis involves several steps including ketalization, bromination, and ester hydrolysis to yield a 92:8 mixture of diastereoisomers. This mixture of diastereoisomers rearranges on heating to 90°C to produce an upgraded mixture of 1-bromonaproxen esters. Reductive cleavage of the 1-bromo substituent followed by ester hydrolysis affords (*S*)-naproxen (ee >98%). The yield from MPN is 70-75%<sup>206</sup>. Apparently, the process is too complicated. There was also some concern about the mechanics of tartaric acid recycle. Finally, the problems associated with manufacture of MAN are also associated with manufacture of MPN: the regioisomer problem and generation of aluminum hydroxide wastes in the Friedel-Crafts acylation.

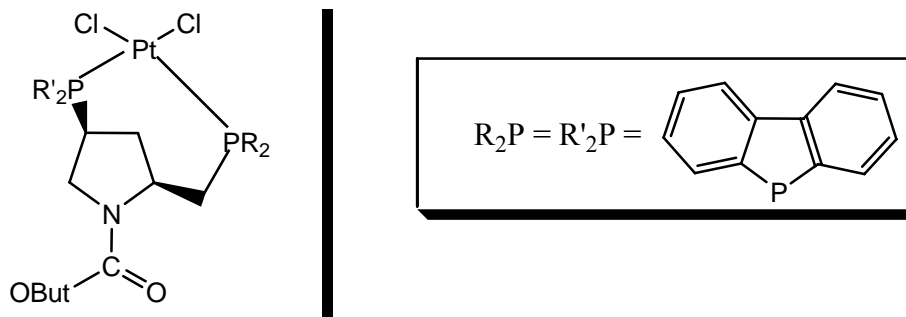
Catalytic asymmetric hydrogenation of a naphthacrylic acid using a ruthenium (*S*)-BINAP catalyst (135 atm) yields (*S*)-naproxen (ee >98%). A *tol*-BINAP based catalyst would mediate hydrogenation at a significantly lower pressure (30 atm)<sup>207</sup>. Such high pressures would necessitate a significant capital investment for any manufacturing

facility. Perhaps of greater importance is the cost associated with the hydrogenation substrate, the naphthacrylic acid. Retrosynthetic analysis suggests the naphthylacetic acid or naphthylacetylene precursors, which in turn, might be derived from BMN or MAN208. In any event, manufacture of the naphthacrylic acid would involve at least two and more likely three-process steps.

Catalytic asymmetric hydroformylation (Figure 1.7), reported by Stille *et al*<sup>209</sup>, starting with 2-methoxy-6-vinylnaphthalene (MVN) and using a rhodium catalyst with BINAPHOS ligand can produce an optically active aldehyde, which on oxidation yields (S)-naproxen. Stille *et al*<sup>209</sup> have reported the asymmetric hydroformylation of several vinylarenes using platinum catalysts. The authors examined the activity of three complexes of Pt(II) containing the chiral ligands 1-(tert-butoxycarbonyl)-(2S,4S)-2-[(diphenylphosphino)methyl]-4-(dibenzophospholyl)pyrrolidine, 1-(tert-butoxycarbonyl)-(2S,4S)-2-[(dibenzophospholyl)methyl]-4-diphenylphosphino pyrrolidine, and 1-(tert-butoxycarbonyl)-(2S,4S)-4-(dibenzophospholyl)-2-[(dibenzophospholyl)methyl] pyrrolidine for the asymmetric hydroformylation of styrene.



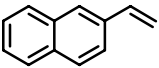
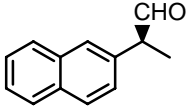
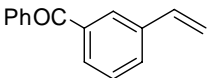
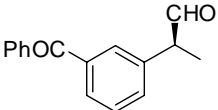
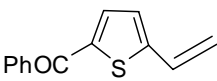
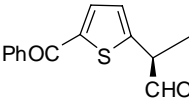
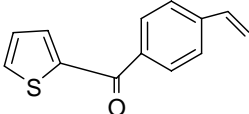
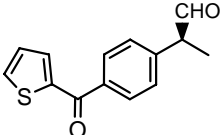
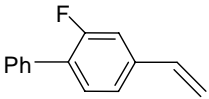
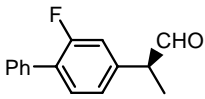
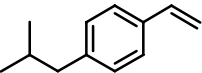
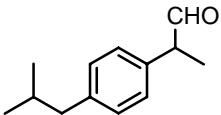
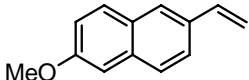
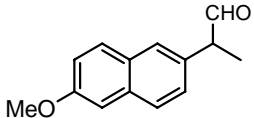
**Figure 1.7.** Scheme for the asymmetric hydroformylation of MVN for direct synthesis of (S)-naproxen



**Figure 1.8.** (b) The most active catalyst for asymmetric hydroformylation of MVN

Various branched/normal (b/n) ratios (0.5-3.2) and enantiomeric excess (*ee*) values (12-77%) were obtained. When the reactions were carried out in the presence of triethyl orthoformate, all catalysts gave virtually complete enantioselectivity (*ee* > 96%) and similar b/n ratios. The complex 1-(tert-butoxycarbonyl)-(2S,4S)-4-(dibenzophospholy1)-2-[(dibenzophospholy1)methyl] pyrrolidine gave the highest b/n (3.3), and was also used for the asymmetric hydroformylation of diverse vinyl aromatic compounds that are the precursors to anti-inflammatory agents. With the platinum complex, however, the *ee*'s were low because of in-situ racemization, and the n/iso ratios depended strongly on the structure of the aromatic substituent. However, when the reactions were carried out in the presence of triethyl orthoformate, enantiomerically pure acetals were obtained. Some of hydroformylation of vinyl aromatic compounds are tabulated in 1.9.

**Table 1.9.** Hydroformylation of vinyl aromatic compounds

| Sr. | Substrate   | Time, h | Product  | Conv., % | b/n | (S)ee % |
|-----|---|---------|--|----------|-----|---------|
| 1.  |    | 38      |    | 95       | 10  | 39      |
| 2.  |    | 44      |    | 100      | 3.3 | 27      |
| 3.  |    | 38      |    | 90       | 5.0 | >96     |
| 4.  |    | 64      |    | 65       | 4.0 | 9       |
| 5.  |   | 70      |   | 95       | 3.8 | 19      |
| 6.  |  | 37      |  | 45       | 2.0 | 39      |
| 7.  |  | 48      |  | 100      | 3.3 | 37      |

There are several potential problems with this technology. First, the ligand must provide not only good stereoselectivity but also the correct regioselectivity. A linear aldehyde is often the major product of an alkene hydroformylation. Second, the branched aldehydes can racemize under the hydroformylation conditions. The racemization can be avoided by converting the aldehyde to an acetal in situ (with an orthoformate), but this approach necessitates an acetal hydrolysis later in the sequence. Other related technologies for naproxen manufacture from MVN include: catalytic asymmetric



hydroesterification<sup>210</sup>, hydrocarboxylation<sup>211</sup>, or hydrocyanation<sup>212</sup>. These approaches have not received as much attention even though they may be more efficient in some respects. All of the naproxen-specific technologies discussed thus far fall into the “asymmetric synthesis” category (nuncatalytic or catalytic).

One example of (*S*)-naproxen manufacture using the chiral pool approach was developed at Syntex in 1982. Ethyl lactate is one of a very few chiral compounds which can be used in stoichiometric quantity in a cost effective synthesis of (*S*)-naproxen. (*S*)-Ethyl lactate is converted to a mesylate. Ester hydrolysis and conversion of the acid to the acid chloride provides a chiral acylating agent. Acylation of the BMN-derived Grignard reagent yields an optically pure ketone. Ketalization with 2,2-dimethyl-1,3-propanediol, followed by rearrangement and ester hydrolysis, yields (*S*)-naproxen. The overall yield from BMN to (*S*)-naproxen is 75%.

It becomes obvious from the literature available on the hydroformylation of vinylarenes and synthetic procedures for NSAIDs that, the former holds good potential for development of an atom-economical, convenient and more eco-friendly route for the synthesis of NSAIDs. The limitations of the asymmetric MVN hydroformylation with regard to the cost of the ligands, regioselectivity issues and overall yields also indicate that the racemic synthesis using the hydroformylation-oxidation approach followed by resolution of racemates holds good potential.

#### **1.4.3. Hydroformylation in Tandem and Sequential Synthesis**

Tandem as well as sequential syntheses using cheaper feedstocks as starting materials have gained a lot of interest in an attempt to avoid the old generation multi-step syntheses and development of cleaner and cheaper alternatives. Following a general trend in organic chemistry, hydroformylation can also be integrated in tandem or domino reaction sequences<sup>213, 214, 215</sup>. In short, this implies that under hydroformylation conditions reduction, nucleophilic addition or aldol condensation can be achieved directly. The application of hydroformylation in this manner is quite extensive and for this reason only a few applications in the synthesis of important organic molecules are mentioned herein.

Hydroformylation followed by C-O, C-N and C-C bond forming steps offers a convenient and versatile method for the construction of new carbon skeletons that give access to a wide variety of natural products, pharmaceuticals and other modern synthetic materials. Hydroformylation of alkenes or alkynes having another reactive functionality, or a reaction of simple alkenes or alkynes in the presence of other organic compounds can lead to formation of cyclic or linear derivatives, some of which are of considerable value in organic synthesis due to their applications in drug chemistry. For example, direct acetal formation under hydroformylation conditions have been reported in several hydroformylation reaction sequences<sup>216, 217</sup>. This have been applied to various substrates e.g.  $\alpha$ -olefins, allylic and homoallylic alcohols<sup>218</sup>, cyano olefins<sup>219</sup>, etc. More importantly, perhaps in organic synthesis, is intramolecular acetalation. The products obtained by this type of tandem hydroformylation process offer access to a wide variety of interesting compounds which can be used as subunits in the synthesis of natural occurring products with biological and pharmacological activities<sup>220,221</sup>. Borole *et al.*<sup>222</sup> have reported synthesis of 1,2-propanediol (1,2-PDO) and 1,3-propanediol (1,3-PDO) by hydroformylation of VAM followed by hydrogenation of aldehydes and hydrolysis of acetoxy propanols with high yields.

The important tandem or sequential hydroformylation reactions reported in the literature has been illustrated in the Table 1.10. The importance of the reactions basically lies in access to high value-added products starting with cheaper feedstock, in lesser number of steps. Synthesis of non-steroidal anti-inflammatories starting from hydroformylation of vinylarenes, followed by oxidation of the aldehyde is another example of these types of reactions.

**Table 1.10.** Examples of tandem or sequential synthesis

| Sr. | Reaction sequence   | Starting material                                    | Final Product   | Application of product                       | References  |
|-----|---|--|---|--|-------------|
| 1   | Hydroformylation- acetalation                                       | 1,2-disubstituted alcohols                           | Prelog Djerassi lactone                               | Pharma-antibiotics                           | 223,224,225 |
| 2   | Hydroformylation - amination  | D- serine  | prosopine   | Pharmaceutical                               | 226,227,228 |
| 3   | Hydroformylation - amination  | <i>o</i> -alkenylamino benzylamines                  | quinazolines  | Anti-cancer activity                         | 229,230     |
| 4   | Hydroformylation – amination  | benzamides   | quinazolinones  | Antibacterial, analgesic                     | 231,232     |
| 5   | Hydroformylation - aldol  | silyl enol ethers                                    | $\beta$ -silyloxy substituted cyclic ketones          |  | 233,234     |
| 6   | Hydroformylation -aldol   | 1,3-butadiene  | furnish formylcyclopentenes                           |  | 235         |
| 7   | Hydroformylation - aldol  | 1,1- <i>bis</i> ( <i>p</i> -fluorophenyl)-2-propynol | 4,4- <i>bis</i> ( <i>p</i> fluorophenyl) butylbromide | Neuroleptic agent                            | 236,237,238 |
| 8   | Hydroformylation –hydrogenation - hydrolysis                        | Vinyl acetate monomer                                | 1,2-propanediol and 1,3-propanediol                   | Antifreeze agent in food and pharmaceuticals | 222         |
| 9   | Hydroformylation – oxidation - hydrolysis                           | Vinyl acetate monomer                                | 2-hydroxy propionic acid                              | Preservative and stabilizer in food products | 239         |
| 10  | Hydroformylation – amination- hydrogenation (Hydroaminomethylation) | Olefins  | Secondary and tert aliphatic amines                   | Bulk and fine chemicals, pharmaceuticals     | 240         |

#### 1.4.4. Mechanism of Hydroformylation

Hydroformylation of olefins is one of the most well studied reaction in terms of mechanism. Among the industrial hydroformylation catalysts major differences are observed between modified and unmodified systems. The catalyst used in the conventional cobalt catalyzed hydroformylation process is the hydridocarbonyl complex,  $\text{HCo}(\text{CO})_4$ . This catalyst is stable only at higher temperatures and  $\text{CO}/\text{H}_2$  pressures, and therefore the reaction conditions are usually very severe (20-35 MPa and 383-453 K). The discovery of rhodium catalyst for hydroformylation of olefins was a significant development in the oxo process technology. Schiller (1956) was the first to report the use of Rh carbonyls  $\text{HRh}(\text{CO})_4$  as a catalyst in hydroformylation reaction. The generally accepted hydroformylation mechanism for the unmodified cobalt and rhodium catalysts are shown in Figure 1.9, which involves seven elementary steps such as, (1) reaction of the metal carbonyl  $\text{Co}_2(\text{CO})_8$  with hydrogen to form the hydridometal carbonyl species  $\text{HCo}(\text{CO})_4$ ; (2) dissociation of CO to generate the unsaturated 16e species  $\text{HCo}(\text{CO})_3$ ; (3) coordination of the olefin  $\text{RCH}=\text{CH}_2$  (18e);

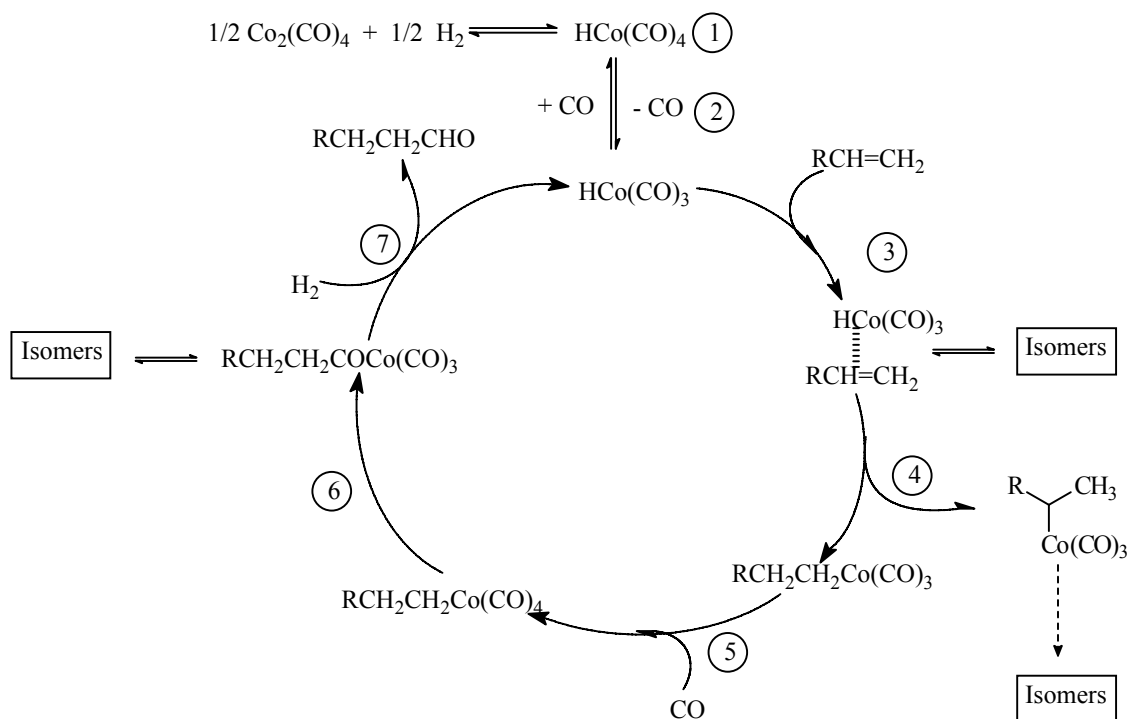


**Figure 1.9.** Catalytic cycle of hydroformylation with unmodified cobalt catalysts.

(4) formation of alkylmetal carbonyl species (16e); (5) coordination of CO (18e); (6) insertion of CO to form the acylmetal carbonyl  $\text{RCH}_2\text{CH}_2\text{COCO}(\text{CO})_3$  (16e); (7) cleavage of the acylmetal species by hydrogen to form the aldehyde and regeneration of the hydridometal carbonyl  $\text{HCo}(\text{CO})_3$ . This mechanism was originally proposed by Heck and Breslow (1960, 1961) for unmodified cobalt catalysts, but the mechanism is valid for unmodified rhodium complexes as well.

Considerable improvements in terms of high chemo and regioselectivities, milder reaction conditions and reaction rates were achieved when rhodium catalysts were explored in detail. This improvement in activity and selectivity was achieved by use of triphenylphosphine as a ligand. It is used commercially for the hydroformylation of propylene in the LP oxo process and also in the Union oil process. This was followed with numerous studies on the role of ligands, solvents and substrates in Rh catalysed hydroformylation. According to Wilkinson *et al.*,  $\text{HRh}(\text{CO})_2(\text{PPh}_3)_2$  is the key intermediate even though several species might exist in solution in equilibrium. It has been shown from NMR studies that out of  $\text{HRh}(\text{CO})(\text{PPh}_3)_3$  and  $\text{HRh}(\text{CO})_2(\text{PPh}_3)_3$ , only the latter reacts with ethylene at 298K and 0.1 MPa. Two different pathways involving associative and dissociative mechanism as proposed by Evans *et al.* are shown in Figure 1.10. The dissociative pathway is initiated by dissociation of a phosphine ligand from  $\text{HRh}(\text{CO})_2(\text{PPh}_3)_2$  followed by the addition of olefin to give coordinately unsaturated square planar complex (step 9, Figure 1.10). The addition of olefin via  $\pi$  complex gives  $\sigma$  alkyl complex (species C<sub>3</sub>, Figure 1.9). Alkyl migration or CO insertion leads to the formation of acyl complex, which on oxidative addition of hydrogen give rise to a dihydride complex (species G, Figure 1.10). This is reported to be the rate-controlling step in the mechanism. Finally, the dihydride complex reductively eliminates the products and the catalyst is regenerated. In the associative mechanism, the alkyl complex is formed, by the addition of olefin to the bisphosphine complex (species C, Figure 1.10).

The catalytic cycle again operates through the above

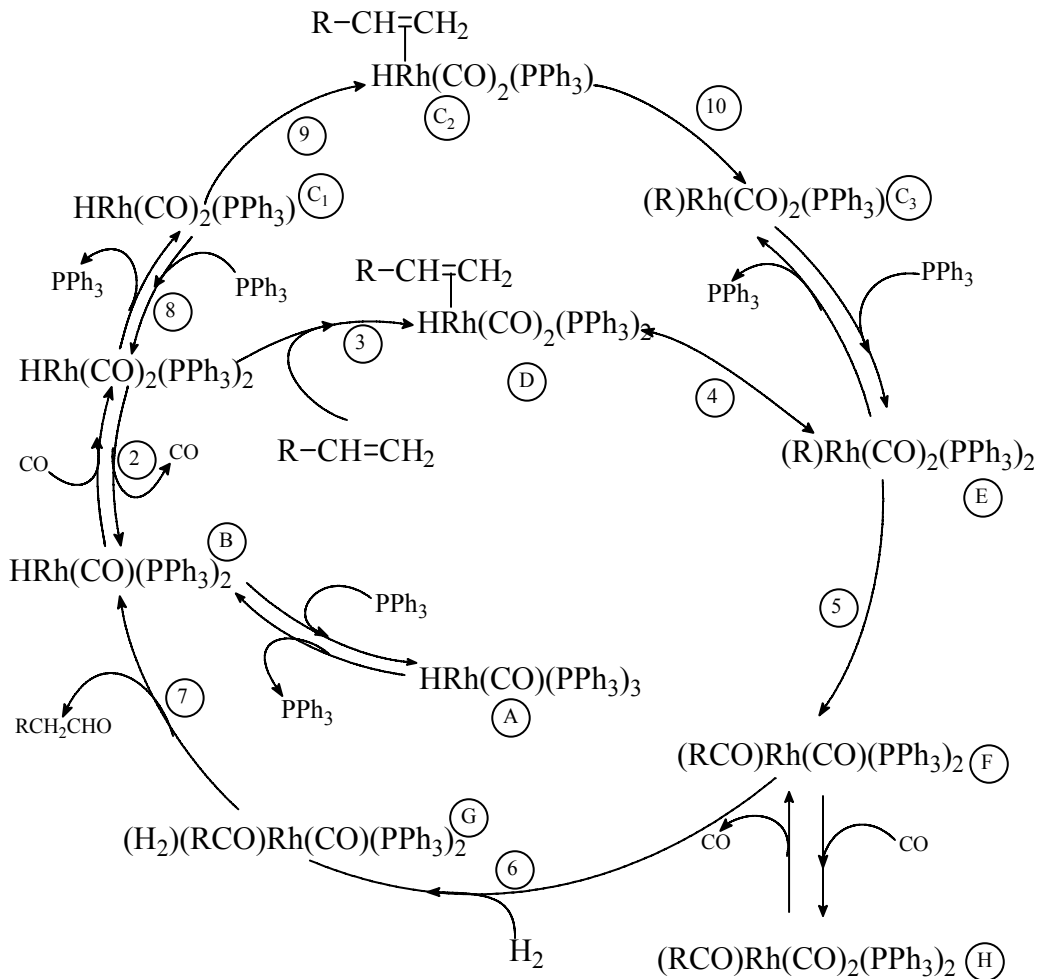


**Figure 1.10.** Mechanism for hydroformylation using modified rhodium catalysts (L= PPh<sub>3</sub>)

steps giving the product and the regeneration of the catalyst. Brown and Wilkinson (1970) studied the kinetics of hydroformylation of 1-hexene using HRh(CO)(PPh<sub>3</sub>)<sub>3</sub> complex catalyst at 298 K. They reported that rate was first order with respect to catalyst and hexene concentration and partial pressure of hydrogen and negative order with respect to partial pressure of carbon monoxide and the concentration of excess PPh<sub>3</sub>. These results have been discussed in detail on the basis of the proposed mechanism.

#### 1.4.5. Kinetics of Hydroformylation Reaction

Compared to the large volume of literature on catalysis of hydroformylation, there are only a few reports on kinetics of this important reaction. Study of kinetics of reaction is essential in understanding the catalyst and molecular process occurring around it. In the present section a brief survey of the kinetic studies on hydroformylation reactions is presented with emphasis on the unmodified and phosphine modified catalyzed reactions.

For the catalysts  $\text{Co}_2(\text{CO})_8$  and  $\text{Rh}_4(\text{CO})_{12}$  the rate of reaction is positively influenced by increase in the concentration of catalyst, olefin and hydrogen<sup>241</sup>. While increasing the carbon monoxide partial pressure, the rate passes through a maximum. At lower partial pressures (1 MPa) an increasing concentration of carbon monoxide enhances the overall reaction rate, indicating the necessity of carbon monoxide to generate hydridocobalt carbonyls, namely the  $16e^-$  species  $\text{HCo}(\text{CO})_3$ . At higher CO partial pressures the less reactive  $\text{HCo}(\text{CO})_4$  is formed and the reaction rate decreases. Unmodified rhodium catalyst also behaves in the same way. The equation derived by Natta and Ercoli is generally accepted

$$R = k \times [\text{substrate}] \times [\text{catalyst}] \times [\text{P}_{\text{H}_2}]/[\text{P}_{\text{CO}}]$$

Gholap *et al.*<sup>242</sup> reported a detailed study on the kinetics of hydroformylation of propene under industrial hydroformylation conditions (temperature range 383-423K and syngas pressures of up to 10 MPa). A rate equation was derived, which was found to explain the observed kinetic data satisfactorily. The rate of reaction was found to be linearly dependent on the propene concentration and fractional order with respect to catalyst and hydrogen. With carbon monoxide partial pressure, the rate showed a positive dependence up to a CO partial pressure of 1 MPa and negative order beyond 1 MPa. The trends observed were almost similar to that observed by Natta although they were not obtained under industrial conditions.

Brown and Wilkinson<sup>243</sup> studied the kinetics of hydroformylation of 1-hexene using  $\text{HRh}(\text{CO})(\text{PPh}_3)_3$  complex catalyst at 298K. The rate of hydroformylation was first order with respect to catalyst, hexene concentration and hydrogen partial pressure and negative order with respect to partial pressure of carbon monoxide and concentration of excess  $\text{PPh}_3$ . The negative-order dependence of the reaction rate at higher carbon

monoxide pressures is mainly due to the formation of *di*- and *tri*-carbonyl rhodium complexes  $\text{RCORh}(\text{CO})_2(\text{PPh}_3)_2$  and  $\text{RCORh}(\text{CO})_3(\text{PPh}_3)$ , which are un-reactive toward oxidative addition of hydrogen. At lower carbon monoxide partial pressure, the formation of these species is expected to be negligible. A positive-order dependence of the rate is observed as the monocarbonyl species  $\text{RCORh}(\text{CO})(\text{PPh}_3)_2$  is stabilized.

Brown and Wilkinson<sup>244</sup> studied the kinetics of hydroformylation of 1-hexene using  $\text{HRh}(\text{CO})(\text{PPh}_3)_3$  complex catalyst at 298K. The rate of hydroformylation was first order with respect to catalyst and hexene concentration and hydrogen partial pressure. The rate was negative order with respect to partial pressure of carbon monoxide and  $\text{PPh}_3$  concentration. The observed trends have been explained based on the mechanism shown in Scheme 1.2. The negative order dependence of the reaction rate at higher carbon monoxide pressures is mainly due to the formation of *di*- and *tri*- carbonyl rhodium complexes  $(\text{RCO})\text{Rh}(\text{CO})_2(\text{PPh}_3)_2$  and  $(\text{RCO})\text{Rh}(\text{CO})_3(\text{PPh}_3)$ , which are unreactive towards oxidative addition of hydrogen. At lower carbon monoxide partial pressure, the formation of these species is expected to be negligible. A positive order dependence of the rate is observed for CO at low pressure as the mono carbonyl species  $(\text{RCO})\text{Rh}(\text{CO})(\text{PPh}_3)_2$  is stabilized.

Deshpande et al<sup>245</sup> have extensively studied kinetics and reaction engineering aspects of hydroformylation of a variety of olefinic substrates such as hexene<sup>245a</sup>, vinyl acetate<sup>66b</sup>, allyl alcohol<sup>66c</sup>, decene<sup>66d</sup> dodecene<sup>66e</sup> styrene<sup>66f</sup> and 1,4 diacetoxy butene<sup>66g</sup>. The trends observed are generally first order with respect to catalyst, substrate (upto a certain concentration) and hydrogen, whereas inhibition was observed with partial pressure of CO. Kalck and co-workers<sup>246</sup> have studied the hydroformylation of terminal olefins using a dimeric  $[\text{Rh}(\mu\text{-S}^t\text{Bu})(\text{CO})(\text{PPh}_3)]_2$  catalyst. Preliminary kinetic studies show that CO has an inhibiting effect but surprisingly the reaction is also inhibited by high pressure of hydrogen.

The kinetics of hydroformylation of propylene<sup>247a</sup>, allyl alcohol<sup>71b</sup> and 1-butene<sup>71c</sup> using supported liquid phase catalyst (SLPC)  $\text{HRh}(\text{CO})(\text{PPh}_3)_3$  has been investigated. The reaction order for propylene was found to be one, while for hydrogen the order was close to zero. The reaction order in CO pressure was found to 0.23 at lower CO pressure



to 0.08 at higher CO pressure. The kinetics of hydroformylation of 1-octene<sup>248</sup>, styrene<sup>67c</sup> and linalool<sup>249</sup> was studied using Rh/TPPTS supported aqueous phase catalyst (SAPC). The trends were similar to those observed in the homogeneous medium except for the substrate inhibition observed at higher concentration. Similar observations were reported for the kinetics of hydroformylation of 1-hexene using Rh/TPPTS complex exchanged on anion exchange resin<sup>250</sup>.

In general, the trends observed for kinetics of hydroformylation using phosphine-modified rhodium catalysts for different parameters can be summarized as follows.

1. First order in catalyst concentration
2. First order in hydrogen partial pressure
3. First order in olefin concentration and in some cases substrate inhibition at higher concentration.
4. At lower CO partial pressure ( $P_{CO} < 1$  MPa), positive order and at high CO partial pressure, negative order

### **1.5. Scope and Objectives of the Thesis**

Multiphase reactions in which reactants in different phases are converted into one or more selective products using homogeneous or heterogeneous catalyst provide the basis for a large number of chemical, petrochemical, biochemical and polymer processes. Liquid Phase Oxidation (LPO) and hydroformylation are two of the most prominent examples of multiphase catalytic reactions in industry. These reactions have been employed for synthesis of a variety of industrial products such as aldehydes, ketones, alcohols, and carboxylic acids etc, which proceed through a cleaner, cheaper and eco-friendly alternate route than the conventional pathways.

The state of the art on multiphase catalytic reactions shows that, the focus to analyze multi-step, complex multiphase reactions has been inadequate. Considering the increasing importance of catalysis in complex catalytic reactions for fine chemicals, pharmaceuticals and specialty products, there is a need to investigate case studies on catalysis and reaction engineering aspects. At the same time, it is also important to explore new types of catalysts and catalytic systems, which can provide better activity,

selectivity to the desired products. In the present era of green chemistry, the major emphasis is on alternative pathways for fine and specialty chemicals with the aim to enhance atom economy, and to reduce use or generation of wastes. The tremendous potential that the area of catalysis carries can further be strengthened and put to commercial use in a better way if the kinetics and reaction engineering aspects of catalytic transformations are thoroughly studied and implemented. Scale-up of new oxidation chemistries from invention to commercial operations can be facilitated and proceed with a higher probability of success if reaction engineering principles are incorporated and applied at various stages in process development program. For example, evaluation of new catalyst technology for activity, selectivity, and other measures of performance requires the use of modern laboratory reactor systems in which transport disguises are negligible so that the true kinetics can be studied as part of the catalyst screening methodology. Proper understanding of all of these may lead to further advancement of the catalysis and reaction engineering of the present age. Keeping these objectives in the background, the specific targets have been chosen for the present work as follows,

- ✓ Selective liquid phase oxidation of toluenes to benzaldehydes
- ✓ Selective oxidation of ethylbenzene using hydrotalcite like compounds as catalyst
- ✓ Hydroformylation of 6-methoxy-2-vinylnaphthalene as a potential route for the synthesis of naproxen
- ✓ Hydroformylation of vinyl acetate monomer as potential route for the synthesis of hydroxy propionic acids

## References

---

1. M.P. Dudukovic, *Catalysis Today* 48 (1999) 5.
2. J.J. Lerou, K.M. Ng, *Chem. Eng. Sci.* 51 (1996) 1595
3. P.L. Mills, R.V. Chaudhari, *Catalysis Today* 48 (1999) 17
4. C. O. Bennett, *Advances in Catalysis* 44 (2000) 329.
5. R.A. Sheldon, R.S. Downing, *Applied Catalysis A: General* 189 (1999) 163
6. F. J. Keil, *Chemical Engineering Science* 59 (2004) 5473
7. P.L. Mills, R.V. Chaudhari, *Catalysis Today* 37 (1997) 367
8. R.A. Sheldon, R.S. Downing *Applied Catalysis A: General* 189 (1999) 163
9. M.Beller, C. Bolm, (Eds.), *Transition Metals for Organic Synthesis: Building Blocks and Fine Chemicals*, VCH, Weinheim 1 (1998)
10. H.U. Blaser, E. Schmidt, Ed., *Asymmetric Catalysis on Industrial Scale: Challenges, Approaches and Solutions*. Wiley-VCH Verlag Gmb H and Co. KGaA, (2004)
11. J. Falbe, *J. Organomet. Chem.* 94 (1975) 213
12. A.G. BASF, *Hydrocarbon Process* 11 (1977) 135
13. A.G. BASF, *Hydrocarbon Process* 11 (1977) 172.
14. J. Roth, J. Craddock, A. Hershmann, F. Paulik, *Chemtech.* (1971) 600
15. (a) J. F. Roth, *Platinum Met. Rev.* 19, (1975) 12 (b) F. E. Paulik, J. F. Roth, *Chem. Commun.* (1968) 1578.
16. C. S. Garland, M. F. Giles, J. G. Sunley, *Eur. Pat.* 643034 (1995)
17. C. S. Garland, M. F. Giles, A. D. Poole, J. G. Sunley, *Eur. Pat.* 728726 (1994)
18. K. Zeigler, *Brit. Pat.* 799392 (1958).
19. H. Hohenshutz, N. Kutepow, W. Himmele, *Hydrocarbon Process* 45 (1966) 141
20. A. Onopchenko, J.G. D. Schultz, R. Seekircher, *U.S. Patent* 3644512 (1972)
21. M. Beller, C. Bolm, Ed. *Transition Metals for Organic Synthesis: Building Blocks and Fine Chemicals*, VCH, Weinheim 1 (1998)
22. H.U. Blaser, E. Schmidt, *Asymmetric Catalysis on Industrial Scale: Challenges, Approaches and Solutions*. Wiley-VCH Verlag GmbH and Co. KGaA (2004)
23. B. Cornils, W.A. Herrmann, Ed. *Aqueous-Phase Organometallic Catalysis*. VCH, Weinheim (1998)
24. G.W. Parshall, W.A. Nugent, *CHEMTECH* 18 (1988) 184.
25. C. Mathieu, E. Dietrich, H. Delmas and H. Jenck, *J. Chem. Eng. Sci.* 47 (1992) 2289.
26. C. Neff and E Bounomo, *Eur. Pat. Appl.* 102 (1984) 997
27. M. Besson, G. Fleche, P. Fuertes, P. Gallezot, E Lahmer, paper presented at the

- 
- Europacat Meeting, Montpellier, France Paper abstract of the conference abstracts 2 (1993) 416.
28. I. Nikov and K. Paev, *Catal. Today* 24 (1995) 41.
  29. Y. Yamamoto, Y. Inoue, H. Suzuki, *Shokubai (Catalyst)* 37 (1995) 179.
  30. M. Otake, *Chem. Tech.* 36 (1995).
  31. H. Loewe and A. Forsch, *ECT* 15 (1981) 757.
  32. G.W. Parshall and W.A. Nugent, *Chem. Tech.* (1988) 184.
  33. S.C. Stinson, *Chem. Eng. News*, June and September (1986).
  34. H. van Bekkum and H.W. Kouwenhoven, *Stud. Surf. Sci. Catal.* 41 (1988) 45.
  35. J.B. Powell, L.H. Slauch, S.B. Mullin, T.B. Thomason, P.R. Weider US 5981808 (1999).
  36. I.V. Kozhevnikov, *Catal. Rev. Sci. Eng.* 37 (1995) 311
  37. Japan Kokai Patents 81255 (1991).
  38. R. Jira, *Ethylene and its industrial derivatives*, Miller S.A. (Ed.), Ernest Benn Ltd. (1969) 650
  39. G. Cao, A. Servida, M. Pisu and M. Morbidelli, *AIChE J.* 40 (1994) 1156
  40. S.J. Tremont, P.L. Mills and P.A. Ramachandran, *Chem. Eng. Sci.* 43 (1988) 2221
  41. R.A. Sheldon and J.K. Kochi, *Metal-Catalyzed Oxidations of Organic Compounds*, Academic Press, New York (1981).
  42. P.L. Millsa, R.V. Chaudhari, *Catalysis Today* 48 (1999) 17
  43. R.A. Sheldon, in: L.I. Simandi (Ed.), *Dioxygen Activation and Homogeneous Catalytic Oxidation*, Elsevier, Amsterdam (1991) 573
  44. R.A. Sheldon, J. Dakka, *Catalysis Today* 19 (1994) 215
  45. A. K. Suresh, M. M. Sharma, T. Sridhar, *Ind. Eng. Chem. Res.* 39 (2000) 3958
  46. A. Farkas, *Catal. Rev. Sci. Eng.* 21 (1980) 183.
  47. D. Jones, *Chemistry and Industry*; Ed.; Clarendon Press: Oxford, U.K. (1967) 33.
  48. R. Landau, A. Saffer, *Chem. Eng. Prog.* 64 (1968) 20.
  49. W. Partenheimer, *Catal. Today* 2 (1995) 69.
  50. S. Ciborowski, L. Simandi, Ed. *Studies in Surface Science and Catalysis Series*; Elsevier: Amsterdam (1991) 66.
  51. K. Weissermel, H. J. Arpe, *Industrial Organic Chemistry 2<sup>nd</sup> Ed.*; VCH: Weinheim, Germany, translated by C. R. Lindley (1993).
  52. N. M. Emanuel, E.T. Denisov, Z.K. Maizus, *Liquid-Phase Oxidation of Hydrocarbons*; Plenum Press: New York, translated by B. J. Hazzard. (1967)
  53. A.K. Roby, J. P. Kingsley, *Oxidize safely with pure oxygen. CHEMTECH* 26 (1996) 26
  54. W.D. Jones, *Science* 287 (2000) 1942.
  55. F. Wang, J. Xu, X. Li, J. Gao, L. Zhou, R. Ohnishi, *Adv. Synth. Catal.* 347 (2005) 1987.
  56. T. Tzedakis, A.J. Savall, *Ind. Eng. Chem. Res.* 31 (1992) 2475.
  57. R.A. Sheldon, N. de Heij, *Stud. Org. Chem.* 33 (1988) 234.
  58. C. Jongasma, W. Laugs, EP 0026507 (1981).
  59. S. Imamura, K. Fukuda, T. Nishida, T. Inui, *J. Catal.* 93 (1985) 186.

- 
60. C. Subrahmanyam, B. Louis, F. Rainone, B. Viswanathan, A. Renken, T. K. Varadarajan, *Catal. Commun.* 3 (2002) 3.
  61. A. Martin, U. Bentrup, A. BrPckner, B. LPcke, *Catal.Lett.* 59 (1999) 61.
  62. H.V. Borgaonkar, S.R. Raverkar, S.B. Chandalla, *Ind. Eng. Chem. Prod. Res. Dev.* 23 (1984) 455
  63. S.K. Ray, P.N. Mukherjee, *Indian J. Technol* 21 (1983) 4137
  64. F. Bruhne, E. Wright, *Ullmanns Encyclopedia of Technical Chemistry* 6<sup>th</sup> Ed., (1998).
  65. F. Konietzni, U. Kolb, U. Dingerdissen, W.F. Maier, *J.Catal.* 176 (1998) 527.
  66. F. Konietzni, H.W. Zanthoff, W.F. Maier, *J. Catal.* 188 (1999) 154.
  67. Y. Ishii, S. Sakaguchi, T. Iwahama, *Adv. Synth. Catal.* 343 (2001) 393.
  68. K. Nomiya, K. Hashino, Y. Nemoto, M. Watanabe, *J.Mol. Catal. A* 176 (2001) 79.
  69. T. Garrell, S. Cohen, G. C. Dismukes, *J. Mol. Catal. A* 187 (2002) 3.
  70. A. R. Zhu, S. C. Tsang, *Chem. Commun.* (2002) 2044.
  71. K. R. Seddon, A. Stark, *Green Chem.* 2 (2002) 119
  72. C. F. Hendriks, H. C. A. van Beek, P. M. Heertjes, *Ind. Eng. Chem. Prod. Res. Dev.* 17 (1978) 256.
  73. C. Guo, Q. Liu, X. Wang, H. Hu, *App. Catal A: General* 282 (2005) 55.
  74. H.V. Borgaonkar, S.R. Raverkar, S.B. Chandalla, *Ind. Eng. Chem. Prod. Res. Dev.* 23 (1984) 455.
  75. C. Guo, Q. Liu, T. Xu, H. Hu, *Applied Catalysis A: General* 282 (2005) 55
  76. M.A. Gonzalez, S.G. Howell, S.K. Sikdar, *J. Catal.* 183 (1999) 159.
  77. D. Mansuy, *Coord. Chem. Rev.* 125 (1993) 129
  78. W. Partenheimer, *Catal. Org. Reactions* Ed. Herkes, EF.E., Marcel Dekker, Inc. New York (1998).
  79. W. Parteinheimer, *J.Mol.Catal. A: General* 67 (1991) 35.
  80. M. L. Kantam, B. M. Choudary, P. Sreekanth, K. K. Rao, K. Naik, T. Prathap Kumar, A. Khan US 6495726 (2002).
  81. M. L. Kantam, P. Sreekanth, K. K. Rao, T. P. Kumar, P.C. Bhavanari, B.M. Choudary, *Catal. Lett.* 81 (2002) 223.
  82. K. Bahranowski, R. Dula, M. Labanowska, A. Michalik, L.A.Vartikian, E.M. Serwick, *Appl. Clay Sci.* 18 (2001) 93.
  83. J. Gao, X. Tong, X. Li, H. Miao, J.J.Xu, *Chem. Technol. Biotechnol.* 82 (2007) 620.
  84. C. F. Hendriks, H. C. A. van Beek, and P. M. Heertje, *Ind. Eng. Chem. Prod. Res. Dev.* 17 (1978) 3.
  85. J. Gao, X. Tong, X. Li, H. Miao and J. Xu, *J Chem Technol Biotechnol* 82 (2007) 620
  86. F. Wang, J. Xu, X. Li, J. Gao, L. Zhou, R. Ohnishi, *Adv. Synth. Catal.* 347 (2005)

- 
- 1987.
87. J. Carpentier, J.F. Lamonier, S. Siffert, E.A. Zhilinskaya, A. Abouka, *Applied Catalysis A: General* 234 (2002) 91
88. C. Guo, Q. Liu, X. Wang, H. Hu *Applied Catalysis A: General* 282 (2005) 55
89. J. Wang, H. Fang, Y. Li, J. Li, Z. Yan, *J. of Molecular Catalysis A: Chemical* 250 (2006) 75.
90. A. Hu, C. Lu, H. Wang, B. Li, *Catalysis Communications* 8 (2007) 1279
91. B. Chou, J.Tsai, S. Cheng, *microporous and mesoporous materials* 48 (2001) 309
92. J.A.A. Hoorn, P.L. Alsters G.F. Versteeg, *International J. of Chemical Reactor Engineering* 3 (2005) A6
93. R. V. Chaudhari, V. H. Rane, A.S. Deshmukh, S.S. Divekar. US 0135820 A1 (2006)
94. R. V. Chaudhari, K.B. Rajurkar, S.S. Tonde., V. H. Rane., US7411099B2 (2008)
95. G.A. Olah, *Friedel–Crafts and Related Reactions*, Wiley–Interscience, New York, (1963)
96. P.H. Groggins, R.H. Nagel, *Ind. Eng. Chem.* 26 (1934) 1313
97. S.D. Borkar, B.M. Khadilkar, *Synth. Commun.* 29 (1999) 4295
98. N.D. Valechha, A. Pradhan, *J. Indian Chem. Soc.* 61 (1984) 909
99. A. Shaabani, A. Bazgir, F. Teimouri, D.G. Lee, *Tet. Lett.* 43 (2002) 5165
100. V.R. Chaudhari, J. R. Indurkar, V.S. Narkhade, R. Jha, *Journal of Catalysis* 227 (2004) 257
101. B.B. Wentzel, M.P.J. Donners, P.L. Alsters, M.C. Feiters, R.J.M. Nolte, *Tetrahedron* 56 (2000) 7797
102. V.R. Chaudhari, J. R. Indurkar, V.S. Narkhade, R. Jha, *J. of Catalysis* 227 (2004) 257.
103. B. Notari, *Stud. Surf. Sci. Catal.* 37 (1987) 413.
104. B. Notari, *Stud. Surf. Sci. Catal.* 60 (1991) 343
105. J.S. Reddy, R. Kumar, P. Ratnasamy, *Appl. Catal.* 58 (1990) L1
106. P. Kumar, R. Kumar, B. Pandey, *Syn. Lett.* (1995) 289.
107. P. Ratnasamy, R. Kumar, *Stud. Surf. Sci. Catal.* 97 (1995) 501.
108. J.D. Chen, R.A. Sheldon, *J. Catal.* 153 (1995) 1.
109. J.D. Chen, M.J. Haanepen, J.H.C. van Hooff, R.A. Sheldon, *Stud.Surf. Sci. Catal.* 84 (1994) 973.
110. R.H. Fish, K.J. Oberhausen, S. Chen, J.F. Richardson, W. Pierce, R.M. Buchanan, *Catal. Lett.* 18 (1993) 357.

- 
111. S. Menage, J.M. Vincent, C. Lambeaux, M. Fontecave, *J. Chem. Soc., Dalton Trans.* (1994) 2081.
112. N. Kitajima, M. Ito, H. Fukui, Y. Moro-oka, *J. Chem. Soc., Chem. Commun.* (1991) 102.
113. S. Vetrivel, A. Pandurangan, *J. of molecular catalysis A: Chemical* 217 (2004) 165.
114. J.D. Chen, M.J. Haanepen, J.H.C. van Hooff, R.A. Sheldon, *Stud. Surf. Sci. Catal* 84 (1994) 973.
115. D. Tetrard, A. Rabion, J.B. Verlhac, J. Guilhem, *J. Chem. Soc. Chem. Commun.* (1995) 531.
116. F. Cavani, F. Trifiro, A. Vaccari, *Catal. Today* 11 (1991) 173
117. S. Vetrivel, A. Pandurangan., *J. of Molecular Catalysis A: Chemical* 217 (2004) 165
118. N.D. Valechha, A. Pradhan, *J. Indian Chem. Soc.* 61 (1984) 909.
119. T.H. Bennur, D. Srinivas, S. Sivasanker *Journal of molecular catalysis A: Chemical* 207 (2004) 163
120. B. Notari, *Stud. Surf. Sci. Catal.* 37 (1987) 413
121. T.K. Das, K. Chaudhari, E. Nandan, A.J. Chandwadkar, A. Sudalai, T. Ravindeanathan and S. Sivasanker, *J. Catalysis.* 38 (1997) 3631
122. S.S. bhoware, S. Shylesh, K.R. Kamble, A.P. Singh *Journal of molecular catalysis* 255 (2006) 123
123. G.L. Tambe, P.A. Ganeshpure, *Indian Journal of Chem.. Sect. B.: Org. Chem. Incl. Med. Chem.* 38B (1999) 611
124. T.H. Bennur, S. Sabne, S.S. Deshpande, D. Srinivas, S. Sivasanker *Journal of molecular catalysis A: Chemical* 185 (2002) 71
125. K.O. Xavier, J. Chacko, K.K. Mohammed Yusuff, *Applied catalysis A: General* 258 (2004) 251
126. M. Klopstra, R. Hage, R. M. Kellogg and B. L. Feringa *tetrahedron letters* 44 (2003) 4581
127. Z. Lounis, A Riahi, F. Djafri, J. Muzart, *Applied Catalysis A:General* 309 (2006) 270
128. N. Mizuno, M. Misono, *Chem. Rev.* 98 (1998) 199.
129. D. H. R. Martell, A. E. Sawyer, *The Activation of Dioxygen and Homogeneous Catalytic Oxidation*; Barton,., Eds.; Plenum Press: New York, (1993)
130. L. Simandi, , *Catalytic Activation of Dioxygen by Metal Complexes*; Kluwer Academic Publisher: Boston, (1992).
131. Y. Owobi-Andely, *Catal. Today* 56 (2000) 173
132. M. Misono, *Catal. Rev. Sci. Eng.* 29 (1987) 269
133. N. Mizuno, M. Misono, *Chem. Rev.* 98 (1998) 199.
134. A. Corma, A. Martinez, *Catal. Rev. Sci. Eng.* 36 (1993) 483.

- 
135. S. Mukhopadhyay *Org. Proc. Res. Dev.* 3 (1999) 365
  136. P. Fristrup, L. B. Johansen, C. H. Christensen *Chem. Commun.* (2008) 2750.
  137. J. Choi, Y. Chang, S. Hong *Tetrahedron Letters* 29 (1988) 1967
  138. B. Bhatia and J. Iqbal, *Tetrahedron Letters* 33 (1992) 7961
  139. M. Wenkin, R. Touillaux, P. Ruiz, B. D. M. Devillers, *Applied Catalysis A: General* 148 (1996) 181
  140. J.K Choi, Y.K Chang, S. Y. Hong *Tetrahedron Lett.* 29 (1988) 1967.
  141. S. Mukhopadhyay, *Organic Process Research and Development* 3 (1999) 365
  142. F. Vocanson, Y.P. Guo, J.L. Nay and H.B. Kagan, *Synthetic Communications* 28 (1998) 2577
  143. B. Hwang, *Ind Eng chem. Res.* 33 (1994) 1897
  144. B.Bhatia, J. Iqbal, *Tetrahedron Letters* 33 (1992) 7961
  145. S. Biella, L. Prati, M. Rossi, *J. of Molecular Catalysis A: Chemical* 197 (2003) 207
  146. A. N. Kharat, P. Pendleton, A. Badalyan, M. Abedini, M. M. Amini, *Journal of Molecular Catalysis A: Chemical* 175 (2001) 277.
  147. H. Chen, T. An, Y. Fang, K. Zhu *Journal of Molecular Catalysis A: Chemical* (1999) 165
  148. E. Dalcanele, F. Montanari, *J. Org. Chem.* 51 (1986) 567
  149. H. Wojtowicz, M. Brzasczcz, J. Malochowski, *Tetrahedron letter* 57 (2001) 9743
  150. K. Sato, M. Hyodo, J. Takagi, M. Aoki, R. Noyori, *Tetrahedron Letters* 41 (2000) 1439
  151. M. Lim, C. Yoon, G. Anc, H. Rhee, *Tetrahedron Letters* 48 (2007) 3835
  152. O.A. Kholdeeva, M.P. Vanina, M.N. Timofeeva, R.I. Maksimovskaya, T.A. Trubitsina, M.S. Melgunov, E.B. Burgina, J. Mrowiec-Bialon, A.B. Jarzebski, C.L. Hill, *Journal of Catalysis* 226 (2004) 363.
  153. K. Kervinen, H. Korpi, M. Leskelä, T. Repo, *J. of Molecular Catalysis A: Chemical* 203 (2003) 9
  154. C.C.Hobbs, E.H. Drew, H.A. Van't Hof, F.G. Mesich, M.J. Onore, *Ind. Eng. Chem. Prod. Res. Dev.* 11 (1972) 220.
  155. G.W. Parshall, *Homogeneous Catalysis*, Wiley-Interscience, New York, (1980)
  156. J.K. Kochi, *Organometallic Mechanisms and Catalysis*, Academic Press, New York, (1978).
  157. C. Masters, *Homogeneous Transition-Metal Catalysis*, Chapman and Hall, London, (1981).
  158. A.K. Suresh, M. M. Sharma, T. Sridhar, *Ind. Eng. Chem. Res.* 39 (2000) 3958
  159. S.J. Tremont, P.L. Mills, P.A. Ramachandran, *Chem. Eng.Sci.* 43 (1988) 2221
  160. N.M. Emanuel, E.T. Denisov, Z.K. Maizus, *Liquid-Phase Oxidation of Hydrocarbons*; Plenum Press: New York, translated by B. J. Hazzard., (1967)
  161. R. A. Sheldon, J.K. Kochi, *Metal-Catalyzed Oxidations of Organic Compounds*; Academic Press: New York (1981).



- 
162. I.V. Berezin, E.T. Denisov, N.M. Emanuel, *The Oxidation of Cyclohexane*; Pergamon Press: Oxford, U.K. translated by K. A. Allen. (1966)
163. W. Partenheimer, *Catal. Today* 23 (1995) 69.
164. W. Partenheimer, A chemical model for the Amoco "MC" oxygenation process to produce terephthalic acid. In *Catalysis of organic reactions*; Blackburn, D., Ed.; Marcel Dekker: New York (1990) 321.
165. I.C.W.E. Arends, R.A. Sheldon *App. Catal. A: General* 212 (2001) 175
166. W. Partenheimer, *Catal. Today* 23 (1995) 69.
167. R.A. Sheldon, J.K. Kochi, *Metal-Catalyzed Oxidations of Organic Compounds*; Academic Press: New York, (1981).
168. R.A. Sheldon, *Top. Curr. Chem.* 164 (1993) 21.
169. R.A. Sheldon, *Chemtech.* (1991) 566.
170. P.A. MacFaul, I.W.C.E. Arends, K.U. Ingold, D.D.M. Wayner, *J. Chem. Soc. Perkin Trans.*, 2 (1997) 135.
171. I.W.C.E. Arends, K.U. Ingold, D.D.M. Wayner, *J. Am. Chem. Soc.* 117 (1995) 4710.
172. W.A. Herrmann, B. Cornils, *Angew. Chem. Int. Ed. Engl.*, 36 (1997) 1048
173. B.M. Trost, *Angew. Chem. Int. Ed. Engl.*, 34 (1995) 259
174. O. Rolen DE 849548, (1938).
175. (a) B. Cornils, *New Synthesis with Carbon Monoxide* (Eds. J. Falbe) Springer-Verlag, Berlin, Heidelberg, New York, (1980). (b) P. W. N. M. van Leeuwen C. Claver (Ed.) *Rhodium catalyzed Hydroformylation* Kluwer Academic Publishers (2000).
176. (a) H. Moell, BASF AG DE 1272911, (1966). (b) F. M. Hibbs, ICI Ltd. GB 1458375 (1976). (c) R. Papp, F. Mongenet, DE-OS 2927979 (1980). (d) Ruhrchemie AG., *Hydrocarbon Proc.*, 11 (1977) 134.
177. C. R. Greene, R. E. Meeker, Shell Oil Co. US 3274263, (1966)
178. R. L. Pruett, J. A. Smith, US 3917661, (1975).
179. E. G. Kuntz, *CHEMTECH* (1987) 570.
180. M. Beller, *J. Mol. Catal A: Chemical* 104 (1995) 17.
181. J. T. Carlock, *Tetrahedron* 40 (1984) 185.
182. (a) F.A. Cotton, B. Hong, *Progress Inorg. Chem.* 40 (1992) 179. (b) H.A. Mayer, W. C. Kaska, *Chem. Rev.* 94 (1994) 1239.
183. L. H. Pignolet (Ed.) *Homogeneous Catalysis with Metal Phosphine Complexes*, Plenum Press, London (1983).
184. (a) A. J. Arduengo, R. L. Harlow, M. Kline, *J. Am. Chem. Soc.* 113 (1991) 361. (b) D. A. Dixon, A. J. Arduengo, *J. Phys. Chem.* 95 (1991) 4180. (c) A. J. Arduengo, H. V. Rasika-Diaz, R. L. Harlow, M. Kline, *J. Am. Chem. Soc.* 114 (1992) 5530.
185. P.W.N. M. van Leeuwen, C. Claver (Eds.) *Rhodium catalyzed Hydroformylation*

- 
- Kluwer Academic Publishers (2000).
186. K. Weissemel, H.J. Arpe., *Industrial Organic Chemistry*, 3<sup>rd</sup> Ed., Verlag Chemie, Weinheim (1997) 76.
  187. A. Yamamoto, Ed. in *Kirk-Othmer, Encyclopedia of Chemical Tehnology*, 3rd edn., Wiley, New York 2 (1978) 410
  188. H. Distler, R. Widder, E. Pommer, DOS 2019535 (1970), BASF; *Chem. Abstr.*, 76 (1972) 46068
  189. B. Zeeh, F. Linhart, E. H. Pommer, DBP 2455082 (1974), BASF *Chem. Abstr.* 85, (1976) 142972.
  - 190 H. B. Tinkar US4072709 (1978)
  191. S. Owaki, S. Kitamura *Japan. Kokai* 76 (1976) 122034
  192. G. Papadogianakis, L. Matt, R.A. Sheldon, *J. Chem. Tech., Biotechnol.* 70 (1997) 83.
  193. P. Papadogianakis, R.A. Sheldon, in *Aqueous-Phase Organometallic Catalysis* (B. Cornils, W.A. Hermann (Eds.)) Wiley- VCH, New York, (1998).
  194. G.W. Parshall, *Homogeneous Catalysis*, Wiely-Insterscience Pub., (1980).
  195. H Shimizu, H. Hirano, Y. Matsumura, Y. Nomura, S. Uchida, A. Sato, *Eur. Pat. Appl.* 170 (1986) 147.
  196. G. Muller, D. Sainz and J.J. Sales, *J. Mol. Catal.* 63 (1990) 173.
  197. D. Neibecker, R. Reau, S.J. Lecolier , *Org. Chem.* 54 (1989) 5208.
  198. C. Bergounhou, D. Neibecker and D. Reau, *Chem. Commun.* (1988) 1370.
  199. P.W.N.M. van Leeuwen, C.F. Roobeek, *J. Organomet. Chem.* 258 (1983) 343.
  200. V. Elango, M.A. Murphy, B.L. Smith, K.G. Davenport, G.N. Mott,G. L. Moss, US 4,981,995 (1991)
  201. P.J.Harrington, E. Lodewijk, *Org. Process Res. Dev.* 1 (1997) 72
  202. C. Jordano, G. Castaldi, F. Uggeri , *Angew. Chem., Int. Ed. Engl.* 23 (1984) 413.
  203. J.P. Rieu, A. Boucherle,H. Coussr, G. Mouzin, *Tetrahedron* 42 (1986) 4095.
  204. D. Neibecker, R Reau, S.J. Lecolier, *J. Org. Chem.* 54 (1989) 5208
  205. H.R. Sonawane, N.S. Bellur, J.R. Ahuja, D.G. Kulkarni, *Tetrahedron Asymmetry* 3 (1992) 163.
  206. C. Giordano, G. Castaldi, S. Cavicchioli, M. Villa, *Tetrahedron* 1989, 45, 4243.
  207. T. Ohta, H. Takaya, M. Kitamura, K. Nagai, R.J. Noyori, *J. Org. Chem.* 52 (1987) 3174.
  208. J.H. Wagenknecht, U.S. 4,601,797 (1986).
  209. J.K.Stille, H. Su,P. Brechot,G. Parinello,L.S. Hegedus, *Organometallics* 10 (1991) 1183.
  210. T. Hiyama, N. Wakasa, T. Kusumoto, *Synlett* (1991) 569.
  211. (a) H. Alper, N.J. Hamel, *J. Am. Chem. Soc.* 112 (1990) 2803. (b) H. Alper, WO 91 03452 (1991).

- 
212. (a) T.V. RajanBabu, A.L. Casalnuovo, *J. Am. Chem. Soc.* 114 (1992) 6265. (b) A.L. Casalnuovo, T.V. RajanBabu, U.S. 5175335 (1992)
213. L.F. Tietze, U. Beifuss, *Angew. Chem.* 105 (1993) 137.
214. R.A. Bunce, *Tetrahedron* 51 (1995) 131.
215. L.F. Tietze, *Chem. Rev.* 96 (1996) 115.
216. R.L. Pruet, *Adv. Organomet. Chem.* 17 (1979) 1.
217. H. Siegel, W. Himmele, *Angew. Chem.* 92 (1980) 182.
218. A.W.S. Currie, J.A. Andersen, *Catal. Lett.* (1997) 109.
219. C. Botteghi, R. Ganzerla, M. Lenarda, G. Moretti, *J. Mol. Catal.* 40 (1987) 129.
220. R. Baker, R.H. Herbert, *Nat. Prod. Rep.* 1 (1984) 299.
221. T.L.B. Boivin, *Tetrahedron* 43 (1987) 3309.
222. Y. L. Borole, R. V. Chaudhari *Ind. Eng. Chem. Res.* 44 (2005) 9601
223. L.F. Tietze, *Chem. Rev.* 96 (1996) 115.
224. R.L. Pruet, *Adv. Organomet. Chem.* 17 (1979) 1.
225. H. Siegel, W. Himmele, *Angew. Chem.* 92 (1980) 182.
226. C. Jaramillo, S. Knapp, *Synthesis* (1994) ,1.
227. B. Kitsos-Rzychon, P. Eilbracht, *Tetrahedron* 54 (1998) 10721
228. E.N. Campi, W.R. Jackson, A.E. Trnacek, *Aust. J. Chem.* 49 (1996) 219.
229. C.L. Kranemann, P. Eilbracht, *Synthesis* (1998) 71.
230. C. Hollmann, P. Eilbracht, *Tetrahedron* (2000) 1685.
231. B. Fell, P. Hermanns, H. Bahrmann, *J. Prakt. Chem.* 340 (1998) 459
232. T. Sugioka, S.W. Zhang, N. Mori, T. Joh, S. Takahashi, *Chem. Lett* (1996) 249.
233. E. Yoneda, T. Sugioka, K. Hirao, S.W. Zhang, S. Takahashi, *J. Chem. Soc. Perkin Trans. I* (1998) 477.
234. T. Sugioka, E. Yoneda, K. Noitsuka, S.W. Zhang, S. Takahashi, *Tetrahedron Lett* 38 (1997) 4989.
235. C. Botteghi, M. Marchetti, S. Paganelli, F. Persi-Paoli, *Tetrahedron* 57 (2001) 1631.
236. B. Breit, W. Seiche, *Synthesis* 1 (2001) 1.
237. B. Fell, P. Hermanns, H. Bahrmann, *J. Prakt. Chem.* 340 (1998) 459.
238. T. Sugioka, S.W. Zhang, N. Mori, T. Joh, S. Takahashi, *Chem. Lett* (1996) 249.
239. T. Sugioka, S.W. Zhang, N. Mori, T. Joh, S. Takahashi, *Chem. Lett* (1996) 249.
240. M. Ahmed, A.M. Seayad, R. Jackstell, M. Beller, *J. Am. Chem. Soc.* 125 (2003) 10311
241. B. Cornils, *New Synthesis with carbon monoxide* Ed. J. Falbe, Springer-Verlag, Berlin, Heidelberg, New York (1980).
242. R.V. Gholap, O.M. Kunt, J.R. Bourne, *Ind. Eng. Chem. Res.* 31 (1992) 1597.
243. C.K. Brown, G. Wilkingson, *Journal of Chemical Society: A* (1970) 2753.
244. C. K. Brown, G. Wilkingson, *J. Chem. Soc. A* (1970) 2753
245. (a) R. M. Deshpande, R. V. Chaudhari, *Journal of catalysis* 115 (1989) 326. (b) R. M. Deshpande, R. V. Chaudhari, *Ind. Eng. Chem. Res.* 27 (1988) 133 (c) R. M. Deshpande, R. V. Chaudhari, *J. Mol. Catal.* 57 (1989) 177 (d) S. S. Divekar, R. M. Deshpande, R. V. Chaudhari, *Catal. Lett.* 21 (1993) 191. (e) B. M. Bhanage, S. S. Divekar, R. M. Deshpande, R. V. Chaudhari, *J. Mol. Catal. A: Chemical* 115 (1997)

- 
247. (f) V. S. Nair, S. P. Mathew, R. V. Chaudhari, *J. Mol. Catal. A: Chemical* 143 (1999) 99. (g) R. Chansarkar, K. Mukhopadhyay, A. A. Kelkar, R. V. Chaudhari, *Catalysis Today*, 51 (2003) 79. (h) R. M. Deshpande, B. M. Bhanage, S. S. Divekar, S. Kanagasabapathy, R. V. Chaudhari, *Ind. Eng. Chem. Res.*, 37 (1998) 2391
246. P. Kalck, F. Monteil, *Adv. in Organomet. Chem.* 34 (1992) 219.
247. (a) L. A. Girritsen, W. Klut, M. H. Vreugdenhil, J. J. F. Scholten, *J. Mol. Catal.* 9 (1980) 265. (b) N. A. Munck, J. P. A. Notenboom, J. E. Deleur, J. J. F. Scholten *J. Mol. Catal.*, 11 (1981) 233. (c) H. E. Pelt, R. P. J. Verburg, J. J. F. Scholten, *J. Mol. Catal.* 32 (1985) 77.
248. (a) U. J. Jauregui-Haza, E. P. Fontdevila, P. Kalck, A. M. Wilhelm, H. Delmas, *Catal. Today*, 409 (2003) 79 (b) U. J. Jauregui-Haza, O. Diaz-Abin, A. M. Wilhelm, H. Delmas, *Ind. Eng. Chem. Res.* 44 (2005) 9636.
249. M. Benaissa, U. J. Jauregui-Haza, I. Nikov, A. M. Wilhelm, H. Delmas, *Catalysis Today* 41 (2003) 79.
250. M. M. Diwakar, R. M. Deshpande, R. V. Chaudhari, *J. Mol. Catal. A: Chemical* 232 (2005) 179

## **Chapter 2**

# **Selective Liquid Phase Oxidation of Toluenes to Benzaldehydes**

Selective liquid phase air oxidation of toluenes using manganese based catalyst system consisting of Lewis acidic salts as co-catalysts and metal bromide as a promoter has been studied as a route for the synthesis of benzaldehydes. The experimental results on liquid phase oxidation of toluenes to benzaldehydes has been demonstrated and a detailed study has been reported using  $\text{Mn}(\text{OAc})_2/\text{FeCl}_3/\text{NaBr}$  as a catalyst system with toluene as a model substrate. The roles of the catalyst, co-catalyst, promoter, solvents and the reaction conditions on the catalyst activity and selectivity to benzaldehyde have been reported. With  $\text{Mn}(\text{OAc})_2 / \text{FeCl}_3$  as the catalyst system and  $\text{NaBr}$  as a promoter, 57.8 % selectivity to benzaldehyde has been achieved with a moderate conversion of toluene (19.2%). A possible mechanism to explain the liquid phase oxidation of toluene has also been discussed. Kinetics of liquid phase oxidation of toluene has been investigated and a rate equation proposed. This study would be valuable in developing an economical and environmentally benign route for synthesis of benzaldehydes via liquid phase oxidation of toluenes.

## 2.1. Introduction

Selective oxidation of the C-H bonds in methylbenzenes (e.g. toluene and derivatives) is a challenge as the intermediate products, aldehydes and alcohols formed are prone to further oxidation to corresponding carboxylic acids, lowering the selectivity<sup>1,2</sup> to the desired products. Liquid phase oxidation of aromatic hydrocarbons using molecular oxygen is a very attractive route from commercial and environmental viewpoint, as a wide range of oxygenated compounds can be produced by this process.<sup>3</sup> Aromatic aldehydes like benzaldehyde, chlorobenzaldehyde, fluorobenzaldehyde etc. are FDA approved synthetic flavoring substances and have extensive applications in food, pharmaceutical, dye, agricultural and perfumery industries<sup>4</sup>. Particularly, benzaldehyde is the most important aromatic aldehyde concerning industrial applications, and has a wide range of applications from food and pharmaceuticals to perfumery industry. Conventionally, benzaldehyde has been synthesized by chlorination of toluene followed by hydrolysis of the benzyl chloride<sup>5</sup>. From an industrial viewpoint, chlorination method suffers from disadvantages like high production cost, large amount of polluting residues, formation of byproducts, and troublesome product purification; besides the use of toxic chlorine and associated corrosion problems. However, for the production of benzaldehydes, of the grade acceptable to perfumery and pharmaceutical applications chlorine free products are required for which, the vapour phase oxidation of toluenes is an obvious alternative route. However, in the vapour phase oxidation of toluenes, the lower value carboxylic acids are formed as major products and benzaldehyde is only a minor product.<sup>6,7</sup> From the previous literature, it is also evident that, in vapour phase oxidation, the reaction conditions are too stringent; with temperatures  $> 773\text{K}$  and pressures in the range of 0.5-2.5 MPa, to achieve an optimum selectivity (best obtained ~25) to benzaldehyde<sup>8,9</sup>. The major challenge is to avoid the formation of benzoic acid and the loss of carbon in the form of gaseous products such as CO and CO<sub>2</sub><sup>10,11,12</sup> which is highly undesirable and adversely affects the atom economy. Hence, the interest in the development of an efficient and selective catalytic system for the air oxidation of toluene to benzaldehyde at milder reaction conditions is being revitalized.

The liquid phase catalytic oxidation of toluene to benzaldehyde has major advantages like avoiding the use of hazardous and toxic chlorine and mineral acids as raw

materials, improving the product quality and overall process economics due to cheaper oxidant (air). In most of the literature reports<sup>13,14,15</sup> the catalyst systems used for this reaction contain mainly cobalt or its salts. The cobalt bromide is shown to be a highly active catalyst for oxidation of methyl benzenes in acetic acid medium, yielding corresponding carboxylic acids as the major products<sup>16,17</sup> (e.g. toluene to benzoic acid). However, as the conversion increases, selectivity to aldehydes is lowered. With  $\text{MnCO}_3$  as a catalyst oxidation of toluene has been reported with poor conversion (6%) and 41.7% selectivity to benzaldehyde.<sup>18</sup> Attempts have been made for low temperature oxidation of toluene using Zn, Cu, Al-layered double hydroxide catalyst with hydrogen peroxide as the oxidant.<sup>19</sup> In MC-type (Mid Century, as it is used from 1950, mid of the century) catalyst systems with acidic solvents (acetic acid, benzoic acid and propionic acid) the aldehyde formed is usually further oxidized to the aromatic acid, thus reducing the aldehyde selectivity.<sup>20,21</sup> Recent developments showed significant improvement in the benzaldehyde selectivity by incorporation of metal salts like Mn, Cr, Ni, Mo etc.

In this chapter, a detailed study on the selective liquid phase air oxidation of toluenes to benzaldehydes using  $\text{Mn(OAc)}_2/\text{FeCl}_3/\text{NaBr}$  catalyst system is presented. Screening of different Lewis acid salt promoters and their effect on the conversion of toluenes and selectivity to aldehydes were investigated. The detailed parametric study was carried out using  $\text{Mn(OAc)}_2/\text{FeCl}_3/\text{NaBr}$  catalyst system and toluene as a model substrate. Comparative studies with cobalt catalyzed reaction have also been reported. The effect of catalyst and toluene concentration and oxygen partial pressure was studied on concentration-time profiles in a temperature range of 373-393K. Based on the results of these studies, a detailed kinetic analysis of oxidation of toluene is presented and rate equations proposed. This study would be valuable in developing an economical and environmentally benign catalytic route for the synthesis of benzaldehydes.

## **2.2. Experimental Section**

### **2.2.1. Materials**

Manganese (II) acetate tetrahydrate, cobalt, molybdenum (II) acetate dimer ( $\text{Mo(OCOCH}_3)_2$ ), ferric (III) chloride and sodium bromide were purchased from Loba Chemie, Mumbai (India) and used as such without further purification. Copper (II)

chloride, nickel (II) chloride, antimony (II) chloride, zinc (II) chloride, aluminium (III) chloride were purchased from Merck-India. The methylbenzenes like toluene, 2-chlorotoluene, 4-chlorotoluene, 2-bromotoluene, 4-bromotoluene, 2-iodotoluene, 4-iodotoluene, 2-fluorotoluene, 4-fluorotoluene were purchased from SD fine chemicals, Mumbai, India. Air and oxygen with 99% purity (Industrial Oxygen Company, Mumbai, India) were used as received. The solvents acetic acid, propionic acid, benzoic acid, NMP, methyl ethyl ketone, methanol, etc were purchased from SD Fine Chemicals, Mumbai, India and were freshly distilled and dried prior to use.

### **2.2.2. Experimental Procedure**

The liquid phase oxidation of toluene was carried out in a 300 ml capacity autoclave (Parr Instrument Co., IL, USA), which was equipped with arrangements for cooling, gas inlet/outlet and sampling of liquid and gas phases. Automatic temperature control, variable agitation speed, safety rupture disc, high temperature cut off and pressure recording by a transducer were also provided. A reservoir containing pure oxygen was used along with a constant pressure regulator for supply of oxygen to the reactor (Figure 2.1). Predetermined quantities of catalyst, promoter, substrate and acetic acid were charged in the reactor at room temperature. It was pressurized with air initially and the contents were then heated to a desired temperature. The depletion in the pressure (due to oxygen consumption) was made up by oxygen from a reservoir attached to the autoclave through a constant pressure regulator. For kinetic study the intermittent samples were taken through the sampling valve using chilled water condenser. The reactor was cooled to room temperature after completion of the reaction. The gases were analyzed by gas chromatography (GC) for the CO and CO<sub>2</sub> content. The liquid products were analyzed by GC and also confirmed by GCMS.



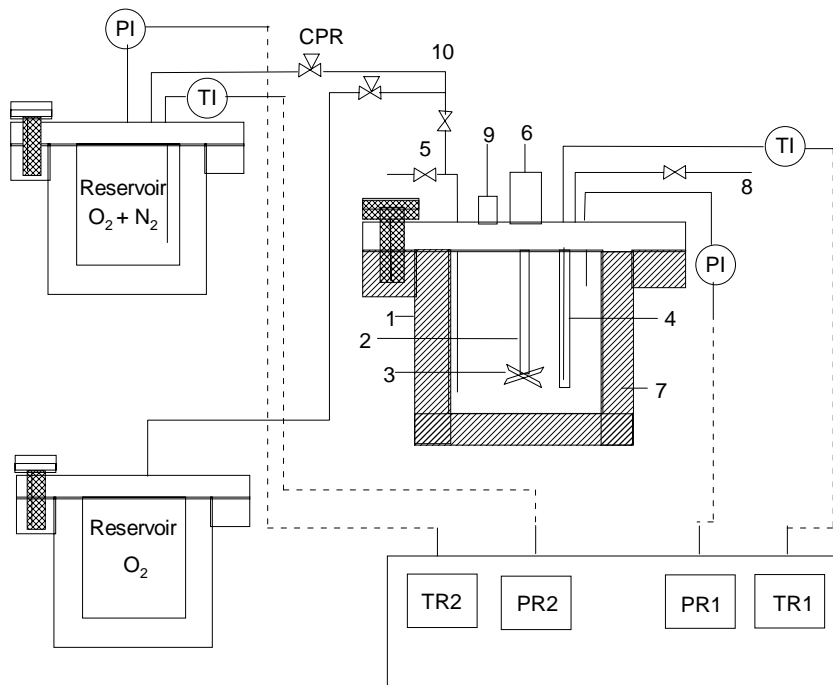


**Figure 2.1.** A schematic of the reactor setup for batch oxidation reactions (1) Reactor, (2) Stirrer Shaft, (3) Impeller, (4) Thermo-well, (5) Sampling valve, (6) Magnetic Drive Stirrer, (7) Furnace, (8) Outlet, (9) Rupture Disc, (10) O<sub>2</sub>-gas Inlet, TI: Thermocouple, PI: Pressure Transducer, CPR: Constant Pressure Regulator, TR1: Reactor Temperature Indicator, PR1: Reactor Pressure Indicator, PR2: Reservoir Pressure Indicator, TR2: Reservoir Temperature Indicator

### 2.2.3. Catalyst Recycle Procedure

After completion of the reaction, the reaction mixture was cooled to 283K and the gas inside the autoclave was slowly vented off. The liquid contents of the autoclave were concentrated at reduced pressure and at lower temperature (393K) to remove the volatiles. To the concentrate, about 20 ml toluene and equal volume of water were added, and mixed vigorously in a separating funnel. The organic layer was then separated, and washed with water ( $3 \times 25$  ml) to extract completely the water soluble catalyst components. The aqueous layers were mixed and concentrated on a rotary evaporator (rotavap) to obtain the catalyst solution, which was used for recycle experiments. The experimental procedure for recycle experiments was kept exactly the same as that of the typical oxidation procedure except that, instead of the fresh catalysts, the catalyst components recovered as above were used in recycle experiments.

#### 2.2.4. Work up Procedure for Isolation of Product

The organic layer separated in the catalyst recovery and recycle procedure as above was subjected to vacuum distillation to separate the organic products. The distillation was carried out under inert conditions by purging nitrogen through the distillation assembly. The reaction components, which comprised of unreacted toluene, benzaldehyde, benzyl alcohol and benzyl acetate, were isolated as separate distillation fractions.

#### 2.2.5. Analytical Methods

IR spectra were obtained using a Bio-Rad FTS 175C machine in transmission mode using KBr pellets. The products of the reactions were identified using GCMS analysis on an Agilent series 6890N GC equipped with a 5973N mass selective detector. Liquid samples were quantitatively analyzed for reaction products and unreacted toluene on a Hewlett-Packard 6890 series GC controlled by the HP-Chemstation software and equipped with an auto sampler unit, using an HP-FFAP capillary column (0.32 mm ID, 60 meters, 0.25 $\mu$ m film thickness. The oven temperature was programmed between 303-484 K. The products benzaldehyde, benzyl alcohol, benzyl acetate and benzoic acid were also identified using GC-MS (Agilent GC series 6890N equipped with a 5973N mass detector). The quantification of toluene, benzaldehyde, benzyl alcohol, benzyl acetate, benzoic acid were done based on the respective calibration curve. The results are discussed in terms of conversion, selectivity, turn over number (TON), turn over frequency (TOF) which are calculated as given below.

$$\text{Conversion, (\%)} = \frac{\text{Initial concentration of toluene} - \text{Final concentration of toluene}}{\text{Initial concentration of toluene}} \times 100$$

$$\text{Selectivity}_{\text{benzaldehyde}}, (\%) = \frac{\text{Number of moles of benzaldehyde formed}}{\text{Number of moles toluene converted}} \times 100$$

$$\text{Selectivity}_{\text{benzylalcohol}}, (\%) = \frac{\text{Number of moles of benzylalcohol formed}}{\text{Number of moles toluene converted}} \times 100$$

$$\text{Selectivity}_{\text{benzylacetate}}, (\%) = \frac{\text{Number of moles of benzyl acetate formed}}{\text{Number of moles toluene converted}} \times 100$$

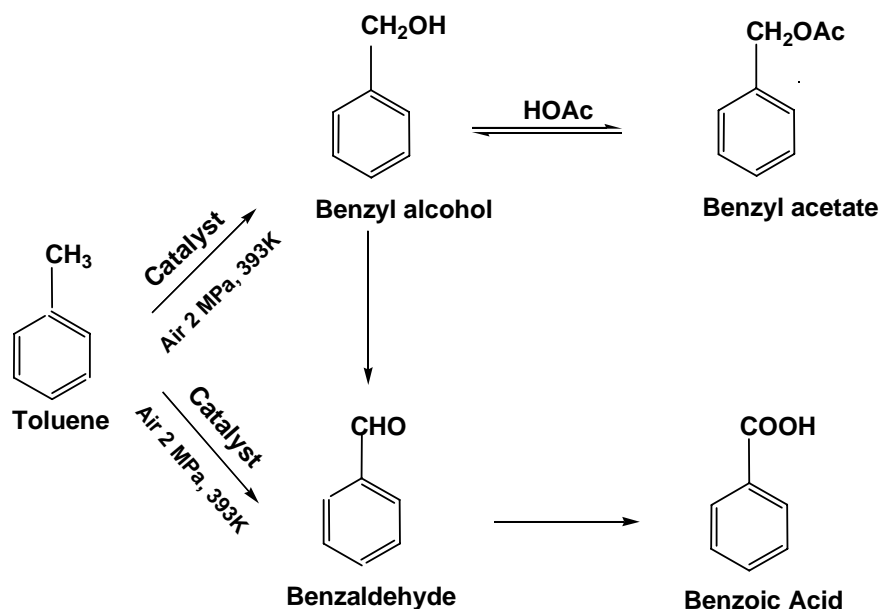
$$\text{Selectivity}_{\text{benzoicacid}}, (\%) = \frac{\text{Number of moles of benzoic acid formed}}{\text{Number of moles toluene converted}} \times 100$$

$$\text{TON} = \frac{\text{Number of moles of oxidation products formed}}{\text{Number of moles of catalyst}}$$

$$\text{TOF}, (h^{-1}) = \frac{\text{Number of moles of oxidation products formed}}{\text{Number of moles of catalyst} \times \text{time in hours}}$$

### 2.3. Results and Discussion

Liquid phase oxidation of toluene is a complex reaction system including various reactions in series and parallel as shown in the scheme 2.1. The oxidation of toluene is believed to proceed through benzyl alcohol. The free radical chain mechanism gives the oxidizability<sup>22</sup> of toluene, benzyl alcohol and benzaldehyde as 0.05, 0.85, and 290 respectively. Accordingly, for most of the catalyst systems known, it has been observed that the major product of toluene oxidation is benzoic acid. The side reaction of formation of benzyl acetate was also observed, because the esterification of benzyl alcohol takes place due to the presence of the acetic acid solvent. As the esterification is a reversible reaction, the benzyl alcohol gets converted into the benzyl acetate and vice versa as shown in the Scheme 2.1.



**Scheme 2.1.** Schematic of liquid phase oxidation of toluene

Oxidation experiments for toluene as substrate were carried out using air as the oxidant and  $\text{Mn}(\text{OAc})_2$  as a catalyst along with a co-catalyst ( $\text{FeCl}_3$ ) and promoter ( $\text{NaBr}$ ). The objectives of the present work were:

1. Develop active, selective and reusable catalyst system for liquid phase oxidation of toluene and its derivatives.
2. Optimize reaction conditions to achieve high selectivity to aldehydes and to minimize carbon loss in the form of  $\text{CO}$  or  $\text{CO}_2$ .
3. Kinetics of oxidation of toluene using  $\text{Mn}(\text{OAc})_2/\text{FeCl}_3/\text{NaBr}$  catalyst

The specific results are discussed below:

### 2.3.1. Liquid Phase Oxidation Experiments

#### 2.3.1.1. Preliminary Experiments

A few preliminary experiments were carried out to find the best catalyst system for liquid phase oxidation of toluene and to assess the effect of metal salts concentration on the overall reaction rate to achieve high selectivity to benzaldehyde. The soluble salts of transition metals like cobalt, molybdenum, manganese etc as the principle catalysts in

monometallic or bimetallic forms were screened with sodium bromide as a promoter, The results on the catalytic performance in oxidation of toluene are presented in Table 2.1. The transition metal catalysts screened were  $\text{Co}(\text{OAc})_2$ , molybdenum (II) acetate and  $\text{Mn}(\text{OAc})_2$ , while NaBr was used as the halide promoter (entry 1-3). When the reactions were carried out using  $\text{Co}(\text{OAc})_2$  catalyst, high conversion of toluene (20.0%) was observed, the major product being benzoic acid, while a very low selectivity to benzaldehyde (29.8%) was achieved. When molybdenum (II) acetate was used as a catalyst along with NaBr as a promoter, (13.1%) conversion of toluene was observed with selectivity (26.1%) to benzaldehyde. Benzoic acid was found to be the major product with both the catalyst (Co and Mo) systems.  $\text{Mn}(\text{OAc})_2$ , however, was found to give higher selectivity to benzaldehyde (38.1%), at comparable conversion of toluene (20.8%).

Chaudhari and coworkers<sup>23</sup> have reported enhancement in the selectivity to benzaldehyde upon the addition of ammonium meta-vanadate (AMV) as a co-catalyst in Co-Br and Mo-Br catalyst systems. Also, Chaudhari and co-workers have demonstrated marked improvement in the selectivity towards benzaldehyde upon incorporation of a transition metal co-catalyst like salts of iron or vanadium in the Mn-Br catalyst system. It was therefore interesting to further study the effect of such Lewis acidic transition metal co-catalysts on the product profile in toluene oxidation. Therefore, the vanadium salt was incorporated in the catalyst system in the present study. Enhancement in the selectivity (38.1 to 54.6%) was observed, when the manganese (II) acetate was used as catalyst (entry 6) and NaBr as a promoter in combination with the AMV. A very high selectivity to benzaldehyde (76.1 %) but very poor conversion (1.3%) was observed when the reaction was carried out in the presence of co-catalyst AMV and promoter NaBr without any principle catalyst (entry 7). This shows that a principle catalyst is required to achieve a high conversion of toluene. When the reaction was carried out in the absence of NaBr, using manganese acetate as the principle catalyst and ammonium metavanadate as a co-catalyst, no catalytic activity was observed (entry 8 and 9) even after 15 hours of reaction time. This result clearly indicates that the presence of bromide is essential to initiate the reaction. The reaction generally proceeds through the formation of free radical chain mechanism using the combination of metal and bromide promoter<sup>21</sup>.

**Table 2.1.** Screening of catalyst

| Sr. | Catalyst system, (kmol/m <sup>3</sup> ) |       |       | Toluene/<br>Catalyst | Time,<br>hrs | Conversion,<br>% | Selectivity, % |                   |                   |                 |
|-----|---|-------|-------|----------------------|--------------|------------------|----------------|-------------------|-------------------|-----------------|
|     | Catalyst                                | AMV   | NaBr  |                      |              |                  | Benzaldehyde   | Benzyl<br>alcohol | Benzyl<br>acetate | Benzoic<br>acid |
| 1   | Co                                      | 0.000 | 0.024 | 69.2                 | 0.5          | 20.0             | 29.8           | 2.1               | 6.2               | 60.0            |
| 2   | Mo                                      | 0.000 | 0.024 | 69.2                 | 0.5          | 13.1             | 26.1           | 2.6               | 4.2               | 63.8            |
| 3   | Mn                                      | 0.000 | 0.024 | 69.2                 | 3.0          | 20.8             | 38.1           | 2.5               | 11.5              | 42.2            |
| 4   | Co                                      | 0.024 | 0.024 | 69.2                 | 0.5          | 21.3             | 30.8           | 2.1               | 6.2               | 60.0            |
| 5   | Mo                                      | 0.024 | 0.024 | 69.2                 | 0.5          | 13.5             | 27.3           | 2.6               | 4.2               | 63.8            |
| 6   | Mn                                      | 0.024 | 0.024 | 69.2                 | 3.0          | 19.9             | 54.6           | 5.2               | 15.2              | 23.2            |
| 7   | Mn                                      | 0.024 | 0.024 | -                    | 3.0          | 1.3              | 76.1           | 2.8               | 17.6              | 2.5             |
| 8   | Mn                                      | 0.024 | 0.000 | 69.2                 | 3.0          | 0.0              | 0.0            | 0.0               | 0.0               | 0.0             |
| 9   | Mn                                      | 0.024 | 0.000 | 69.2                 | 15.0         | 0.0              | 0.0            | 0.0               | 0.0               | 0.0             |

**Reaction Conditions:** Toluene,  $1.8 \times 10^{-3}$  kmol/m<sup>3</sup>; Catalyst, 0.024 kmol/m<sup>3</sup>; Temperature, 393K;  $P_{O_2}$ , 2.1 MPa; Agitation speed, 20 Hz; Solvent, Acetic acid; Time, 3 h; Total charge,  $7 \times 10^{-5}$  m<sup>3</sup>

### 2.3.1.2. Screening of Co-catalysts

The screening of transition metal co-catalysts was carried out to determine their effect on selectivity of benzaldehyde, and the results are illustrated in the Table 2.2. It was observed that benzaldehyde selectivity increased in the presence of AMV with the principle catalyst and NaBr as a promoter. Specifically, Mn(OAc)<sub>2</sub>/AMV/NaBr catalyst system showed very significant improvement in the selectivity to benzaldehyde from 38.1% for Mn-Br system to 54.6 % for Mn-V-Br system (Table 2.1) at comparable conversion of toluene. Therefore the screening of co-catalysts like FeCl<sub>3</sub>, SbCl<sub>2</sub>, NiCl<sub>2</sub>, CuCl<sub>2</sub>, AlCl<sub>3</sub>, SnCl<sub>2</sub> etc, was carried out in the presence of Mn (II) acetate and NaBr. It was observed that there was significant increase in the selectivity to benzaldehyde and decrease in formation of benzoic acid with incorporation of co-catalyst. AMV and FeCl<sub>3</sub> were found to give good activity for oxidation of toluene along with Mn (OAc)<sub>2</sub> as a catalyst. Among the co-catalysts screened, FeCl<sub>3</sub> was found to give the best results, i.e., a moderate toluene conversion of 19.2% and the highest selectivity to benzaldehyde 57.8% (Table 2.2, entry 3). FeCl<sub>3</sub> was chosen as a co-catalyst as it gave the best results in terms of benzaldehyde selectivity among the co-catalysts screened. Other co-catalysts showed similar trends of improvement in the selectivity to benzaldehyde.

**Table 2.2.** Screening of co-catalysts

| Sr. | Co-catalyst       | Conversion, % | Selectivity % |                |                |              | Rate x 10 <sup>5</sup> , kmol/m <sup>3</sup> /s |
|-----|-------------------|---------------|---------------|----------------|----------------|--------------|---|
|     |                   |               | Benzaldehyde  | Benzyl alcohol | Benzyl acetate | Benzoic acid |   |
| 1   | -                 | 20.8          | 38.1          | 2.5            | 11.5           | 42.2         | 3.22  |
| 2   | AMV               | 19.9          | 54.6          | 5.2            | 15.2           | 23.2         | 3.08  |
| 3   | FeCl <sub>3</sub> | 19.2          | 57.8          | 3.7            | 18.1           | 20.3         | 2.97  |
| 4   | AlCl <sub>3</sub> | 15.9          | 55.3          | 2.5            | 20.1           | 22.0         | 2.46  |
| 5   | SbCl <sub>2</sub> | 15.0          | 54.0          | 2.0            | 12.8           | 31.2         | 2.32  |
| 6   | CuCl <sub>2</sub> | 18.2          | 50.1          | 2.2            | 12.6           | 34.2         | 2.82  |
| 7   | ZnCl <sub>2</sub> | 16.1          | 47.9          | 2.2            | 15.2           | 27.9         | 2.49  |
| 8   | SnCl <sub>2</sub> | 15.4          | 55.8          | 3.2            | 15.7           | 23.9         | 2.38  |

**Reaction Conditions:** Toluene, 1.8 x 10<sup>-3</sup> kmol/m<sup>3</sup>; Mn (OAc)<sub>2</sub>, 0.18 kmol/m<sup>3</sup>; NaBr, 0.24 kmol/m<sup>3</sup>; Temperature, 393K; P<sub>O<sub>2</sub></sub>, 0.41 MPa; Agitation speed, 20 Hz; Solvent, Acetic acid; Time, 3 h; Total charge, 7 x 10<sup>-5</sup> m<sup>3</sup>

### 2.3.1.3. Selection of Catalyst System

The oxidation of toluene with MC-type catalyst proceeds via benzyl alcohol. As clearly observed from Table 2.2 the incorporation of a Lewis acidic co-catalyst, enhances the rate of toluene oxidation, i.e. the formation of benzyl alcohol and benzaldehyde while the selectivity to benzoic acid remains low. However, significant difference in the activity of the cobalt and manganese catalysts was observed. Cobalt (II) acetate gave higher rates of reaction compared to  $\text{Mn}(\text{OAc})_2$  (~6 times) in the initial period, but the selectivity of benzaldehyde was significantly lower for the cobalt catalyst. In a consecutive oxidation reaction like toluene oxidation, it is difficult to arrest the reaction at an intermediate product like benzaldehyde, which was achieved to a large extent in the case of manganese acetate as a catalyst. Though the activity of the manganese catalyst for liquid phase oxidation is lower (20.8%) the selectivity towards benzaldehyde is much higher.

The optimization of the reaction conditions and concentrations was carried out to achieve highest possible conversion of toluene and selectivity to benzaldehyde. Several experiments were carried out with  $\text{Mn}(\text{OAc})_2$  as a catalyst, sodium bromide as a promoter along with  $\text{FeCl}_3$  as a co-catalyst to optimize their concentrations and reaction conditions. The results on the catalytic performance in oxidation of toluene are presented in Table 2.3.



**Table 2.3.** Effect of catalyst and promoter concentrations

| Sr. | Catalyst system,<br>(kmol/m <sup>3</sup> ) |                   |       | Toluene/<br>Catalyst | C:LA:Br   | Time,<br>hrs | Conversion,<br>% | Selectivity, % |                   |                   |                 | RateX<br>10 <sup>4</sup> ,<br>kmol/m <sup>3</sup> /s |
|-----|--|-------------------|-------|----------------------|-----------|--------------|------------------|----------------|-------------------|-------------------|-----------------|--|
|     | Mn<br>(OAc) <sub>2</sub>                   | FeCl <sub>3</sub> | NaBr  |                      |           |              |                  | Benzaldehyde   | Benzyl<br>alcohol | Benzyl<br>acetate | Benzoic<br>acid |  |
| 1   | 0.024                                      | 0.024             | 0.024 | 69.2                 | 1:1:1     | 3.0          | 19.2             | 57.8           | 3.7               | 18.1              | 20.3            | 0.30   |
| 2   | 0.018                                      | 0.018             | 0.024 | 92.2                 | 1:1:1.3   | 3.0          | 18.4             | 60.2           | 2.8               | 16.5              | 18.2            | 0.28   |
| 3   | 0.018                                      | 0.018             | 0.018 | 92.2                 | 1:1:1     | 3.0          | 11.8             | 60.9           | 4.8               | 16.8              | 17.3            | 0.18   |
| 4   | 0.012                                      | 0.018             | 0.024 | 138.3                | 1:1.3:2   | 3.0          | 9.9              | 61.1           | 3.8               | 18.1              | 16.2            | 0.15   |
| 5   | 0.006                                      | 0.018             | 0.024 | 276.7                | 1:3:4     | 3.0          | 5.5              | 66.4           | 4.5               | 20.8              | 8.1             | 0.09   |
| 6   | 0.018                                      | 0.012             | 0.024 | 92.2                 | 1:0.6:1.3 | 3.0          | 18.1             | 51.1           | 2.9               | 13.4              | 31.8            | 0.28   |
| 7   | 0.018                                      | 0.006             | 0.024 | 92.2                 | 1:0.5:2   | 3.0          | 18.8             | 47.3           | 2.1               | 11.1              | 38.2            | 0.29   |
| 8   | 0.018                                      | 0.000             | 0.024 | 92.2                 | 1:0:1.3   | 3.0          | 19.1             | 38.8           | 1.8               | 14.2              | 42.0            | 0.30   |
| 9   | 0.018                                      | 0.018             | 0.012 | 92.2                 | 1:1:0.6   | 3.0          | 11.7             | 62.3           | 3.2               | 17.4              | 16.5            | 0.18   |

**Reaction Conditions:** Toluene,  $1.8 \times 10^{-3}$  kmol/m<sup>3</sup>; Temperature, 393K;  $P_{O_2}$ , 0.41 MPa; Agitation speed, 20 Hz; Solvent, Acetic acid; Time, 3 h; Total charge,  $7 \times 10^{-5}$  m<sup>3</sup>

#### 2.3.1.4. Effect of solvents

In the oxidation of alkylbenzenes using MC-type catalyst systems the solvent used in almost every case is a carboxylic acid. Additionally, the most preferred carboxylic acid solvent has been acetic acid, for following reasons<sup>24</sup>

1. MC catalysts are apparently significantly active only in solvents containing a carboxylic acid moiety. As postulated by Kantam and coworkers the oxidation of toluene with MC-Type catalyst triggers off with the formation of per acetic acid, which transforms the catalysts with higher oxidation state, thus initiating the catalytic cycle (Scheme 2.4). Also, the carboxylic acid solvents are known to stabilize free radicals<sup>25</sup> and therefore are favorable for free radical reactions. This justifies the necessity and hence the occurrence of the use of acetic acid in this liquid phase oxidation reaction in several literature report.
2. Acetic acid is one of the most inert solvents in an autoxidation environment. The longer chain fatty acids, such as propionic acid, are as active as acetic acid, but they autoxidize much are prone to auto-oxidation more easily to carbon oxides (CO + CO<sub>2</sub>) and methyl acetate<sup>24</sup>.
3. The enormous volume of commercially produced aromatic acids requires that the solvent be readily available and less expensive. The carbonylation and autoxidation routes to acetic acid produced  $4.59 \times 10^6$  tonnes of acetic acid worldwide in 1991.  $0.50 \times 10^6$  tonnes, 11% by weight, was required as a solvent in terephthalic acid and dimethylterephthalic acid manufacture in 1991.<sup>26</sup>

To assess the suitability of a solvent for liquid phase oxidation of toluene, the reactions were conducted using different carboxylic acid solvents like butyric acid, propionic acid and acetic acid. The results are shown in Figure 2.2. Conversion of toluene was found to decrease in the following order: acetic acid > propionic acid > butyric acid. However, the benzaldehyde selectivity was not found to vary with these solvents. The results show that the effect of the solvent on the product selectivities is marginal. When the reaction was carried out in the absence of any solvent (solventless conditions), no substrate conversion was observed. This could be because, the acidic solvents stabilize the free radicals formed in the reaction course, which helps the reaction to proceed.<sup>25</sup>

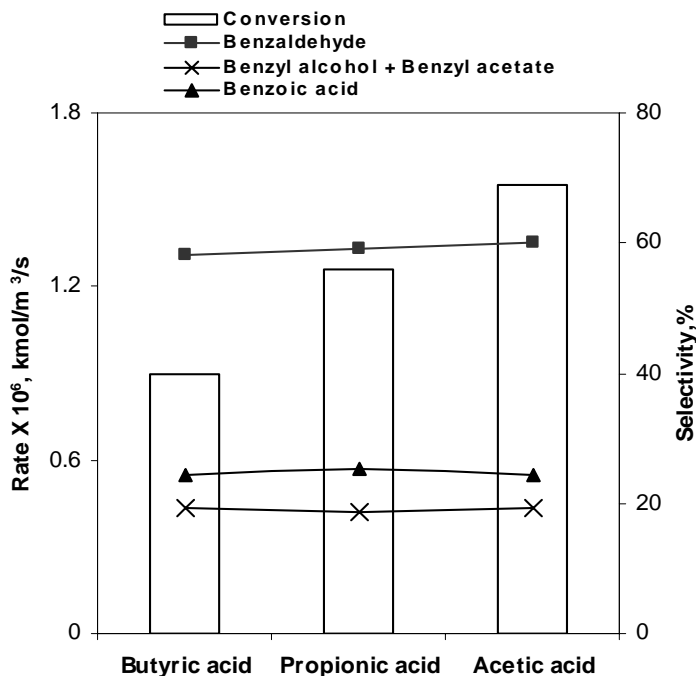


**Figure 2.2.** Effect of solvents

**Reaction Conditions:** Toluene,  $1.8 \times 10^{-3}$  kmol/m<sup>3</sup>; Mn (OAc)<sub>2</sub>, 0.18 kmol/m<sup>3</sup>; FeCl<sub>3</sub>, 0.18 kmol/m<sup>3</sup>; NaBr, 0.24 kmol/m<sup>3</sup>; Temperature, 393K;  $P_{O_2}$ , 0.41 MPa; Agitation speed, 20 Hz; Time, 3 h; Total charge,  $7 \times 10^{-5}$  m<sup>3</sup>

### 2.3.1.5. Effect of Temperature

The effect of temperature on the conversion of toluene and product selectivities in the liquid phase oxidation of toluene over Mn(OAc)<sub>2</sub>/FeCl<sub>3</sub>/ NaBr catalyst was studied in the temperature range of 373-413K and the results are presented in Figure 2.3. It was found that the conversion of toluene increases from 5.8 to 40.3 % with increase in the temperature from 373 to 413K. However, the selectivity to benzaldehyde decreased from 68.3 to 30.5 %, with increase in selectivity to benzoic acid (15.5-44.3%). Alkyl benzene oxidations are known to lose selectivity towards the desired oxidation products i.e. alcohols, aldehydes or carboxylic acids at temperatures beyond 423K, and result in the formation of CO and CO<sub>2</sub>, thus yielding lower atom economy. It was observed in the present study that there is no such loss of carbon in the temperature range studied.

The results obtained from the temperature study, however, showed that the selectivity towards benzaldehyde is affected adversely with increasing temperature, with consequent increase in the selectivity towards benzoic acid.

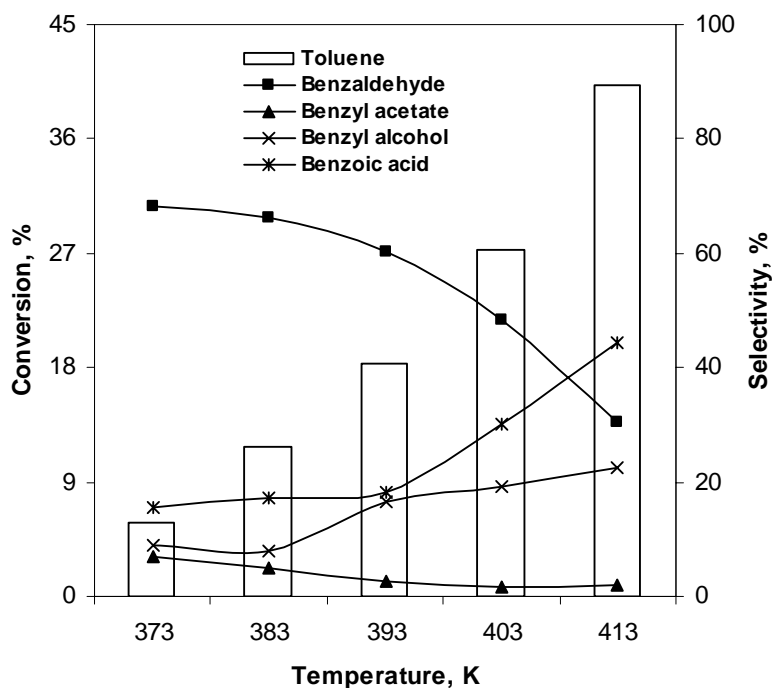


**Figure 2.3.** Effect of temperature in Mn (OAc)<sub>2</sub> / FeCl<sub>3</sub>/ NaBr catalyzed oxidation of toluene

**Reaction Conditions:** Toluene,  $1.8 \times 10^{-3}$  kmol/m<sup>3</sup>; Mn (OAc)<sub>2</sub>, 0.18 kmol/m<sup>3</sup>; FeCl<sub>3</sub>, 0.18 kmol/m<sup>3</sup>; NaBr, 0.24 kmol/m<sup>3</sup>;  $P_{O_2}$ , 0.41 MPa; Oxidant, air; Agitation speed, 20 Hz; Solvent, Acetic acid; Time, 3 h; Total charge,  $7 \times 10^{-5}$  m<sup>3</sup>

### 2.3.1.6. Effect of Partial Pressure of Oxygen

In order to study the effect of partial pressure on the conversion of toluene and product selectivity, the reactions were carried out using molecular oxygen as the oxidant in the partial pressure range of 0.2-1.2 MPa and the results are presented in Figure 2.4. The results show that with increase in the partial pressure of oxygen in the reactor, there is marginal increase in conversion of toluene. The increase in conversion is significant at lower partial pressure (0.69 MPa) beyond which the effect was marginal. On the other

hand oxygen partial pressure has negative effect on the benzaldehyde selectivity and positive effect on benzoic acid selectivity. The decrease in selectivity to benzaldehyde (62.6-55.4%) and increase in benzoic acid (15.9 -21.3%) was observed with increase in oxygen partial pressure of oxygen pressure (0.2-1.03 MPa).

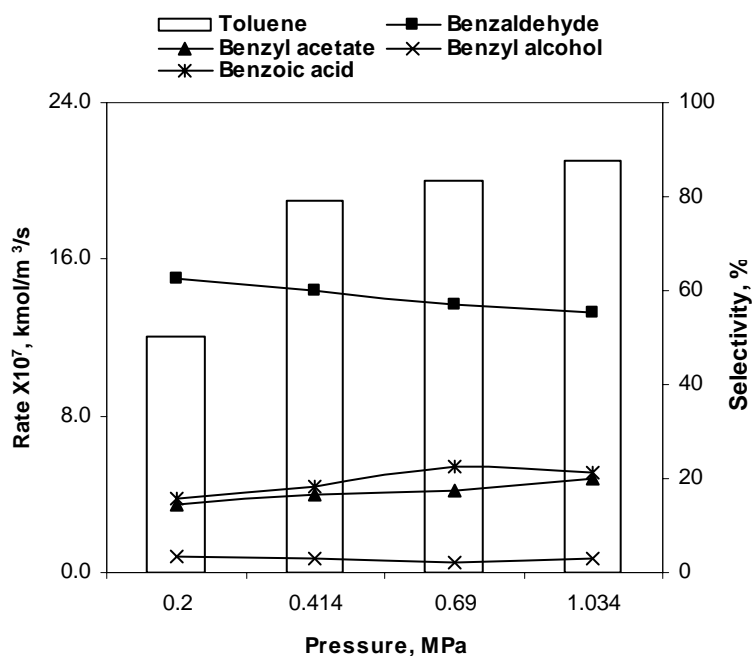


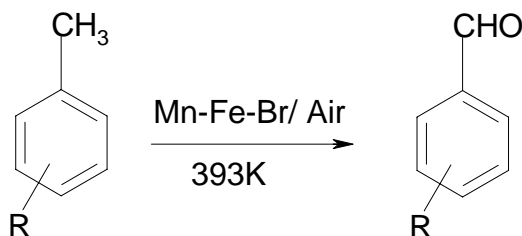
**Figure 2.4.** Effect of O<sub>2</sub> partial pressure

**Reaction Conditions:** Toluene,  $1.8 \times 10^{-3}$  kmol/m<sup>3</sup>; Mn (OAc)<sub>2</sub>, 0.18 kmol/m<sup>3</sup>; FeCl<sub>3</sub>, 0.18 kmol/m<sup>3</sup>; NaBr, 0.24 kmol/m<sup>3</sup>; Temperature, 393K; Agitation speed, 20 Hz; Solvent, Acetic acid; Time, 3 h; Total charge,  $7 \times 10^{-5}$  m<sup>3</sup>

### 2.3.1.7. Effect of substrates (substituted toluenes)

The oxidation of various substituted toluene substrates was examined using Mn (OAc)<sub>2</sub> as a catalyst along with FeCl<sub>3</sub> as a co-catalyst and NaBr as a promoter. It was observed that increase in selectivity to corresponding aldehydes and decrease in selectivity to corresponding carboxylic acids in the presence of Lewis acid co-catalyst was also observed for substituted toluenes. The oxidation activity increased in the following order toluene < fluoro < bromo < Iodo < chloro however, selective formation of the

corresponding aldehydes was observed with the catalyst system. The results are presented in the Table 2.4.



**Scheme 2.2.** Liquid phase oxidation of substituted toluenes to benzaldehyde derivatives

**Table 2.4.** Results with substituted toluene substrates

| Sr | R    | Conv., % | Selectivity % |                       |          |        | Ratex10 <sup>4</sup> kmol/m <sup>3</sup> /s |
|----|------|----------|---------------|-----------------------|----------|--------|---|
|    |      |          | Ar-CHO        | Ar-CH <sub>2</sub> OH | Ar-COOMe | ArCOOH |   |
| 1  | -    | 10.5     | 62.5          | 3.1                   | 15.6     | 18     | 1.63  |
| 2  | 4-F  | 12.6     | 60.3          | 1.8                   | 14.1     | 22     | 1.95  |
| 3  | 4-Br | 13.9     | 64.1          | 2.9                   | 18.7     | 13.6   | 2.15  |
| 4  | 4-I  | 15.1     | 61.2          | 3.2                   | 15.0     | 18.9   | 2.34  |
| 5  | 4-Cl | 16.9     | 64.3          | 4.1                   | 12.6     | 17.3   | 2.62  |

**Reaction Conditions:** Mn (OAc)<sub>2</sub>, 0.18 kmol/m<sup>3</sup>; FeCl<sub>3</sub>, 0.18 kmol/m<sup>3</sup>; NaBr, 0.24 kmol/m<sup>3</sup>; Temperature, 393K; P<sub>O<sub>2</sub></sub>, 0.41 MPa; Agitation speed, 20 Hz; Solvent, Acetic acid; Time, 3 h; Total charge, 7 x 10<sup>-5</sup> m<sup>3</sup>

### 2.3.1.8. Catalyst Recycle

To assess the reusability of the catalyst, experiments were carried out in which Mn (OAc)<sub>2</sub> and FeCl<sub>3</sub> components of the catalyst system were extracted in water while NaBr was needed to be replenished in each recycle, as bromide is consumed partially during the oxidation reaction showing a loss of approximately 32% of the original loading of bromide. The results of this study are shown in Figure 2.5. The catalyst was

found to retain its activity even after the third recycle without any considerable adverse effect on the conversion of toluene; however, the selectivity for benzaldehyde was marginally affected. The GC analysis of the vent gas at the end of the fifth recycle showed no formation of CO or CO<sub>2</sub>, supporting that the recycled catalyst is unaffected after the reaction and is not prone to carry out over oxidation of toluene and intermediate to carbon oxides. This establishes, a robust and reusable catalyst system for the liquid phase oxidation of toluene.

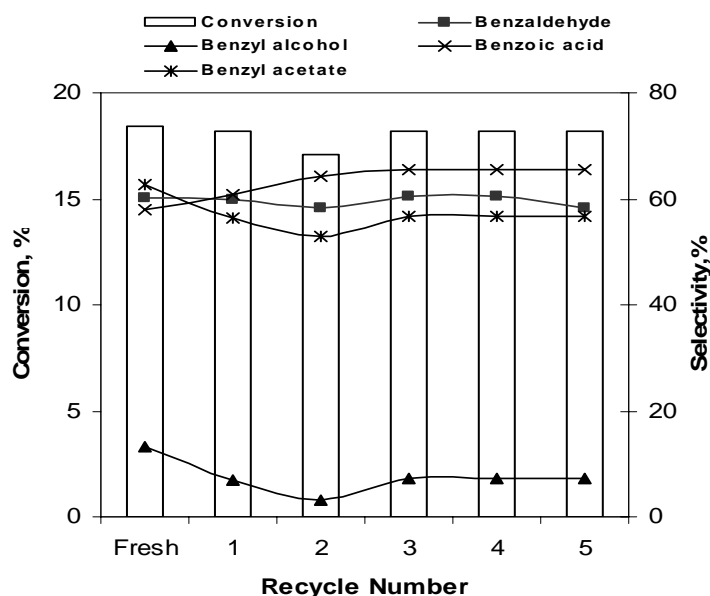


**Figure 2.5.** Effect of catalyst recycle

**Reaction Conditions:** Toluene,  $1.8 \times 10^{-3}$  kmol/m<sup>3</sup>; Mn (OAc)<sub>2</sub>, 0.18 kmol/m<sup>3</sup>; FeCl<sub>3</sub>, 0.18 kmol/m<sup>3</sup>; NaBr, 0.24 kmol/m<sup>3</sup>; Temperature, 393K;  $P_{O_2}$ , 0.41 MPa; Agitation speed, 20 Hz; Solvent, Acetic acid; Time, 3 h; Total charge,  $7 \times 10^{-5}$  m<sup>3</sup>

### 2.3.1.9. Solubility of Oxygen in Solvent

For interpretation of the kinetic data, a knowledge of the concentration of the gaseous reactants in the reaction medium is essential. The solubility of oxygen in acetic acid was determined experimentally at 373-403K, using a method described by Chaudhari and coworkers.<sup>27</sup> The data was found to be in good agreement with the solubility data available in the literature<sup>28</sup>. The solubility of air measured in stirred autoclave supplied by Parr Instrument Company, USA designed for 25 MPa pressure.

The equipment was provided with automatic temperature control and a pressure recording system. A pressure transducer having a precession of  $\pm 1$  kPa was used to measure the autoclave pressure.

In a typical experiment for the measurement of solubility of oxygen, a known volume of solvent was introduced in to the autoclave and the contents were heated to a desired temperature. After a steady temperature reading was attained, the void space in the reactor was carefully flushed with oxygen and pressurised to the level required. The contents were then stirred for about ten minutes to equilibrate the liquid phase with the solute gas. The change in the pressure in the autoclave was recorded on-line as function of time till it remained constant, indicating saturation of the liquid phase. From the initial and final pressure readings, the solubility was calculated in mole fraction as

$$X_a = \frac{(P_i - P_f)V_g M_s}{RTV_L \rho_s} \quad 2.1$$

Where  $X_a$  represents the mole fraction of the solute gas in the liquid phase at the partial pressure of the oxygen prevailing at  $P_f$ ,  $P_i$  and  $P_f$  are the initial and final pressure readings in the autoclave,  $V_g$  and  $V_L$  are the volumes of the gas and liquid phases, respectively,  $R$  is the gas constant,  $T$  is the temperature,  $M_s$  is the molecular weight of the solvent and  $\rho_s$  is the molar density of the liquid. The Henry's law constant,  $H$  was then calculated as

$$H = \frac{P_f}{X_a} \quad 2.2$$

The results are presented as Henry's law constant in Table 2.5

**Table 2.5.** Henry's law constant

| Temperature, K                             | 373  | 383  | 393  | 403  |
|--|------|------|------|------|
| $H_A$ for $O_2$ , kmol/m <sup>3</sup> /MPa | 28.6 | 29.1 | 29.5 | 29.8 |



## 2.4. Kinetics of Liquid Phase Oxidation of Toluene

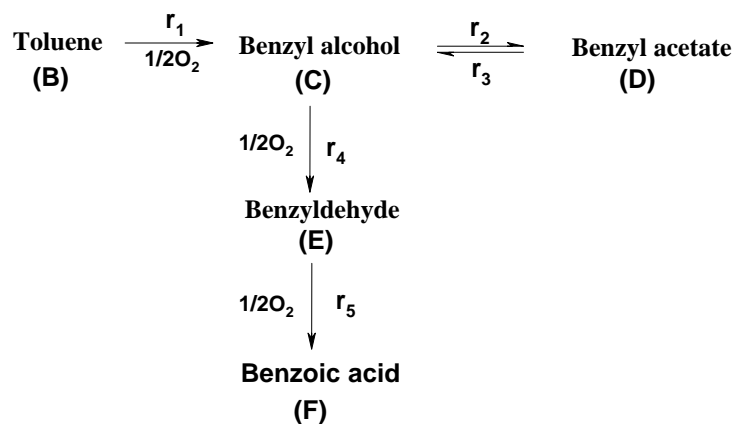
Though, liquid phase oxidation of toluene is an important reaction in chemical process industry, very scanty published literature is available on kinetics of this reaction. Liquid phase oxidation toluene using molecular oxygen as oxidant involve consecutive and parallel reactions (Scheme 2.1). The main objective of this work was to study the kinetics and develop rate equation for liquid phase oxidation of toluene using  $\text{Mn}(\text{OAc})_2/\text{FeCl}_3/\text{NaBr}$  catalyst and air as oxidant. The effect of concentration of catalyst, co-catalyst, promoter, toluene and partial pressure of oxygen on the rate of oxidation and concentration-time profile was studied in the temperature range of 383-403K. The range of concentrations and other parameters used for this study are summarized in Table 2.6.

**Table 2.6.** Range of operating conditions

| Parameter   | Range                |
|---|----------------------|
| Concentration of $\text{Mn}(\text{OAc})_2$ ( $\text{kmol}/\text{m}^3$ ) | 0.09 - 0.036         |
| Concentration of $\text{FeCl}_3$ ( $\text{kmol}/\text{m}^3$ )           | 0.04 - 0.036         |
| Concentration of $\text{NaBr}$ ( $\text{kmol}/\text{m}^3$ )             | 0.04 - 0.036         |
| Concentration of toluene ( $\text{kmol}/\text{m}^3$ )                   | 0.78- 3.5            |
| $P_{\text{O}_2}$ (MPa)  | 0.2 – 1.04           |
| Temperature (K)   | 110 - 130            |
| Solvent   | Acetic acid          |
| Reaction Volume, ( $\text{m}^3$ )                                       | $7.0 \times 10^{-5}$ |

In order to establish the mass balance of liquid components at various time intervals, concentration-time profile was obtained, which is as shown in the Figure 2.6. The GC analysis of all intermediate samples showed the balance of toluene and products formed in the range of 91-99%. Concentration of toluene decreased as a function of time and was converted to the oxidation products like benzyl alcohol, benzyl acetate, benzaldehyde and benzoic acid. A reaction sequence in the oxidation toluene is shown in the Scheme 2.3 for the sake of simplicity, the catalyst components, and solvents are excluded from the scheme and only the substrate, intermediate oxidation products and oxygen are shown in the scheme, the stoichiometry in the reaction sequence indicates that, for every mole of toluene, three moles of oxygen are consumed when the oxidation proceeds upto the formation of benzoic acid. A side reaction of equilibrium esterification of benzyl alcohol to benzyl acetate in presence of acetic acid solvent was observed. Thus,

during liquid phase oxidation of toluene, benzyl acetate, and benzoic acid were formed as by products along with benzyl alcohol and benzaldehyde.



**Scheme 2.3.** Simplified reaction scheme for liquid phase oxidation of toluene

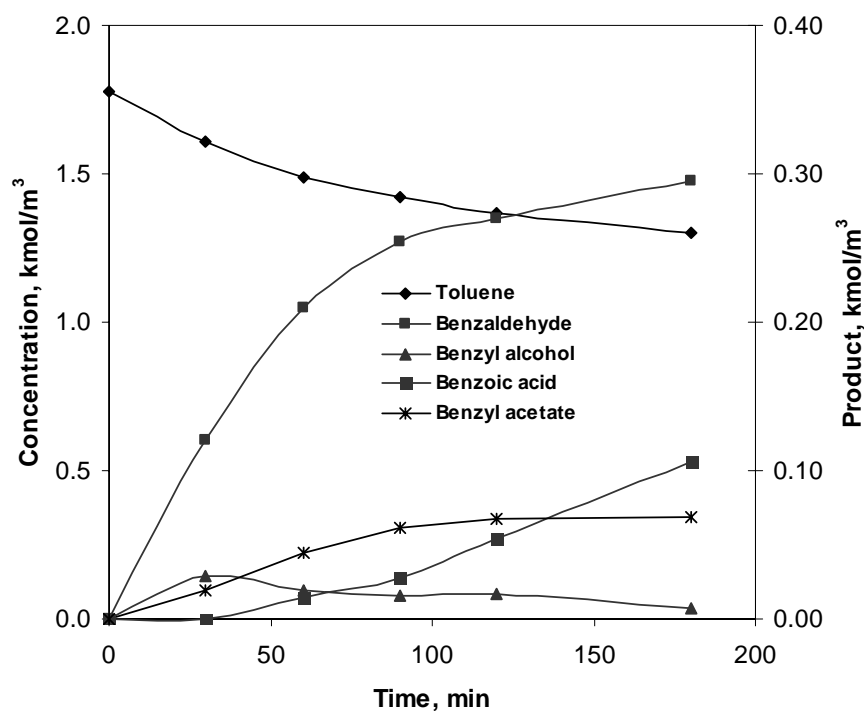


**Figure 2.6.** Concentration time profile at 393K

**Reaction Conditions:** Toluene,  $1.8 \times 10^{-3}$  kmol/m<sup>3</sup>; Mn (OAc)<sub>2</sub>, 0.18 kmol/m<sup>3</sup>; FeCl<sub>3</sub>, 0.18 kmol/m<sup>3</sup>; NaBr, 0.24 kmol/m<sup>3</sup>; Temperature, 393K;  $P_{\text{O}_2}$ , 0.41 MPa; Agitation speed, 20 Hz; Solvent, Acetic acid; Time, 3 h; Total charge,  $7 \times 10^{-5}$  m<sup>3</sup>

### 2.4.1. Mass Transfer Effects

The analysis of overall rate of reaction for a two-phase (gas-liquid) catalytic reactions is given by Ramachandran *et al*<sup>29</sup>. The following criteria described by Ramachandran and Chaudhari<sup>20</sup> were used to check the significance of various mass-transfer effects.

#### 2.4.1.1. Gas-liquid Mass Transfer Effect

The significance of gas-liquid mass transfer resistance was analyzed by comparing the initial rate of oxygen consumption and maximum possible rate of gas-liquid mass transfer. The gas-liquid mass transfer resistance is negligible if a factor  $\alpha_1$  defined as follows is less than 0.1 for the experimental conditions used.

$$\alpha_{1,A} = \frac{R_{exp}}{k_L a_B C_{A,aq.}} \quad 2.3$$

Where,  $R_{exp}$  is the observed rate of oxidation (kmol/m<sup>3</sup>/s),  $k_L a_B$  the gas-liquid mass transfer coefficient and  $C_A$  represent the saturation solubility of oxygen in equilibrium with the gas phase concentration at the reaction temperature (kmol/m<sup>3</sup>). The gas-liquid mass transfer coefficient ( $k_L a_B$ ) used in above equations was estimated by using a correlation (Equation 5.3) proposed by Chaudhari and coworkers<sup>30</sup> for a reactor similar to that used in this work for agitation speed of 1200 rpm.

$$k_L a_B = 1.48 \times 10^{-3} (N)^{2.18} \times (V_g / V_L)^{1.88} \times (d_I / d_T)^{2.1} \times (h_1 / h_2)^{1.16} \quad 2.4$$

The terms involved in above equation are described in Table 2.7 along with the respective values obtained from the reactor and charge used in the present case.

**Table 2.7.** Parameters used for  $k_{LA_B}$  calculations

| Parameters | Description                                | Value                |
|------------|--|----------------------|
| $V_g$      | Gas volume (m <sup>3</sup> )               | $4.5 \times 10^{-5}$ |
| N          | Agitation Speed (Hz)                       | 20                   |
| $V_L$      | Liquid volume (m <sup>3</sup> )            | $2.5 \times 10^{-5}$ |
| $d_I$      | Impeller diameter (m)                      | $1.6 \times 10^{-2}$ |
| $d_T$      | Tank diameter (m)                          | $4.0 \times 10^{-2}$ |
| $h_1$      | Height of the impeller from the bottom (m) | $1.1 \times 10^{-2}$ |
| $h_2$      | Liquid height (m)                          | $2.1 \times 10^{-2}$ |

The  $k_{LA_B}$  value for 1200 rpm (20 Hz) was evaluated as  $0.24 \text{ s}^{-1}$ .

The equilibrium solubilities for the gases given in Table 5.4 were used. The factor  $\alpha_I$  was calculated (taking  $R_{\text{exp}}$  as  $4.02 \times 10^{-4}$  i.e. highest) found to be  $8.41 \times 10^{-2}$ . Since the values of  $\alpha_I$  are very much less than 0.1, gas-liquid mass transfer resistance can be assumed to be negligible.

#### 2.4.2. Parametric Effects

Effect of different parameters such as concentration of Mn (OAc)<sub>2</sub>, FeCl<sub>3</sub>, NaBr, toluene, and oxygen partial pressure on concentration-time profile was studied at three different temperatures in the range 383-403 K. The initial rates of reactions  $r_1$  and  $r_3$  (benzyl alcohol),  $r_2$  (benzyl acetate),  $r_4$  (benzaldehyde) and  $r_5$  (benzoic acid) (see Scheme 2.2) were evaluated from the data in the range of less than 10 % conversion of toluene, which were analyzed to understand the nature of the reaction. These data represent formation of oxidation products, which were primarily used to understand the rate dependence on different parameters. For evaluation of rate equations and kinetic parameter estimation, integral concentration-time data were used. The effect of agitation speed on the rate of reaction was studied at 403K. In a gas liquid reaction, mass transfer issue becomes important at higher catalyst concentrations. Insignificant effect of agitation speed on the reaction rate is one of the criteria to ensure that the reaction is in kinetic

regime. As shown in Figure 2.7, the rate of total oxygen consumption was independent of agitation speed indicating that the reaction was not mass transfer controlled. For kinetic study, the effect of various parameters was studied at 20 Hz to ensure kinetic regime.

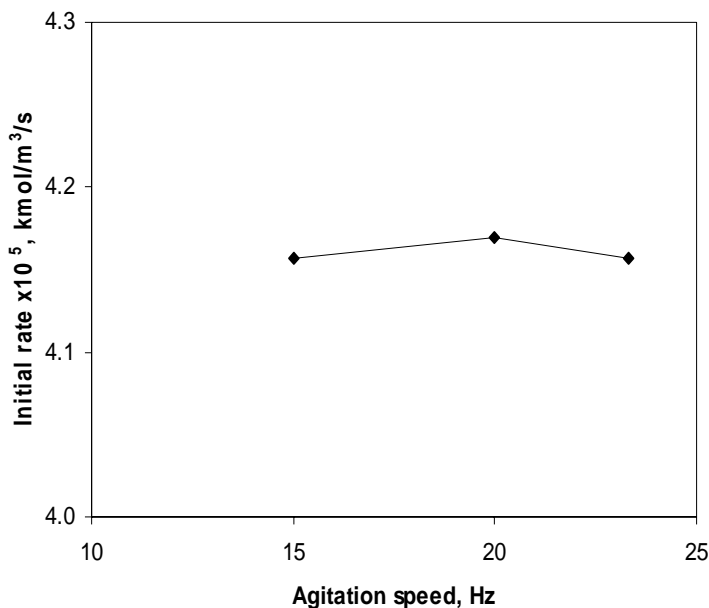


**Figure 2.7.** Effect of agitation speed

**Reaction Conditions:** Toluene,  $1.8 \times 10^{-3}$  kmol/m<sup>3</sup>; Mn (OAc)<sub>2</sub>, 0.28 kmol/m<sup>3</sup>; FeCl<sub>3</sub>, 0.18 kmol/m<sup>3</sup>; NaBr, 0.24 kmol/m<sup>3</sup>; Temperature, 403K;  $P_{O_2}$ , 0.41 MPa; Solvent, Acetic acid; Total charge,  $7 \times 10^{-5}$  m<sup>3</sup>

#### 2.4.2.1. Effect of Mn (OAc)<sub>2</sub> Concentration

Effect of Mn (oAc)<sub>2</sub> concentration was investigated in the concentration range ( $9 \times 10^{-3}$ ) to ( $3.6 \times 10^{-2}$ ) kmol/m<sup>3</sup>. Increasing the Mn(oAc)<sub>2</sub> concentration increases the reaction rate of toluene conversion ( $r_1$ ) linearly at all of the temperatures studied. Such a linear increase in the rate of toluene oxidation with Mn(OAc)<sub>2</sub> concentration also suggests that the reaction occurs in kinetic regime. Rate of formation of benzyl alcohol ( $r_1$  and  $r_3$ ) and benzoic acid ( $r_5$ ) (Figure 2.8 a, b, d). were found to increase with increase in concentration of Mn(OAc)<sub>2</sub>. Rate of formation of benzaldehyde ( $r_4$ ) (Figure 2.8c) was found to increase linearly at lower concentration of catalyst ( $< 1.8 \times 10^{-2}$  kmol/m<sup>3</sup>) after which it was found to be independent of catalyst concentration. This may be due to the over oxidation to benzoic acid with higher concentration of Mn catalyst. Though the rate

of reaction of benzyl alcohol to benzyl acetate ( $r_2$ ) increased with catalyst concentration in the beginning, it can be noted that the reaction occurs even without catalyst due the presence of acetic acid, which acts as catalyst for esterification reaction. Thus, the reaction  $r_2$  generates benzyl acetate (Figure 2.8b) even in absence of catalyst, which increases with catalyst concentration. This increase in reaction rate was because of reaction  $r_1$  generating benzyl alcohol with increase in catalyst concentration, which after esterification gives benzyl acetate.

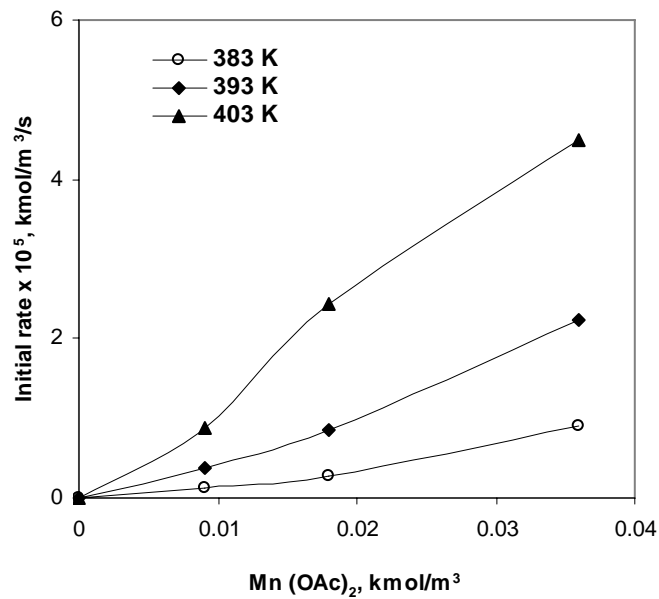


**Figure 2.8a.** Effect of Mn(OAc)<sub>2</sub> concentration on rate of formation of benzyl alcohol

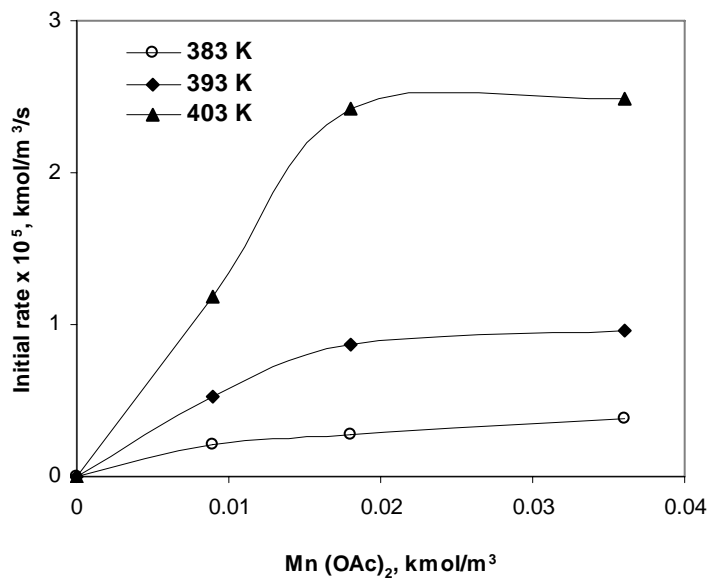


**Figure 2.8b.** Effect of  $\text{Mn}(\text{OAc})_2$  concentration on rate of formation of benzyl acetate

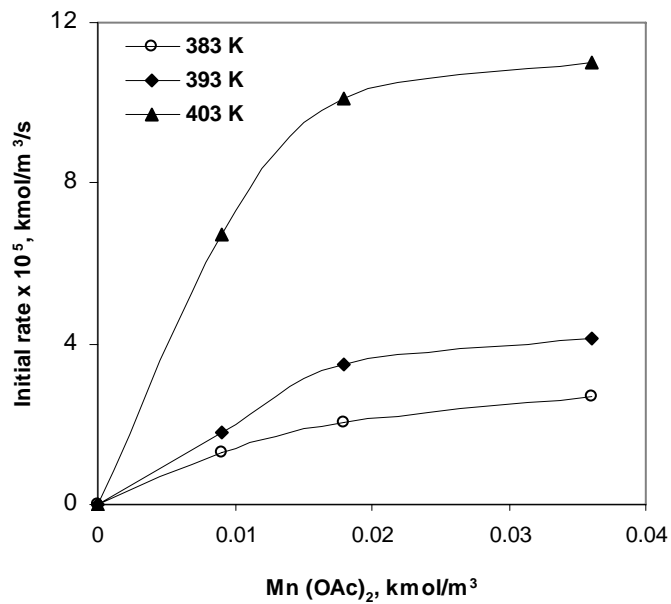


**Figure 2.8c.** Effect of  $\text{Mn}(\text{OAc})_2$  concentration on rate of formation of benzaldehyde

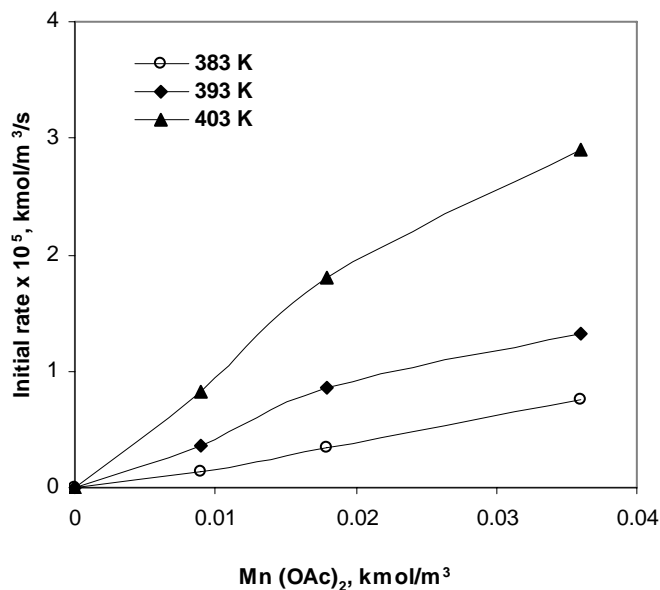


**Figure 2.8d.** Effect of  $\text{Mn}(\text{OAc})_2$  concentration on rate of formation of benzoic acid  
**Figure 2.8.** Effect of  $\text{Mn}(\text{OAc})_2$  concentration on liquid phase toluene oxidation

**Reaction Conditions:** Toluene,  $1.8 \times 10^{-3} \text{ kmol/m}^3$ ;  $\text{FeCl}_3$ ,  $0.18 \text{ kmol/m}^3$ ;  $\text{NaBr}$ ,  $0.24 \text{ kmol/m}^3$ ; Temperature, 383-403K;  $P_{\text{O}_2}$ , 0.41 MPa; Agitation speed, 20 Hz; Solvent, Acetic acid; Time, 3 h; Total charge,  $7 \times 10^{-5} \text{ m}^3$

#### 2.4.2.2. Effect of $\text{FeCl}_3$ Concentration

Effect of  $\text{FeCl}_3$  concentration was studied in the range of  $9 \times 10^{-3}$  to  $3.6 \times 10^{-2} \text{ kmol/m}^3$ . (Figure. 2.9). Rates of the reaction of formation of benzyl alcohol ( $r_1$  and  $r_3$ ) was found to increase with increase in  $\text{FeCl}_3$  concentration initially then becomes independent of concentration at higher concentration of  $\text{FeCl}_3$  and rate of formation of benzyl acetate was found to increase marginally with increase in  $\text{FeCl}_3$  concentration (Figure 2.9 a, c) because of acidic nature of  $\text{FeCl}_3$  acting as catalyst for esterification reaction. Rate of the formation of benzaldehyde was found to increase with increase in  $\text{FeCl}_3$  concentration in the studied range of concentration and at all temperatures. The rate of formation of benzoic acid was found to decrease with increase in the concentration of  $\text{FeCl}_3$ . (Figure 2.9 d).



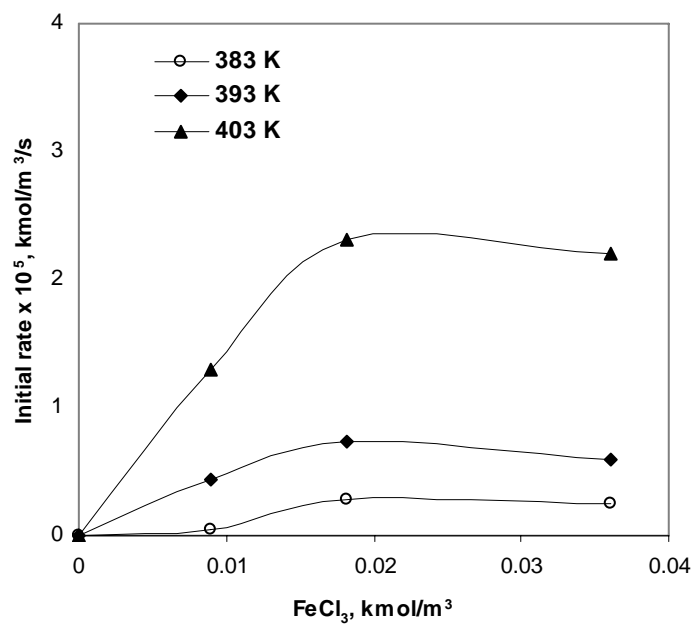


**Figure 2.9a.** Effect of FeCl<sub>3</sub> concentration on rate of formation of benzyl alcohol

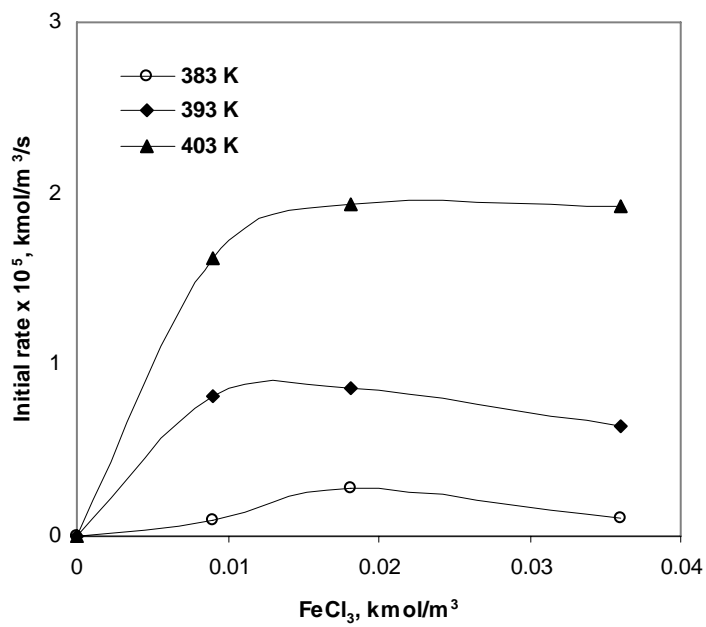


**Figure 2.9b.** Effect of FeCl<sub>3</sub> concentration on rate of formation of benzyl acetate

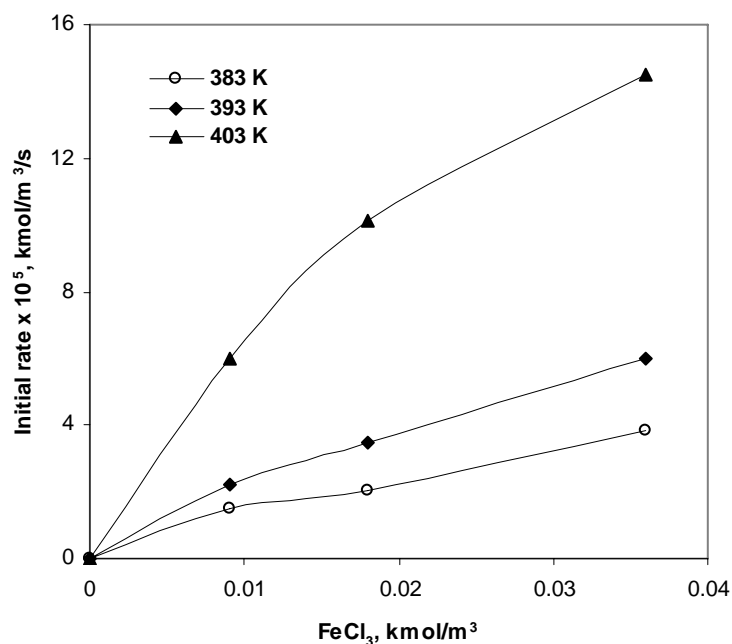


**Figure 2.9c.** Effect of FeCl<sub>3</sub> concentration on rate of formation of benzaldehyde

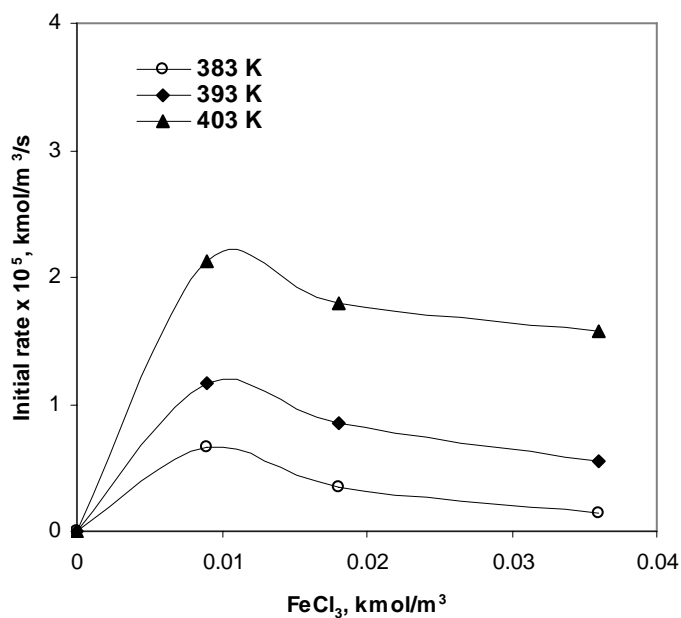


**Figure 2.9d.** Effect of FeCl<sub>3</sub> concentration on rate of formation of benzoic acid

**Figure 2.9.** Effect of FeCl<sub>3</sub> concentration on liquid phase toluene oxidation

**Reaction Conditions:** Toluene,  $1.8 \times 10^{-3}$  kmol/m<sup>3</sup>; Mn (OAc)<sub>2</sub>, 0.18 kmol/m<sup>3</sup>; NaBr, 0.24 kmol/m<sup>3</sup>; Temperature, 383-403K;  $P_{O_2}$ , 0.41 MPa; Agitation speed, 20 Hz; Solvent, Acetic acid; Time, 3 h; Total charge,  $7 \times 10^{-5}$  m<sup>3</sup>

### 2.4.2.3. Effect of NaBr Concentration

Bromide is the essential component of the reaction, without which there was no reaction observed. Increase in NaBr concentration increased the rate of formation of benzyl alcohol linearly in the lower concentration range ( $< 1.8 \times 10^{-2} \text{ kmol/m}^3$ ), beyond that it becomes independent of the concentration of NaBr (Figure 2.10 a). Rate of formation of benzaldehyde increase with increase in the concentration of NaBr initially, further increase in concentration showed marginal increase in the rate (Figure 2.10 c). Benzoic acid formation rate increases with increase in the NaBr concentration (Figure 2.10 d).

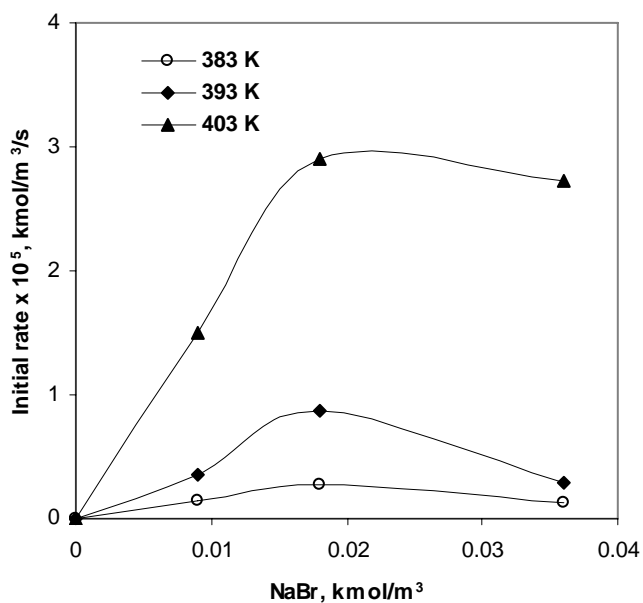


**Figure 2.10a.** Effect of NaBr concentration on rate of formation of benzyl alcohol

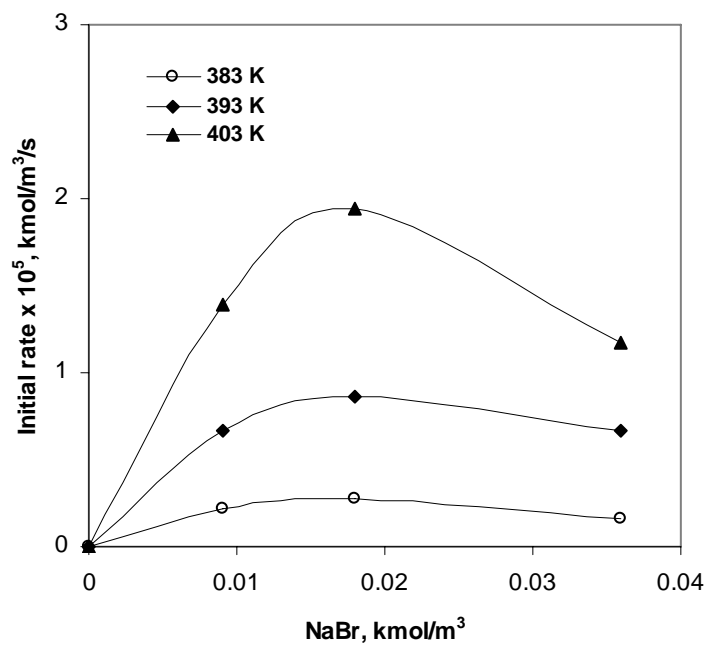


**Figure 2.10b.** Effect of NaBr concentration on rate of formation of benzyl acetate

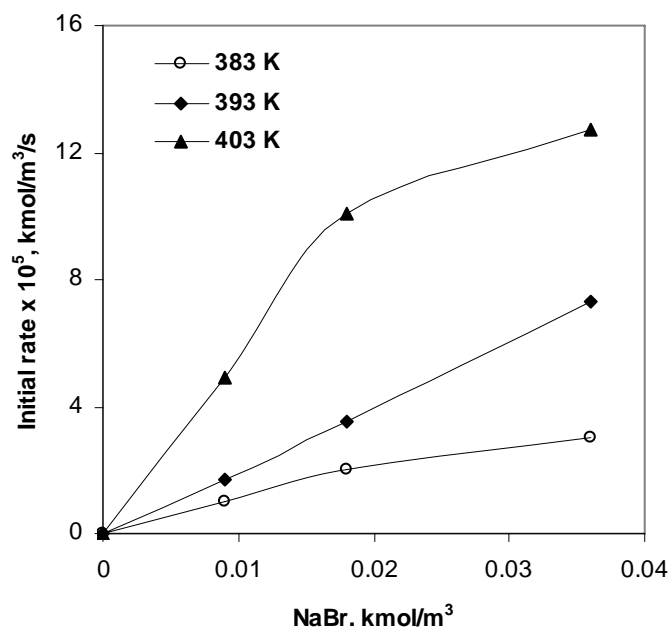


**Figure 2.10c.** Effect of NaBr concentration on rate of formation of benzaldehyde

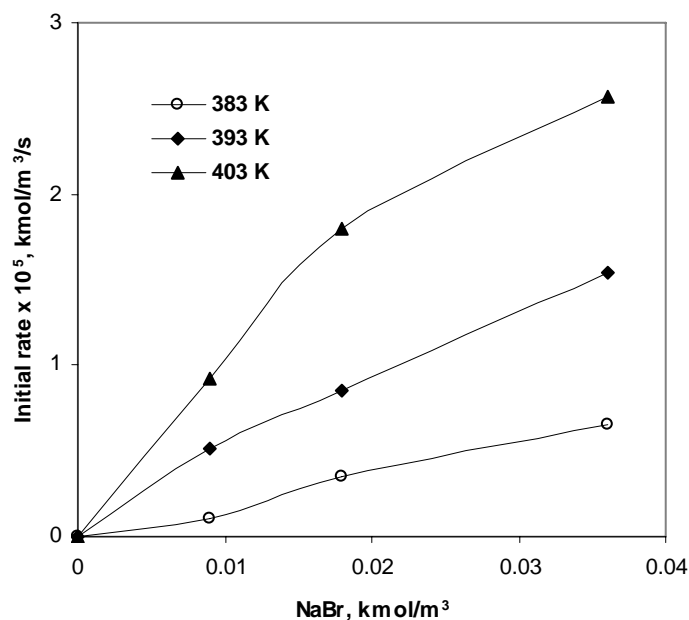


**Figure 2.10d.** Effect of NaBr concentration on rate of formation of benzoic acid

**Figure 2.10.** Effect of NaBr concentration on liquid phase toluene oxidation

**Reaction Conditions:** Toluene,  $1.80 \times 10^{-3}$  kmol/m<sup>3</sup>; Mn (OAc)<sub>2</sub>, 0.18 kmol/m<sup>3</sup>; FeCl<sub>3</sub>, 0.18 kmol/m<sup>3</sup>; Temperature, 383-403K;  $P_{O_2}$ , 0.41 MPa; Agitation speed, 20 Hz; Solvent, Acetic acid; Time, 3 h; Total charge,  $7 \times 10^{-5}$  m<sup>3</sup>

#### 2.4.2.4. Effect of Toluene Concentration

Increase in toluene concentration increased the rate of formation of benzyl alcohol and benzaldehyde initially and showed marginal increase in the rate of formation of both the products (Figure 2.11 a, c). The rate of formation of benzyl acetate was found to increase marginally initially and then decreases with increase in the concentration of toluene (Figure 2.11 b). Benzoic acid formation rate is marginally increased with increase in the toluene concentration (Figure 2.11 d). However, in neat toluene (without acetic acid), there was no reaction observed. This could be due to insolubility of catalyst components in toluene in absence of radical carrier medium.

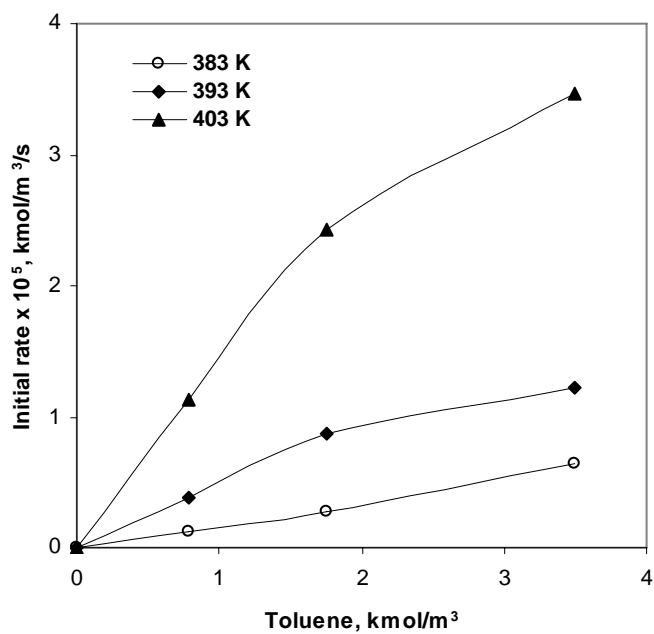


**Figure 2.11a.** Effect of toluene concentration on rate of formation of benzyl alcohol

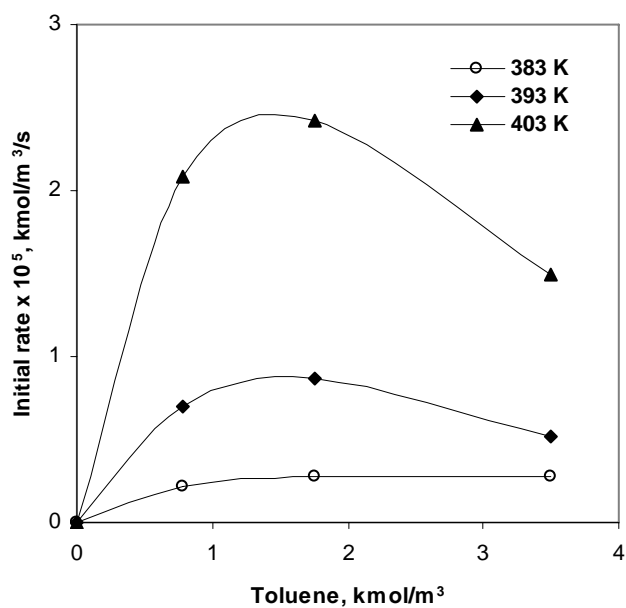


**Figure 2.11b.** Effect of toluene concentration on rate of formation of benzyl acetate

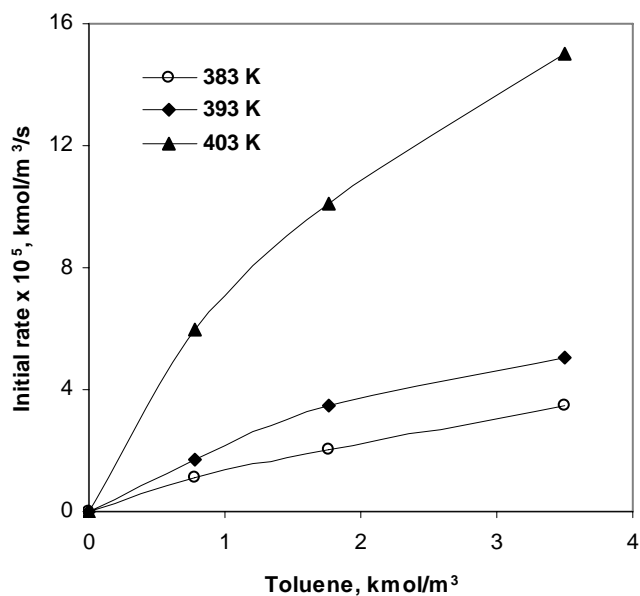


**Figure 2.11c.** Effect of toluene concentration on rate of formation of benzaldehyde

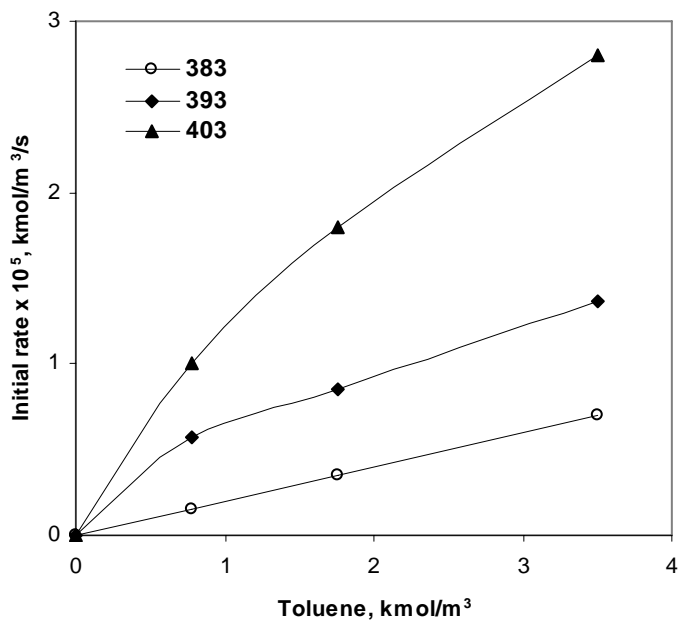


**Figure 2.11d.** Effect of toluene concentration on rate of formation of benzoic acid

**Figure 2.11.** Effect of toluene concentration on liquid phase toluene oxidation

**Reaction Conditions:** Mn (OAc)<sub>2</sub>, 0.18 kmol/m<sup>3</sup>; FeCl<sub>3</sub>, 0.18 kmol/m<sup>3</sup>; NaBr, 0.24 kmol/m<sup>3</sup>; Temperature, 383-403K; P<sub>O<sub>2</sub></sub>, 0.41 MPa; Oxidant, air; Agitation speed, 20 Hz; Solvent, Acetic acid; Time, 3 h; Total charge, 7 x 10<sup>-5</sup> m<sup>3</sup>

### 2.4.2.5. Effect of Oxygen Partial Pressure

Experiments were carried using air as the oxidant at various partial pressures of oxygen. Increasing the oxygen partial pressure decreased the selectivity to benzaldehyde with increase in the rate of toluene conversion and selectivity to benzoic acid. The effect of oxygen partial pressure was studied in the range of 0.2 to 0.62 MPa. Marginal increase in the rate of conversion of toluene was observed, however, selectivity to benzoic acid was found to increase. Decrease in the rate of formation of benzyl alcohol and benzyl acetate was observed with increase in the partial pressure of oxygen (Figure 2.12 a, b). Marginal decrease in the formation of benzaldehyde was observed, which may be due to over oxidation of benzaldehyde to benzoic acid (Figure 2.12 c). A linear dependence of the rate of formation of benzoic acid was observed with the increase in partial pressure of oxygen (Figure 2.12 d).

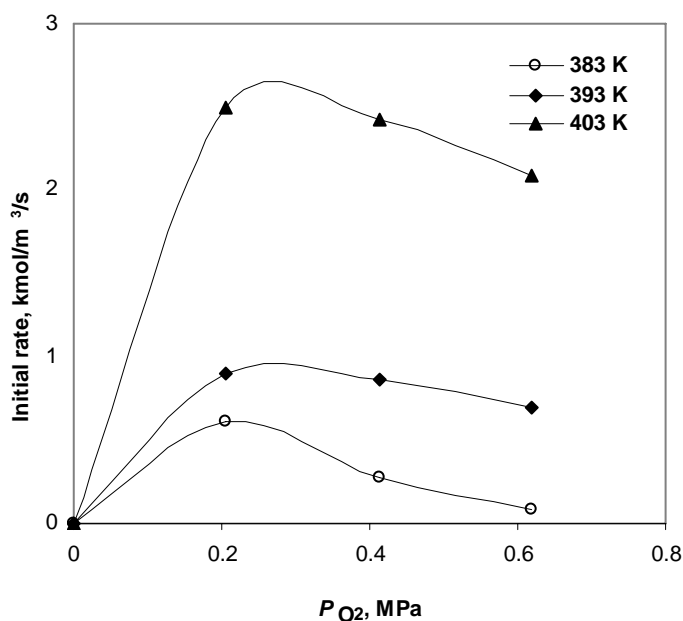


**Figure 2.12a.** Effect of oxygen partial pressure on rate of formation of benzyl alcohol



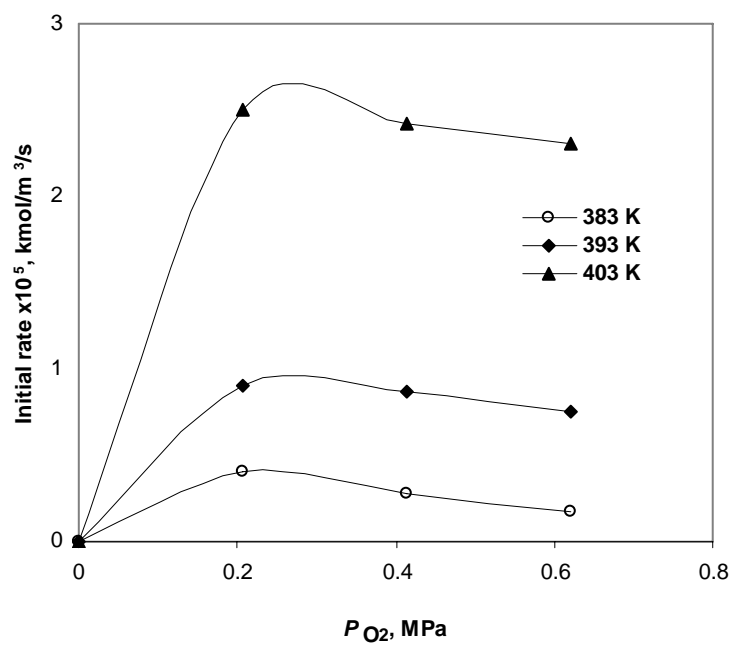


**Figure 2.12b.** Effect of oxygen partial pressure on rate of formation of benzyl acetate

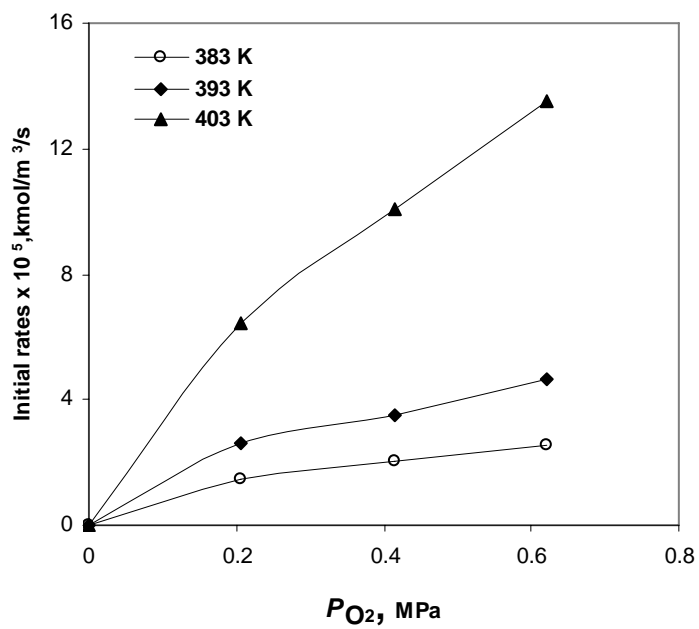


**Figure 2.12c.** Effect of oxygen partial pressure on rate of formation of benzaldehyde

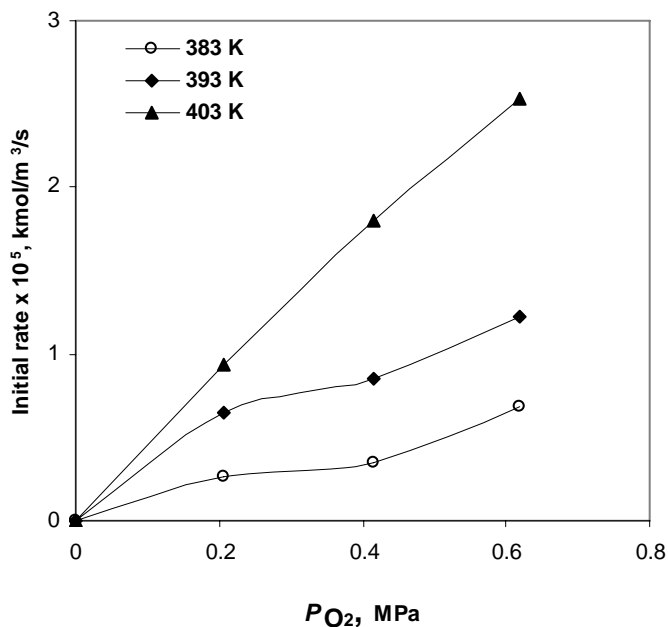


**Figure 2.12d.** Effect of oxygen partial pressure on rate of formation of benzoic acid

**Figure 2.12.** Effect of oxygen partial pressure on liquid phase toluene oxidation

**Reaction Conditions:** Toluene,  $1.8 \times 10^{-3}$  kmol/m<sup>3</sup>; Mn (OAc)<sub>2</sub>, 0.18 kmol/m<sup>3</sup>; FeCl<sub>3</sub>, 0.18 kmol/m<sup>3</sup>; NaBr, 0.24 kmol/m<sup>3</sup>; Temperature, 383-403K; Agitation speed, 20 Hz; Solvent, Acetic acid; Time, 3 h; Total charge,  $7 \times 10^{-5}$  m<sup>3</sup>

### 2.4.3. Kinetic Model

The experimental concentration-time data in the kinetic regime were used to evaluate the different rate equations for liquid phase oxidation of toluene. Liquid phase oxidation of toluene is a complex reaction system as summarized in Scheme 2.1. The reaction Scheme 2.1 was simplified as shown in Scheme 2.2, where it was assumed that the formation of benzaldehyde can also be from toluene as well as benzyl alcohol. Based on the observed trends in liquid phase oxidation of toluene using Mn-Fe-Br as a catalyst system, three different rate models were selected to evaluate the most suitable rate model for liquid phase oxidation of toluene.

In order to check the applicability of the rate models derived under isothermal and integral conditions, a semi batch reactor model was developed. Material balance of the liquid phase components based on Mode I are given below as an example:

M.B. Equation for toluene

$$\frac{dB}{dt} = -r1 \quad 2.5$$

M.B. Equation for benzyl alcohol

$$\frac{dC}{dt} = r1 + r3 - r2 - r4 \quad 2.6$$

M.B. Equation for benzyl acetate

$$\frac{dD}{dt} = r2 - r3 \quad 2.7$$

M.B. Equation for benzaldehyde

$$\frac{dE}{dt} = r4 - r5 \quad 2.8$$

M.B. Equation for benzoic acid

$$\frac{dF}{dt} = r5 \quad 2.9$$

With initial conditions

$$t=0, B=B_0, C=0, D=0, E=0, F=0$$

#### 2.4.4. Estimation of Kinetic Parameters and Model Discrimination

The integral concentration-time data obtained at 383, 393 and 403K were used for evaluation of kinetic models, since complex reactions are involved. A non-linear least square regression analysis was used to obtain the best-fit values of the parameters. For this purpose, an optimization program based on Marquardt's method combined with a Runge-Kutta method<sup>31</sup> was used to solve the set of equations shown in Table 2.7. The model parameters were estimated by minimizing the following objective function:

$$\Phi_{\min} = \sum_{i=1}^n [C_{\text{exp}} - C_{\text{pre}}]^2 \quad 2.10$$

Where  $C_{(exp)}$  is the concentration observed experimentally,  $C_{(pre)}$  is the predicted concentration using nonlinear regression analysis and  $n$  is number of data points. The mean average of relative residuals (% RR) was also calculated based on the following expression:

$$\%RR = \sum_{i=1}^4 \sum_{i=1}^n \frac{(C_{exp} - C_{pre})}{C_{exp}} \times 100 \quad 2.11$$

All three models were thus evaluated for this analysis to obtain the rate parameters. The values of rate parameters at different temperatures are presented in Table 2.8. The values of  $\Phi_{min}$  indicate the extent of fit of the kinetic models. As three different rate models were considered for the mathematical calculations, few models have to be discriminated in order to get an appropriate model for this reaction. Model II and Model-III gave higher values of the  $\Phi_{min}$ , suggesting lack of fit of these models. Therefore, the Models II and III were rejected on the basis of their lack of fit. The analysis of experimental data was performed using nonlinear regression analysis that has purely mathematical basis, further model discrimination was done based on thermodynamic considerations. Thus, the discrimination of the proposed models based on the objective function and thermodynamic constrains suggests that the Model- I was found to be the best fit for  $Mn(OAc)_2$ - $FeCl_3$ - $NaBr$  the liquid phase oxidation of toluene.

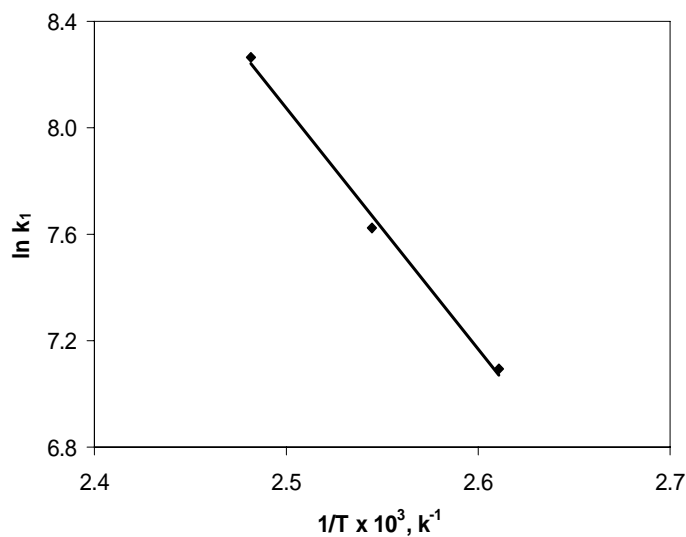


**Figure 2.13.** Arrhenius plot

In order to verify the applicability of the kinetic model under integral conditions, experimental data on the liquid phase concentrations of toluene, benzyl alcohol, benzyl acetate and benzoic acid as a function of time were obtained. The variation of the concentration of Toluene, benzyl alcohol, benzyl acetate, benzaldehyde and benzoic acid can be represented by the following mass balance equations, for conditions of constant synthesis gas pressure in the reactor.

The equations were solved numerically by using the Runge-Kutta method to obtain the concentration of toluene, benzyl alcohol, benzyl acetate, benzaldehyde, and benzoic acid as a function of time. For this purpose intrinsic rates were used. The comparison of the experimental and the predicted results for 393K are presented in Figure 2.14, which show excellent agreement. These results indicate that the rate model proposed were applicable over a wide range of conditions and can be used for design and scale up purposes. To show the difference in fitting between the Model 1 and other models, a typical experimental vs predicted concentration time profiles is shown in Figure 2.14 – 2.16, which clearly indicate the suitability of Model 1.

**Table 2.8.** Model discrimination

| Sr. No | Model  | Temp, K | k <sub>1</sub> | K <sub>2</sub> | K <sub>3</sub> | K <sub>4</sub> | K <sub>5</sub> | K <sub>6</sub> | K <sub>7</sub> | K <sub>8</sub> | K <sub>9</sub> | K <sub>10</sub> | Φ min    | %PP |
|--------|--|---------|----------------|----------------|----------------|----------------|----------------|----------------|----------------|----------------|----------------|-----------------|----------|-----|
| 1      | $r_1 = \frac{k_1 w_1 w_3 BA^*}{(1 + K_2 w_3)(1 + K_3 B) (1 + K_4 A^*)^2}$      | 383     | 1545.5         | 920.1          | 2034.3         | 927.8          | 487.6          | 1343.6         | 2510.6         | 624.1          | 25.2           | 588.5           | 2.5E-04  | 14  |
|        | $r_2 = K_5 C$  |         |                |                |                |                |                |                |                |                |                |                 |          |     |
|        | $r_3 = K_6 D$  | 393     | 2046.7         | 1135.1         | 2699.3         | 1025.9         | 641.9          | 1639.7         | 2870.5         | 814.3          | 35.3           | 853.2           | 2.2E-04  | 13  |
|        | $r_4 = \frac{k_7 w_1 w_2 w_3 CA^*}{(1 + K_8 w_1)(1 + K_9 B)}$                  |         |                |                |                |                |                |                |                |                |                |                 |          |     |
|        | $r_5 = K_{10} w_1 w_2^{0.5} w_3 EA^*$  | 403     | 2513.6         | 1445.7         | 2900.0         | 1446.0         | 753.0          | 1594.3         | 2967.2         | 1106.7         | 63.2           | 1245.2          | 2.2E-04  | 11  |
| 2      | $r_1 = \frac{k_1 w_1 w_3 BA^*}{(1 + K_2 w_3)^2 (1 + K_3 B)^3 (1 + K_4 A^*)^2}$ | 383     | 1930.5         | 1096.8         | 2477.8         | 1223.1         | 493.2          | 1299.5         | 1498.7         | 602.6          | 66.1           | 660.8           | 1.31E-01 | 52  |
|        | $r_2 = K_5 C$  |         |                |                |                |                |                |                |                |                |                |                 |          |     |
|        | $r_3 = K_6 D$  | 393     | 2123.5         | 1206.5         | 2725.6         | 1345.4         | 542.5          | 1429.5         | 2547.8         | 1024.5         | 112.4          | 1123.4          | 2.34E-02 | 60  |
|        | $r_4 = \frac{k_7 w_1 w_2 w_3 CA^*}{(1 + K_8 w_1)^2 (1 + K_9 B)}$               |         |                |                |                |                |                |                |                |                |                |                 |          |     |
|        | $r_5 = K_{10} w_1 w_2 w_3 EA^*$  | 403     | 2335.9         | 2292.4         | 5178.6         | 2556.3         | 1030.8         | 2716.1         | 2802.6         | 1127.0         | 123.6          | 1235.7          | 1.15E-01 | 40  |
| 3      | $r_1 = \frac{k_1 w_1 w_3 BA^*}{(1 + K_2 w_3)^3 (1 + K_3 B) (1 + K_4 A^*)}$     | 383     | 1360.3         | 514.2          | 1255.9         | 609.1          | 527.3          | 791.3          | 855.1          | 387.9          | 21.9           | 87.4            | 8.11E-01 | 112 |
|        | $r_2 = K_5 C$  |         |                |                |                |                |                |                |                |                |                |                 |          |     |
|        | $r_3 = K_6 D$  | 393     | 2312.5         | 874.2          | 2135.1         | 1035.4         | 896.4          | 1345.2         | 1453.7         | 659.4          | 37.2           | 148.6           | 7.43E-01 | 140 |
|        | $r_4 = \frac{k_7 w_1 w_2 w_3 CA^*}{(1 + K_8 w_1)(1 + K_9 B)^2}$                |         |                |                |                |                |                |                |                |                |                |                 |          |     |
|        | $r_5 = K_{10} w_1 w_2^2 w_3 EA^*$  | 403     | 4393.8         | 1661.0         | 4056.7         | 1967.3         | 1703.2         | 2555.9         | 2762.0         | 1252.9         | 70.7           | 282.3           | 6.11E-02 | 130 |

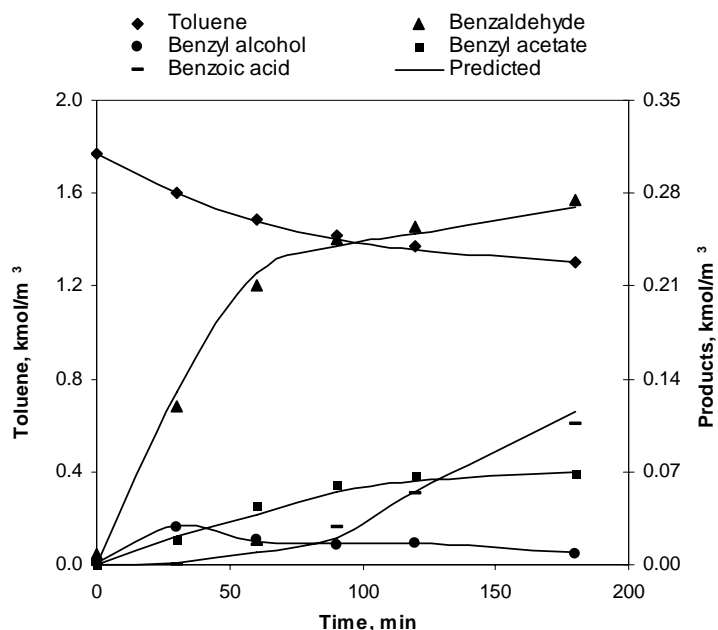


**Figure 2.14.** Experimental Vs predicted concentration time profile at 393K

**Reaction Conditions:** Toluene,  $1.8 \times 10^{-3}$  kmol/m<sup>3</sup>; Mn (OAc)<sub>2</sub>, 0.18 kmol/m<sup>3</sup>; FeCl<sub>3</sub>, 0.18 kmol/m<sup>3</sup>; NaBr, 0.24 kmol/m<sup>3</sup>; Temperature, 393K;  $P_{O_2}$ , 0.41 MPa; Agitation speed, 20 Hz; Solvent, Acetic acid; Time, 3 h; Total charge,  $7 \times 10^{-5}$  m<sup>3</sup>

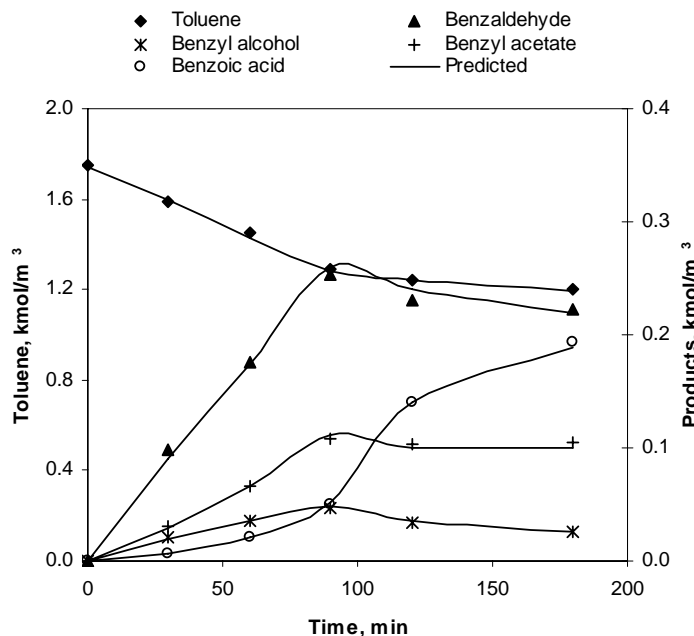


**Figure 2.15.** Experimental Vs predicted concentration time profile at 403K

**Reaction Conditions:** Toluene,  $1.8 \times 10^{-3}$  kmol/m<sup>3</sup>; Mn (OAc)<sub>2</sub>, 0.18 kmol/m<sup>3</sup>; FeCl<sub>3</sub>, 0.18 kmol/m<sup>3</sup>; NaBr, 0.24 kmol/m<sup>3</sup>; Temperature, 403K;  $P_{O_2}$ , 0.41 MPa; Agitation speed, 20 Hz; Solvent, Acetic acid; Time, 3 h; Total charge,  $7 \times 10^{-5}$  m<sup>3</sup>

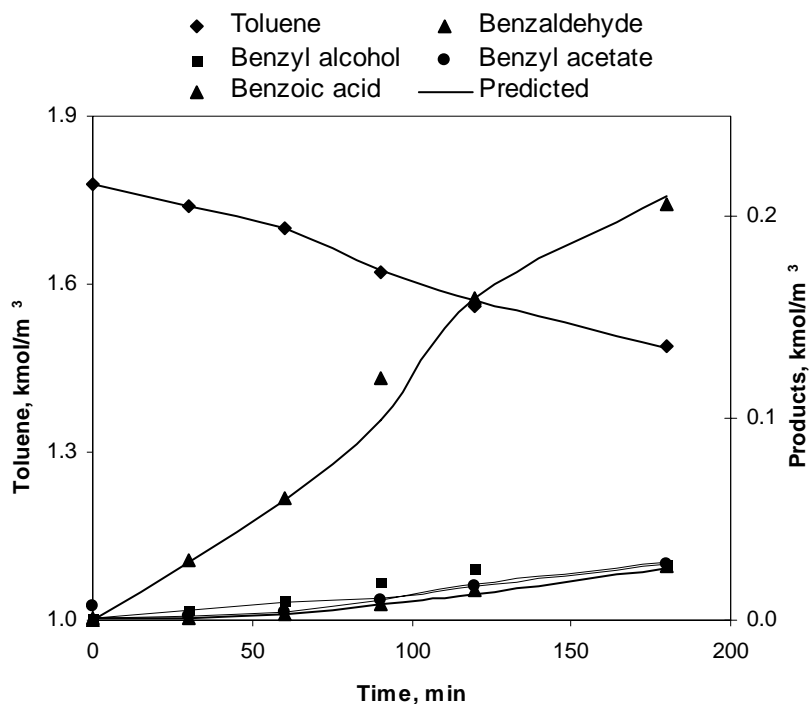


**Figure 2.16.** Experimental Vs predicted concentration time profile at 383K

**Reaction Conditions:** Toluene,  $1.8 \times 10^{-3}$  kmol/m<sup>3</sup>; Mn (OAc)<sub>2</sub>, 0.18 kmol/m<sup>3</sup>; FeCl<sub>3</sub>, 0.18 kmol/m<sup>3</sup>; NaBr, 0.24 kmol/m<sup>3</sup>; Temperature, 383K;  $P_{O_2}$ , 0.41 MPa; Agitation speed, 20 Hz; Solvent, Acetic acid; Time, 3 h; Total charge,  $7 \times 10^{-5}$  m<sup>3</sup>

## 2.5. Reaction Pathway

The general MC type catalysts involving a transition metal catalyst and a bromide promoter are known to oxidize alkyl benzenes via a free radical chain mechanism. A similar mechanism has been proposed for the present reaction system involving manganese as the principle oxidation catalyst. In an attempt to understand the reaction pathway, the transition of Mn(II) to Mn(III) in presence and absence of other components in the catalysts system was investigated by UV spectroscopic analysis. The UV spectrum of a solution of Mn(OAc)<sub>2</sub> in acetic acid showed a marked difference when exposed to oxygen pressure. A peak at 462 nm appeared, which was assigned to Mn(OAc)<sub>3</sub> formation (Figure 2.17). It was further observed that this peak disappeared when NaBr was added to this solution and heated to 353K under inert (nitrogen) atmosphere, which causes the reduction of Mn(III) to Mn(II). Addition of NaBr to Mn(OAc)<sub>3</sub> generates Br<sup>-</sup>



radical and regenerates  $\text{Mn}(\text{OAc})_2$  in solution. Though the formation of  $\text{Br}^\cdot$  radical was not traced directly by UV,  $\text{Mn}(\text{III})$  to  $\text{Mn}(\text{II})$  reduction after addition of  $\text{NaBr}$  in inert atmosphere supports the formation of  $\text{Br}^\cdot$  radical necessary to initiate the oxidation reaction. These observations support the sequence of reactions in the catalytic cycle. The bromide free radical generated by this pathway is known to abstract a hydrogen atom from the methyl group of toluene molecule and initiate the free radical oxidation. This abstraction of hydrogen atom is known to be the rate-limiting step.<sup>32</sup> The methyl benzene free radical thus generated forms benzyl peroxide radical. This is followed by several redox reactions as shown in scheme 2.4, giving benzyl alcohol, benzaldehyde and consequently benzoic acid. The benzyl acetate formed in the reaction is an esterification product of benzyl alcohol, which implies that the oxidation of benzyl alcohol and its esterification are competitive reactions.

The transition metal co-catalyst  $\text{FeCl}_3$  added in the reaction apparently doesn't have a direct role in the catalysis of the oxidation, which is also relevant to the observation that there is no enhancement in the rate of toluene oxidation as studied in  $\text{FeCl}_3$  concentration effect (refer Table 2.2). The enhancement in the selectivity of benzaldehyde due to its addition, however, suggests that the further oxidation of aldehyde to acid is arrested to some extent by addition of such a Lewis acidic transition metal salt. Previously, similar effect of Lewis acids in the alkylation reaction has been observed, where it was found to quench the aldehyde moiety<sup>33,34,35</sup>. The effect of addition of Lewis acid to aldehyde was investigated using IR spectroscopy. The carbonyl frequency  $\nu_{(\text{CO})}$  was found to shift from its original value of  $1703 \text{ cm}^{-1}$  to  $1688 \text{ cm}^{-1}$  on addition of  $\text{FeCl}_3$ . The red shift in carbonyl frequency is well known upon coordination of the carbonyl oxygen with transition metals.<sup>34</sup> Such a coordination of the aldehyde with the Lewis acid may cause the retardation of further oxidation to benzoic acid.

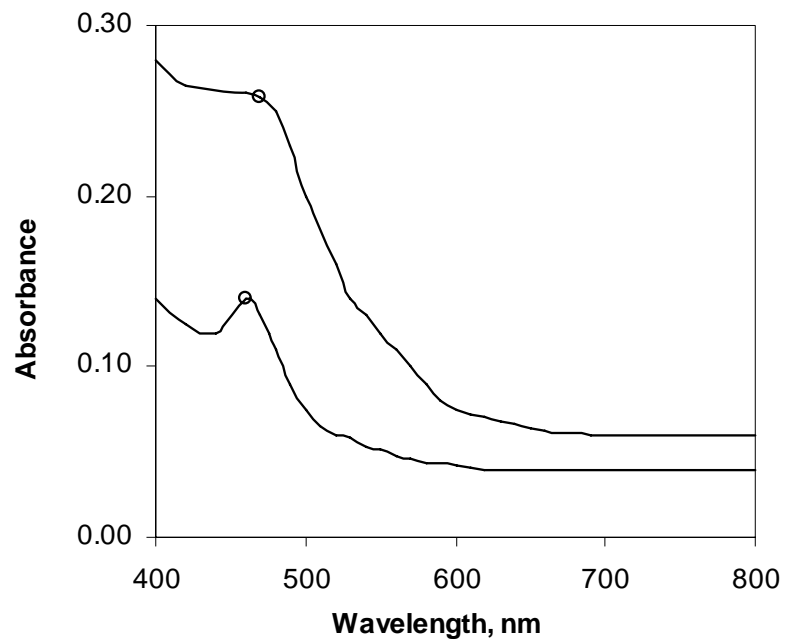
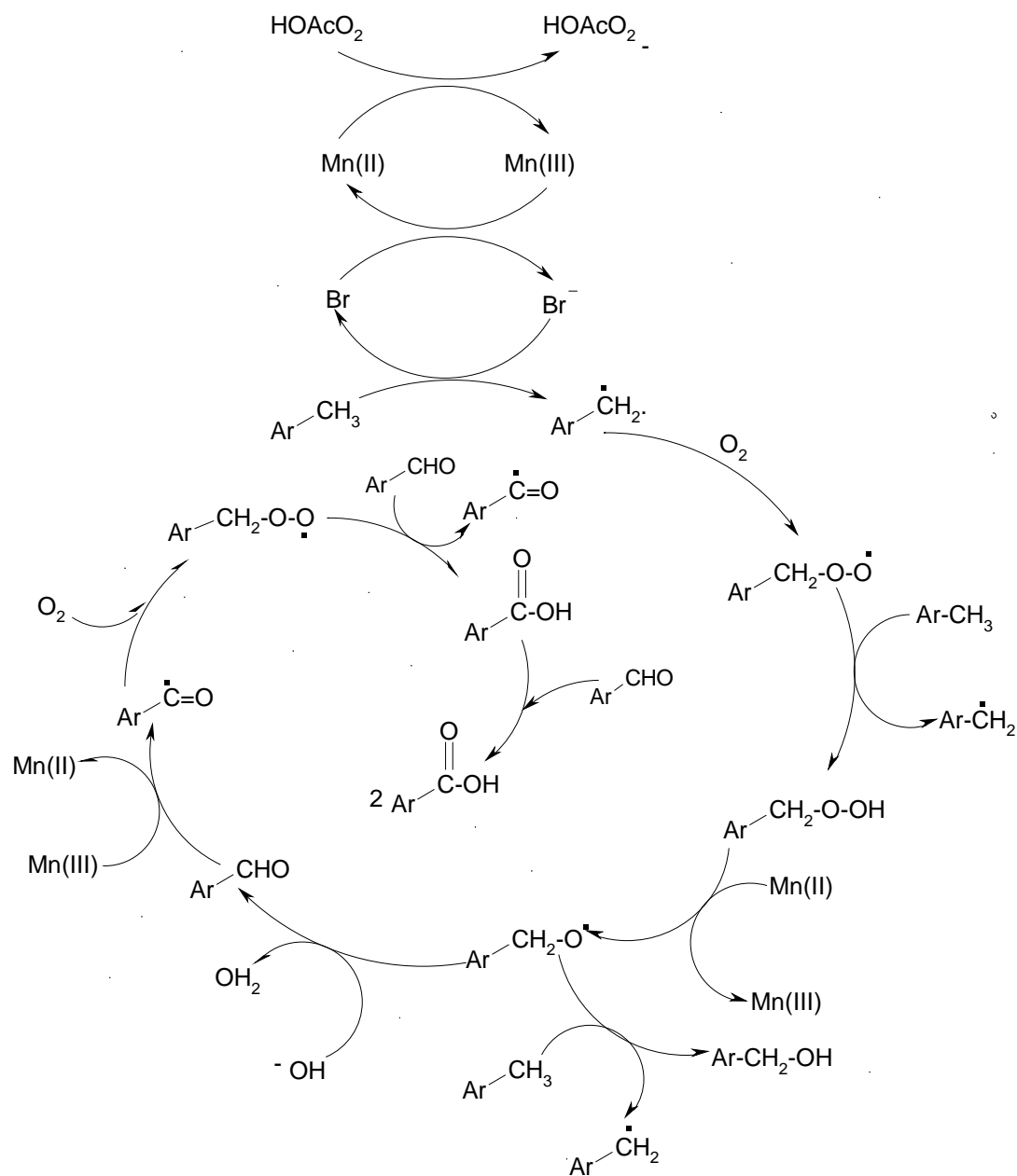


**Figure 2.17.** Spectroscopic analysis



**Scheme 2.4.** Mechanism of liquid phase oxidation of toluene

## 2.6. Conclusions

Liquid phase selective oxidation of toluene was investigated in detail using Mn(OAc)<sub>2</sub> as catalyst, Lewis acidic salt of transition metal as co-catalyst, sodium bromide as promoter and air as oxidant. The effect of different catalyst precursors, co-

catalysts, and solvents on the behaviour of the reaction were studied, and following trends were observed-

1. A simple MC-type catalyst system with Mn as the principle oxidation catalyst was established and the reaction conditions were optimized to achieve optimum toluene conversions with excellent selectivity to benzaldehyde.
2. Screening of Lewis acidic transition metal salts as co-catalyst was carried out, and  $\text{FeCl}_3$  was found to result in high selectivity to benzaldehyde (%).
3. Recycle efficiency of the catalyst system was evaluated. Except for the requirement of replenishment of bromide, the catalyst was found to retain its activity and selectivity upon recycle.
4. The effect of reaction components and parameters was studied in detail. The nature of solvent was found to have marked effect on the product profile. Increase in polarity was found to favour the rate of reaction. Acetic acid was found to be the best solvent.
5. Kinetics of Mn-Fe-Br catalyzed liquid phase oxidation of toluene was investigated in the temperature range of 373 – 393K and rate equations were proposed.

Parametric effects were studied in the kinetic regime. The parametric studies showed that liquid phase oxidation of toluene is first order with respect to catalyst, first order tending to zero order with respect to  $\text{FeCl}_3$ , NaBr, toluene concentration and oxygen partial pressure.

Considering the industrial significance of liquid phase oxidation of toluenes for benzaldehydes manufacture, it is always rewarding to search new catalysts as alternatives to existing ones.  $\text{Mn}(\text{OAc})_2$  and  $\text{FeCl}_3$  catalysts, though well known for a variety of oxidation reactions, have not been explored for liquid phase oxidation of toluene. The results presented in this chapter show that Mn-Fe-Br catalyst system can give higher selectivity to benzaldehyde compared to the conventional MC-type catalyst systems, although at the cost of rate of toluene conversion. It should also be taken into account that the replacement of Co by Mn in an MC-type catalyst systems should favour the economy of the process to a great extent.

An in-depth analysis of the results presented in this study shows a great potential for developing industrially competitive, economical and recyclable Mn based catalyst system.

### **Nomenclature**

|                                 |   |
|---------------------------------|---|
| A                               | Concentration of oxygen, kmol/m <sup>3</sup>  |
| B                               | Concentration of toluene, kmol/m <sup>3</sup>   |
| C                               | Concentration of benzyl alcohol, kmol/m <sup>3</sup>                                      |
| D                               | Concentration of benzyl acetate, kmol/m <sup>3</sup>                                      |
| E                               | Concentration of benzaldehyde, kmol/m <sup>3</sup>  |
| F                               | Concentration of benzoic acid, kmol/m <sup>3</sup>  |
| H                               | Henry constant defined by equation 2.3  |
| k <sub>1</sub>                  | Intrinsic rate constants, m <sup>3</sup> /kmol  |
| k <sub>2</sub> - k <sub>9</sub> | Constant in reaction m <sup>3</sup> /kmol   |
| P <sub>f</sub>                  | Final pressure MPa  |
| P <sub>i</sub>                  | Initial pressure MPa  |
| R                               | Universal gas constant, kJ/kmol/K   |
| r                               | Rate of hydroformylation, kmol/m <sup>3</sup> /s.   |
| C <sub>exp</sub>                | Experimental concentrations, kmol/m <sup>3</sup>  |
| C <sub>pre</sub>                | Predicted concentrations, kmol/m <sup>3</sup>   |
| R <sub>i</sub>                  | Reaction rate for the oxidation reaction (kmol/m <sup>3</sup> /s)                         |
| t                               | Reaction time, h.   |
| T                               | Temperature, K  |
| V <sub>g</sub>                  | Gas volume, m <sup>3</sup>  |
| V <sub>L</sub>                  | Total liquid volume, m <sup>3</sup>   |
| X <sub>a</sub>                  | Solubility of gas of the solute gas at pressure P <sub>f</sub> , kmol/m <sup>3</sup> /MPa |
| Φ                               | Parameter defined by Eq-2.8   |

## References

---

1. R. A. Sheldon, H. van Bekkum, *Fine Chemicals Through Heterogeneous Catalysis*, Wiley-VCH, Weinheim (2001) 1.
2. M. Thomas, R. Raja, G. Sankar, R. G. Bell, *Nature* 398 (1999) 227.
3. A. E. Shilov, G. B. Shul'pin, *Chem. Rev.* 97 (1997) 2879.
4. F. Wang, J. Xu, X. Li, J. Gao, L. Zhou, R. Ohnishi, *Adv. Synth. Catal.* 347 (2005) 1987.
5. W. Parteinheimer, *J.Mol.Catal. A: General* 67 (1991) 35
6. C. Jongsma, W. Laugs, EP 0026507 (1981).
7. S. Imamura, K. Fukuda, T. Nishida, T. Inui, *J. Catal.* 93 (1985) 186.
8. C. Subrahmanyam, B. Louis, F. Rainone, B. Viswanathan, A. Renken, T. K. Varadarajan, *Catal. Commun.* 3 (2002) 345.
9. A. Martin, U. Bentrup, A. BrPckner, B. LPcke, *Catal.Lett.* 59 (1999) 61.
10. F. Bruhne, E. Wright, *Ullmanns Encyclopedia of Technical Chemistry* 6<sup>th</sup> Ed., (1998).
11. F. Konietzni, U. Kolb, U. Dingerdissen, W.F. Maier, *J.Catal.* 176 (1998) 527.
12. F. Konietzni, H.W. Zanthoff, W.F. Maier, *J. Catal.*, 188 (1999) 154.
13. C. F. Hendriks, H. C. A. van Beek, P. M. Heertjes, *Ind. Eng. Chem. Prod. Res. Dev.* 17 (1978) 256.
14. C. Guo, Q. Liu, X. Wang, H. Hu, *App. Catal A: General* 282 (2005) 55.
15. H.V. Borgaonkar, S.R. Raverkar, S.B. Chandalla, *Ind. Eng. Chem. Prod. Res. Dev.* 23 (1984) 455.
16. W. Partenheimer, *Catal. Org. Reactions Ed. Herkes, EF.E., Marcel Dekker, Inc. New York*, (1998).
17. W. Parteinheimer, *J.Mol.Catal. A: General* 67 (1991) 35.
18. J. Gao, X. Tong, X. Li, H. Miao, J.J.Xu, *Chem. Technol. Biotechnol.* 82 (2007) 620.
19. K. Bahranowski, R. Dula, M. Labanowska, A. Michalik, L.A.Vartikian, E.M. Serwick, *Appl. Clay Sci.* 18 (2001) 93.
20. M. L. Kantam, B. M. Choudary, P. Sreekanth, K. K. Rao, K. Naik, T. Prathap Kumar, A. Khan, US 6495726 (2002).
21. M. L. Kantam, P. Sreekanth, K. K. Rao, T. Prathap Kumar, P.C. Bhavanari, B.M. Choudary, *Catal. Lett.* 81 (2002) 223.
- 22 R.A. Sheldon, J. K. Kochi, *Metal Catalyzed Oxidations of Organic Compounds* (Academic Press), New York, (1981)
- 23 R.V. Chaudhari, V.H. Rane, A.S. Deshmukh, S.S. Divekar, US 2006/0135820 (2006) A1
- 24 W. Partenheimer, *Catalysis Today*, 23 (1995) 69.
- 25 C. F. Hendriks, H. C. A. van Beek, P. M. Heertjes, *Ind. Eng. Chem. Prod. Res. Dev.* 17 (1978) 260.
- 26 K. Weissermel and H.J. Arpe, *Industrial Organic Chemistry*, Vedag Chemie, Weinheim, New York, 2 Ed., (1993), 176.
- 27 R.M. Deshpande, B.M. Bhanage, S.S. Divekar, S.Kanagasabapathy, R.V. Chaudhari, *Ind. Eng. Chem. Res.* 37 (1998) 2391.
- 28 R. Battino, T. R. Rettich, T. Tominaga, *J. Phys. Chem. Ref. Data* 12 (1983) 163
29. P.A. Ramachandran, R.V. Chaudhari, *Multiphase Catalytic Reactors Gordon and*

- 
- Breach, London, (1983).
30. R.V. Chaudhari, R.V. Gholap, G. Emig, H. Hofmann, *Can. J. Chem.* 65 (1987) 744.
32. L. Kiwi-Minsker, D. A. Bulushev, F. Rainone, A. Renken, *J. Mol. Catal A: Chemical* 184 (2002) 223.
33. P.W.H. Chan , S. Kamijo, Y. Yamamoto, *Synth. Lett.* (2001), 910.
34. C. Zhao , J. Yan, Z. Xi, *J.Org. Chem.* 68 (2003) 4355.
35. S. Liu, I. D. Hills, G. C. Fu, *J. Am. Chem. Soc.* 127 (2005) 15352.

## **Chapter 3**

# **Selective Oxidation of Ethylbenzene Using Hydrotalcite-like Compounds as Catalysts**

Liquid phase oxidation of ethylbenzene using hydrotalcite-like compounds as catalysts in non-acidic medium in the presence of *tert*-butyl hydroperoxide (TBHP) as the oxidant was investigated. Cobalt-containing hydrotalcite was found to give high catalytic activity and excellent selectivity to acetophenone (Acph). The effect of temperature and the concentration of ethylbenzene, catalyst and TBHP on ethylbenzene conversion and the product distribution has been studied. The reaction rates and product distribution was found to be strongly influenced by the metal ions in the hydrotalcite like compound (HTlc), the concentration of the metal ions in the catalyst, the solvent used and the reaction conditions. High selectivity to acetophenone (>98%) with moderate ethylbenzene conversion was achieved using Co-Al hydrotalcite as catalyst. A detailed kinetic study was carried out using Co-Al Hydrotalcite as a catalyst and TBHP as the oxidant.



### 3.1. Introduction

Aromatic ketones are of significant importance in synthetic chemistry as intermediates in perfumery and pharmaceuticals. For example, acetophenone (Acph) is an important intermediate in perfumery, drug and pharmaceutical industry<sup>1</sup>. The industrial synthesis of aromatic ketones involves Friedel-Craft's acylation of aromatic compounds by acid halide or acid anhydride, using stoichiometric amounts of anhydrous aluminium chloride or homogeneous acid catalysts, leading to formation of large volumes of highly toxic and corrosive wastes.<sup>2,3</sup> In the past extensive work has been done to synthesize the aromatic ketones by oxidizing the methyl group attached to an aromatic ring using stoichiometric oxidation reagents like  $\text{KMnO}_4$ . A few illustrations of this kind of oxidations are the oxidation of diphenylmethane to benzophenone by  $\text{KMnO}_4$ ,  $\text{SeO}_2$  or  $\text{CrO}_3\text{-SiO}_2$ <sup>4,5</sup> and the oxidation of alkylarenes by  $\text{KMnO}_4$  supported on Mont-K<sup>6</sup>. These reactions produce large amounts of waste inorganic salts, and also, the separation and isolation of the products and unconverted substrate from the reaction mixture is difficult. Recently, there has been an increasing interest in developing cleaner, economical catalytic processes for synthesizing value-added products like ketones by benzylic oxidation of alkyl aromatics.<sup>7</sup>

Acetophenone can also be produced by liquid phase air oxidation of ethylbenzene using soluble salts of Co, Mn, Cu or Fe as catalysts and using acetic acid as a solvent<sup>8</sup>. Although the metal salts used in these processes are in catalytic amounts, the reaction conditions are harsh<sup>7</sup>; the ketone selectivity is poor, corrosive promoters like bromide ions are essential along with the catalyst. Also the recovery and recycle of the catalyst is tedious and expensive which becomes complicated due to formation of tarry compounds<sup>7</sup>. In industrial processes, the cost centre is obviously the metal catalyst used, which implies that the reactions to be carried out in a manner that simplifies the separation, isolation and reuse of the catalyst. Due to this fact, extensive research work has been done in heterogenization of catalysts, recovery of the catalyst, catalyst poisoning etc.

The oxidation of many organic substrates using  $\text{H}_2\text{O}_2$  as oxidant over  $\text{Ti}^{4+}$  analogues of ZSM-5 (TS-1) and ZSM-11 (TS-2) has been well-documented.<sup>9,10,11</sup> Titanium substituted silicates have been thought to catalyze ring hydroxylation of arenes with  $\text{H}_2\text{O}_2$ , but vanadium<sup>12</sup>, tin<sup>13</sup> and chromium<sup>14,15</sup> substitution into a variety of zeolites

and aluminophosphate molecular sieves have led to favored oxidation at the side-chain. The presence of molecular oxygen or single oxygen atom donors such as *tert*-butyl hydroperoxide (TBHP) for the oxidation of alkanes to alcohols and ketones are shown to be important<sup>16,17,18</sup>.

Oxidation using hydroperoxide as an oxidant is attracting great interest because of the fact that they yield the desired oxidation product with high selectivity under mild reaction conditions and generate easily separable co-products like water or aliphatic alcohols<sup>19</sup>. Among the various transition metal catalyst systems reported for ethylbenzene oxidation, the most effective ones are the heterogenized cobalt catalysts like cobalt-containing hexagonal mesoporous materials (Co-HMS)<sup>1</sup> and cobalt-substituted silicate xerogels<sup>2</sup>. Chromium substituted aluminophosphate catalysts are found to yield ketones with high selectivity from alkyl arenes with TBHP as the oxidant<sup>20</sup>. Manganese analogues of these systems have also been shown to catalyze oxidation of alkanes using TBHP<sup>21</sup>.

Most of the work has been done on the homogeneous<sup>1,22</sup> and supported Co, Cu, Ni, V, Sn etc as catalyst<sup>23</sup> using TBHP as the oxidant for liquid phase oxidation of ethylbenzene. Layered double hydroxides (hydrotalcites) have received significant attention because of their potential as bulk catalysts, catalyst supports, and ion exchangers. The structural studies of hydrotalcites have shown that they are laminar structures consisting of positively charged brucite-type metal hydroxide layers with balancing anions and water molecules in the interlayer space, the most common and representative of this category being the Mg-Al hydrotalcite having the molecular formula  $Mg_3Al(OH)_8(CO_3)_{0.5} \cdot 2H_2O$ . Hydrotalcite-like compounds (HTlcs) have attracted much attention in recent years as catalyst precursors and catalyst supports. This is due to (i) their ability to accommodate a large variety of bivalent and trivalent cations, (ii) the homogeneous mixture of the cations on an atomic scale, and (iii) the formation of thermo stable mixed oxides with a high surface area. The first two properties are a result of the precursor, while the last property appears to be related to the decomposition mechanism<sup>24</sup>.

In this chapter, a detailed study of synthesis, characterization, and evaluation of a few transition metal-containing (Co, Cu, Ni, Fe etc) HTlcs as catalysts for the liquid

phase oxidation of ethylbenzene (EB) to acetophenone (Acph) using TBHP as oxidant. The effects of concentration of ethylbenzene, catalyst and oxidant on activity and selectivity were studied in a temperature range of 303-353 K, using Co-Al HTlcs as the catalyst. With this catalyst, high conversion of ethylbenzene (>80%) and high selectivity to acetophenone (>96%) at mild reaction conditions (333K) has been achieved. Based on the results of these studies, a detailed kinetic analysis of the liquid phase oxidation of ethyl benzene is presented and rate equations proposed. This study would be valuable in understanding the behavior of HTlcs as catalyst for the oxidation of ethylbenzene using TBHP as oxidant.

## 3.2. Experimental

### 3.2.1. Chemicals

The salts like magnesium nitrate ( $\text{Mg}(\text{NO}_3)_2 \cdot 6\text{H}_2\text{O}$ ), aluminium nitrate ( $\text{Al}(\text{NO}_3)_3 \cdot 9\text{H}_2\text{O}$ ), copper nitrate ( $\text{Cu}(\text{NO}_3)_2 \cdot 3\text{H}_2\text{O}$ ), cobalt nitrate ( $\text{Co}(\text{NO}_3)_2 \cdot 6\text{H}_2\text{O}$ ), iron nitrate ( $\text{Fe}(\text{NO}_3)_3 \cdot 9\text{H}_2\text{O}$ ), nickel nitrate ( $\text{Ni}(\text{NO}_3)_2 \cdot 6\text{H}_2\text{O}$ ), zinc nitrate ( $\text{Zn}(\text{NO}_3)_2 \cdot 6\text{H}_2\text{O}$ ), chromium chloride ( $\text{CrCl}_3 \cdot 6\text{H}_2\text{O}$ ), etc. were purchased from Merck India Ltd., Mumbai. NaOH and  $\text{Na}_2\text{CO}_3$  were purchased from S.D. Fine chemicals. Solvents like *tert*-Butanol, ethanol, methanol, acetonitrile, N-Methyl-2-Pyrrolidone, ethyl acetate, etc. were purchased from Merck India Ltd, Mumbai. Ethylbenzene and the substituted ethylbenzenes were purchased from Merck India Ltd., Mumbai.

### 3.2.2. Synthesis of HTlcs

HTlcs were prepared by co-precipitation at static pH and temperature at low super saturation conditions, as previously described in the literature.<sup>25</sup> The assembly used is as shown in Figure 3.1. Slow and constant addition of an aqueous solution of the metal nitrates ( $\text{Co}(\text{NO}_3)_2 \cdot 6\text{H}_2\text{O}$ , w99.0%, Merck and  $\text{Al}(\text{NO}_3)_3 \cdot 9\text{H}_2\text{O}$ , >99.0%, Fluka) in the desired molar ratio ( $x = \text{Al}^{3+} / (\text{Co}^{2+} + \text{Al}^{3+}) = 0.25$ ) with a total cation concentration of 1.5 M was mixed slowly at 25<sup>0</sup>C under vigorous agitation with an alkaline solution of  $\text{Na}_2\text{CO}_3/\text{NaOH}$ , with a carbonate concentration in the molar  $\text{CO}_3^{2-}/\text{Al}^{3+}$  ratio of 2. The pH of the mixtures was kept at 9.5 by adjusting the addition rate of the alkaline solution. Following this addition, the slurry was aged at 338K for 18 h under mild stirring. A

reflux condenser was mounted on top of the vessel to prevent water evaporation. Finally, the material was cooled to room temperature, filtered, washed with a large volume of warm (303K) deionized water until the  $\text{Na}^+$  had been completely removed ( $<0.01$  vol%) and dried at  $90^\circ\text{C}$  for 12 h.

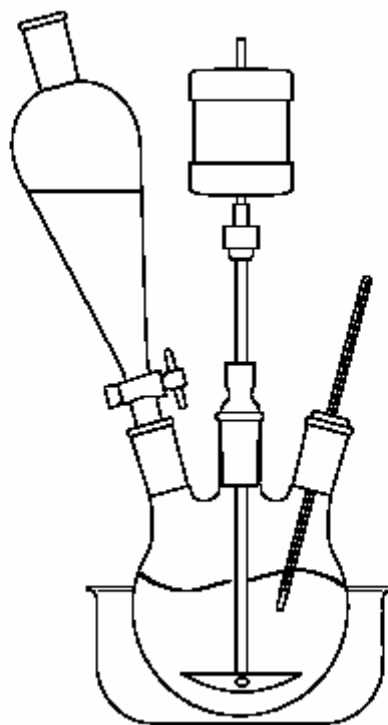
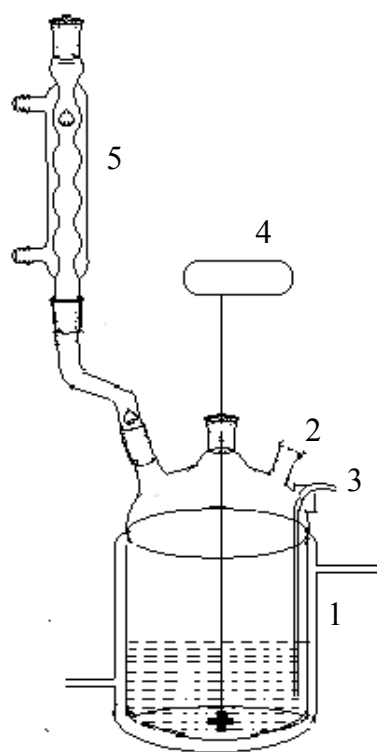


**Figure 3.1.** Hydrotalcite synthesis set up

### 3.2.3. Experimental Procedure

All the liquid phase oxidation reactions were carried out in a jacketed stirred glass reactor of 100 ml capacity. The reactor was equipped with heating arrangement, overhead stirrer, thermo well, and sampling port. There was a separate controller for agitation speed, while the reaction temperature was maintained using thermostat. A schematic of the glass reactor set-up is shown in Figure 3.2. In a typical experiment,

required amounts of ethylbenzene and *tert*-butyl hydroperoxide (TBHP) dissolved in solvent were charged into the reactor. The total volume of the reaction mixture in all the experiments was kept 50 ml ( $5 \times 10^{-5} \text{m}^3$ ). An initial sample for GC analysis was drawn. Measured amount of powdered HTlc as a catalyst was charged into the reactor containing reaction mixture at desired temperature. The reaction was started by putting the agitation to a set value. Samples were drawn at regular intervals and analyzed by gas chromatography. The reaction was stopped after a certain time and the reactor contents were cooled to room temperature.



(1) Jacketed glass reactor (2) Sampling port (3) Gas Sparger (4) Overhead stirrer (5) Condenser

**Figure 3.2.** Liquid phase oxidation reactor set up

### 3.2.4. Catalyst Recycle Procedure

For the recycle experiments, the reaction mixture after a typical oxidation experiment was cooled to room temperature, and the allowed to settle for 30 minutes. As the fine catalyst settled at the bottom of the reactor, the liquid was siphoned off carefully. The catalyst was soaked in methanol that was then siphoned off carefully, taking care not to lose any catalyst. This washing was repeated twice, after which, the catalyst was dried at low temperature (313K) under reduced pressure. The dry catalyst was then kept in oven at 363K for 12 hr and then used for the recycle experiment. The experimental procedure for carrying out the recycle experiments was kept similar to that of the typical oxidation experiment.

### 3.2.5. Analytical Methods

IR spectra were obtained using a Bio-Rad FTS 175C machine in transmission mode using KBr pellets as well as liquid cells. GC-MS analysis was carried out on an Agilent GC machine of 6890N series equipped with 5973N Mass Selective Detector.

Liquid samples were analyzed on a Hewlett Packard 6890 Series GC controlled by the HP-Chemstation software and equipped with an auto sampler unit, by using a HP-1 capillary column (30 m x 30  $\mu$ m x 0.25  $\mu$ m film thickness with a stationary phase of polymethyl siloxane). The oven temperature was programmed in the range of 333-573K at constant pressure of 10 psi. The quantitative analysis was obtained by constructing calibration curve in the range of concentrations studied. The conversion and selectivities were calculated using the following formulae % Conversion was always calculated based on the liquid substrate charged. Total aldehyde selectivity was calculated by addition of both linear and branched products. The quantifications of ethylbenzene, acetophenone, 1-phenyl ethanol (PE) were done based on the respective calibration curve. The results are discussed in terms of conversion, selectivity, turn over number (TON), turn over frequency (TOF), which are defined below.

$$\text{Conversion, (\%)} = \frac{\text{Initial ethylbenzene concentration} - \text{Final ethylbenzene concentration}}{\text{Initial ethylbenzene concentration}} \times 100$$

$$\text{Selectivity}_{\text{acetophenone}}, (\%) = \frac{\text{Number of moles of acetophenone formed}}{\text{Number of moles ethylbenzene converted}} \times 100$$

$$\text{Selectivity}_{\text{phenyl-ethanol}}, (\%) = \frac{\text{Number of moles of phenylethanol formed}}{\text{Number of moles ethylbenzene converted}} \times 100$$

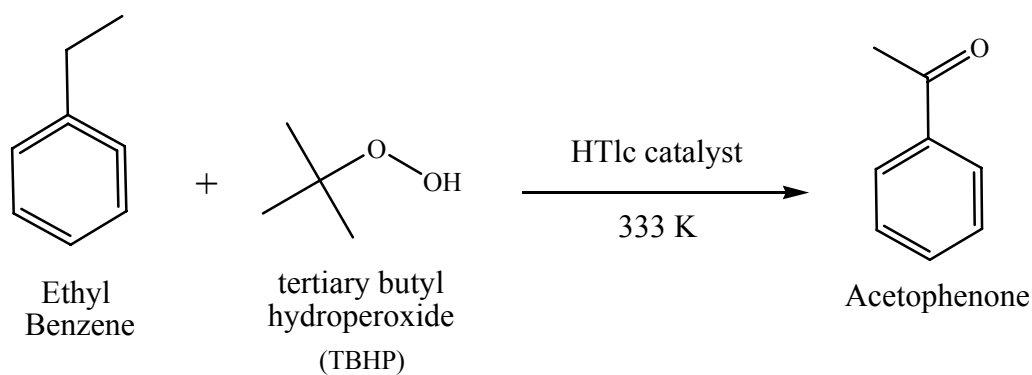
### 3.2.5.1 Analysis of TBHP Consumption

To determine the consumption of TBHP in a typical experiment, the unreacted TBHP was estimated by titration method (more commonly known as the residual oxidizing power) according to the procedure published in literature,<sup>26</sup> with minor changes. 20 ml reaction mixture was added gradually to a solution of pure potassium iodide in 10 ml of 2 N sulfuric acid contained in a stoppered conical flask. The mixture was allowed to stand for 15 minutes and then 100 ml of distilled water was added to the mixture with washing the wall of the conical flask. The liberated iodide was titrated with standard 0.1 N thiosulfate solution with the addition of 2 ml of starch solution when the color of the iodine solution was nearly discharge. The end point was from blue to colourless solution. A blank run was also carried out at the same time. To get the accurate reading of thiosulfate, the value of blank run was subtracted from the value of the reaction mixture. The amount of TBHP in the reaction mixture was then calculated by using the following equation.

$$1 \text{ ml } 1 \text{ N Na}_2\text{S}_2\text{O}_3 \equiv 0.09 \text{ g of TBHP.}$$

### 3.3. Results and Discussion

Liquid phase oxidation of ethylbenzene operates through formation of 1-phenyl ethanol (PE), which further oxidized to acetophenone, where the intermediate alcohol (PE) formed is further oxidized to give another products. For most of the catalyst systems known, it has been observed that selective synthesis of acetophenone is a major challenge as formation of byproducts such as benzaldehyde and benzoic acid, which reduces the selectivity. The general scheme is as shown in below.



**Scheme 3.1.** Schematic of liquid phase oxidation of ethylbenzene

Liquid phase oxidation of ethylbenzene was investigated using non-noble metal containing HTlcs as catalysts and 70% TBHP (aq) as the oxidant. The important objectives of the work presented in this chapter are addressed below.

1. Synthesis of non-noble transition metal containing HTlcs and their detailed spectroscopic characterization.
2. Evaluation of the synthesized HTlcs for liquid phase oxidation of ethylbenzene, and selection of the catalyst.
3. Tailoring reaction conditions to achieve high selectivity to acetophenone and to establish reusability of catalyst for liquid phase oxidation of ethylbenzene using TBHP as oxidant.
4. Detailed kinetic investigation to assess the feasibility of the proposed catalyst system for the liquid phase oxidation of ethylbenzene.

These objectives have been achieved with detailed experimentation and the results obtained are discussed in a view to understand the catalysis and kinetics of the reaction.

### 3.3.1. Characterizations of the Solid Catalysts

For characterization of the synthesized materials at different stages of synthesis and after the reactions numerous techniques have been employed to identify, understand and confirm our postulates. XRD, FT-IR spectra were obtained using a Perkin Elmer Spectrum-2000 in transmission mode using KBr pellets as well as in Shimadzu Hyper IR



in DRS (Diffused Reflectance Spectroscopy) mode by mixing samples with KBr. TGA profiles of carefully weighed quantities ( approximately 18 mg) of powders of HTlcs were recorded on a Seiko Instruments model TG/DTA 32 instrument in flowing air, in the temperature range of 30°C to 1000°C at a heating rate of 10°C/min. Powder X-ray diffraction (XRD) measurements were performed on a Philips PW 1830 instrument consisting of a rotating anode generator with a copper target (Cu  $K_{\alpha}$  radiation,  $\lambda=1.5418\text{\AA}$ ) operating at 40 kV and a current of 30 mA. The XRD patterns of the HTlcs were recorded in the range 5° - 85° at a scan rate of 1° per minute. X-ray photoelectron spectra (XPS) were recorded on a VG – Microtech ESCA 3000 spectrometer using the Mg- $K_{\alpha}$  emission ( $E = 1253\text{ eV}$ ) under a vacuum of  $\sim 10^{-9}$  torr. Scanning electron microscopy (SEM) was performed using a Philips XL 30 instrument – the catalyst materials were suspended in isopropanol, cast on gold plated discs followed by drying under vacuum and coating with a conducting material and then were imaged.

### 3.3.1.1. Powder X-Ray Diffraction

Powder X-ray diffraction is one of the most important tools for the determination of the phasic composition of the materials as well as some other derived aspects such as the size of the crystallites, their crystallographic properties etc. The hydrotalcite-like materials synthesized using various M(II)-M(III) combinations were characterized by powder XRD. All these materials were expected to have characteristic powder XRD fingerprints of those of the basic hydrotalcite Mg-Al HT, i.e.  $(\text{Mg}_2\text{Al}_6(\text{OH})(\text{CO}_3))$ -JCPDS file no. 22-700), which were used to identify the materials synthesized. Selected XRD patterns are shown in Figure 3.3. All the catalysts showed the characteristic crystallinity pattern of the hydrotalcite-like structure, and no other crystalline phase was identified.

Since the model catalyst chosen for the reaction was the Co-Al-HT (2:1), more emphasis was given on the characterization of the same. The XRD patterns of Co-Al-HTlcs CoAlHT-1 (1:1), CoAlHT-2 (2:1) and CoAlHT-3 (3:1) clearly indicated the presence of pure hydrotalcite as the only crystalline phase in all the three cases. Further, the fresh CoAlHT-2 and recovered CoAlHT-2a, CoAlHT-2b catalysts were checked for the presence of crystalline phases of the hydrotalcite. It is clearly observed that the crystallinity of the material is maintained even upon recycle. However, the only minor

change observed in the fresh and sequentially reused catalysts is that of a small shift in the  $2\theta$  values. Pérez-Ramirez and coworker have studied the high temperature XRD patterns of Co-Al-HTlcs, wherein the authors quote the effect of temperature increase on the  $2\theta$  values of the Co-Al-HT (3:1). Upon heating of the layered double material from 298K to 373K in air, the authors have observed that reflection of the basal spacing  $d$  (003) shifts slightly to lower  $d$  values, as a result of the removal of physically adsorbed water and the partial release of the interlayer water from the hydrotalcite, causing a slight decrease in the interlayer spacing. The procedure for the recovery and recycle of the catalyst in the present study (Section 3.2.3) involves washing the recovered catalyst with methanol several times, drying under vacuum, followed by further drying at 363K for 12 hours. This seems to have caused partial removal of adsorbed and interlayer water in the Co-Al-HT, as similar shift in the  $2\theta$  values have been observed upon sequential recycling of the catalyst. (Figure 3.3). The XRD patterns of all the HTlcs in general show the hydrotalcite structure as the only crystalline component, exhibiting sharp and symmetric reflections of the basal (003), (006), and (009) planes, and broad and asymmetric reflections for the non-basal (012), (015), and (018) planes. The (009) and (012) reflections overlap result in the broad signal between 32 and 38°  $2\theta$ . Furthermore, the two reflections of (110) and (113) can be clearly distinguished around 60°  $2\theta$ .

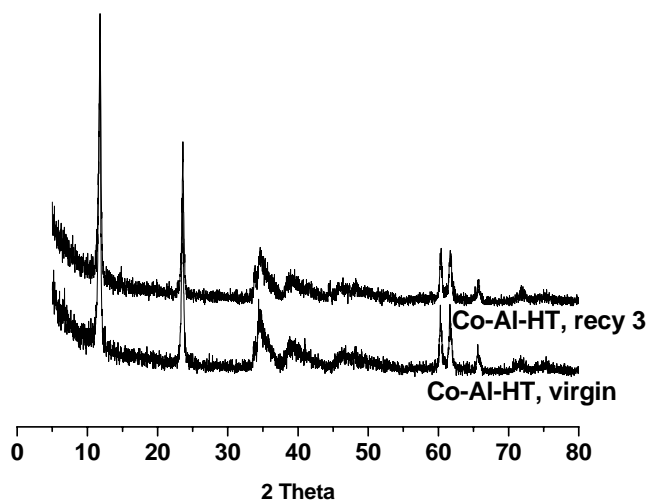


**Figure 3.3.** Powder XRD patterns for unused and recovered Co-Al-HT catalyst

### 3.3.1.2. Scanning Electron Microscopy

Scanning electron microscopy is a straightforward technique used widely to probe the morphological features of heterogeneous or bulk catalysts. SEM scans over a sample surface with a probe of electrons (5-50 eV) and detects the yield of either secondary or back-scattered electrons as a function of the position of the primary beam, and provides the sight of the morphological pattern of the synthesized materials in a sub-micron level. The SEM micrographs of the unused and recycled samples are presented in Figure 3.4. It was observed that the average particle size  $\sim 230$  nm and it was also found to maintain after recycle.

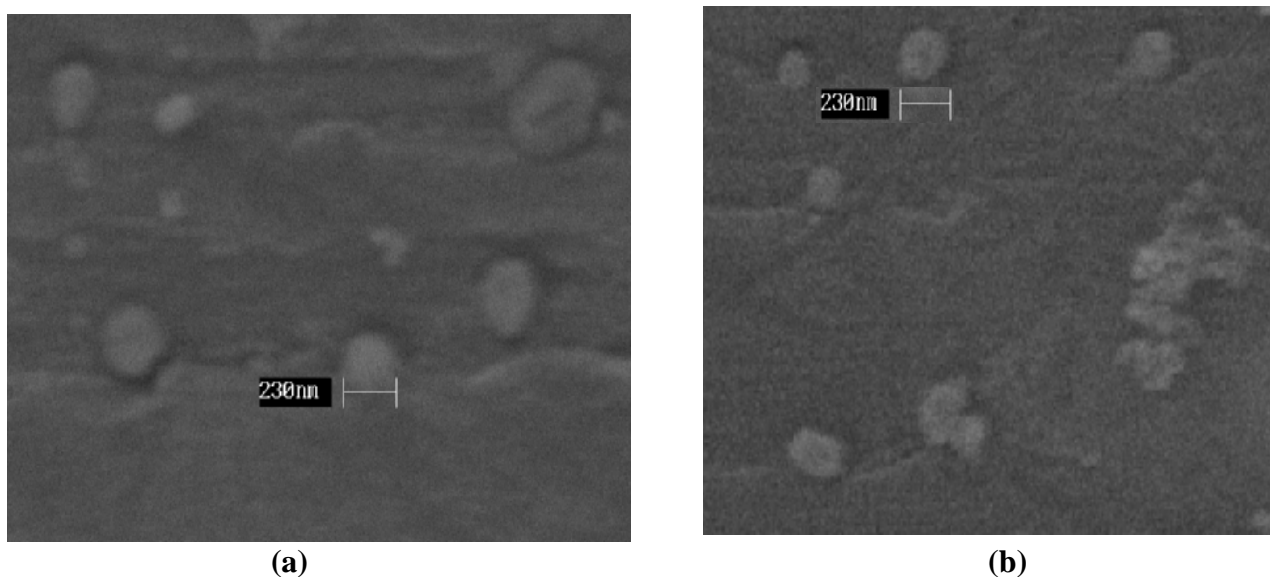


**Figure 3.4.** Scanning Electron Microscopy patterns of for unused and recovered Co-Al-HT catalyst a) unused catalyst b) recovered catalyst.

### 3.3.1.3. X-Ray Photoelectron Spectroscopy

The oxidation state present in the catalyst is typically analyzed using the X-ray photoelectron spectroscopy (XPS). For the hydrotalcite Co-Al-HTlc, the XPS spectrum is shown in Figure 3.5., which shows a full scale binding energy data for the catalyst. The peaks in the spectra are typically identified as the different elements and the binding energies were used to assign the oxidation states of the respective elements. All the

values were corrected to the standard carbon 1s peak arising out of the adventitious carbon at 285 eV.

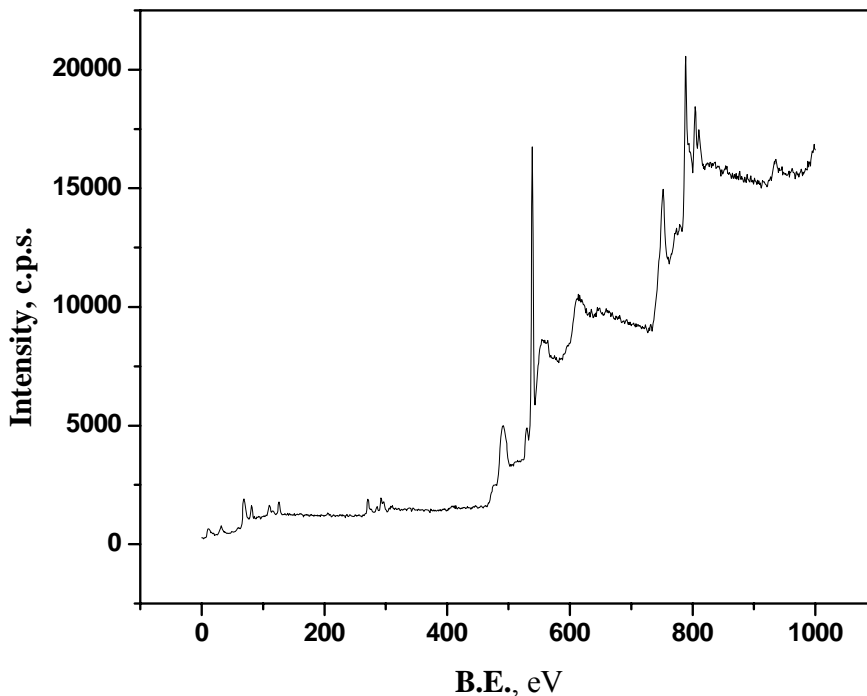


**Figure 3.5.** Full-range XPS spectrum of Co-Al-HTlc

The XPS spectrum of Co-Al-HT clearly shows the presence of Co  $2p_{3/2}$  at the B.E. of 780.8 and  $2p_{1/2}$  at 796.8. It is known that the intensity of these peaks depends on the metal content. The higher metal contents cause increase in the intensity and broadening of the peaks. The energy difference between the  $2p_{3/2}$  and  $2p_{1/2}$  for the Co-Al-HT was found to be  $\sim 16.1$ , which clearly shows that the cobalt in the hydrotalcite exists as  $\text{Co}^{2+}$  and not as  $\text{Co}^{3+}$  <sup>27</sup>.

The XPS spectrum of fresh Co-Al-HT was also compared with the spectrum of catalyst recovered from the reaction. The used catalyst was recovered, washed and dried as explained in section 3.2.3, and its XPS spectrum was also recorded. The comparison can be seen in Figure 3.6. The comparison shows that the oxidation state of cobalt remains unaltered at 2+ after the oxidation experiment.

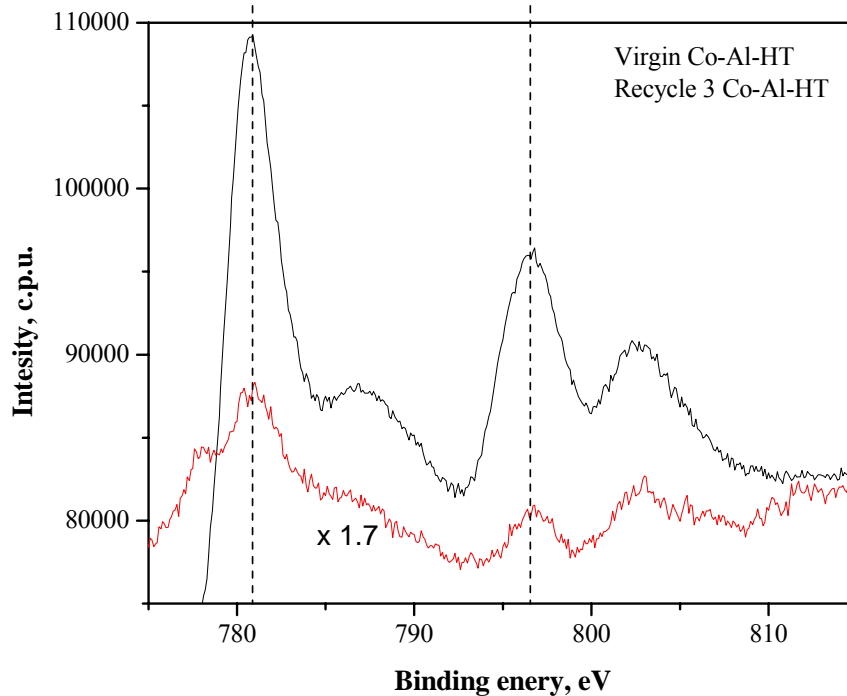


**Figure 3.6.** XPS spectra of unused and recovered Co-Al-HT catalyst

### 3.3.1.4. Fourier Transform Infra Red Spectroscopy

The IR spectra of the hydrotalcite catalyst Co-Al-HT was recorded in the range of 400-4000  $\text{cm}^{-1}$ . Kloprogge and coworker have done the band component analysis of Co, Mg and Ni containing hydrotalcites, wherein they have observed four major bands in the Co-Al-HT, and they have been assigned frequencies based on literature reports and spectral interpretation<sup>28</sup>. A similar pattern has been observed in the IR spectrum in the present study. The band at 3046  $\text{cm}^{-1}$  can be assigned as the  $\text{CO}_3^{2-}$ -H<sub>2</sub>O bridging mode of carbonate and water in the interlayer frequency. The broad band at 3423  $\text{cm}^{-1}$  is due to the Co-OH bond, which masks the band due to the hydrogen-bonded interlayer water, as revealed by the band component analysis. The broad band probably also masks the band due to the Al-OH, which is expected to appear at a frequency more than that due to the Co-OH band, since the Al-OH band is weaker than the Co-OH bond. The hydroxyl translation modes mainly influenced by the divalent Co in the hydrotalcite structure can be observed at 598  $\text{cm}^{-1}$ . The band at 546  $\text{cm}^{-1}$  is assigned to the Al-OH translation mode.

Incidentally, the band at 598 and 546  $\text{cm}^{-1}$  are observed as two distinct bands, which could be resolved only by band component analysis by Kloporgge and coworker<sup>29</sup>. The bands at 790  $\text{cm}^{-1}$  and 867  $\text{cm}^{-1}$  are characteristic for the  $\nu_4$  and  $\nu_2$  modes of the interlayer carbonate group. The band at 1627  $\text{cm}^{-1}$  is characterized by the bending mode of interlayer water. The two  $\nu_3$  modes (symmetric stretch) are known to appear at 1365 and 1401  $\text{cm}^{-1}$  associated with the interlayer carbonate<sup>30</sup>. In case of the Co-Al-HT catalyst, the band at 1365  $\text{cm}^{-1}$  is seen, but that at 1401 is probably masked.

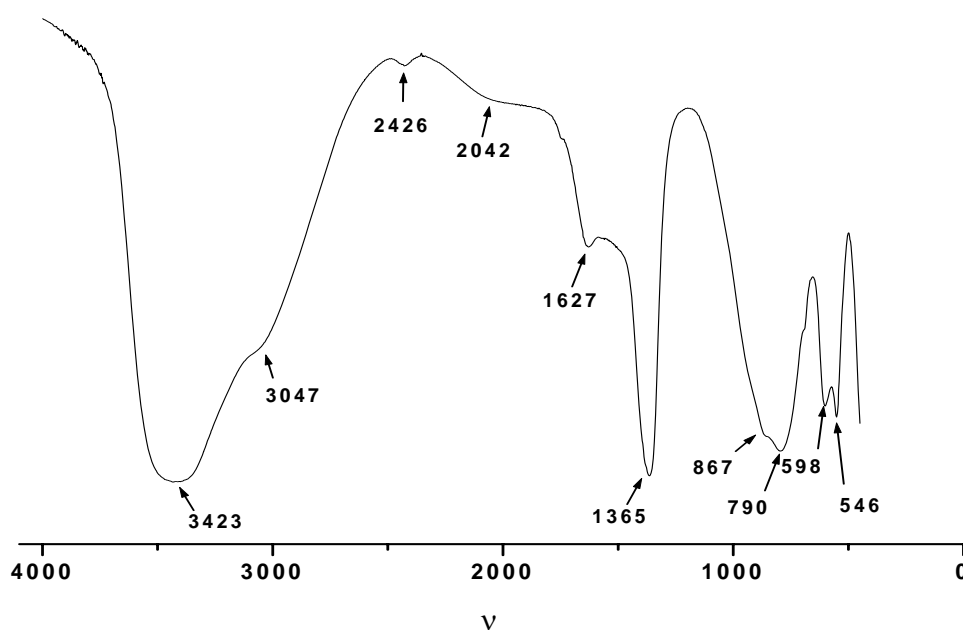


**Figure 3.7.** FTIR spectra of Co-Al-HT catalyst

### 3.3.1.5. TGA-DTA

The Co-Al-HTlc was subjected to thermogravimetric analysis. The pattern of weight loss observed in this study is presented in Figure 3.8. This profile is similar to that observed by Perez-Ramirez and coworkers,<sup>31</sup> who have also done the mass spectroscopic analysis to ascertain the nature of decomposition of the layered material. The decomposition pattern obtained for Co-Al-HTlc has been reported to be considerably different from the pattern observed in thermal analysis of other layered double hydroxides.<sup>32</sup> Also, the nature of decomposition is different in air and inert medium.

Perez-Ramirez and coworkers have reported that, in inert gas the main transitions appear to be more separated, and a two-step weight loss occurs, while in the sample decomposed in air, the simultaneous occurrence of the different processes appears as a single-step weight loss in the TGA profile. A similar pattern has been observed in the TGA of Co-Al-HTlc, and the weight losses due to dehydroxylation and decarbonation cannot be clearly defined. However, the initial weight loss of up to 14.5%, caused by dehydroxylation, is clearly observed in the temperature interval of 38-243<sup>0</sup>C, while the weight loss of ca. 6.5% is observed in the further temperature interval of 243-523<sup>0</sup>C, which apparently masks the weight loss due to decarbonation. The total weight loss observed in the thermal decomposition was approximately 22.9%. The thermal analysis of the cobalt catalyst thus indicates that the catalyst retains its hydrotalcite-like nature under the experimental conditions, and there is no dehydroxylation or decarbonation of the layered material under experimental conditions (maximum 90<sup>0</sup>C).

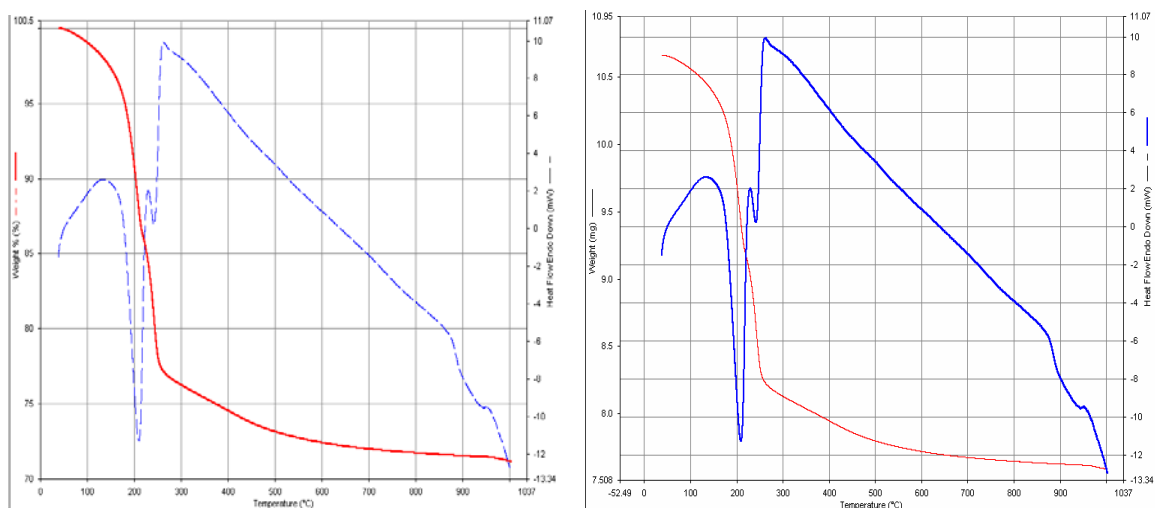


**Figure 3.8.** TGA and DTA patterns of Co-Al-HT catalyst

### 3.3.1.6. Surface Area Measurement

The HTlcs were analyzed for the determination of the surface area of the crystalline bulk catalysts formed. It was important from the viewpoint of the activity of the catalyst, as the larger the surface area, greater is the accessibility of the reactants to the catalytic sites, and better is the activity. The surface area analysis of the HTlcs were

done using N<sub>2</sub>-physisorption - desorption technique, using the BET formula. The results are presented in Table 3.1. It is clearly observed from the data in Table 3.1 that the HTlcs have low surface areas, in the range of 45 to 61 m<sup>2</sup>g<sup>-1</sup>.

**Table 3.1.** Surface area of HTlcs

| Sr | HTlc (M <sup>II</sup> -M <sup>III</sup> ) | Surface area, m <sup>2</sup> g <sup>-1</sup> |
|----|---|--|
| 1  | Mg-Al                                     | 55.3   |
| 2  | Co-Al                                     | 58.6   |
| 3  | Ni-Fe                                     | 57.2   |
| 4  | Ni-Cr                                     | 53.1   |
| 5  | Cu-Cr                                     | 48.9   |
| 6  | Mg-Al                                     | 60.7   |
| 7  | Cr-Zn                                     | 55.3   |
| 8  | Mg-Al-Cu                                  | 53.1   |
| 9  | Ni-Al                                     | 44.3   |
| 10 | Co-Cr                                     | 57.2   |
| 11 | Co-Fe                                     | 51.4   |

### 3.3.2. Catalysis Using HTlcs

Hydrotalcite-like anionic clays are synthetic or natural crystalline materials consisting of positively charged two-dimensional sheets with water and exchangeable charge-compensating anions in the interlayer region. Their general formula is  $[M_{1-x}^{2+}M_x^{3+}(OH)_2]^{x+} (A_{x/n}^{n-})_m H_2O$ , where M<sup>2+</sup> and M<sup>3+</sup> represent divalent and trivalent cations in the brucite-type layers, A is the interlayer anion with charge n, x is the fraction of the trivalent cation (x values in the general formula are in the range of 0.20–0.50), and m is the water of crystallization. Hydrotalcites are useful as catalysts in three possible ways: 1) Solid base catalysis- the hydrated HTlcs carry hydroxyl anions, while the water-free calcined materials contain the strong Lewis basic O<sup>2-</sup>—M pairs. 2) Catalysis with exchangeable anions, a very prominent example of which is WO<sup>4-</sup> exchanged HT, which has been extensively used for oxidation and hydrobromination reactions; and 3) Catalysis due to transition metals which constitute the cationic framework of the hydrotalcite. This property has been exploited in several reactions including partial or complete oxidation which mainly employed Co as the catalytically active cation, hydrogenations especially with Ni containing HTlcs, whereas, a few Co and Cu containing HT precursors may even



be applied for the Fischer–Tropsch synthesis of hydrocarbons from CO/H<sub>2</sub> mixtures.<sup>33</sup> Because of the fact that transition metal containing hydrotalcites have their framework made of the cations, they offer stable, crystalline, non-leaching bulk catalysts. The TBHP-mediated oxidations using transition metal catalysts are known to operate via free-radical mechanism, and the ionic form of the metals is known to be active for catalysis. It was therefore an objective of the present study to investigate the catalytic activity of such transition metal-containing HTlcs for the liquid phase oxidation of ethylbenzene.

### 3.3.2.1. Screening of HTlcs

The non-catalytic oxidation of ethylbenzene with TBHP was first attempted as a control experiment. Very less conversion of ethylbenzene (0.9%) was observed with ~50 % selectivity to acetophenone. Thereafter, an experiment with the basic Mg-Al-HT as a catalyst was carried out. Marginal catalytic activity of the hydrotalcite was observed, with only 2.9 % ethylbenzene conversion and an acetophenone selectivity of 69%. After this, the screening of HTlcs containing different M(II)-M(III) combinations with metals like Co, Cu, Fe, Ni, Zn was carried out. The catalyst screening results were compared in terms of ethylbenzene conversion and selectivity to acetophenone and the results are shown in Table 3.2. From the results, it is envisaged that under identical set of reaction conditions, Co-HTlc gave the highest selectivity to acetophenone. Mg-Al-Fe and Cr-Zn were also found to give good activity (14.3 % and 18.3 %), but the selectivity to acetophenone was comparatively low (~ 80%). The formation of acetophenone in this reaction is supposed to be a consecutive oxidation reaction, in which 1-phenylethanol (PE) is an intermediate. Alternatively, it has been reported that benzaldehyde is formed as a byproduct in this reaction, which may also further oxidize to benzoic acid. In the present study, the nickel-containing HTlcs, namely Ni-Al, Ni-Cr and Ni-Fe yielded benzaldehyde and benzoic acid as byproducts, although in trace quantities. The incorporation of cobalt into HTlcs was found to enhance the activity as well as selectivity in case of liquid phase oxidation to ethylbenzene. The best catalytic performance was observed when the reaction was carried out using Co-Al HTlcs, wherein high conversion of ethylbenzene (43.9%) was achieved with good selectivity of acetophenone (92.7%).

**Table 3.2.** Screening of hydrotalcite for liquid phase oxidation of ethylbenzene

| Sr. | HTlcs    | Ethylbenzene<br>Conversion,<br>% | Selectivity, % |      |     |     |
|-----|----------|----------------------------------|----------------|------|-----|-----|
|     |          |                                  | Acph           | PE   | BzH | BAc |
| 1   | Non-cat  | 0.9                              | 50.0           | 35.0 | 8.0 | 3.0 |
| 2   | Mg-Al    | 2.9                              | 69.0           | 26.0 | 2.0 | 1.0 |
| 3   | Ni-Fe    | 5.9                              | 70.0           | 25.0 | 3.0 | 2.0 |
| 4   | Ni-Cr    | 11.3                             | 73.0           | 22.0 | 4.0 | 1.0 |
| 5   | Cu-Cr    | 11.2                             | 84.0           | 10.0 | 2.0 | 1.0 |
| 6   | Mg-Al-Fe | 14.3                             | 80.2           | 12.3 | 4.0 | 1.5 |
| 7   | Cr-Zn    | 18.3                             | 85.0           | 12.0 | 2.0 | 1.0 |
| 8   | Mg-Al-Cu | 13.8                             | 76.0           | 19.0 | 3.0 | 1.0 |
| 9   | Ni-Al    | 12.4                             | 74.0           | 18.0 | 5.0 | 3.0 |
| 10  | Co-Cr    | 17.3                             | 86.4           | 9.3  | 3.0 | 1.0 |
| 11  | Co-Fe    | 27.6                             | 88.0           | 9.0  | 2.0 | 1.0 |
| 12  | Co-Al    | 43.9                             | 92.7           | 6.9  | 0.6 | 0.0 |

**Reaction Conditions:** Ethylbenzene, 0.69 kmol/m<sup>3</sup>; catalyst, 2.2 kg/m<sup>3</sup>; TBHP, 2.1 kmol/m<sup>3</sup>; Temperature, 333K; Agitation speed, 16.7 Hz; Solvent, t-BuOH; Time, 3 h; Total charge 5 x 10<sup>-5</sup> m<sup>3</sup>

### 3.3.2.2. Optimization of Reaction Parameters

The effect of different reaction parameters on the behavior of the reaction was investigated in order to optimize the concentrations of reaction components. For this purpose, the effect of catalyst concentration, i.e. Co-Al-HT (22% Co; Co:Al = 2) was first studied. The results are shown in the Table 3.3. The conversion of ethylbenzene was found to increase linearly with the increase in concentration of Co-Al-HT till 3 kg/m<sup>3</sup> (entry 1-4). High selectivity to Acph (92.5%) was observed at 24.4 % conversion of ethylbenzene (entry 2). At higher catalyst concentration, the selectivity to acetophenone was hampered, as formation of benzaldehyde and benzoic acid was observed (entry 4). Increase in rate of reaction observed with increase in ethylbenzene concentration (entry 5,6). Also the formation of PE was more with increase in ethylbenzene concentration. A few reactions were carried to optimize the TBHP concentration (entry 8-10), where increase in the rate was observed till 3.1 kmol/m<sup>3</sup>/s (ethylbenzene: TBHP ratio 1:3) (entry 2).

**Table 3.3.** Optimization of reaction parameters for liquid phase oxidation of ethylbenzene

| Sr.             | Co-Al HTLc, kg/m <sup>3</sup> | Ethylbenzene Conversion, % | Selectivity, % |      |     |     | Rate x 10 <sup>5</sup> , kmol/m <sup>3</sup> /s |
|-----------------|-------------------------------|----------------------------|----------------|------|-----|-----|---|
|                 |                               |                            | Acph           | PE   | BzH | BAc |   |
| 1               | 0.7                           | 11.6                       | 87.0           | 11.5 | 0.1 | 0.0 | 1.5   |
| 2               | 1.7                           | 24.4                       | 92.5           | 6.9  | 0.0 | 0.0 | 3.1   |
| 3               | 3.0                           | 33.6                       | 91.3           | 5.3  | 1.2 | 0.0 | 4.3   |
| 4               | 4.5                           | 34.4                       | 92.6           | 7.2  | 2.5 | 1.8 | 4.4   |
| 5 <sup>a</sup>  | 1.7                           | 32.1                       | 93.2           | 5.4  | 0.0 | 0.0 | 2.1   |
| 6 <sup>b</sup>  | 1.7                           | 12.3                       | 86.2           | 10.4 | 1.7 | 0.9 | 3.4   |
| 7 <sup>c</sup>  | 1.7                           | 07.6                       | 86.2           | 10.4 | 1.7 | 0.9 | 3.5   |
| 8 <sup>d</sup>  | 1.7                           | 13.6                       | 90.4           | 9.1  | 0.0 | 0.0 | 1.7   |
| 9 <sup>e</sup>  | 1.7                           | 16.7                       | 92.1           | 7.8  | 0.0 | 0.0 | 2.1   |
| 10 <sup>f</sup> | 1.7                           | 25.1                       | 91.8           | 5.3  | 1.2 | 0.8 | 3.2   |

**Reaction Conditions:** Ethylbenzene, 0.69 kmol/m<sup>3</sup>; TBHP, 2.1 kmol/m<sup>3</sup>; Temperature, 333K; Agitation speed, 16.6 Hz; Solvent, t-BuOH; Time, 1.5 h; Total charge 5 x 10<sup>-5</sup> m<sup>3</sup>; a ethylbenzene, 0.5 kmol/m<sup>3</sup>; b ethylbenzene, 1.5 kmol/m<sup>3</sup>; c ethylbenzene, 2.5 kmol/m<sup>3</sup>; d TBHP, 1 kmol/m<sup>3</sup>; e TBHP, 2 kmol/m<sup>3</sup>; f TBHP, 4 kmol/m<sup>3</sup>.

### 3.3.2.3. Effect of Co:Al Ratio on Ethylbenzene Oxidation

Since the Co-Al-HT is a bulk, crystalline catalyst the amount of cobalt and its dispersion in the solid matrix was expected to yield varying catalytic activities for the TBHP mediated oxidation. To study the effect of dispersion of cobalt in the hydrotalcite, a few experiments were also carried out using Co-Al-HTlcs with different Co:Al ratios (Table 3.4). The investigations revealed that the conversion of ethylbenzene increased with increase in Co:Al ratio of 2, whereas the Co:Al ratio of 3 did not result in any visible increase in the catalytic activity. Therefore, further study was carried out using Co-Al HTlc as catalyst, with a Co:Al ratio of 2. A few other properties like surface area, pH and basicity of the Co-Al HTlcs were also investigated. The surface areas of the modified hydrotalcites were determined by BET technique, the pH and quantitative estimation of the basic sites on the surface of the layered material was calculated by methods similar to those employed by Jana and coworkers.<sup>34</sup> The results of these investigations are

illustrated in Table 3.5. The surface areas of the hydrotalcites varied marginally, and lower Co:Al ratio hydrotalcite were found to have larger higher surface areas. The basicity was found to increase slightly on increasing the Co-Al ratio.

**Table 3.4.** Effect of Co-Al ratio on ethyl benzene oxidation

| Sr. | Co/Al | Ethylbenzene Conversion, % | Selectivity, % |     |     |     |
|-----|-------|----------------------------|----------------|-----|-----|-----|
|     |       |                            | Acph           | PE  | BzH | BAc |
| 1   | 0.5   | 11.2                       | 92.6           | 7.2 | 0.0 | 0.0 |
| 2   | 1     | 16.3                       | 91.3           | 8.0 | 0.0 | 0.0 |
| 3   | 2     | 24.4                       | 92.5           | 6.9 | 0.0 | 0.0 |
| 4   | 3     | 25.6                       | 92.8           | 4.3 | 1.1 | 0.9 |

**Reaction Conditions:** Ethylbenzene, 0.69 kmol/m<sup>3</sup>; Cobalt, 0.37 kg/m<sup>3</sup>; TBHP, 2.1 kmol/m<sup>3</sup>; Temperature, 333K; Agitation speed, 16.6 Hz; Solvent, t-BuOH; Time, 1.5 h; Total charge 5 x 10<sup>-5</sup> m<sup>3</sup>

**Table 3.5.** Properties of Co-Al HTlc

| Sr. | Co:Al | XRD phases   | Surface area, m <sup>2</sup> -gm <sup>-1</sup> | Pore volume, ml-gm <sup>-1</sup> | pH of suspension in water <sup>a</sup> | μmol basic sites/gm HTlc Basicity <sup>b</sup> |
|-----|-------|--------------|--|----------------------------------|--|--|
| 1   | 3     | hydrotalcite | 47.31  | 0.07                             | 8.7                                    | 27.7   |
| 2   | 2     | hydrotalcite | 58.69  | 0.19                             | 8.2                                    | 26.7   |
| 3   | 1     | hydrotalcite | 74.43  | 0.18                             | 7.8                                    | 25.9   |

<sup>a</sup> Suspension of 0.3 gm hydrotalcite in 20 ml deionized water

<sup>b</sup> 0.15 gm hydrotalcite suspended in 2 ml phenolphthalein indicator solution, and titrated with 0.01M benzoic acid.

#### 3.3.2.4. Effect of Solvents

Effect of different solvents was studied using Co-Al HTlc as catalyst at 333K (Table 3.6). An attempt was made to correlate the experimental results obtained with the polarities of the solvents. It was observed that, solvents with low polarities favored the conversion of ethylbenzene and also increases the selectivity to Acph. Among the solvents screened, ethyl acetate was found to be the best solvent, however, the solvent was found to be reactive under the experimental conditions employed, and therefore was not considered for further studies. *Tert*-butyl alcohol was found to be the most effective,

non-participating solvent, in which an ethylbenzene conversion of 24.4% with 92.5 % selectivity to acetophenone could be achieved.

**Table 3.6.** Screening of solvents for liquid phase oxidation of ethylbenzene

| Sr. | Solvents | Dielectric constant, e | Ethylbenzene Conversion, % | Selectivity, % |      |     |     | Rate x 10 <sup>6</sup> , kmol/m <sup>3</sup> /s |
|-----|----------|------------------------|----------------------------|----------------|------|-----|-----|---|
|     |          |                        |                            | Acph           | PE   | BzH | BAC |   |
| 1   | EtOAc    | 6.02                   | 26                         | 92.8           | 6.9  | 0.0 | 0.0 | 1.73  |
| 2   | t-BuOH   | 18                     | 24.4                       | 92.5           | 6.9  | 0.0 | 0.0 | 1.63  |
| 3   | MeOH     | 33                     | 15.3                       | 89.2           | 7.9  | 0.5 | 0.1 | 1.02  |
| 4   | NMP      | 32.4                   | 11.9                       | 88.0           | 8.3  | 0.3 | 0.0 | 0.79  |
| 5   | EtOH     | 24.3                   | 10                         | 81.1           | 12.0 | 0.1 | 0.0 | 0.67  |

**Reaction Conditions:** Ethylbenzene, 0.69 kmol/m<sup>3</sup>; catalyst, 1.7 kg/m<sup>3</sup>; TBHP, 2.1 kmol/m<sup>3</sup>; Temperature, 333K; Agitation speed, 16.6 Hz; Solvent, t-BuOH; Time, 1.5 h; Total charge 5 x 10<sup>-5</sup> m<sup>3</sup>

### 3.3.2.5. Effect of Temperature

Significant effect of temperature was observed in Co-Al HTlc catalyzed liquid phase oxidation of ethylbenzene. At 303 K, a TOF of 82 h<sup>-1</sup> was observed without catalyst deactivation. When the temperature was increased from 303 K to 343 K, in Co-Al-HTlc catalyst system, significant increase in rate of reaction was observed (Figure 3.9). Simultaneously, increase in conversion levels increased the selectivity to acetophenone decreasing the selectivity to PE. The optimum temperature range observed was 303-333K. High conversion of ethylbenzene (24.4%) was observed at 333K with selectivity of 92.5% to acetophenone at 333K. Beyond 333 K, no prominent enhancement in ethylbenzene conversion and acetophenone selectivity was observed; therefore further exploration was carried out at 333 K.

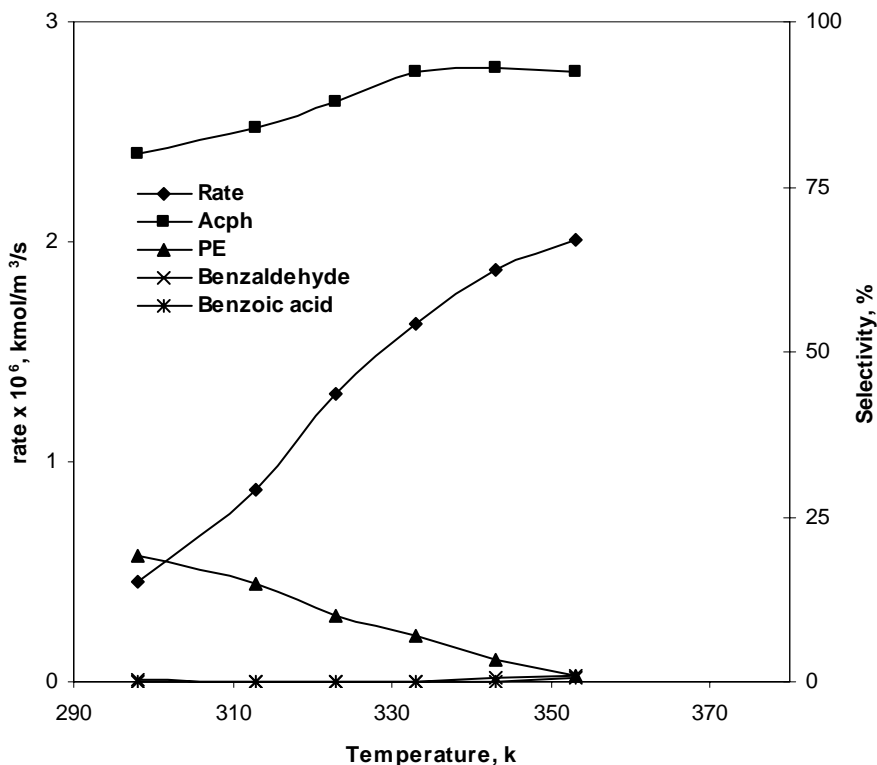


**Figure 3.9.** Effect of temperature on ethylbenzene oxidation

**Reaction Conditions:** Ethylbenzene, 0.69 kmol/m<sup>3</sup>; catalyst, 1.7 kg/m<sup>3</sup>; TBHP, kmol/m<sup>3</sup>; Agitation speed, 16.6 Hz; Solvent, t-BuOH; Time, 1.5 h; Total charge 5 x 10<sup>-5</sup> m<sup>3</sup>

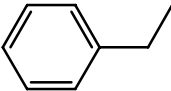
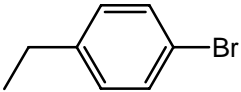
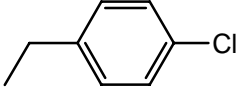
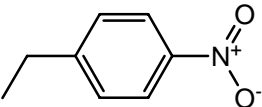
### 3.3.2.6. Screening of Ethylbenzenes

The oxidation of alkylbenzene are as shown in Table 3.7. In all cases, the -CH<sub>2</sub>- group of alkylaromatics is selectively converted to the -CO- group, indicating high chemoselectivity in the oxidation. The nature of the substituents strongly influence the yield of the oxidation products. It is observed that, alkylbenzenes having electron donating ring substituents facilitate the oxidation, while electron withdrawing ring substituents result in lower conversions of the alkyl group to the corresponding ketone. For example, the conversion levels are good in case of ethylbenzene and isobutyl benzene; however, the ethylbenzenes with ring deactivating substituents like Br-, Cl- or NO<sub>2</sub>- give lower conversions. These results are in accordance with the observations by S.

K. Jana and coworkers,<sup>35</sup> wherein the authors have distinctly observed the effect of the nature of substituents on the liquid phase oxidation of alkylbenzenes using heterogeneous manganese containing hydrotalcite catalyst.

In the present study, in all cases, only the benzylic C–H bonds of alkylaromatics are oxidized to their corresponding ketones with high selectivity, while the alcohols were also found in low amounts.

**Table 3.7.** Screening of alkylbenzene for liquid phase oxidation

| Sr | Alkylbenzene  | Conversion, % | Aryl ketone | Aryl alcohol | Rate x 10 <sup>5</sup> , kmol/m <sup>3</sup> /s |
|----|---|---------------|-------------|--------------|---|
| 1  |    | 24.4          | 92.5        | 6.9          | 3.1   |
| 2  |    | 10.6          | 89.4        | 10.8         | 1.4   |
| 3  |   | 8.2           | 86.3        | 13.9         | 1.0   |
| 4  |  | 1.2           | 90.2        | 7.8          | 0.2   |

**Reaction Conditions:** Alkylbenzene, 0.69 kmol/m<sup>3</sup>; catalyst, 1.7 kg/m<sup>3</sup>; TBHP, 2.1 kmol/m<sup>3</sup>; Temperature, 333K; Agitation speed, 16.6 Hz; Solvent, t-BuOH; Time, 1.5 h; Total charge 5 x 10<sup>-5</sup> m<sup>3</sup>

### 3.3.2.7. Catalyst Recycle Study

Though Co-Al-HTlc showed very good activity for oxidation of ethylbenzene as well as high selectivity to acetophenone, it was necessary to confirm that the active catalyst doesn't leach into the reaction medium. For a heterogeneous catalyst, the major advantage is its reusability, which would be lost if cobalt was leached out of the hydrotalcite. Recycle experiments were therefore carried out to study the reusability of Co-Al-HTlc. The results obtained are presented in Figure 3.10. It was observed that the

catalyst retains its activity in terms of ethylbenzene conversion as well as acetophenone selectivity up to at least 4 recycles. It should also be noted that the various spectroscopic investigations of fresh and recovered Co-Al-HTlc confirm the unaltered oxidation state of cobalt ( $\text{Co}^{2+}$ ), as well as the crystallinity of the hydrotalcite material, as established from the XPS and XRD spectral analyses of the catalysts, respectively. The SEM micrographs also support this conclusion, which shows no change in the morphology or shape and size of the hydrotalcite crystallites.

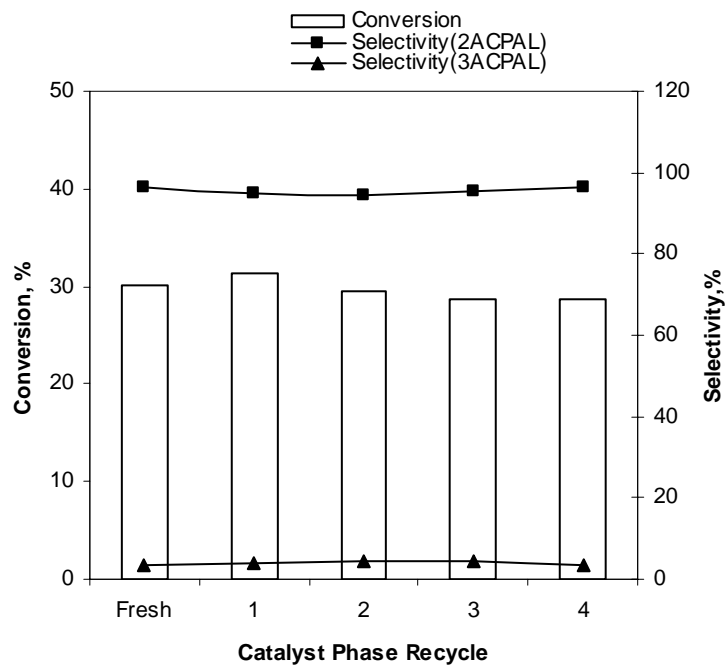


**Figure 3.10.** Recycle study of Co-Al-HTlc for ethylbenzene oxidation

**Reaction Conditions:** Ethylbenzene,  $0.69 \text{ kmol/m}^3$ ; catalyst,  $1.66 \text{ kg/m}^3$ ; TBHP,  $2.1 \text{ kmol/m}^3$ ; Temperature,  $333\text{K}$ ; Agitation speed,  $16.6 \text{ Hz}$ ; Solvent, t-BuOH; Time,  $1.5 \text{ h}$ ; Total charge  $5 \times 10^{-5} \text{ m}^3$

Although the recycle experiments do give an idea of reusability, it was also necessary to confirm that the filtered liquid reaction mixture did not contain any soluble form of cobalt, which could catalyze the oxidation. This study was carried out for ethylbenzene oxidation in two parallel experiments, for which, the concentration-time profiles were plotted by drawing periodic samples and analyzing the liquid samples by G.C. In one experiment, the reaction mixture was cooled after allowing the reaction to



take place for 1 hours (Conversion ~ 20%), and then it was filtered through a Whatman filter paper (Number 1) to remove all the hydrotalcite. To this, fresh TBHP and ethylbenzene was added and the reaction was further continued at the same temperature and agitation. The concentration-time profiles plotted for the two sets of experiments are shown in Figure 3.11. It can be clearly observed that the conversion of ethylbenzene completely ceased in the experiment where the catalyst was removed. To further confirm the outcome of this observation, the liquid reaction mixture was concentrated and analyzed by AAS for the presence of cobalt. It was found that there was negligible cobalt leaching (0.1% of the originally charged cobalt) into the reaction mixture. These results confirm that there is indeed no cobalt leaching during the Co-Al-HT catalyzed oxidation of ethylbenzene using TBHP as the oxidant, and it constitutes a robust, reusable and active catalyst.

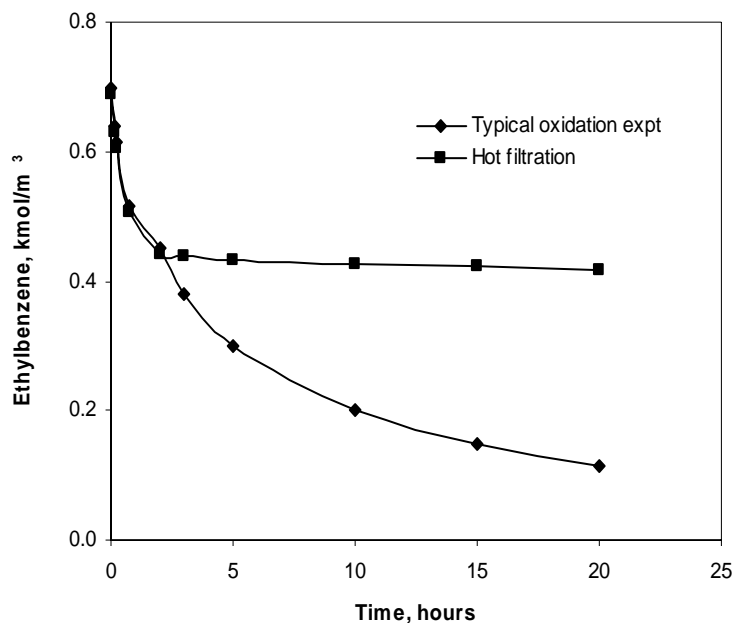


**Figure 3.11.** Hot filtration experiment for confirming the reusability of the catalyst Co-Al-HT

**Reaction Conditions:** Ethylbenzene, 0.69 kmol/m<sup>3</sup>; catalyst, 1.66 kg/m<sup>3</sup>; TBHP, 2.1 kmol/m<sup>3</sup>; Temperature, 333K; Agitation speed, 16.6 Hz; Solvent, t-BuOH; Total charge 5 x 10<sup>-5</sup> m<sup>3</sup>

### **3.3.3. Kinetics of Liquid Phase Oxidation of Ethylbenzene**

A detailed kinetic investigation has been carried out for the Co-Al HTlc catalyzed liquid phase oxidation of ethylbenzene to PE and Acph. There is no previous report on the investigation of intrinsic kinetics on liquid phase oxidation of ethylbenzene using HTlcs as catalyst and TBHP as oxidant. The knowledge of kinetics and development of rate equations is also important in understanding the mechanistic features of such complex catalytic reactions. Considering the industrial importance of this reaction in synthesis of Acph, such a study would be useful. The effect of Co-Al HTlc, ethylbenzene and TBHP concentration on initial rate of concentration time profile has been investigated in the temperature range of 313 - 333K.

#### **3.3.3.1. Preliminary Experiments**

Preliminary experiments were carried out to select a range of reaction conditions suitable for studying the reaction kinetics and establish the product distribution, material balance etc. A typical concentration time profile of ethylbenzene conversion and formation of products i.e. PE and Acph at 333K is shown in Figure 3.12. A component balance analysis of the consumption of ethylbenzene and the formation of oxidation products showed good agreement, and the mole balance was more 97% through out the reaction profile. The conversion of TBHP was also monitored by titrimetric analysis as described in section 3.2.5.1 as well as by using GC analysis for the formation of *tert*-butyl alcohol. The mass balance of TBHP was found to be in the range of 87-96%.

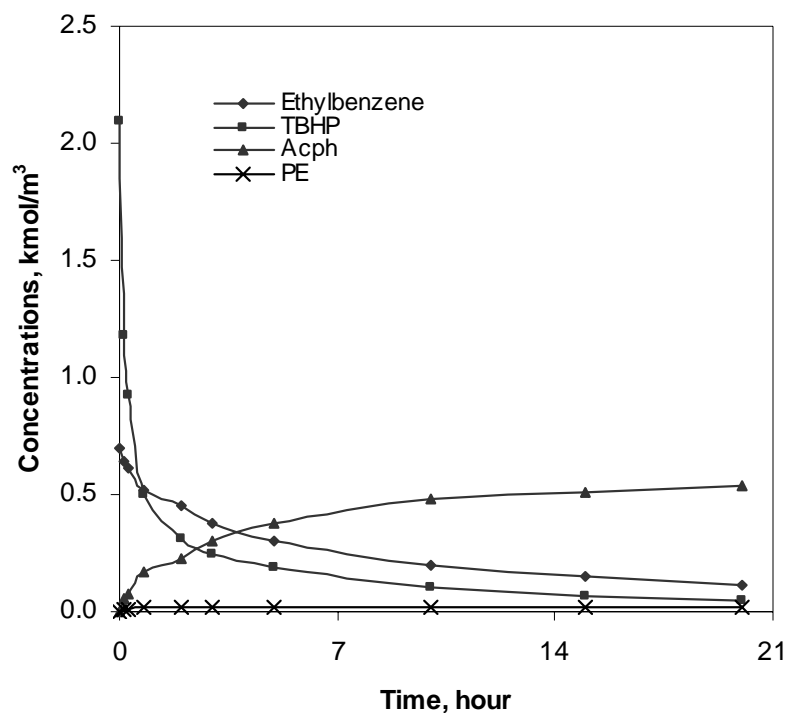


**Figure 3.12.** Concentration - time profile of liquid phase oxidation of ethylbenzene.

**Reaction Conditions:** Ethylbenzene,  $0.69 \text{ kmol/m}^3$ ; catalyst,  $1.7 \text{ kg/m}^3$ ; TBHP,  $2.1 \text{ kmol/m}^3$ ; Agitation speed,  $16.6 \text{ Hz}$ ; Solvent,  $t\text{-BuOH}$ ; Total charge  $5 \times 10^{-5} \text{ m}^3$

### 3.3.3.1.1. Evaluation of Kinetic Regime

#### 3.3.3.1.2. Effect of Agitation Speed

For the kinetic study, it is essential that reaction should operate in the kinetic regime and not under the condition where mass transfer is controlling. For that purpose, the effect of agitation speed on the rate of reaction was studied and the results are presented in Figure 3.13. The rate of ethylbenzene conversion was found to be independent of the agitation speed beyond  $1000 \text{ rpm}$  ( $16.6 \text{ Hz}$ ), which clearly indicates that the reaction is in kinetic regime beyond  $16.6 \text{ Hz}$ . Therefore, all the reactions for kinetic studies were carried out at an agitation speed of  $1200 \text{ rpm}$  ( $20 \text{ Hz}$ ) to ensure that the reaction occurred in the kinetic regime.

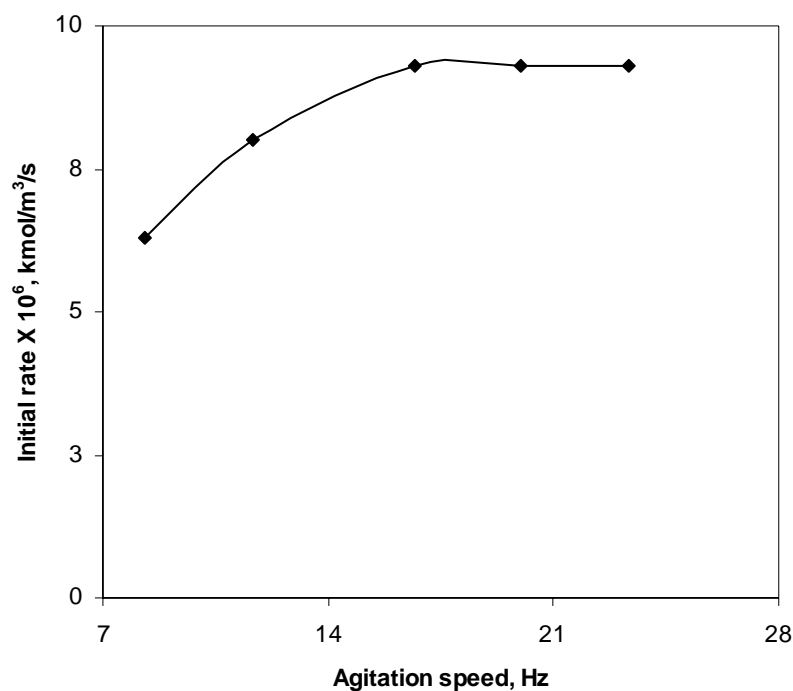


**Figure 3.13.** A plot of rate of liquid phase oxidation of ethylbenzene vs. agitation speed

**Reaction Conditions:** Ethylbenzene, 1.4 kmol/m<sup>3</sup>; catalyst, 3.2 kg/m<sup>3</sup>; TBHP, 2.1 kmol/m<sup>3</sup>; Temperature, 333K; Solvent, t-BuOH; Time, 0.20 h; Total charge 5 x 10<sup>-5</sup> m<sup>3</sup>

### 3.3.3.2. Analysis of Initial Rate Data with HTlcs as Catalyst

The analysis of initial rate data is useful in understanding the dependency of the reaction rate on individual parameters. It also useful in evaluating significance of mass transfer effects. The rates of liquid phase oxidation of ethylbenzene were calculated from concentration of ethylbenzene consumed and the products formed. This approach would be more relevant to obtain the meaningful kinetics of the consecutive reactions. The ranges of the operating conditions used for the kinetic study are given in the Table 3.8. Initial rates for the consumption of ethylbenzene and formation of phenyl ethanol and acetophenone were calculated.

**Table 3.8.** Range of operating conditions for liquid phase oxidation of ethylbenzene

---

|   |           |
|---|-----------|
| Reaction temperature, K                     | 313 - 333 |
| Agitation speed, Hz                         | 20        |
| Co-Al HTlc concentration, kg/m <sup>3</sup> | 0.7- 3    |
| Ethylbenzene, kmol/m <sup>3</sup>           | 0.5-1.5   |
| TBHP, kmol/m <sup>3</sup>                   | 1- 4      |

---

### 3.3.3.2.1. Effect of Co-Al HTlc Concentration

Effect of Co-Al HTlc concentration was investigated in the range (0.7-3 Kg/m<sup>3</sup>). Increasing the Co-Al HTlc concentration was found to increase the reaction rate of ethylbenzene conversion ( $r_1$ ) linearly at all of the temperatures studied. Such a linear increase in the rate of ethylbenzene oxidation with Co-Al HTlc concentration also suggests that the reaction occurs in kinetic regime. Rate of formation of Acph ( $r_2$ ) (Figure 3.14 a) was found to increase with increase in concentration of catalyst. The rate of formation of PE was found unaffected. With the increase in catalyst concentration the rate of formation of PE is expected to increase, at the same time catalyst has much stronger influence on the formation of Acph from PE. A combined influence of the two effect results in the almost independent behavior of initial rate of PE with respect to catalyst as seen from the Figure (3.14b). The observation of the higher PE concentration at lower temperature indirectly shows that under conditions where the rate of Acph, formation is low, slightly higher concentration of PE was observed. The first order behavior of the formation of Acph with catalyst concentration is thus expected. The zero order dependence of the PE with respect to catalyst concentration is no way indication of any mass transfer resistance, but a combined effect of the catalyst concentration on the rates of formation and consumption of PE.

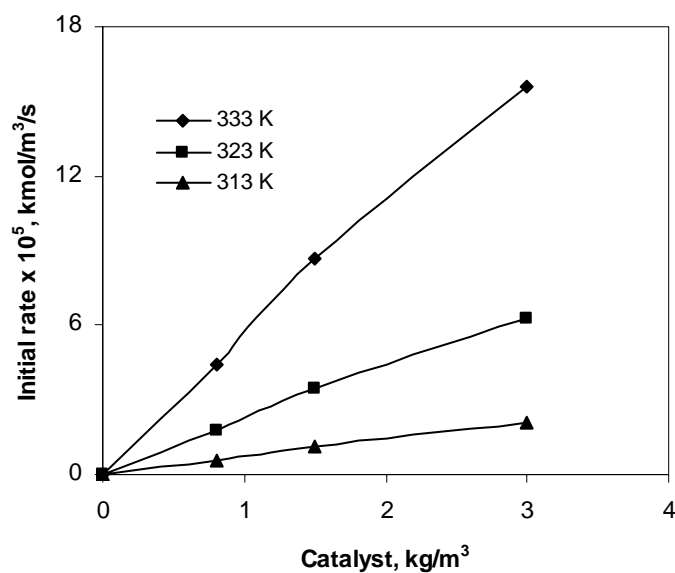


**Figure 3.14a.** Effect of Co-Al HTlc concentration on rate of formation of Acph

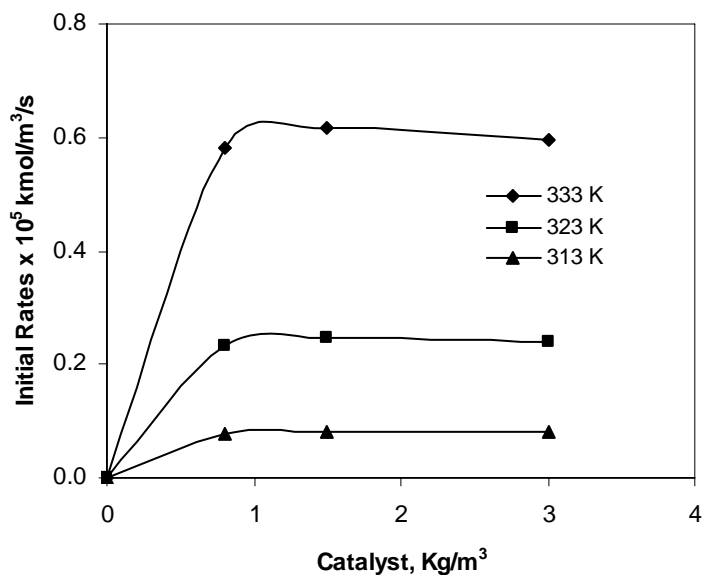


**Figure 3.14b.** Effect of Co-Al HTlc concentration on rate of formation of PE

**Reaction Conditions:** Ethylbenzene, 0.69 kmol/m<sup>3</sup>; TBHP, 2.1 kmol/m<sup>3</sup>; Temperature, 313-333K; Agitation speed, 20 Hz; Solvent, t-BuOH; Time, 1.5 h; Total charge 5 x 10<sup>-5</sup> m<sup>3</sup>

### 3.3.3.2.2. Effect of Ethylbenzene Concentration

The effect of ethylbenzene concentration on the rate of formation of Acph and PE was investigated at a constant catalyst and TBHP concentration, in the ethylbenzene concentration range of 0.3–1.4 kmol/m<sup>3</sup> in the temperature range of 313-333K and the results are shown in Figure 3.15. With the increase in ethylbenzene concentration, there was increase in the rate of formation of PE (3.15b).

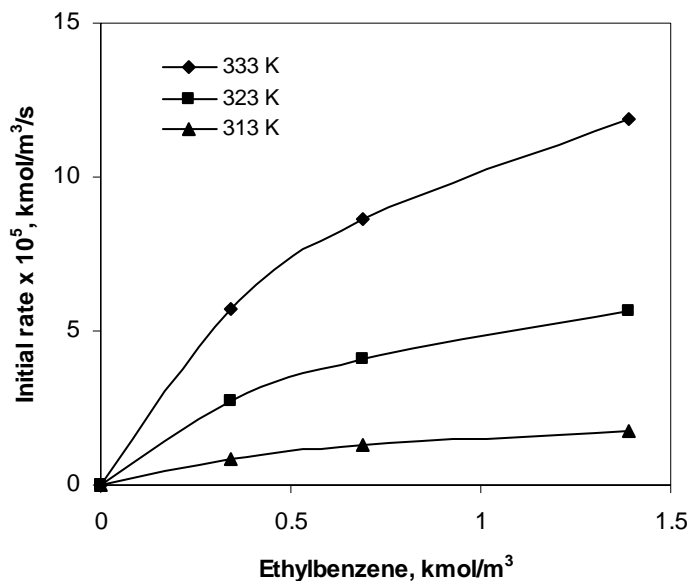


**Figure 3.15a.** Effect of ethylbenzene concentration on rate of formation of Acph

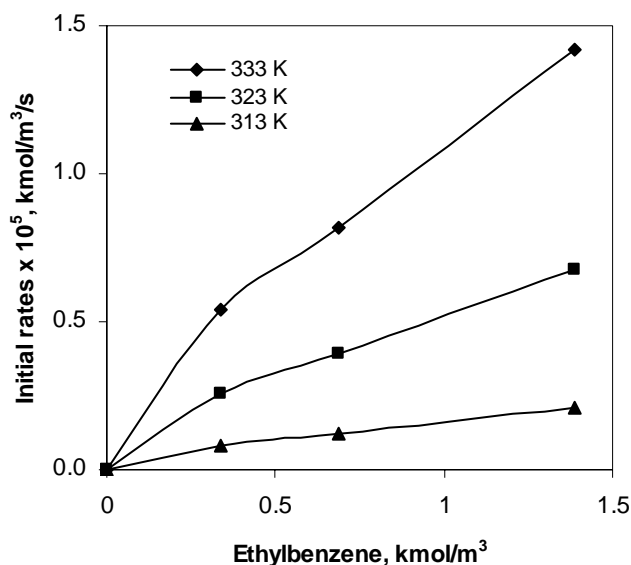


**Figure 3.15b.** Effect of ethylbenzene concentration on rate of formation of PE

**Reaction Conditions:** catalyst, 1.66 kg/m<sup>3</sup>; TBHP, 2.1 kmol/m<sup>3</sup>; Temperature, 313-333K; Agitation speed, 20 Hz; Solvent, t-BuOH; Time, 1.5 h; Total charge 5 x 10<sup>-5</sup> m<sup>3</sup>

### 3.3.3.2.3. Effect of TBHP Concentration

The effect of TBHP concentration on the rate of formation of Acph and PE was investigated in the temperature range of 313-333K. In the studied range it was observed that increase in the concentration of TBHP initially increases the rate of formation of Acph (ethylbenzene:TBHP = 1:1) and then it becomes independent of the concentration of TBHP. The rate of formation of PE increases initially and then further increase in TBHP concentration it decreases. The results are shown in the Figure (3.16a,b).



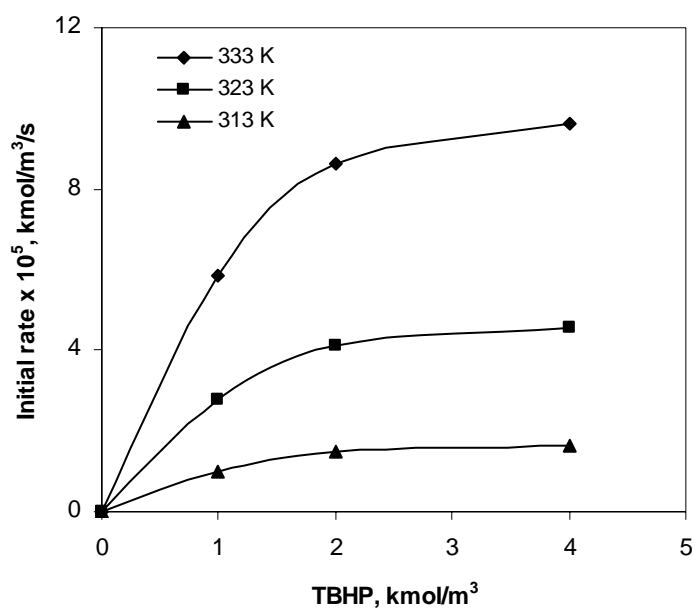


**Figure 3.16a.** Effect of TBHP concentration on rate of formation of Acph

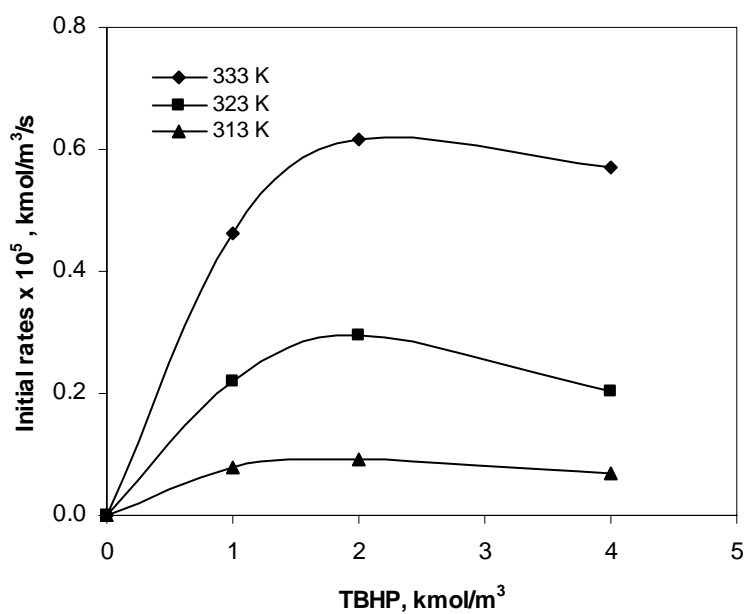
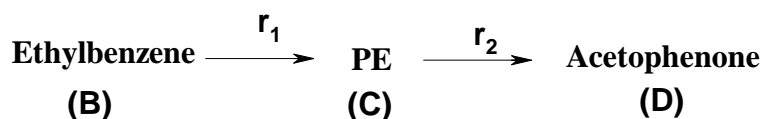


**Figure 3.16b.** Effect of TBHP concentration on rate of formation of PE

**Reaction Conditions:** Ethylbenzene, 0.69 kmol/m<sup>3</sup>; catalyst, 1.66 kg/m<sup>3</sup>; Temperature, 313-333K; Agitation speed, 20 Hz; Solvent, t-BuOH; Time, 3 h; Total charge 5 x 10<sup>-5</sup> m<sup>3</sup>

### 3.3.4. Kinetic Model

The kinetic modeling of complex multiphase catalytic reactions needs a careful consideration of various complexities. The initial rate analysis gives idea about the effect of various parameters on rates of the reaction, which may not be adequate to explain the integral batch reactor performance. Considering the complexities it was thought appropriate to use mainly the integral rate data for developing the suitable kinetic model. The simplified reaction scheme is shown in the scheme 3.2



**Scheme 3.2.** Simplified reaction scheme for liquid phase oxidation of ethylbenzene

Initially power law model was applied for the simplicity of analysis. Since the kinetics of complex multiphase catalytic oxidation reactions were analyzed by using single, double site L-H type of models, similar models were tested. The details of the different models screened are as given below:

**Model 1** A power law model was considered for the fitting of the data. The rate equations used are as given below considering excess TBHP.

$$r_1 = k_1 w B^{n_1}$$

$$r_2 = k_2 w C^{n_2}$$

Where  $n_1$  and  $n_2$  are the powers of reacting species B and C.  $k_1$  and  $k_2$  are the reaction rate constants

**Model 2** The Eley-Rideal (E-R model) type reaction scheme was considered and model proposed as given as follows. The reaction of TBHP with adsorbed ethylbenzene is slowest and hence this step considered as rate limiting step.

#### Reaction Mechanism

- TBHP (A) remains in the liquid phase.
- EB (B) comes to catalyst site and gets adsorbed.

- A in liquid phase and adsorbed B react to form adsorbed C (Phenyl Ethanol ) and liquid phase D ( TBA )
- Water molecule is separated from adsorbed C to form the product E (acetophenone ) which is in the adsorbed stage.
- Finally, E gets desorbed.

Following reaction scheme were considered



Reaction Equations

$$r_1 = w.k_1.C_{B.S} \quad 3.5$$

$$r_2 = w.k_2.C_{C.S} \quad 3.6$$

The adsorbed concentrations, are given as

$$C_{B.S} = \left[ \frac{K_B C_B}{1 + K_B C_B + K_C C_C + K_E C_E} \right] \quad 3.7$$

$$C_{C.S} = \left[ \frac{K_C C_C}{1 + K_B C_B + K_C C_C + K_E C_E} \right] \quad 3.8$$

$$C_{E.S} = \left[ \frac{K_E C_E}{1 + K_B C_B + K_C C_C + K_E C_E} \right] \quad 3.9$$

Where K are the adsorption constants for various species.

**Model 3** A Langmuir-Hinshelwood (L-H model) type model was derived based on assumptions of a dual site mechanism which seems to be appropriate based on the general

trends observed. The reaction of adsorbed TBHP with adsorbed EB was slowest and hence considered as rate limiting.

### Assumptions and simplification of reaction scheme

- Isothermal conditions prevail through out the reaction.
- The TBA (D) formation takes place in the bulk liquid and thus the TBA concentration on the catalyst surface is negligible.
- The formation of TBA has no effect on the PE (C) oxidation to Acph (E).
- Only the reactive species are chemisorbed on the active sites and the solvent do not occupy the active sites.
- The adsorption of product, Acph was assumed to be negligible.
- No further oxidation of Acph to any product.

The reaction path considered as follows:



Thus we write first order kinetics with respect to both the reactants for the both forward reaction.

$$r_1 = k_1 C_{A.S} C_{B.S} \quad 3.16$$

$$r_2 = k_2 C_{A.S} C_{C.S} \quad 3.17$$

The surface concentrations for A, B and C are obtained by following equations

$$C_{A.S} = \frac{K_A C_A}{1 + K_A C_A + K_B C_B + K_C C_C} \quad 3.18$$

$$C_{B.S} = \frac{K_B C_B}{1 + K_A C_A + K_B C_B + K_C C_C} \quad 3.19$$

$$C_{C.S} = \frac{K_C C_C}{1 + K_A C_A + K_B C_B + K_C C_C} \quad 3.20$$

As the TBHP was taken in excess, the concentration of TBHP i.e.  $C_A$  remains almost constant and thus we may consider  $k_1 C_A = k'_1$ , where  $k'_1$  is pseudo first order constant and similarly for  $k_2 C_A = k'_2 C_A$ . A non-linear least square regression analysis was used to obtain the best-fit values of the parameters. The comparison of the experimental and the predicted results are presented in Figure 3.17-3.19, which show excellent agreement. To show the difference in fitting between the Model 3 and other models, a typical substrate consumption-time profile is shown in Figure 3.17, which clearly indicates the suitability of Model 3. The rate equations derived for these 1-3 models are concisely presented in Table 3.9.

In order to check the applicability of the rate models derived under isothermal and integral conditions, a batch reactor model was developed. The simulation model for batch reactor under isothermal conditions written for Model 3 is as follows:

$$\frac{dB}{dt} = -r_1 \quad 3.21$$

$$\frac{dC}{dt} = r_1 - r_2 \quad 3.22$$

$$\frac{dE}{dt} = r_2 \quad 3.23$$

With initial conditions

$t=0, B=B_0, C=0, E=0$

In order to evaluate the rate parameters in the kinetic model, the observed concentration time data were simulated by trial and error method.

The rate constants for the heterogeneous reactions were evaluated by simulation of experimental data on concentration time profile using batch reactor model at different temperatures. The approach followed to evaluate the kinetic parameters for overall reaction was same as described in chapter 2. A nonlinear regression analysis combined with Runge-Kutta method was used to solve these equations to obtain best fit values of parameters. The reaction rate constants were optimized. This exercise was repeated for three different temperatures. Three different models are proposed (Table 3.9) and the values of the optimized rate constants are given in table 3.9. Model 1 and 2 gave higher values of  $\Phi_{\min}$  and %RR and hence rejected. Model 3 was found to give lowest value of  $\Phi_{\min}$  and also the value of %RR was found to be less among the model screened.

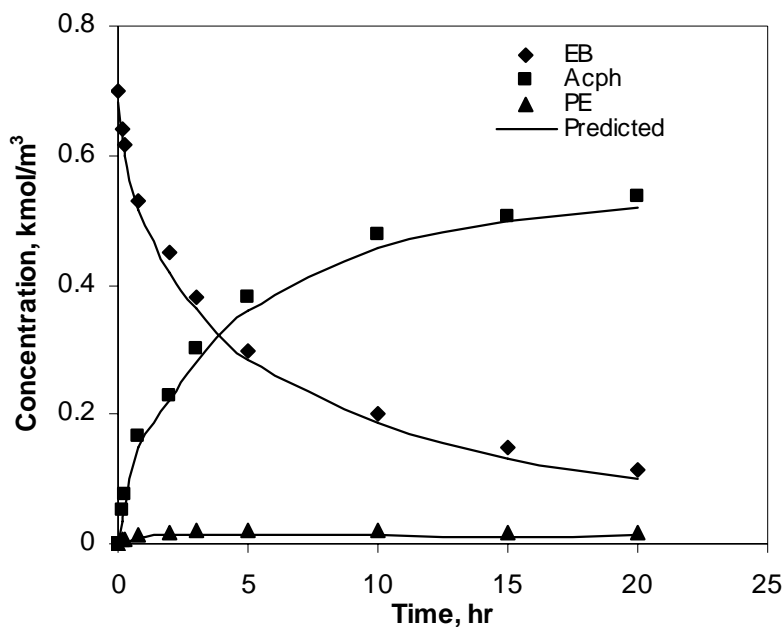


**Figure 3.17.** Experimental Vs predicted concentration time profile for liquid phase oxidation of ethylbenzene at 333K

**Reaction Conditions:** Ethylbenzene,  $0.69 \text{ kmol/m}^3$ ; catalyst,  $1.7 \text{ kg/m}^3$ ; TBHP,  $2.1 \text{ kmol/m}^3$ ; Temperature, 333K; Agitation speed, 16.6 Hz; Solvent, t-BuOH; Total charge  $5 \times 10^{-5} \text{ m}^3$

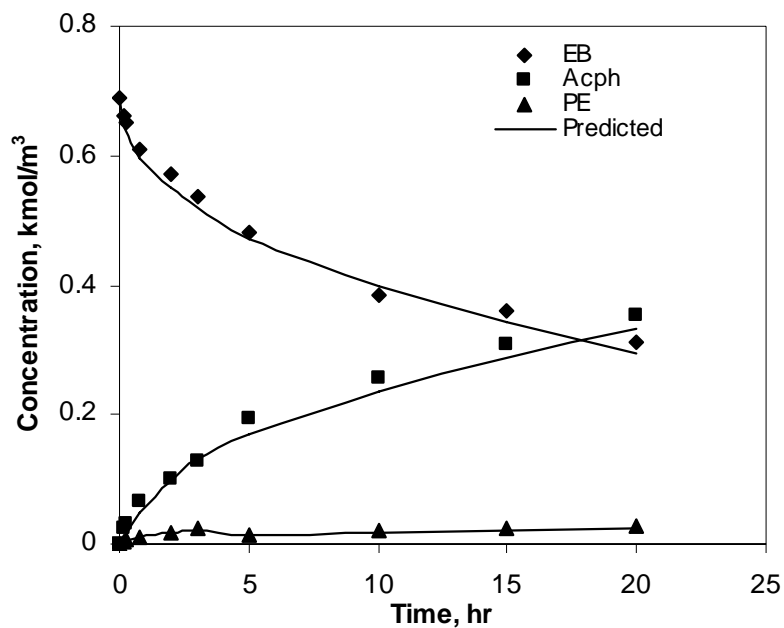


**Figure 3.18.** Experimental Vs predicted concentration time profile for liquid phase oxidation of ethylbenzene at 323K

**Reaction Conditions:** Ethylbenzene,  $0.69 \text{ kmol/m}^3$ ; catalyst,  $1.7 \text{ kg/m}^3$ ; TBHP,  $2.1 \text{ kmol/m}^3$ ; Temperature, 323K; Agitation speed, 16.6 Hz; Solvent, t-BuOH; Total charge  $5 \times 10^{-5} \text{ m}^3$

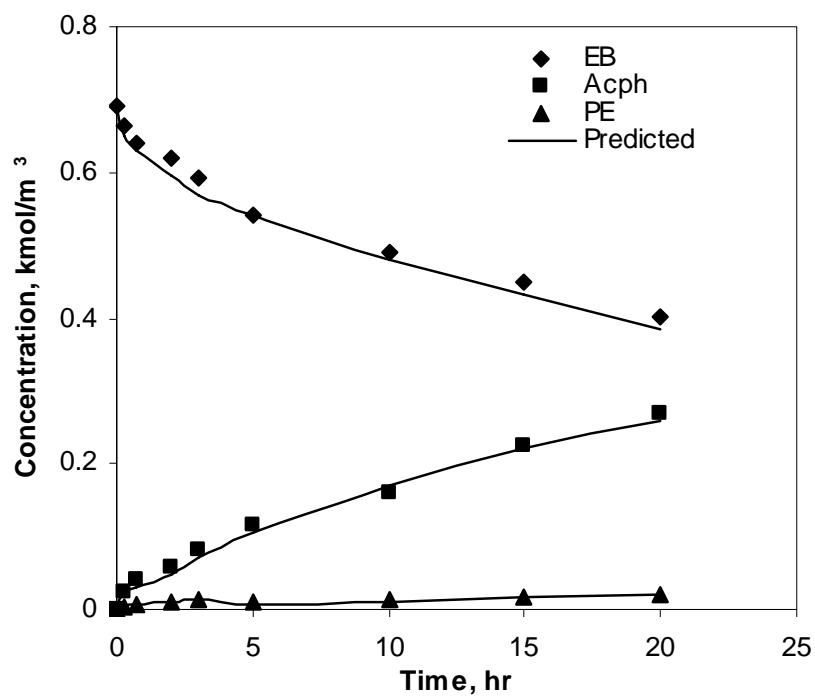


**Figure 3.19.** Experimental Vs predicted concentration time profile for liquid phase oxidation of ethylbenzene at 313K

**Reaction Conditions:** Ethylbenzene, 0.69 kmol/m<sup>3</sup>; catalyst, 1.7 kg/m<sup>3</sup>; TBHP, 2.1 kmol/m<sup>3</sup>; Temperature, 313K; Agitation speed, 16.6 Hz; Solvent, t-BuOH; Total charge 5 x 10<sup>-5</sup> m<sup>3</sup>



**Table 3.9.** Model Discrimination

| Sr. | Model  | Temperature, K | $n_1$ | $n_2$ | $k_1$   | $k_2$   | $k_3$   | $K_4$   | $K_A$   | $K_B$   | $K_C$   | $K_E$   |
|-----|--|----------------|-------|-------|---------|---------|---------|---------|---------|---------|---------|---------|
| 1   | $r_1 = k_1 w A B^{n_1}$<br>$r_2 = k_2 w C^{n_2}$           | 313            | 0.80  | 1.25  | 1.2E-01 | 2.3E-01 | -       | -       | -       | -       | -       | -       |
|     |  | 323            | 0.67  | 2.21  | 1.4E-01 | 2.0E-01 | -       | -       | -       | -       | -       | -       |
|     |  | 333            | 1.25  | 1.20  | 6.0E-01 | 2.1E-01 | -       | -       | -       | -       | -       | -       |
| 2   | $r_1 = w k_1 C_{B,S}$<br>$r_2 = w k_2 C_{C,S}$             | 313            | -     | -     | 8.6E-01 | 5.4E-01 | 9.6E-01 | 3.2E-01 | 1.8E-02 | -       | 1.9E-01 | 8.1E-01 |
|     |  | 323            | -     | -     | 3.4E-01 | 4.5E-01 | 1.3E+00 | 5.5E-01 | 5.6E-01 | -       | 1.1E-01 | 4.4E-01 |
|     |  | 333            | -     | -     | 1.2E+00 | 5.6E-01 | 3.4E-01 | 1.2E+00 | 8.6E-01 | -       | 8.0E-01 | 5.4E-01 |
| 3   | $r_1 = k_1 C_{A,S} C_{B,S}$<br>$r_2 = k_2 C_{A,S} C_{C,S}$ | 313            | -     | -     | 1.0E-02 | 6.1E-01 | -       | -       | -       | 8.4E-02 | 6.5E-02 | 4.3E-02 |
|     |  | 323            | -     | -     | 1.7E-02 | 7.7E-01 | -       | -       | -       | 9.8E-02 | 7.2E-02 | 5.2E-02 |
|     |  | 333            | -     | -     | 2.5E-02 | 8.2E-01 | -       | -       | -       | 1.6E-01 | 8.1E+00 | 9.0E-02 |

### 3.4. Conclusions

In this chapter, it is demonstrated that transition metal containing hydrotalcite-like compounds (HTlcs) are highly active, recyclable heterogeneous catalysts for liquid phase oxidation of ethylbenzene to acetophenone using TBHP as oxidant. These catalysts were characterized by various spectroscopic and chemical techniques to understand their morphological and chemical properties. The observations of the characterization can be summarized as follows

1. Powder XRD analysis of the HTlcs established that all the catalysts are crystalline, and they contain only the HT (hydrotalcite) crystalline phase. The spectra of fresh and recovered Co-Al-HTlc confirmed that there was no change in the crystallinity pattern of the catalyst after the oxidation experiment.
2. Thermal studies TGA and DTA for Co-Al-HT showed weight losses due to dehydroxylation and decarbonation. The study also confirmed the thermal stability of the catalyst under the experimental conditions employed for the oxidation of ethylbenzene.
3. XPS analysis of the HTlc indicates that the cobalt in the hydrotalcite material is in +2 oxidation state, even after its use for liquid phase oxidation of ethylbenzene.

The synthesized HTlcs showed varying catalytic activities for oxidation of ethylbenzene using TBHP as the oxidant; Co-Al-HT was found to be the best catalyst in terms of ethylbenzene conversion (24.4% under optimized experimental conditions) and acetophenone selectivity (92.4%). Cobalt catalysts with oxidation state of 2+ were found to be excellent catalysts for alkylbenzene oxidation.

Kinetics of liquid phase oxidation of ethylbenzene to acetophenone was studied in *tert*-butyl alcohol as solvent and TBHP as oxidant over a temperature range of 313-333K. It was found that the experimental data were in the kinetic regime in all the reactions at the agitation speed of 16 Hz. Different rate models were developed and based on the observed concentration-time data, intrinsic kinetic parameters were estimated. A rate model considering adsorption of TBHP on the catalyst surface followed by reaction with the liquid phase components as the rate-limiting step was found to give the best fitting of

the experimental concentration-time data at different initial sets of reaction conditions. Activation energy was evaluated and found to be for  $k_1$  (57.2 kJ/mol) and for  $k_2$  (13.6 kJ/mol)

### **Nomenclature**

|                  |   |
|------------------|---|
| A                | Concentration of TBHP, kmol/m <sup>3</sup>                        |
| B                | Concentration of EB, kmol/m <sup>3</sup>                          |
| C                | Concentration of PE, kmol/m <sup>3</sup>                          |
| D                | Concentration of TBA, kmol/m <sup>3</sup>                         |
| E                | Concentration of Acph, kmol/m <sup>3</sup>                        |
| $k_1, k_2$       | Intrinsic rate constants, m <sup>3</sup> / (kmol s)               |
| K                | Adsorption constant, (m <sup>3</sup> /kmol)                       |
| r                | Rate of hydroformylation, kmol/m <sup>3</sup> /s.                 |
| $C_{\text{exp}}$ | Experimental concentrations, kmol/m <sup>3</sup>                  |
| $C_{\text{pre}}$ | Predicted concentrations, kmol/m <sup>3</sup>                     |
| $R_i$            | Reaction rate for the oxidation reaction (kmol/m <sup>3</sup> /s) |
| t                | Reaction time, h.   |
| T                | Temperature, K  |
| $V_L$            | Total liquid volume, m <sup>3</sup>                               |
| $\Phi$           | Parameter defined by Eq-2.8                                       |

## References

---

1. G.A. Olah, *Friedel–Crafts and Related Reactions*, Wiley–Interscience, New York, (1963).
2. G.A. Olah, *Friedel–Crafts and Related Reactions*, Wiley–Interscience, New York, (1963).
3. P.H. Groggins, R.H. Nagel, *Ind. Eng. Chem.* 26 (1934) 1313.
4. S.D. Borkar, B.M. Khadilkar, *Synth. Commun.* 29 (1999) 4295.
5. N.D. Valechha, A. Pradhan, *J. Indian Chem. Soc.* 61 (1984) 909.
6. A. Shaabani, A. Bazgir, F. Teimouri, D.G. Lee, *Tet. Lett.* 43 (2002) 5165.
7. V.R. Chaudhari, J. R. Indurkar, V.S. Narkhade, Rani Jha, *Journal of Catalysis* 227 (2004) 257.
8. B.B. Wentzel, M.P.J. Donners, P.L. Alsters, M.C. Feiters, R.J.M. Nolte, *Tetrahedron* 56 (2000) 7797.
9. B. Notari, *Stud. Surf. Sci. Catal.* 37 (1987) 413.
10. B. Notari, *Stud. Surf. Sci. Catal.* 60 (1991) 343.
11. J.S. Reddy, R. Kumar, P. Ratnasamy, *Appl. Catal.* 58 (1990) L1.
12. P. Kumar, R. Kumar, B. Pandey, *Syn. Lett.* (1995) 289.
13. P. Ratnasamy, R. Kumar, *Stud. Surf. Sci. Catal.* 97 (1995) 501.
14. J.D. Chen, R.A. Sheldon, *J. Catal.* 153 (1995) 1.
15. J.D. Chen, M.J. Haanepen, J.H.C. van Hooff, R.A. Sheldon, *Stud. Surf. Sci. Catal.* 84 (1994) 973.
16. R.H. Fish, K.J. Oberhausen, S. Chen, J.F. Richardson, W. Pierce, R.M. Buchanan, *Catal. Lett.* 18 (1993) 357.
17. S. Menage, J.M. Vincent, C. Lambeaux, M. Fontecave, *J. Chem. Soc., Dalton Trans.* (1994) 2081.
18. N. Kitajima, M. Ito, H. Fukui, Y. Moro-oka, *J. Chem. Soc., Chem. Commun.* (1991) 102.
19. S. Vetrivel, A. Pandurangan, *Journal of molecular catalysis A: Chemical* 217 (2004)165.
20. J.D. Chen, M.J. Haanepen, J.H.C. van Hooff, R.A. Sheldon, *Stud. Surf. Sci. Catal.* 84 (1994) 973.
21. D. Tetrard, A. Rabion, J.B. Verlhac, J. Guilhem, *J. Chem. Soc., Chem. Commun.* (1995) 531.
22. C.F. Cullis, J.W. Ladbury, *J. Chem. Soc.* (1955) 2850.
23. M. R. Maurya, M. Kumar, U. Kumar *Journal of Molecular Catalysis A: Chemical* 273 (2007) 133
24. F. Cavani; F. Trifiro; A. Vaccari, *Catal. Today* 11 (1991) 173.
25. F. Cavani,; F. Trifiro; A. Vaccari, *Catal. Today* 1991, 11, 173.
26. D. H. R. Barton, V. N. Le Gloahec, H. Patin, F. Launay *New J. Chem.* (1998) 559.
27. J. P. RamoArez, G. Mul, F. Kapteijn and J. A. Moulijn, *J. Mater. Chem.* 11( 2001) 821.
28. J. Theo Kloprogge, Ray L. Frost, *J. Solid State Chem.* 146 (1999) 506.
29. J. T. Kloprogge, R. L. Frost, L. Hickey, *Clays Clay Miner.* in press.
30. J. T. Kloprogge and R. L. Frost, *Phys. Chem. Chem. Phys.* 1, (1999) 1643.
31. J. P. RamoArez, G. Mul, F. Kapteijn and J. A. Moulijn *J. Mater.*

- 
- Chem. 11 (2001) 821.
32. J.M. Hernandez, M.A. Ulibarri, J. Cornejo, M.J. Pena, J.C. Serna, *Thermo chim. Acta* 94 (1985) 257.
33. F. Cavani; F. Trifiro; A. Vaccari, *Catal. Today* 11 (1991) 173.
34. S. K. Jana, P. Wu, T. Tatsumi *J. Catal.* 240 (2006) 268.
35. S. K. Jana, Y. Kubota, T. Tatsumi *J. Catalysis* 247 (2007) 214.

# Chapter 4

## Hydroformylation of 6-Methoxy-2-Vinylnaphthalene as a Potential Route for the Synthesis of *dl*-Naproxen

Hydroformylation of 6-methoxy-2-vinylnaphthalene (MVN) using homogeneous  $\text{Rh}(\text{CO})_2(\text{acac})$  as a catalyst and chelating bidentate ligand, 1,2-bis-(diphenylphosphino) ethane (dppe) followed by oxidation of the hydroformylation product, 2-(6-methoxynaphthyl) propanal (2-MNP) to 2-(6-methoxynaphthyl) propionic acid (Naproxen) has been studied as an alternative route for the synthesis of *dl*-naproxen. A detailed study has been reported on the key hydroformylation step and feasibility of MVN hydroformylation route has been demonstrated. The roles of the catalyst, ligands, and solvents and the effect of reaction conditions on the reaction rate and regioselectivity to the product 2-MNP have been investigated. With  $\text{Rh}(\text{CO})_2(\text{acac})$  as a catalyst and dppe as a ligand, >98% selectivity to 2-MNP (an important precursor to *dl*-naproxen) has been achieved. A possible mechanism to explain the variation in regio-selectivity with  $\text{Rh}(\text{CO})_2(\text{acac})$  as a catalyst and dppe as a ligand has been discussed. Kinetics of the hydroformylation step has been investigated and a rate equation proposed. The second step in the proposed route, oxidation of 2-MNP to Naproxen has been studied using early transition metal salt catalysts and tetrabutyl ammonium hydrogen sulphate (TBAHS) as the phase transfer catalyst with  $\text{H}_2\text{O}_2$  as the oxidant for the first time. Screening of catalysts of the early transition metals like salts of tungsten, vanadium and molybdenum showed that  $\text{Na}_2\text{WO}_4$  gives the best performance for the oxidation step with >80% selectivity to Naproxen. This study would be valuable in developing a new environmentally benign route for naproxen synthesis.

## 4.1. Introduction

Naproxen has significant importance due to its application as non-steroidal anti-inflammatory (NSAI) agent.<sup>1</sup> The latter is one of the largest classes of drugs due to its high demand and therapeutic interest, which include ketoprofen and ibuprofen as the important representatives. Ibuprofen, which ranks first in the NSAI, is commercially being produced using Boots Process and by Pd-catalyzed carbonylation of *p*-isobutylphenyl ethanol, the latter being an excellent example of a successful commercialization of an environmentally benign three step catalytic process<sup>2,3,4</sup>. Naproxen, which is the second most important drug in this category and fourth in sales of optically pure pharmaceuticals, lack study in catalytic and environmentally benign route for its synthesis. It is currently manufactured by multistep stoichiometric synthetic routes: (a) Syntex Process<sup>5</sup> starting with  $\beta$ -naphthol and involving stoichiometric bromination, methylation and alkylmetal coupling reactions to yield naproxen, (b) Zambon Process<sup>6</sup> involving acylation of nerolin (2-methoxynaphthalene), ketalization, bromination, hydrolysis and reductive cleavage as the key steps and (c) asymmetric hydrogenation of 6-methoxy naphthacrylic acid using Ru-(*S*)-BINAP catalyst<sup>7</sup>. The attempts towards direct synthesis of chiral naproxen *via* chiral pool using (*S*)-lactate<sup>8</sup>, and asymmetric hydroformylation followed by oxidation were also made<sup>9</sup>. These routes suffer from the drawbacks like use of hazardous reagents and generation of undesired waste consisting of inorganic salts. Therefore, it is most desirable to develop an environmentally benign catalytic route for the synthesis of naproxen.

Extensive work has been done on hydroformylation of styrene with respect to mechanism and kinetics<sup>10,11</sup> but scanty literature is available on hydroformylation of substituted styrenes<sup>12,13</sup>. One such example is asymmetric hydroformylation of 6-methoxy-2-vinylnaphthalene (MVN) to 2-(6-methoxynaphthyl) propanal (2-MNP), which upon oxidation gives (*S*)-Naproxen. The exotic ligands used in the chiral hydroformylation and the large reaction time, however, make its applicability on an industrial scale difficult to bring about. Also, there is a possibility that the branched aldehyde can racemize under the hydroformylation conditions. Moreover the regioselectivity to the branched aldehyde product is a major issue.

Barner et al<sup>14</sup> have reported good yields (83-86%) of profens in two steps i.e. asymmetric hydroformylation of MVN followed by oxidation of corresponding aldehyde using 2,6-lutidine in peracetic acid solution at 2<sup>0</sup>C. It has major drawback of use of peracid and pyridine derivatives in stoichiometric quantity. Catalytic oxidation of aldehydes is one of the most promising reactions to achieve corresponding carboxylic acids in high yields. Oxidation of aryl aldehydes to get pharmaceutically important carboxylic acids using green oxidants like air, oxygen or hydrogen peroxide is much desirable. Hydrogen peroxide is a weak oxidant compared to peracids and dioxiranes, and it produces only water as the byproduct.<sup>15</sup> Some derivatives of a few transition metal elements like W, Mo, V have been studied as the most effective catalysts<sup>16</sup> for oxidation reactions involving hydrogen peroxide in organic synthesis, and the chemistry of the reaction has been understood very well<sup>17</sup>. Thus, oxidation of 2-(6-methoxynaphthyl) propanal (MNP) is a convenient method for the synthesis of *dl*-naproxen. However, scanty literature is available on such synthesis of profens via aldehyde oxidation.

In this chapter, the detailed study on the two-step hydroformylation-oxidation route for the synthesis of *dl*-naproxen is reported. In the first step, hydroformylation of MVN is carried out using a soluble rhodium complex catalyst to achieve high conversion of MVN (>96%) and regioselectivity (98%) to the branched isomer, 2-MNP at milder reaction conditions (373 K, 5.51 MPa). A detailed kinetic analysis of the hydroformylation step is presented and rate equations proposed. In the second step, oxidation of 2-(6-methoxynaphthyl) propanal with H<sub>2</sub>O<sub>2</sub> as oxidant is investigated to obtain *dl*-naproxen with high yield. Activity of a few transition metal catalysts (Na<sub>2</sub>WO<sub>4</sub>, Na<sub>2</sub>MoO<sub>4</sub>, Na<sub>2</sub>VO<sub>4</sub>), phosphotungstic acid (PTA), and phosphomolybdic acid (PMA) is studied for oxidation of MNP. Effects of concentration of substrate, catalyst and oxidant on the selectivity to *dl*-naproxen are studied in a temperature range of 273-313K. This study would be valuable in developing an environmentally benign route for Naproxen synthesis.



## 4.2. Experimental Section

### 4.2.1. Materials

Rhodium trichloride ( $\text{RhCl}_3 \cdot 3\text{H}_2\text{O}$ ), dppb (Diphenyl phosphino butane), dppp (diphenyl phosphino propane), dppe (Diphenyl phosphino ethane), and triphenyl phosphine were procured from Aldrich, U.S.A. and used as received without further purification.  $\text{Rh}(\text{CO})_2(\text{acac})$  was prepared according to the literature procedure.<sup>18</sup>  $\text{Na}_2\text{WO}_4$ ,  $\text{Na}_2\text{MoO}_4$ ,  $\text{Na}_2\text{VO}_4$ , tetrabutyl ammonium hydrogen sulphate, oxalic acid and hydrogen peroxide were procured from SD Fine Chemicals, Mumbai, India. Carbon monoxide with 99.9% purity (Matheson, U.S.A.) and  $\text{H}_2$  with 99% purity (Industrial Oxygen Company, Mumbai, India) were used as received, and synthesis gas mixture in the required  $\text{CO}:\text{H}_2$  ratio was prepared in a reservoir. The solvents toluene, ethanol, ethyl methyl ketone, N- methyl pyrrolidone etc from SD Fine Chemicals, Mumbai, India and were freshly distilled and dried prior to use.

### 4.2.2. Hydroformylation Experiments

The reactions were carried out in a 50 ml high-pressure stainless steel reactor manufactured by Parr Instrument Co., USA equipped with a pressure transducer, a temperature sensor, control with automatic heating and cooling, and a magnetic stirrer with variable speed (Figure 4.1). A reservoir filled with synthesis gas ( $\text{CO}:\text{H}_2$ , 1:1) was connected to the reactor *via* a constant pressure regulator. This enabled continuous feeding of the synthesis gas from the reservoir, as per the consumption in the reactor, while maintaining the pressure in the reactor constant. The reaction was monitored by observing the pressure drop in the reservoir. For the reaction, the reactants and catalyst were charged into the reactor and was flushed with nitrogen and synthesis gas. Following this, the reactor contents were heated to the desired temperature under low stirring (200 rpm). Once the temperature was attained, the stirring was stopped and the synthesis gas was pressurized as required into the reactor. The reaction was started by increasing the agitation speed to 1000 rpm. During the course of the reaction, samples were withdrawn periodically and analyzed by GC for reactant and products. The gas absorption data were collected by reading the pressure drop in the reservoir. For kinetic measurements, the reactions were conducted for fixed time duration, whereas for the screening studies the

reactions were conducted to high levels of conversion of MVN. At the end of the reaction the autoclave was cooled and final samples were taken for analysis and confirmation of the mass balance.

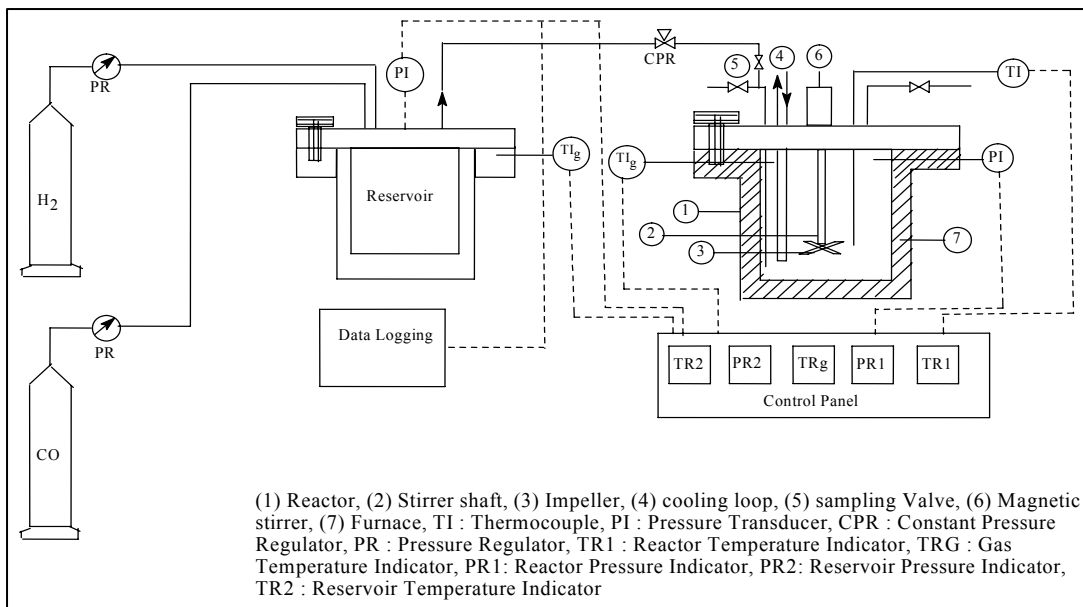
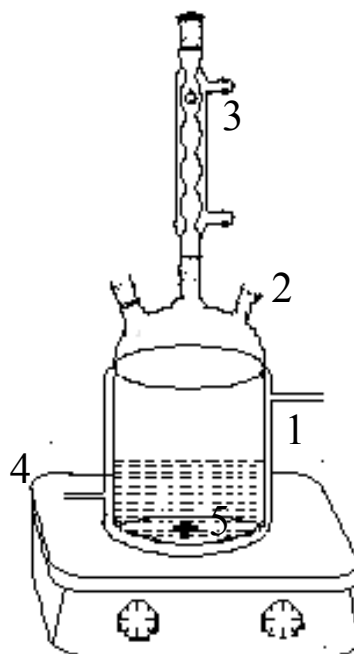


**Figure 4.1** A schematic of the reactor setup for hydroformylation of MVN

#### 4.2.3. Oxidation Experiments

Oxidation of 2-(6-methoxynaphthyl) propanal (2-MNP) was carried out in a 25 ml two-necked jacketed reactor in methyl ethyl ketone (MEK) as solvent as shown in the Figure 4.2. Desired amounts of 2-MNP, MEK, Na<sub>2</sub>WO<sub>4</sub> as a catalyst and TBAHS as co catalyst or promoter and 30% H<sub>2</sub>O<sub>2</sub>, as a oxidant were mixed and stirred at desired temperature using a magnetic stirrer. 2-MNP was analyzed by GC and the naproxen, 2-Acetyl-6-methoxynaphthalene, (ketone) etc were analyzed by HPLC.



(1) jacketed glass reactor (2) Sampling port (3) Condenser (4) Magnetic stirrer (5) Magnetic needle

**Figure 4.2** A schematic of the reactor setup for oxidation reactions

#### 4.2.4. Analytical Methods

The analysis of the liquid samples was done by GC and HPLC. The products of the reactions were identified using GC-MS analysis on an Agilent series 6890N GC equipped with a 5973N mass selective detector. Liquid samples were analyzed for quantification on a Hewlett-Packard 6890 series GC controlled by the HP-Chemstation software and equipped with an autosampler unit, using an HP-1 capillary column (0.32 mm ID, 30 meters, 0.25 $\mu$ m film thickness with a stationary phase of polymethyl siloxane) The oven temperature was programmed between 373-573K. The quantification of reactants and products were done based on a calibration curve. The quantitative analysis of the products, *dl*-naproxen and 2-Acetyl-6-methoxynaphthalene was done using a Symmetry shield RP-8 column (5  $\mu$ , 4.6X250 mm) on a series 1100 Agilent

H.P.L.C. instrument equipped with a DAD, at 210 nm. A solution of 40% acetonitrile and 0.1% glacial acetic acid filtered through a 0.45  $\mu$  Vericel membrane was used as the mobile phase. The flow rate of the mobile phase was kept 1 ml/min (isocratic). IR spectra were obtained using a Bio-Rad FTS 175C machine in transmission mode using KBr pellets as well as liquid cells.

$$\text{Conversion, (\%)} = \frac{\text{Initial concentration of VAM} - \text{Final concentration of VAM}}{\text{Initial concentration of VAM}} \times 100$$

$$\text{TON} = \frac{\text{Number of moles of hydroformylation products formed}}{\text{Number of moles of catalyst}}$$

$$\text{TOF, (h}^{-1}\text{)} = \frac{\text{Number of moles of hydroformylation products formed}}{\text{Number of moles of catalyst} \times \text{time in hours}}$$

#### 4.2.5. Synthesis of Complexes

##### 4.2.5.1. Preparation of Rh(CO)<sub>2</sub>(acac)

Rh(CO)<sub>2</sub>(acac) was prepared by a method used by Varshavskii and coworkers<sup>19</sup>. To a solution of 3 gms of rhodium trichloride trihydrate (40 %) in 60 x 10<sup>-6</sup> m<sup>3</sup> dimethyl formamide, 12 x 10<sup>-6</sup> m<sup>3</sup> acetyl acetate was added with continuous stirring. The solution was refluxed for thirty minutes and then cooled to the room temperature. It was diluted to twice the volume with distilled water. Addition of water resulted in a voluminous crimson precipitate. The precipitate was filtered and washed with methanol. The complex was recrystallised from hexane. The needle-shaped red-green crystals were obtained by slow cooling of the hexane solution. The yield was about 70%. The complex was confirmed from its elemental analysis, which is given below. The elemental analysis of Rh(CO)<sub>2</sub>(acac) showed C=32.6%, H=2.9%. Calculated: C=32.4; H=3.08%. Characteristic IR shifts for this complex at 2065 cm<sup>-1</sup>, 2006 cm<sup>-1</sup> and 1525 cm<sup>-1</sup> are shown in Figure- 4.3

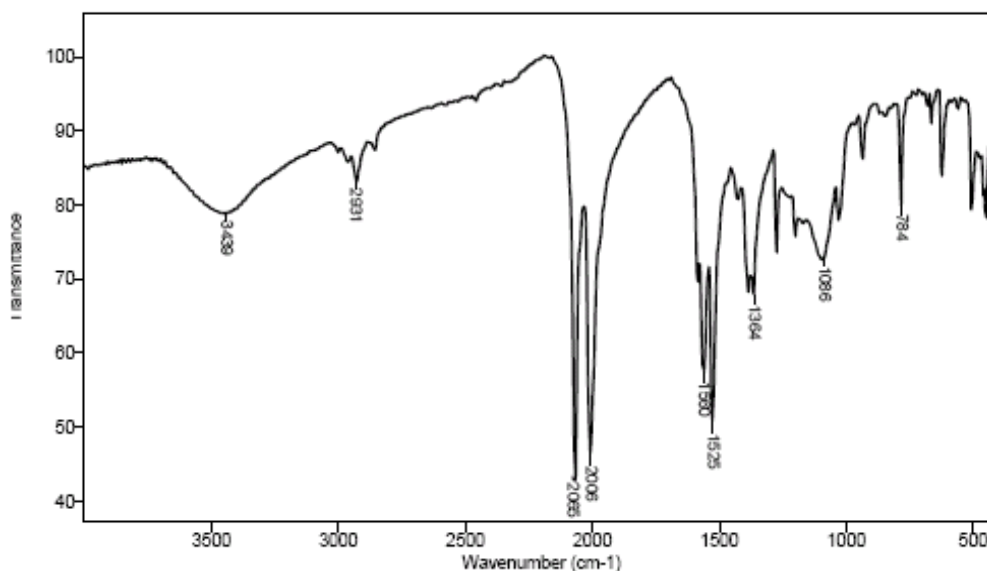


**Figure 4.3:** FTIR spectrum of Rh(CO)<sub>2</sub>(acac)

#### 4.2.5.2. Synthesis of [Rh(COD)Cl]<sub>2</sub>

[Rh(COD)Cl]<sub>2</sub> was prepared according to a procedure reported by Chatt and Venanzi<sup>20</sup>. Rhodium trichloride trihydrate (1 g,  $4.77 \times 10^{-3}$  moles) in ethanol (3 ml) was boiled under reflux with a solution of 1, 5 cyclo-octadiene (COD) (2 ml) for 3 hours. The solution was cooled and the orange solid filtered, washed with ethanol, dried and recrystallized from acetic acid. (Yield, 0.7 g, 60%). Characteristic IR shifts for this complex at  $2874 \text{ cm}^{-1}$ ,  $1468 \text{ cm}^{-1}$  and  $960 \text{ cm}^{-1}$  are shown in Figure-4.4. The elemental analysis of [Rh(COD)Cl]<sub>2</sub> Found: C=39.1%; H=4.85%; Cl=14.3%. Calculated: C=39.05%; H=5.0%; Cl=14.4%.

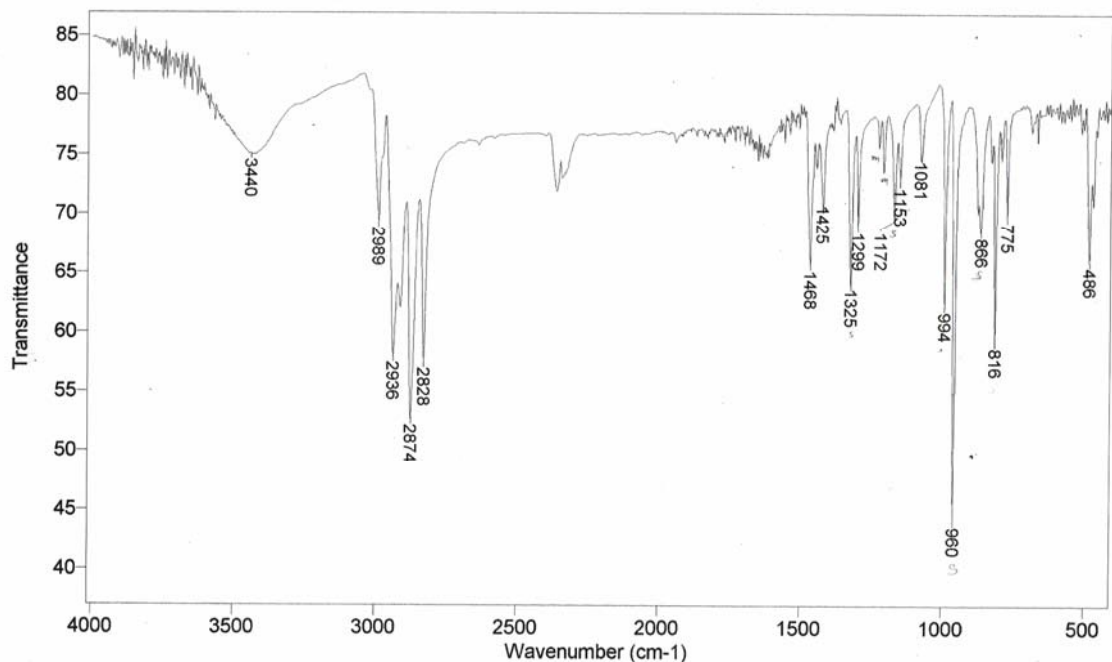


**Figure 4.4.** FTIR spectra of  $[\text{Rh}(\text{COD})\text{Cl}]_2$

#### 4.2.5.3. Preparation of $\text{HRh}(\text{CO})(\text{PPh}_3)_3$

$\text{HRh}(\text{CO})(\text{PPh}_3)_3$ , was prepared in two steps by a method described by Evans and coworkers<sup>21</sup>. In the first step,  $\text{Rh}(\text{CO})\text{Cl}(\text{PPh}_3)_2$  was synthesized and in the next step, it was used as a starting material for the preparation of  $\text{HRh}(\text{CO})(\text{PPh}_3)_3$ .

**(i) Synthesis of  $\text{Rh}(\text{CO})\text{Cl}(\text{PPh}_3)_2$ :** To a refluxing solution of  $\text{PPh}_3$  (7.2 g,  $2.75 \times 10^{-2}$  mole) in ethanol (300 ml),  $\text{RhCl}_3 \cdot 3\text{H}_2\text{O}$  (2 g,  $9.55 \times 10^{-3}$  moles in 70 ml ethanol) was added under constant stirring.  $\text{RhCl}(\text{PPh}_3)_3$  was formed after sometime (indicated by red-brown coloration of the solution). Formaldehyde (40% w/w, 10-20 ml) was added slowly to this red-brown solution, under constant stirring. After 30 minutes,  $\text{RhCl}(\text{PPh}_3)_3$  was converted to  $\text{Rh}(\text{CO})\text{Cl}(\text{PPh}_3)_2$ , as indicated by a color change from red-brown to yellow. This complex was obtained as a solid precipitate, which was filtered from the hot solution and repeatedly washed with hot, and then cold ethanol and dried. The product thus obtained was *trans*- $\text{Rh}(\text{CO})\text{Cl}(\text{PPh}_3)_2$ , a highly crystalline, bright yellow complex, Yield = 4.6 g (70 %). The IR spectrum (KBr pellet) of this complex showed a carbonyl stretch at  $1965 \text{ cm}^{-1}$ , which is typical for this complex (Figure 4.5). The elemental analysis of

$\text{Rh}(\text{CO})\text{Cl}(\text{PPh}_3)_2$  Found: C=64.39%; H=2.43%; P= 9.0%. Calculated: C=64.30%; H=2.46%; P=8.98%.

**(ii) Synthesis of  $\text{HRh}(\text{CO})(\text{PPh}_3)_3$  :** To prepare  $\text{HRh}(\text{CO})(\text{PPh}_3)_3$ ,  $\text{Rh}(\text{CO})\text{Cl}(\text{PPh}_3)_2$  (1.0 g,  $1.44 \times 10^{-3}$  moles) and  $\text{PPh}_3$  (1.5 g,  $5.72 \times 10^{-3}$  moles) were added to ethanol (100 ml) and refluxed under constant stirring. To this solution,  $\text{NaBH}_4$  (0.5 g,  $1.56 \times 10^{-2}$  moles) in ethanol (60 ml) was added very slowly. After complete addition, the mixture was refluxed, till a small sample of the suspended catalyst (washed and dried) showed no absorption at  $1965 \text{ cm}^{-1}$  corresponding to  $\text{Rh}(\text{CO})\text{Cl}(\text{PPh}_3)_2$ . A weak absorption observed at  $2020 \text{ cm}^{-1}$  ( $\nu_{\text{Rh-H}}$ ) and a carbonyl stretch at  $1924 \text{ cm}^{-1}$  is typical of the  $\text{HRh}(\text{CO})(\text{PPh}_3)_3$  complex. The complex was filtered from the hot solution, washed several times with hot ethanol followed by cold ethanol, and dried, Yield=1.3 g (98%). The infrared spectrum of the complex (KBr pellet) showed the characteristic absorption at  $1919 \text{ cm}^{-1}$  and  $2013 \text{ cm}^{-1}$  (Figure-4.6). Elemental analysis of  $\text{HRh}(\text{CO})(\text{PPh}_3)_3$  Found: C=71.96%; H=5.3%; P=10.1%. Calculated: C=71.90%; H=5.12%; P=10.13%.

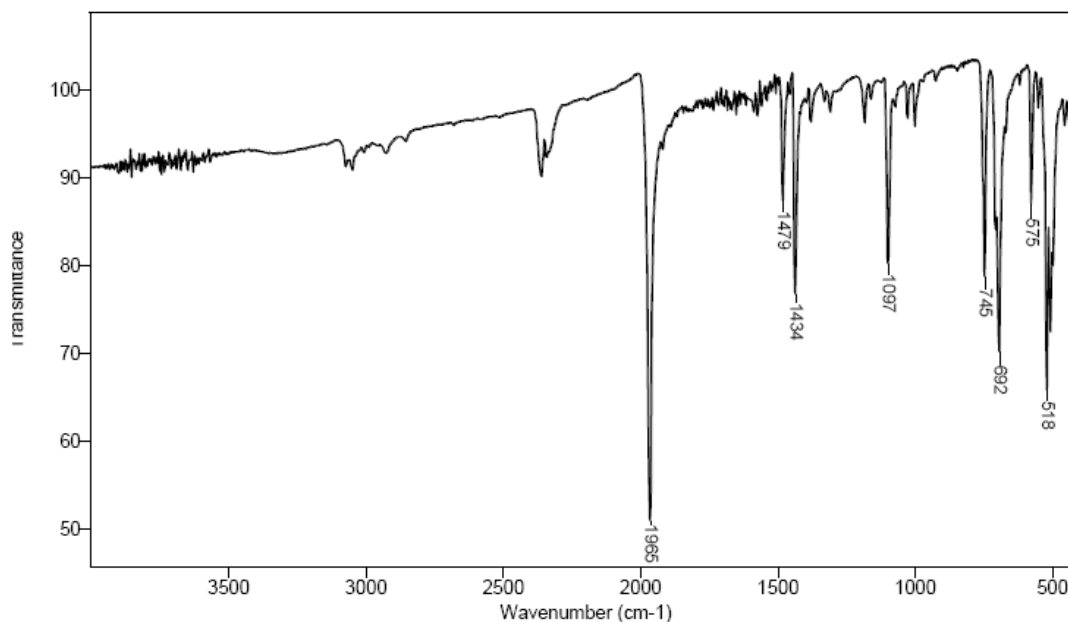


**Figure 4.5.** FTIR spectra of  $\text{Rh}(\text{CO})\text{Cl}(\text{PPh}_3)_2$

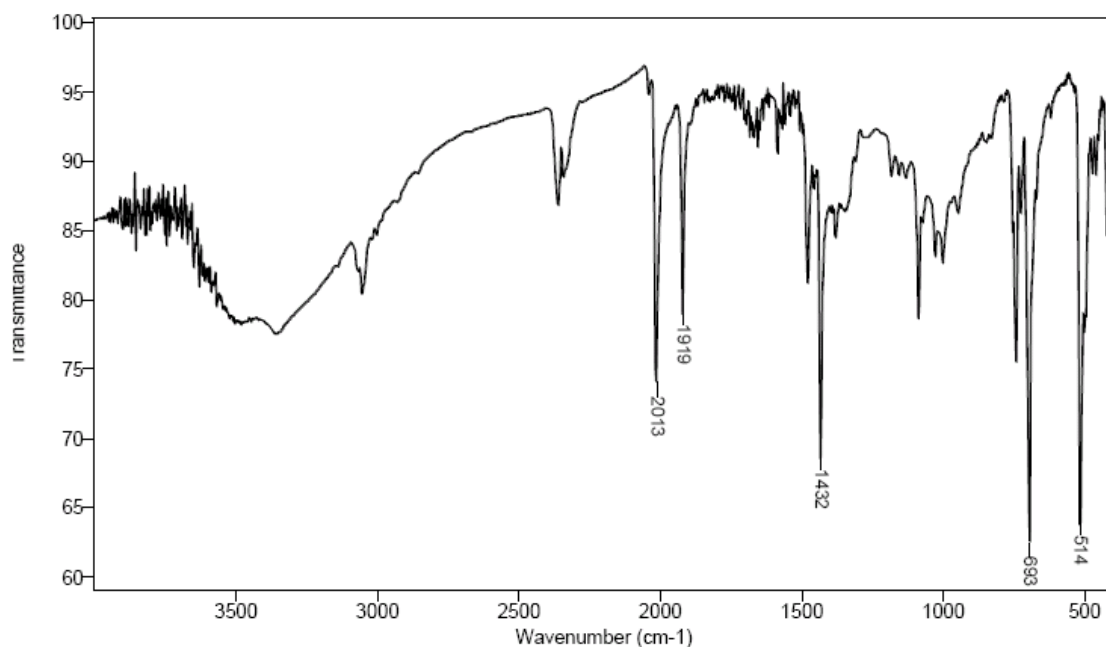
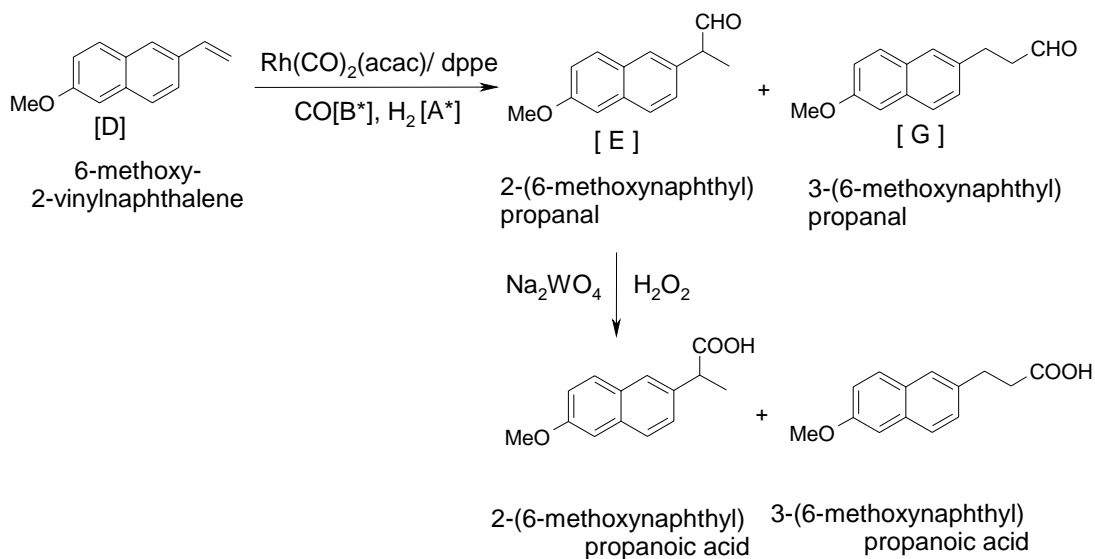


**Figure 4.6** FTIR spectra of  $\text{HRhCO}(\text{PPh}_3)_3$

### 4.3. Results and Discussions

In this chapter, the synthesis of *dl*-naproxen has been investigated in two steps (i) Hydroformylation of MVN to the regioisomers 2-MNP and 3-MNP, and (ii) Oxidation of 2-MNP to *dl*-naproxen, using  $\text{H}_2\text{O}_2$  as the oxidant. The reaction scheme is as shown in the scheme 4.1.



**Scheme 4.1.** Synthesis of *dl*-naproxen by hydroformylation-oxidation route



As it can be noted from the scheme 4.1, only the branched aldehydes product of hydroformylation step i.e. 2-MNP is useful for the synthesis of *dl*-naproxen. Therefore achieving high regioselectivity to 2-MNP was the key issue. The important objectives of the work presented in this chapter are addressed below.

1. Evaluation of hydroformylation-oxidation as an alternative route for selective synthesis of racemic naproxen.
2. Hydroformylation of MVN; screening of Rh catalysts and phosphine ligands as catalyst for achieving high regioselectivity to *iso*-aldehyde.
3. Detailed kinetic investigation of MVN hydroformylation as the key step in the present study.
4. Screening of catalysts and optimization of reaction conditions for the oxidation of 2-MNP for achieving high yields of *dl*-naproxen using H<sub>2</sub>O<sub>2</sub> as the oxidant under mild operating conditions, with good atom economy.

These objectives have been achieved in the present study with detailed experimentation, and the results obtained are presented below in two separate sections- Hydroformylation of MVN, and Oxidation of 2-MNP. The schematic representation is as shown in scheme 4.1.

### **4.3.1. Hydroformylation of MVN: Preliminary Experiments**

#### **4.3.1.1. Screening of Catalysts Precursor**

Even though the active catalytic species in hydroformylation is a metal hydridocarbonyl, different precursors and ligands affect the electronic environment around the metal and thus affect activity and selectivity of the catalyst. Initial hydroformylation experiments were carried out to study the effect of the catalyst precursors. The results for different catalyst precursors like RhCl<sub>3</sub>, Rh(COD)Cl<sub>2</sub>, HRhCO(PPh<sub>3</sub>)<sub>3</sub> and Rh(CO)<sub>2</sub>(acac) are presented in Table 4.1. It was observed that Rh(CO)<sub>2</sub>(acac) with PPh<sub>3</sub> as a ligand, gave the highest activity (TOF = 127.8 h<sup>-1</sup>) with a regioselectivity of 76% to 2-MNP. Under similar conditions, the TOF for RhCl<sub>3</sub>, Rh(COD)Cl<sub>2</sub>, HRhCO(PPh<sub>3</sub>)<sub>3</sub> are 105.7, 107.5 and 120 h<sup>-1</sup> respectively. Thus the Rh(CO)<sub>2</sub>(acac) was found to be the best catalyst precursors.

**Table 4.1.** MVN hydroformylation: screening of catalysts

| Catalyst                              | MVN<br>Conversion<br>% | Regioselectivity,<br>% |            | TOF<br>h <sup>-1</sup> |
|---------------------------------------|------------------------|------------------------|------------|------------------------|
|                                       |                        | <i>iso</i> -           | <i>n</i> - |                        |
| RhCl <sub>3</sub>                     | 79.2                   | 51.4                   | 48.5       | 105.7                  |
| HRhCO(PPh <sub>3</sub> ) <sub>3</sub> | 80.5                   | 64.3                   | 64.0       | 107.5                  |
| [Rh(COD)Cl] <sub>2</sub>              | 90.3                   | 72.0                   | 27.8       | 120.6                  |
| Rh(CO) <sub>2</sub> (acac)            | 95.7                   | 76.3                   | 23.0       | 127.8                  |

**Reaction Conditions:** <sup>a</sup>Catalyst, 8.7X10<sup>-4</sup>kmol/m<sup>3</sup>; PPh<sub>3</sub>:Rh 6:1; MVN,0.108 kmol/m<sup>3</sup>;Pressure (CO:H<sub>2</sub>=1:1), 8.2 MPa; Temperature, 373K; time, 60 min; Solvent, NMP; upto 2.5 X 10<sup>-5</sup>.

#### 4.3.1.2. Ligand Screening and Concentration Effect

The effect of different ligands on the rate of hydroformylation and *n/iso* aldehyde ratio was studied at a CO and H<sub>2</sub> partial pressure of 2.76 MPa each, a catalyst loading of 7.7 × 10<sup>-4</sup> kmol/m<sup>3</sup> in NMP solvent at 373 K. The ratio of L:Rh was kept constant for all the reactions. The results of screening of different monodentate and bidentate ligands are presented in Table 4.2. It was observed that the rate of MVN hydroformylation was higher with PPh<sub>3</sub> as ligand, but the *n/iso* was also higher, which is undesirable. It was observed that the selective formation of *iso* aldehyde is possible with dppe as ligand, even though the rate of MVN hydroformylation was less compared to PPh<sub>3</sub>.

The effect of ligand concentration on rate of hydroformylation of MVN and *n/iso* ratio was also studied at 373 K, using dppe as the ligand. It was observed that the rate of hydroformylation increases with increase in ligand concentration, passes through a maxima at L:Rh of 2:1, and then decreases as shown in Figure 4.2. Beyond a typical L:Rh ratio rate starts decreasing due to formation of the catalytically inactive dimeric species,<sup>15</sup> The *n/iso* ratio also increases with increase in ligand concentration till L:Rh, 4:1 after that it is independent of the concentration of ligand. This is indeed observed in

the ligand concentration effect studied using dppe as the ligand with Rh(CO)<sub>2</sub>(acac) catalyst (Figure 4.7 (b)). The olefin insertion step is reversible at higher temperatures and at low partial pressures of CO or H<sub>2</sub>, in case of *iso* aldehyde formation, while these parameters do not affect the olefin insertion in the formation of the normal product<sup>22</sup>. It is therefore expected that the regioselectivity to the *iso* aldehyde be adversely affected under these conditions as observed in this study.

**Table 4.2.** MVN hydroformylation: screening of ligands

| Sr. | Ligands,<br>kmol/m <sup>3</sup> | MVN<br>Conversion, % | Regioselectivity, % |            | TOF,<br>h <sup>-1</sup> |
|-----|---------------------------------|----------------------|---------------------|------------|-------------------------|
|     |                                 |                      | <i>iso</i> -        | <i>n</i> - |                         |
| 1   | PPh <sub>3</sub>                | 100.0                | 76.0                | 24.0       | 63.9                    |
| 2   | dp <sub>p</sub> h               | 70.0                 | 84.3                | 15.5       | 46.7                    |
| 3   | dp <sub>p</sub> p               | 50.0                 | 86.1                | 14.0       | 33.4                    |
| 4   | dppe                            | 35.0                 | 95.0                | 5.0        | 23.4                    |
| 5   | dppe                            | 79.3                 | 94.3                | 5.4        | -                       |
| 6   | dppe                            | 95.0                 | 95.2                | 5.5        | -                       |

**Reaction conditions:** Rh(CO)<sub>2</sub>(acac), 7.7X10<sup>-4</sup>kmol/m<sup>3</sup>; L:Rh 4:1; MVN,0.108 kmol/m<sup>3</sup>; Temperature, 373K; Pressure (CO:H<sub>2</sub>=1:1), 5.51 MPa; time, 120 min, Solvent, NMP; up to 2.5 X 10<sup>-5</sup>m<sup>3</sup> total volume

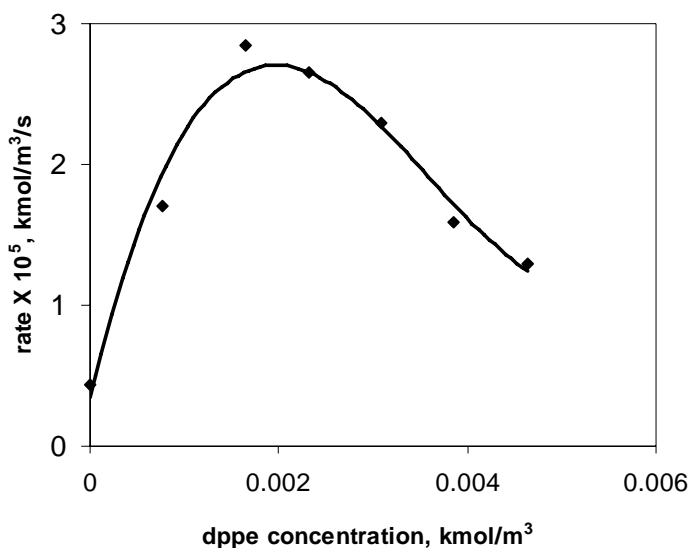


**Figure 4.7(a)** Effect of ligand concentration on the rate of hydroformylation

**Reaction conditions:** MVN 10.7 X 10<sup>-2</sup> kmol/m<sup>3</sup>; Rh(CO)<sub>2</sub>(acac), 7.7X10<sup>-4</sup> kmol/m<sup>3</sup>; Pressure (CO:H<sub>2</sub>=1:1), 5.52 MPa; temperature, 373K; time,120 min; Solvent, NMP; up to 2.5 X 10<sup>-5</sup>m<sup>3</sup> total volume

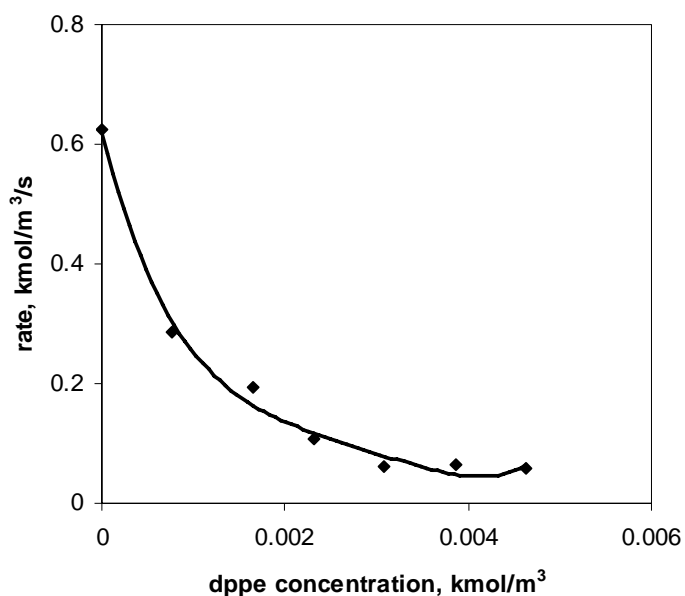


**Figure 4.7(b)** Effect of ligand concentration on *n/iso* ratio

**Reaction conditions:** MVN  $10.7 \times 10^{-2} \text{ kmol/m}^3$ ;  $\text{Rh}(\text{CO})_2(\text{acac})$ ,  $7.7 \times 10^{-4} \text{ kmol/m}^3$ ; Pressure ( $\text{CO}:\text{H}_2=1:1$ ), 5.52 MPa; temperature, 373K; time, 120 min; Solvent, NMP; up to  $2.5 \times 10^{-5} \text{ m}^3$  total volume

#### 4.3.1.3. Screening of Solvents

The results of solvent screening using solvents with varying polarities are shown in Table 4.3. The low solubility of MVN in different solvents was a major constraint, and therefore, non-polar solvents were not used for the screening study. It was observed that MVN conversions of 42% and 38% with >99% selectivity to the aldehyde products (2-MNP and 3-MNP) were obtained using MEK and NMP solvents, respectively. Moderate conversions ranging from 18 to 29% were obtained in hydroformylation experiments using other solvents like THF, ethyl acetate and chlorobenzene. It was observed that the regioselectivity varied only marginally (*n/iso* = 0.0106 to 0.0109), though considerable variations in conversions were observed with the solvents screened. Although MVN has moderate solubility in ethanol, the latter as solvent in hydroformylation of styrenes is known to give acetals<sup>23</sup> as undesirable byproducts in considerable quantities and therefore was not used in the present study. In general, the polar solvents showed a remarkable effect on the activity and regioselectivity in the hydroformylation of MVN.

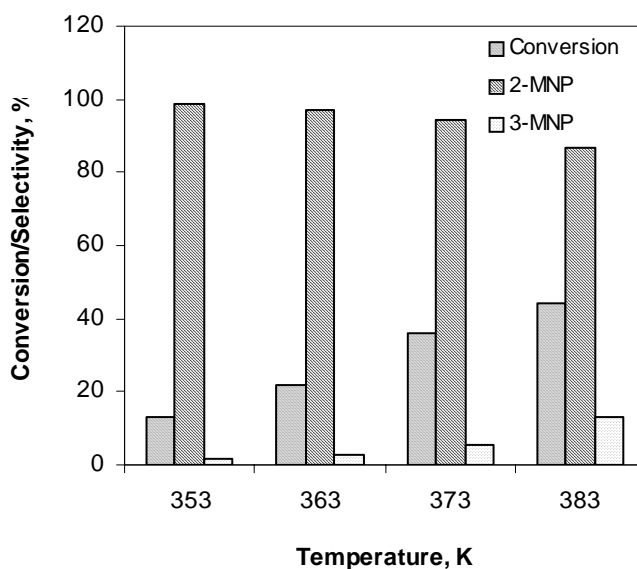
**Table 4.3.** MVN hydroformylation: Solvent screening

| Sr. | Solvents      | MVN<br>conversion,<br>% | Regioselectivity, % |            |
|-----|---------------|-------------------------|---------------------|------------|
|     |               |                         | <i>iso</i> -        | <i>n</i> - |
| 1   | MEK           | 42                      | 94                  | 6          |
| 2   | NMP           | 38                      | 94                  | 6          |
| 3   | Chlorobenzene | 29                      | 91                  | 9          |
| 4   | Ethyl acetate | 22                      | 91                  | 9          |
| 5   | THF           | 18                      | 92                  | 8          |

**Reaction Conditions:** Rh(CO)<sub>2</sub>(acac), 7.7X10<sup>-4</sup>kmol/m<sup>3</sup>; (dppe):Rh 4:1; MVN, 0.108 kmol/m<sup>3</sup>; Temperature,373K; Pressure (CO:H<sub>2</sub>=1:1), 5.51 MPa; time, 180 min; Solvent, up to 2.5 X 10<sup>-5</sup> m<sup>3</sup> total volume

#### 4.3.1.4. Effect of Temperature

The dependency of activity and selectivity for MVN hydroformylation on temperature was studied using Rh(CO)<sub>2</sub>(acac) with dppe as a ligand in the range of 353 to 383 K. It was observed that the conversion increases from 13 % to 48% with increase in temperature from 353 - 383 K. The formation *n*-aldehyde increases (1.5-13%) with increase in temperature as shown in the Figure 4.8.

**Figure 4.8.** Effect of temperature on hydroformylation of MVN

**Reaction Conditions:** Rh(CO)<sub>2</sub>(acac), 7.7X10<sup>-4</sup>kmol/m<sup>3</sup>; (dppe) L:Rh 4:1; MVN, 0.108 kmol/m<sup>3</sup>; Pressure (CO:H<sub>2</sub>=1:1), 5.52 MPa; time, 180 min; Solvent, NMP; up to 2.5 X 10<sup>-5</sup> m<sup>3</sup> total volume

#### 4.3.1.5. Effect of Total Pressure

To study the effect of total pressure on the conversion of MVN and *n/iso* ratio, experiments were carried out using synthesis gas (CO:H<sub>2</sub>; 1:1) in the pressure range of 3.44 – 8.27 MPa. All the reactions were carried out at 373 K, keeping the concentrations of substrate, Rh(CO)<sub>2</sub>(acac) and dppe constant. It was observed that the conversion increased with increase in pressure of synthesis gas without affecting the *n/iso* ratio. The reaction was very slow at 3.44 MPa and the rates increased with the increase in pressure as shown in the Figure 4.9.

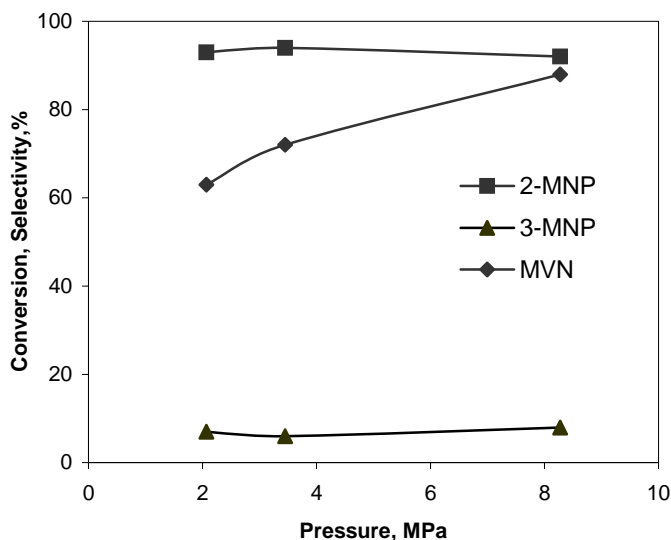


**Figure 4.9** Effect of total pressure on hydroformylation of MVN

**Reaction Conditions:** Rh(CO)<sub>2</sub>(acac),  $8.1 \times 10^{-4}$  kmol/m<sup>3</sup>; (dppe)L:Rh, 4:1; MVN,  $10.8 \times 10^{-2}$  kmol/m<sup>3</sup>; temperature, 373 K; time, 240 min; Solvent, NMP; up to  $2.5 \times 10^{-2}$  m<sup>3</sup> total volume

#### 4.4. Kinetics of Hydroformylation of MVN

Kinetics of hydroformylation of linear styrenes has been extensively studied, however, very few studies using functionalized styrenes substrates are known. The literature lack a detailed investigation of intrinsic kinetics of hydroformylation of MVN. Knowledge of intrinsic kinetics and development of rate equation is also important in understanding the mechanistic features of such complex catalytic reactions. Considering

the industrial importance of this reaction in naproxen synthesis, such a study would also provide useful data for reactor design purpose. Hence, the important objective of this work was to investigate the kinetics of hydroformylation of MVN to 2-MNP and 3-MNP using  $\text{Rh}(\text{CO})_2(\text{acac})$  as a catalyst and dppe as a ligand. For the kinetic studies, only the initial rate data, wherein the concentration of the olefin changed marginally ( $\sim 10\text{-}15\%$ ), was considered. The effect of  $\text{Rh}(\text{CO})_2(\text{acac})$  and MVN concentrations and partial pressures of  $\text{H}_2$  and  $\text{CO}$  on initial rate of hydroformylation as well as concentration time profile have been studied in the temperature range of 372 to 393 K. For this purpose, a few experiments were carried out in which the amount of MVN consumed, products formed and  $\text{CO} + \text{H}_2$  consumed were compared with experiments for higher conversion of MVN. A typical concentration time profile is as shown in the Figure 4.10.

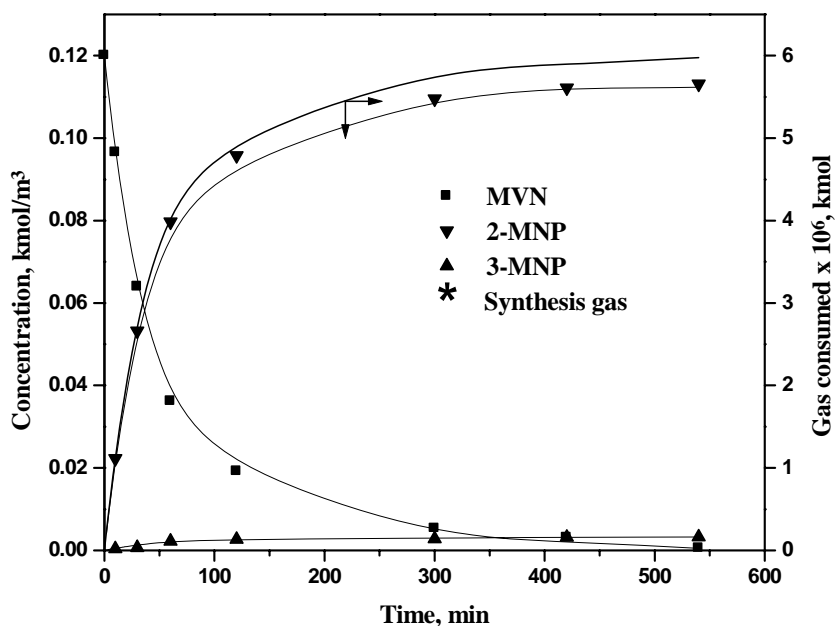


**Figure 4.10.** Hydroformylation of MVN: concentration time profile

**Reaction Conditions:**  $\text{Rh}(\text{CO})_2(\text{acac})$ ,  $8.1 \times 10^{-4} \text{ kmol/m}^3$ ;  $\text{L}(\text{dppe})\text{:Rh}$ , 4:1; MVN,  $10.8 \times 10^{-2} \text{ kmol/m}^3$ ; temperature, 373 K; agitation speed, 16.6 Hz, synthesis gas, 5.51 MPa; Solvent, NMP; up to  $2.5 \times 10^{-2} \text{ m}^3$  total volume

#### 4.4.1. Agitation Effect

In order to study the kinetics, it was important to ensure that the reactions were carried out under kinetic regime. The experiments at different agitation speeds showed that the rate of the reaction was independent of the agitation speed beyond 600 rpm (12.5 Hz), indicating a kinetic regime. All the reactions were therefore carried out at an agitation speed of 1000 rpm (16.66 Hz) to ensure kinetic regime (Figure 4.11)

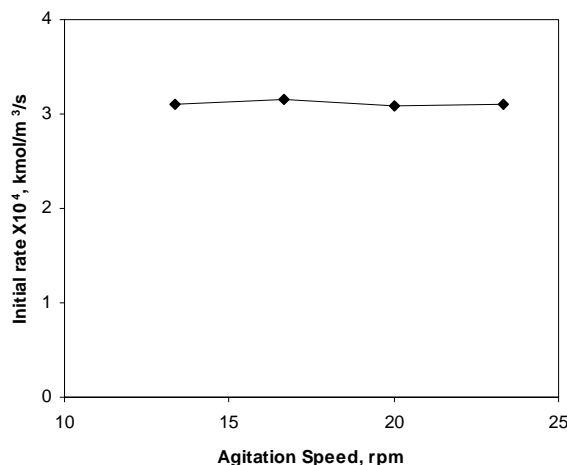


**Figure 4.11.** Hydroformylation of MVN: Effect of agitation speed

**Reaction conditions:** MVN 0.2070 kmol/m<sup>3</sup>; catalyst, 1.2X10<sup>-5</sup> kmol/m<sup>3</sup>, (dppe)L:Rh 4:1; Pressure (CO:H<sub>2</sub>=1:1), 5.52 MPa; Solvent, NMP up to 2.5 X 10<sup>-5</sup> m<sup>3</sup> total volume

#### 4.4.2. Solubility of H<sub>2</sub> and CO in Solvent

For interpretation of kinetic data, knowledge of the concentration of the gaseous reactants in the reaction medium is essential. The solubility of CO and H<sub>2</sub> in NMP, was determined experimentally at 373, 383 and 393 K, using a method described by Chaudhari and coworkers<sup>24</sup>. The solubility of H<sub>2</sub> and CO measured in 6.0 x 10<sup>-4</sup> m<sup>3</sup> capacity stirred autoclave supplied by Parr Instrument Company, USA designed for 25 MPa pressure. The equipment was provided with automatic temperature control and a pressure recording system. The temperature of the liquid in the reactor was controlled within ±1 K. A pressure transducer having a precession of ±1 kPa was used to measure the autoclave pressure.



In a typical experiment for the measurement of solubility of H<sub>2</sub> and CO, a known volume (100 ml) of solvent was introduced into the autoclave and the contents were heated to a desired temperature. After the thermal equilibrium was attained, the void space in the reactor was carefully flushed with a solute gas and pressurised to the level required. The contents were then stirred for about ten minutes to equilibrate the liquid phase with the solute gas. In general, it required, about 5 minutes to saturate the liquid phase. The change in the pressure in the autoclave was recorded on-line as function of time till it remained constant, indicating the saturation of the liquid phase. From the initial and final pressure readings, the solubility was calculated in mole fraction as

$$X_a = \frac{(P_i - P_f) V_g M_s}{RT V_L \rho_s} \quad 4.1$$

Where X<sub>a</sub> represents the mole fraction of the solute gas in the liquid phase at the partial pressure of the solute gas prevailing at P<sub>f</sub>, P<sub>i</sub> and P<sub>f</sub> are the initial and final pressure readings in the autoclave, V<sub>g</sub> and V<sub>L</sub> are the volumes of the gas and liquid phases, respectively, R is the gas constant, T is the temperature, M<sub>s</sub> is the molecular weight of the solvent and ρ<sub>s</sub> is the molar density of the liquid. The Henry's law constant, H was calculated as

$$H = \frac{P_f}{X_a} \quad 4.2$$

The results are presented as Henry's law constant in Table 4.4

**Table 4.4.** Henry's law Constant

| Temperature<br>K | H <sub>A</sub> for H <sub>2</sub><br>kmol/m <sup>3</sup> /MPa | H <sub>A</sub> for CO<br>kmol/m <sup>3</sup> /MPa |
|------------------|---|---|
| 373              | 52.63   | 35.71   |
| 363              | 63.29   | 40.16   |
| 353              | 76.34   | 44.64   |

#### 4.4.3. Gas-liquid Mass Transfer Effect

The significance of gas-liquid mass transfer resistance was analyzed by comparing the initial rate of reaction and maximum possible rate of gas-liquid mass

transfer. The gas-liquid mass transfer resistance is negligible if a factor  $\alpha_I$  defined as follows is less than 0.1 for the experimental conditions used.

$$\alpha_{1,A} = \frac{R_{exp}}{k_L a_B C_{A,aq.}} \quad 4.3$$

$$\alpha_{1,B} = \frac{R_{exp}}{k_L a_B C_{B,aq.}} \quad 4.4$$

Where,  $R_{exp}$  is the observed rate of hydroformylation ( $\text{kmol/m}^3$ ),  $k_L a_B$  the gas-liquid mass transfer coefficient and  $C_A$  and  $C_B$  represent the saturation solubility of reacting gases *i.e.*  $\text{H}_2$  and  $\text{CO}$  in equilibrium with the gas phase concentration at the reaction temperature ( $\text{kmol/m}^3$ ). The gas-liquid mass transfer coefficient ( $k_L a_B$ ) used in above equations was estimated by using a correlation (Equation 4.3) proposed by Chaudhari and coworkers<sup>25</sup> for a reactor similar to that used in this work for agitation speed of 1200 rpm.

$$k_L a_B = 1.48 \times 10^{-3} (N)^{2.18} \times (V_g / V_l)^{1.88} \times (d_I / d_T)^{2.1} \times (h_1 / h_2)^{1.16} \quad 4.5$$

The terms involved in above equation are described in Table-4.5 along with the respective values obtained from the reactor and charge used in the present case.

**Table 4.5.** Parameters used for  $k_L a_B$  calculations

| Parameter | Description                                | Value                |
|-----------|--|----------------------|
| $V_g$     | Gas volume ( $\text{m}^3$ )                | $4.5 \times 10^{-5}$ |
| $N$       | Agitation Speed (Hz)                       | 20                   |
| $V_L$     | Liquid volume ( $\text{m}^3$ )             | $2.5 \times 10^{-5}$ |
| $d_I$     | Impeller diameter (m)                      | $1.6 \times 10^{-2}$ |
| $d_T$     | Tank diameter (m)                          | $4.0 \times 10^{-2}$ |
| $h_1$     | Height of the impeller from the bottom (m) | $1.1 \times 10^{-2}$ |
| $h_2$     | Liquid height (m)                          | $2.1 \times 10^{-2}$ |

The  $k_L a_B$  value for 1200 rpm (20 Hz) was evaluated as  $0.22 \text{ s}^{-1}$ .

The equilibrium solubilities for the gases given in Table 4.5 were used. The factor  $\alpha_l$  was calculated (taking  $R_{\text{exp}}$  as  $4.3 \times 10^{-5}$  i.e. highest) for both hydrogen and carbon monoxide and found to be  $9.96 \times 10^{-3}$  and  $6.76 \times 10^{-3}$ , respectively. Since the values of  $\alpha_l$  are much less than 0.1 for both the gaseous reactants, gas-liquid mass transfer resistance can be assumed to be negligible.

#### 4.4.4. Initial Rate Data

In order to study the kinetics of the hydroformylation of MVN using  $\text{Rh}(\text{CO})_2(\text{acac})$  in NMP as solvent, several experiments were carried out in the range of conditions as shown in the Table 4.6. The initial rates of hydroformylation were calculated from observed data on the consumption of  $\text{CO} + \text{H}_2$  as a function of time

An important objective of this work was to investigate the kinetics of hydroformylation of MVN to 2-MNP and 3-MNP using  $\text{Rh}(\text{CO})_2(\text{acac})$  as a catalyst and dppe as a ligand. The kinetics of hydroformylation of MVN was studied under the range of conditions as given in Table 4.6. For the kinetic studies, only the initial rate data, wherein the concentration of the olefin changed marginally (~10-15%), was considered. Preliminary experiments were carried out to ensure the material balance and reproducibility of the experiments. The observation that agitation speed has no effect on the rate indicated the absence of mass transfer resistance.

**Table 4.6.** Range of operating conditions

| Parameter  | Range   |
|--|---|
| Concentration of catalyst ( $\text{kmol}/\text{m}^3$ ) | $3.86 \times 10^{-4}$ - $1.23 \times 10^{-3}$ |
| Concentration of MVN ( $\text{kmol}/\text{m}^3$ )      | 0.05 – 0.21                                   |
| Partial pressure of hydrogen, MPa                      | 0.69–3.45                                     |
| Partial pressure of carbon monoxide, MPa               | 0.34–5.51                                     |
| Temperature, K   | 353–373                                       |
| Solvent  | NMP   |
| Reaction volume ( $\text{m}^3$ )                       | $2.5 \times 10^{-5}$                          |

#### 4.4.5. Effect of Catalyst Concentration

The effect of catalyst concentration on the rate of hydroformylation was studied at an MVN concentration of  $0.107 \text{ kmol/m}^3$  and CO and H<sub>2</sub> partial pressures of 2.76 MPa each. The range of catalyst concentration for the study was  $3.86 \times 10^{-4} - 1.23 \times 10^{-3} \text{ kmol/m}^3$ . The L:Rh ratio was kept constant during this study. The rate was found to vary with a linear dependence on catalyst concentration. There is marginal decrease in the *n/iso* ratio with increase in catalyst concentration as shown in the Figure 4.12a and 4.12b.

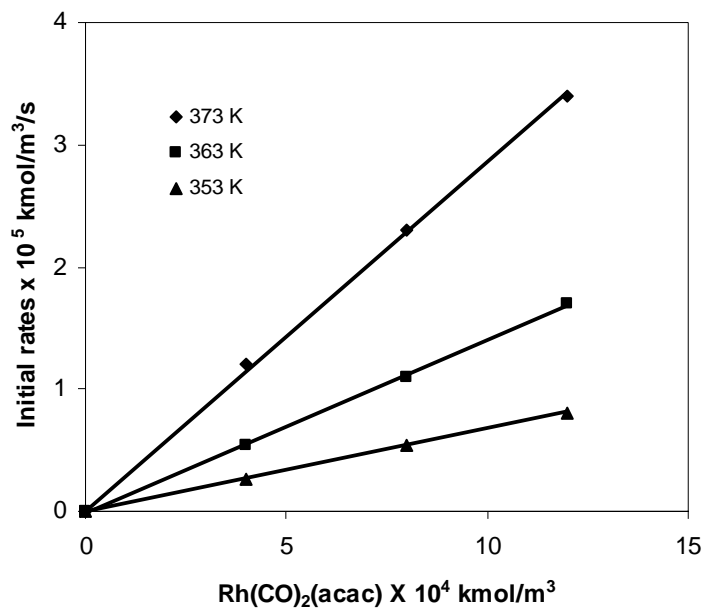


**Figure 4.12 (a).** Effect of catalyst concentration on rate of hydroformylation of MVN

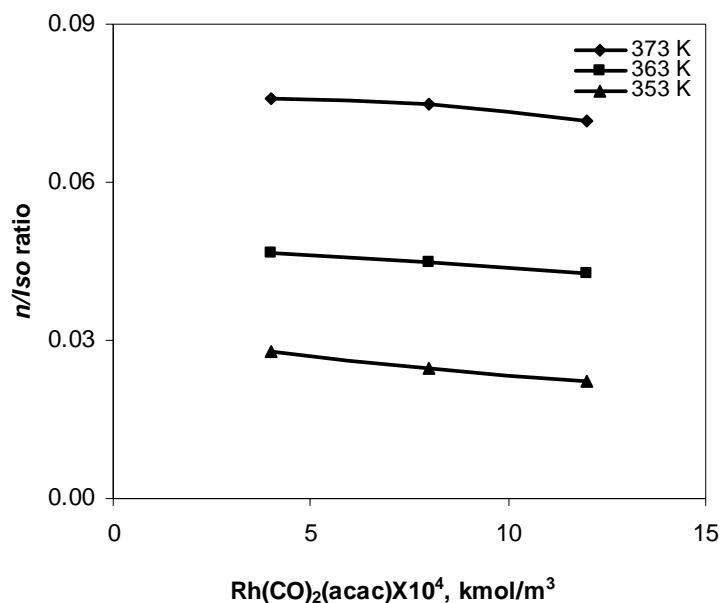


**Figure 4.12 (b).** Effect of catalyst concentration on rate *n/iso* ratio

**Reaction Conditions:** MVN 0.1070 kmol/m<sup>3</sup>; (dppe)L:Rh 4:1; Pressure (CO:H<sub>2</sub>=1:1), 5.52 MPa; time, 120 min; Solvent, NMP up to 2.5 X 10<sup>-5</sup> m<sup>3</sup>total volume.

#### 4.4.6. Effect of MVN Concentration

The effect of MVN concentration on the rate of hydroformylation and regioselectivity of the aldehyde products (2-MNP and 3-MNP) was studied over a range of MVN concentration of 0.053 to 0.21 kmol/m<sup>3</sup>, at a CO and H<sub>2</sub> partial pressure of 2.76 MPa each, a catalyst loading of 7.7×10<sup>-4</sup> kmol/m<sup>3</sup> in NMP as solvent in a temperature range of 353–373K. The results are presented in Figure 4.13(a). The rate increases linearly with increasing MVN concentrations in the range studied. The first order kinetics with MVN is expected in hydroformylation reactions, as the enhanced olefin concentration will increase the formation of active alkyl rhodium species concentration. The *n/iso* ratio of the aldehyde products decreased marginally with increasing MVN concentration as presented in Figure 4.13b

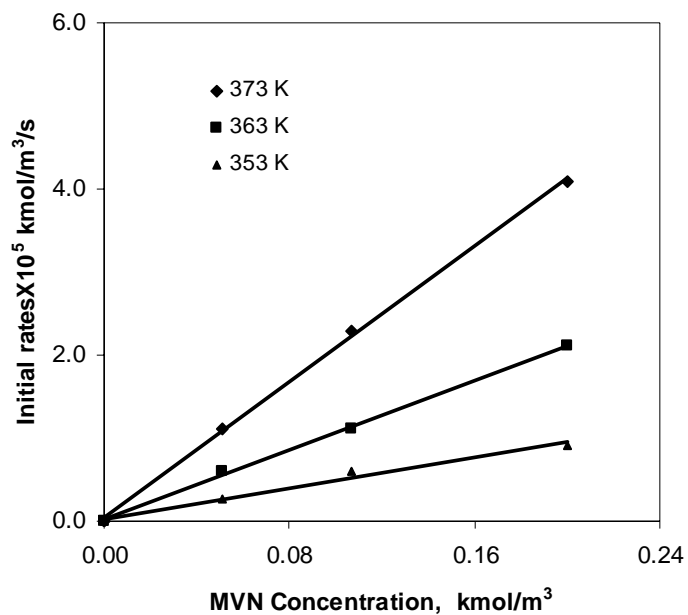


**Figure 4.13 (a).** Effect of MVN concentration on rate of hydroformylation of MVN

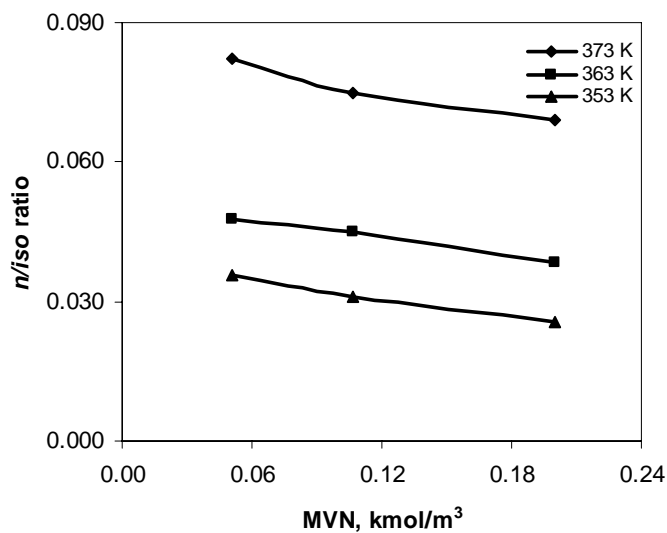


**Figure 4.13 (b).** Effect of MVN concentration *n/iso* ratio

**Reaction Conditions:** Rh(CO)<sub>2</sub>(acac), 7.7X10<sup>-4</sup>kmol/m<sup>3</sup>; (dppe) L:Rh 4:1; Pressure (CO:H<sub>2</sub>=1:1), 5.52 MPa; time,120 min; Solvent, NMP up to 2.5 X 10<sup>-5</sup> m<sup>3</sup> total volume

#### 4.4.7. Effect of Partial Pressure of Carbon Monoxide

The effect of partial pressure of carbon monoxide on the rate of hydroformylation and *n/iso* aldehyde ratio was studied at H<sub>2</sub> partial pressure of 2.76 MPa and a catalyst concentration of  $7.7 \times 10^{-4}$  kmol/m<sup>3</sup> in NMP in a temperature range of 353–373K and an MVN concentration of 0.107 kmol/m<sup>3</sup>. The rate initially increased with increasing  $P_{CO}$  and then decreased with further increase in CO partial pressure. The inhibition in rate with enhanced CO pressure owing to the formation of the inactive dicarbonyl and tricarbonyl species of rhodium is a well-known phenomenon in hydroformylation chemistry.<sup>26</sup> The *n/iso* ratio was also found to be strongly dependent on the partial pressure of CO. The *n/iso* ratio dropped with increasing  $P_{CO}$ . The CO and H<sub>2</sub> partial pressures are known to affect the regioselectivity at higher temperatures, due to the different behavior of the alkyl rhodium intermediate towards the  $\beta$ -hydride elimination. Lazzaroni and coworker<sup>27</sup> have shown, through deuterioformylation experiments at higher temperatures, that the  $\beta$ -hydride elimination from the branched alkylmetal occurs to a larger extent at lower CO and H<sub>2</sub> partial pressures, unlike the  $\beta$ -hydride elimination from the linear one, which occurs only to a small extent even at low pressure. The results obtained in the present study are given in Figure 4.14 (a,b).

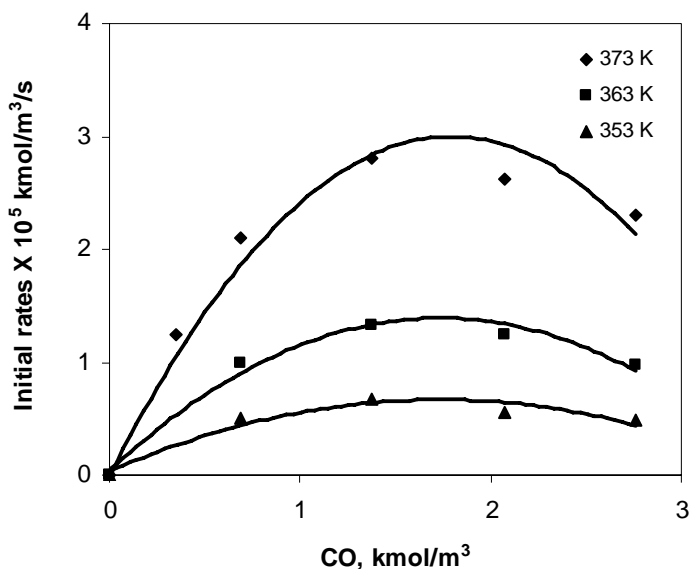


**Figure 4.14 (a).** Effect of  $P_{CO}$  on rate of hydroformylation of MVN

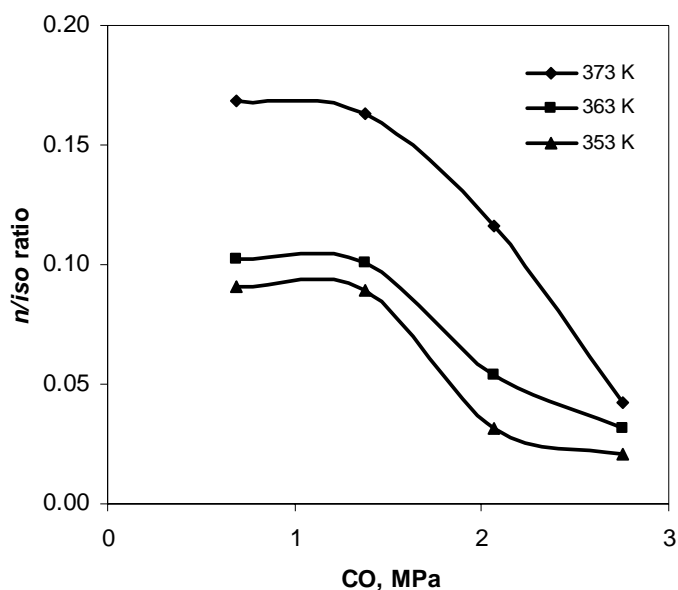


**Figure 4.14 (b).** Effect of  $P_{CO}$   $n/iso$  ratio

**Reaction Conditions:** MVN  $0.1070 \text{ kmol/m}^3$ ;  $\text{Rh}(\text{CO})_2\text{acac}$ ,  $7.7 \times 10^{-4} \text{ kmol/m}^3$ ; (dppe)L:Rh 4:1;  $P_{\text{H}_2}$ , 2.76 MPa; time, 120 min; Solvent, NMP up to  $2.5 \times 10^{-5} \text{ m}^3$  total volume

#### 4.4.8. Effect of Partial Pressure of Hydrogen

The effect of partial pressure of hydrogen on the rate of hydroformylation and  $n/iso$  aldehyde ratio was studied at a CO partial pressure of 2.76 MPa, a catalyst loading of  $7.7 \times 10^{-4} \text{ kmol/m}^3$  in NMP solvent in a temperature range of 353–373 K and an MVN concentration of  $0.107 \text{ kmol/m}^3$ . The results are presented in Figure 4.15(a). The rate was found to be dependent on the hydrogen partial pressure with a first order. Since the oxidative addition of hydrogen to the acyl carbonyl rhodium phosphine species is the rate-determining step, increase in the partial pressure of hydrogen would lead to increased rate of hydroformylation. The  $n/iso$  ratio was found to decrease with increase in hydrogen pressure at all the temperatures studied as seen in Figure 4.15(b). This result is concurrent with the explanation given above. The effect of total pressure on the conversion of MVN and  $n/iso$  ratio is also shown in Figure 4.9. It was observed that the conversion increases from 63% to 85 % with increase in pressure of synthesis gas from 2-8 MPa without affecting the  $n/iso$  ratio.



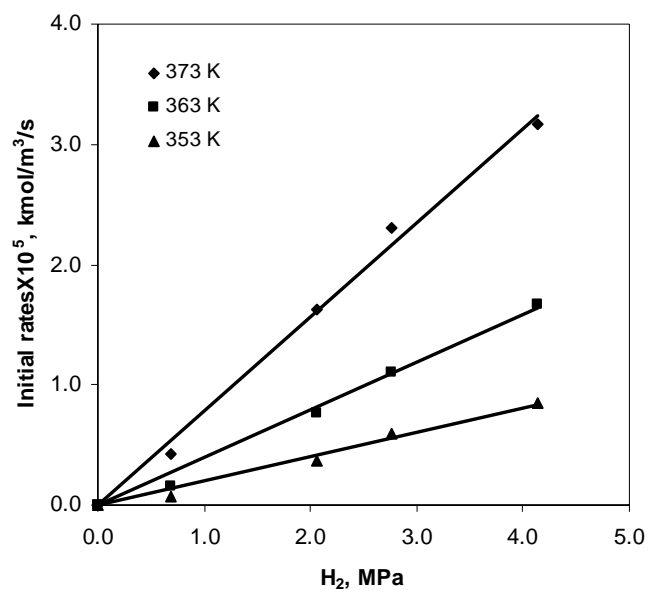


**Figure 4.15 (a).** Effect of  $P_{H_2}$  on rate of hydroformylation of MVN

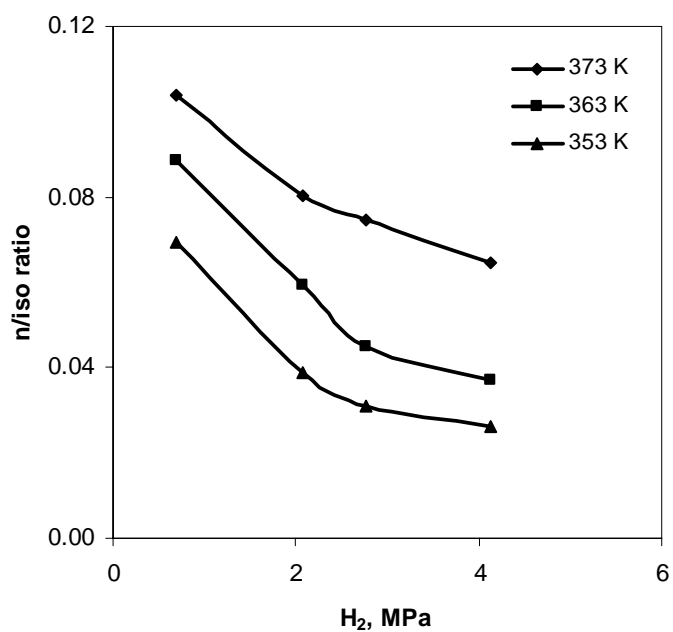


**Figure 4.15 (b).** Effect of  $P_{H_2}$  on  $n/iso$  ratio

**Reaction Conditions:** MVN,  $10.7 \times 10^{-2} \text{ kmol/m}^3$ ;  $\text{Rh}(\text{CO})_2(\text{acac})$ ,  $7.7 \times 10^{-4} \text{ kmol/m}^3$ ; (dppe)L:Rh 4:1;  $P_{\text{CO}}$ , 2.76 MPa; time, 120 min; Solvent, NMP; up to  $2.5 \times 10^{-5} \text{ m}^3$  total volume

#### 4.5. Kinetic Model

For the purpose of development of rate models, an empirical approach was followed. Prior to discrimination of rate equations, the rate data were analyzed for the importance of mass transfer resistances. The effect of agitation speed on the rate was investigated at the highest catalyst concentration and at highest temperature. The rate was found to be independent of the agitation speed, and hence the data were representative of the true kinetics of the reaction. The observed dependency of the rate on different parameters indicates that the hydroformylation of MVN is first order with respect to catalyst and dissolved hydrogen, concentrations, and a negative order with respect to  $P_{CO}$ . The effect of MVN concentration on initial rate showed first order kinetics. In order to fit the rate data, several rate equations were examined using a nonlinear regression analysis. The results on parameters estimated for different models are presented in Table 4.7 for this purpose, an optimization program based on Marquardt's method was used. The objective function was chosen as follows;

$$\Phi_{\min} = \sum_{i=1}^n [R_{Ai} - R_{ai}]^2 \quad 4.6$$

$\Phi_{\min}$ , representing the sums of squares of the difference between the observed and predicted rates,  $n$  is the number of experimental data;  $R_{Ai}$  and  $R_{ai}$  represent experimental and predicted rates, respectively. The minimum absolute squared-error objective function,  $\Phi_{\min}$ , was selected as the basis for the discrimination of the kinetic models. The values of rate parameters and  $\Phi_{\min}$ , are presented in Table 4.7. Models 2, 3 and 4 are not consistent with the observed rate dependence. Also, the values of  $\Phi_{\min}$ , for these models were higher than that for model 1.  $\Phi_{\min}$  for Model 5 is higher than model 1. Therefore, model 1 was considered the best model for representing the kinetics of hydroformylation of MVN using  $\text{Rh}(\text{CO})_2(\text{acac})$  as catalyst and with dppe as ligand. The corresponding rate equations are:

$$r_{iso} = \frac{k_1 A^* B^* CD}{(1 + k_2 B^*)^2} \quad 4.7$$

$$r_n = \frac{k_3 A^* B^* CD}{(1 + k_2 B^*)^2} \quad 4.8$$

where,  $k$  is the intrinsic reaction rate constant ( $\text{m}^3/\text{kmol}$ );  $A^*$ ,  $B^*$  are the concentrations of  $\text{H}_2$  and  $\text{CO}$  in NMP at the gas-liquid interface ( $\text{kmol}/\text{m}^3$ ), respectively, and  $C$  and  $D$  represent the concentrations of the catalyst and MVN ( $\text{kmol}/\text{m}^3$ ) respectively. The rate parameters in Equation 4.7 and 4.8 are presented in Table 4.7. The experimental rates were compared with those predicted by rate model (Equations 4.7 and 4.8) in Figure 4.16, which shows reasonably good fit of the data. The average deviation in the predicted and observed rates was found to be in the range of 5%. The Arrhenius plots showing the effect of temperature on the rate parameter is shown in Figure 4.17, from which the activation energy was evaluated as 13.24 and 31.02 kcal/mol.

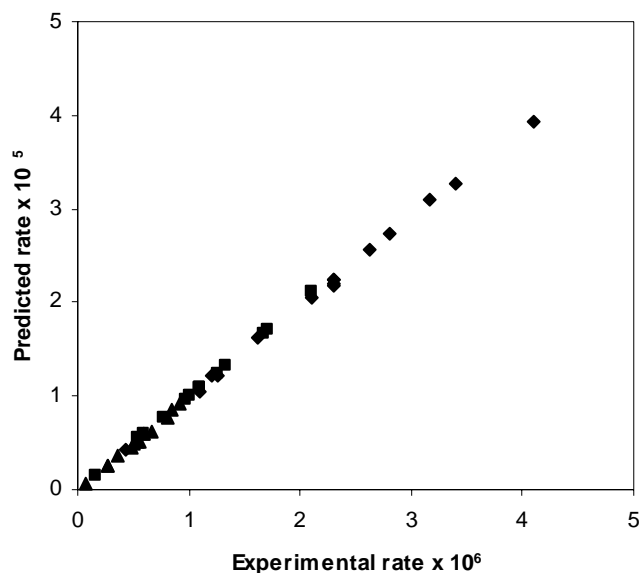


**Figure 4.16.** MVN hydroformylation: Experimental rates vs Predicted rates

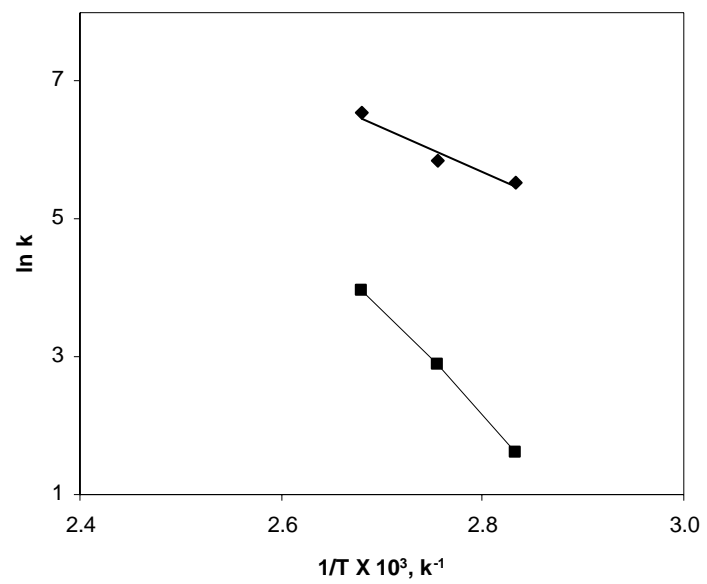


**Figure 4.17.** Hydroformylation of MVN: Arrhenius plot

**Table 4.7.** Rate models examine to fit the data on MVN hydroformylation

| Sr | Rate Model  | T (K) | k <sub>1</sub> | k <sub>2</sub> | k <sub>3</sub> | ϕ <sub>min</sub> |
|----|---|-------|----------------|----------------|----------------|------------------|
| 1  | $r_{iso} = \frac{k_1 A^* B^* CD}{(1 + K_2 B^*)^2}$                  | 353   | 2.53E+02       | 7.64E+00       | 4.99E+00       | 1.31E-14         |
|    | $r_n = \frac{k_3 A^* B^* CD}{(1 + K_2 B^*)^2}$                      | 363   | 3.45E+02       | 1.45E+01       | 1.80E+01       | 8.33E-14         |
|    |   | 373   | 6.96E+02       | 2.47E+01       | 5.26E+01       | 4.52E-14         |
| 2  | $r_{iso} = \frac{k_1 A^* B^* CD}{(1 + K_2 B^*)}$                    | 353   | 4.02E+01       | 5.32E-03       | 1.42E-05       | 2.83E-11         |
|    | $r_n = \frac{k_3 A^* B^* CD}{(1 + K_2 B^*)}$                        | 363   | 4.55E+01       | 7.25E-04       | 1.05E-04       | 1.30E-10         |
|    |   | 373   | 6.12E+02       | 1.15E+02       | 2.07E-02       | 3.99E-11         |
| 3  | $r_{iso} = \frac{k_1 (A^*)^{1.5} B^* (C)^{1.5} D}{(1 + K_2 B^*)^2}$ | 353   | 3.29E+01       | 1.96E-04       | 3.01E-03       | 2.75E-11         |
|    | $r_n = \frac{k_3 (A^*)^{1.5} B^* (C)^{1.5} D}{(1 + K_2 B^*)^2}$     | 363   | 4.55E+01       | 1.21E-04       | 1.50E-03       | 1.30E-10         |
|    |   | 373   | 7.43E+00       | 1.19E-04       | 3.05E-03       | 6.61E-10         |
| 4  | $r_{iso} = \frac{k_1 A^* B^* CD}{(1 + K_2 B^*)^3}$                  | 353   | 3.29E+01       | 1.96E-04       | 3.01E-03       | 2.75E-11         |
|    | $r_n = \frac{k_3 A^* B^* CD}{(1 + K_2 B^*)^3}$                      | 363   | 4.55E+01       | 1.21E-04       | 1.50E-03       | 1.30E-10         |
|    |   | 373   | 7.43E+00       | 1.19E-04       | 3.05E-03       | 6.61E-10         |
| 5  | $r_{iso} = \frac{k_1 A^* B^* CD}{(1 + K_2 (B^*)^2)}$                | 353   | 3.29E+01       | 2.50E-06       | 5.13E-04       | 2.75E-11         |
|    | $r_n = \frac{k_3 A^* B^* CD}{(1 + K_2 (B^*)^2)}$                    | 363   | 4.55E+01       | 5.06E-05       | 1.63E-03       | 1.30E-10         |
|    |   | 373   | 6.40E+01       | 2.92E-04       | 5.20E-03       | 4.19E-10         |

#### 4.6. Semibatch Reactor Model

In order to verify the applicability of the kinetic model under integral conditions, experimental data on the liquid phase concentrations of MVN, 2-MNP and 3-MNP as a function of time were obtained. The variation of the concentration of MVN, 2-MNP and 3-MNP can be represented by the following mass balance equations, for conditions of constant synthesis gas pressure in the reactor.

For 2-methoxy-6-vinylnaphthalene

$$-\frac{dD}{dt} = \frac{k_1 A^* B^* CD}{(1 + K_2 B^*)^2} + \frac{k_3 A^* B^* CD}{(1 + K_2 B^*)^2} \quad 4.9$$

For 2-methoxynaphthylpropanal

$$\frac{dE}{dt} = \frac{k_1 A^* B^* CD}{(1 + K_2 B^*)^2} \quad 4.10$$

For 3-methoxynaphthylpropanal

$$\frac{dG}{dt} = \frac{k_3 A^* B^* CD}{(1 + K_2 B^*)^2} \quad 4.11$$

With initial conditions

$t=0, D=D_0, E=0, G=0$

For the data at a constant synthesis gas pressure, the equations were solved numerically by using the Runge-Kutta method to obtain the concentration of MVN, 2-MNP, and 3-MNP as a function of time. For this purpose intrinsic rates were used. The comparison of the experimental and the predicted results for 373 K are presented in Figure 4.18, which show excellent agreement. These results indicate that the rate model proposed on the basis of initial rate data is also applicable over a wide range of conditions and can be used for design and scale up purposes. To show the difference in fitting between the Model 1 and other models, a typical substrate consumption-time profile is shown in Figure 4.18, which clearly indicates the suitability of Model 1.

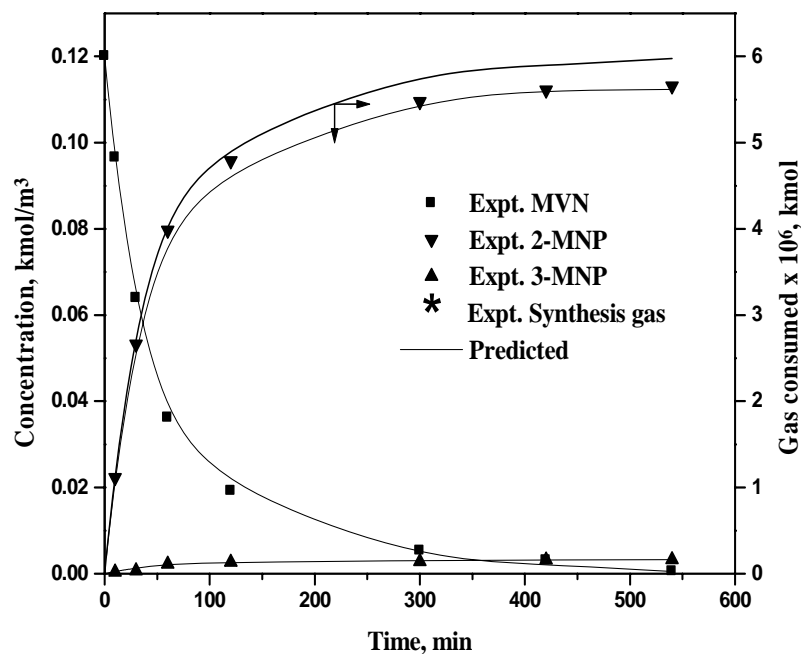


**Figure 4.18.** Hydroformylation of MVN: experimental Vs predicted concentration time profile

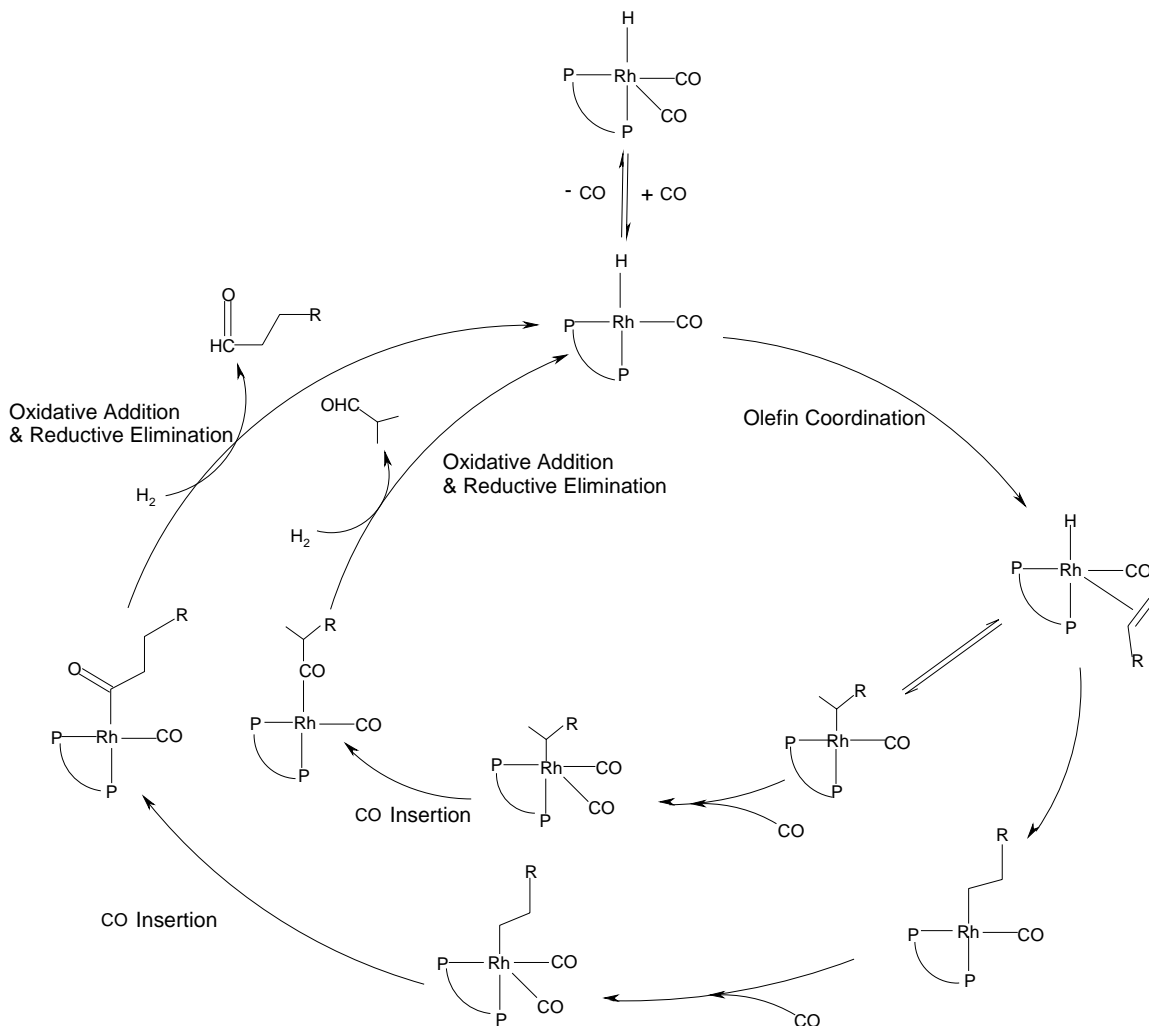
**Reaction Conditions:**  $\text{Rh}(\text{CO})_2(\text{acac})$ ,  $8.1 \times 10^{-4} \text{ kmol/m}^3$ ;  $\text{L}(\text{dppe}):\text{Rh}$ , 4:1; MVN,  $10.8 \times 10^{-2} \text{ kmol/m}^3$ ; temperature, 373 K; agitation speed, 16.6 Hz, synthesis gas, 5.51 MPa; Solvent, NMP; up to  $2.5 \times 10^{-2} \text{ m}^3$  total volume

#### 4.7. Reaction Pathway

The mechanism of the hydroformylation is shown in the scheme 4.2. The ligand being a chelating bidentate ligand, the stability of its complex with Rh depends on the bite angle in the formed complex, and the consequent strain exerted on the complex. In this context, dppe forms a stable complex, since the complex is less than 3 kcal more strained than the free ligand.<sup>28</sup> The bite angle in the Rh-dppe complex is small, i.e. 84, therefore, the ligand prefers apical-equatorial (ae) coordination to the central metal atom.

In case of bidentate ligands, the increasing ligand concentration may cause a reversible formation of the catalytically inactive binuclear rhodium complex species,<sup>29</sup> causing thereby rate retardation. This is indeed observed in the ligand concentration experiments carried out using dppe as the ligand with  $\text{Rh}(\text{CO})_2(\text{acac})$  (Figure 4.7). The

olefin insertion step is reversible at higher temperatures and at low partial pressures of CO or H<sub>2</sub>, in case of the formation of the *iso* aldehyde, while these parameters do not affect the olefin insertion in the formation of the normal product. It is therefore expected that the regioselectivity to the *iso* aldehyde be affected adversely under these conditions<sup>30</sup>, which was also observed in our study.



**Scheme 4.2.** A plausible mechanism for rhodium catalyzed MVN hydroformylation to 2-MNP and 3-MNP



#### 4.8. Liquid Phase Oxidation of 2-MNP

2-MNP, the hydroformylation product was oxidized to *dl*-naproxen using the  $\text{Na}_2\text{WO}_4$ , tetrabutyl ammonium hydrogen sulphate (TBAHS) catalyst system and  $\text{H}_2\text{O}_2$  oxidant. A few preliminary experiments were carried out to investigate the roles of the catalyst and the promoter. To assess the activity of the tungstate catalyst, a few other catalysts were also screened at the same experimental conditions. The effect of different parameters on conversion of aldehyde and selectivity to naproxen was investigated to optimize the reaction conditions and parameters. The effect of catalyst concentration, 2-MNP concentration, and  $\text{H}_2\text{O}_2$  concentration on conversion of 2-MNP and selectivity of *dl*-naproxen has been studied in the temperature range of 273 to 303K.

The oxidation of organic substrates by tungstate catalysts is known to proceed via a peroxy-complex intermediate.<sup>31</sup> Such type of complexes of transition metals like molybdenum, vanadium and especially tungsten etc, particularly heterogenized on supports like hydrotalcites or resins, in their highest oxidation states are known to be excellent oxidation catalysts for the oxidation of benzylic and secondary alcohols<sup>32,33</sup> epoxidation of olefins,<sup>34</sup> oxidative bromination<sup>35,36</sup> of phenols etc. Although reagent-based oxidation of aldehydes has been extensively studied, there are scanty reports on the catalytic oxidation of complex substituted aldehydes.

The material balance and reproducibility of the experiments was confirmed by taking a few experiments in which the amount of 2-MNP consumed and products formed were compared with experiments for higher conversion of 2-MNP. The concentration time profile of oxidation of 2-MNP is as shown in Figure 4.19. It was observed that the prominent byproduct of the reaction was 2-acetyl-6-methoxynaphthalene (2-AMN), which was confirmed by GCMS analysis.

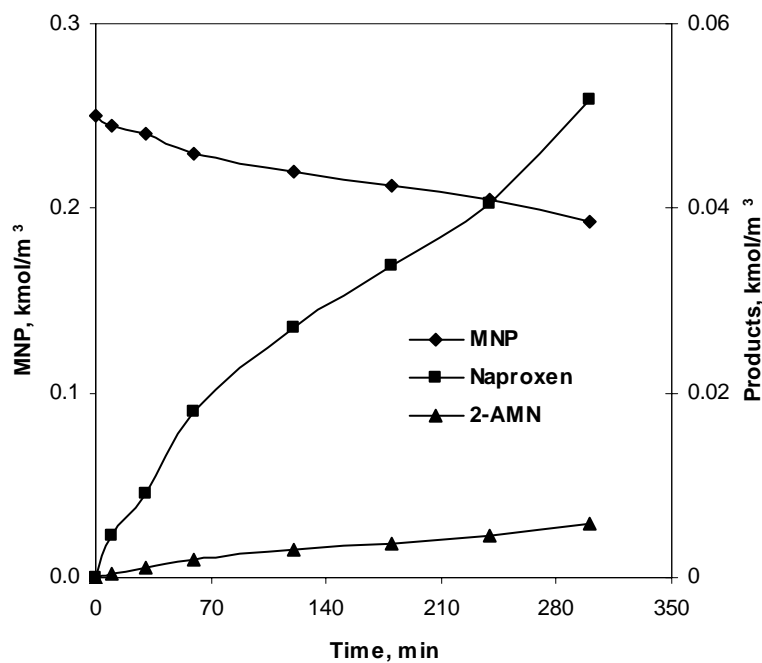


**Figure 4.19.** Concentration time profile of oxidation of 2-MNP

**Reaction conditions:** MNP,  $24.7 \times 10^{-2} \text{ kmol/m}^3$ ; catalyst,  $0.010 \text{ kmol/m}^3$ ; TBAHS,  $0.010 \text{ kmol/m}^3$ ;  $\text{H}_2\text{O}_2$ ,  $0.250 \text{ kmol/m}^3$ ; MEK, up to  $5 \times 10^{-6} \text{ m}^3$  total volume; temperature, 298K; agitation, 16.6 Hz; time, 6 hours; a- reaction in absence of TBAHS.

#### 4.8.1. Preliminary Studies

The screening of different lower transition metals like sodium tungstate, sodium molybdate, sodium vanadate, phosphotungstic acid, phosphomolybdic acid as catalysts was carried out. The results of the screening study are presented in the Table 4.8.

It was observed that the sodium tungstate gave the best conversion of 2-MNP, and high selectivity to the acid. However, the reaction did not proceed in absence of the promoter- TBAHS, as can be noticed from Table 4.8 (entry 1). Although there are several reports on the oxidation of substrates like olefins and alcohols using halide salts as phase transfer catalysts, the use of a halogen-free phase transfer is rewarding, as the corrosive halogens are avoided. Sato and co worker have reported the oxidation of terminal olefins with tungstate catalyst and in the presence of acidic PTCs like alkyl ammonium hydrogen

sulfates<sup>37</sup>. The authors have actually reported lowering of activity when conventional halide-containing PTCs were used instead of alkyl ammoniumhydrogen sulfates.

**Table 4.8.** Screening of catalysts

| Sr             | Catalyst  | 2-MNP<br>Conversion, % | Selectivity, % |       |
|----------------|---|------------------------|----------------|-------|
|                |   |                        | Naproxen       | 2-AMN |
| 1 <sup>a</sup> | Na <sub>2</sub> WO <sub>4</sub> .2H <sub>2</sub> O                    | Trace                  | -              | -     |
| 2              | Na <sub>2</sub> WO <sub>4</sub> .2H <sub>2</sub> O                    | 19.3                   | 82.3           | 12.2  |
| 3              | Na <sub>2</sub> MoO <sub>4</sub> .2H <sub>2</sub> O                   | 6.7                    | 52.3           | 45.2  |
| 4              | NaVO <sub>3</sub>   | 9.3                    | 56.5           | 40.2  |
| 5              | H <sub>3</sub> PO <sub>4</sub> .12WO <sub>3</sub> .xH <sub>2</sub> O  | 4.2                    | 71.2           | 24.7  |
| 6              | H <sub>3</sub> PO <sub>4</sub> .12MoO <sub>3</sub> .xH <sub>2</sub> O | 2.6                    | 66.7           | 28.2  |

**Reaction conditions:** MNP,  $10.7 \times 10^{-2}$  kmol/m<sup>3</sup>; catalyst, 0.010 kmol/m<sup>3</sup>; TBAHS, 0.010 kmol/m<sup>3</sup>; H<sub>2</sub>O<sub>2</sub>, 0.250 kmol/m<sup>3</sup>; MEK, up to  $5 \times 10^{-6}$  m<sup>3</sup> total volume; temperature, 298K; agitation, 16.6 Hz; time, 6 hours; a- reaction in absence of TBAHS.

The solubility of the aldehyde 2-MNP in common organic solvents was found to be less, and this was the constraint in studying the solvent variation effect. In the permanganate oxidation of analogous aldehydes, Barner and coworker<sup>38</sup> have used a polar solvent like acetone. However, the aldehyde under present study, i.e. 2-MNP, was found to be soluble in the desired concentrations only in ethyl acetate and MEK. It was found that the reaction did not proceed well in ethyl acetate, which was not surprising, because hydrogen peroxide forms a separate phase in the reaction mixture. Therefore, MEK has to be used as the solvent.

#### 4.8.2. Sodium Tungstate Concentration Effect

The screening of catalyst showed that sodium tungstate is highly selective and active catalyst for the oxidation of 2-MNP. The effect of sodium tungsten concentration was studied in the range 0.005 to 0.020 kmol/m<sup>3</sup> at the temperature of 298K. It was observed that increase in catalyst concentration increases the conversion of 2-MNP with marginal decrease in the selectivity to naproxen. The highest conversion of 2-MNP

achieved under the optimized reaction conditions was 23.1%, with a high selectivity of 80.7% to *dl*-naproxen. The results are illustrated in Table 4.9.

**Table 4.9.** Effect of sodium tungstate concentration

| <b>Na<sub>2</sub>WO<sub>4</sub>.2H<sub>2</sub>O,<br/>kmol/m<sup>3</sup></b> | <b>2-MNP Conversion,<br/>%</b> | <b>Selectivity, %</b> |              |
|---|--------------------------------|-----------------------|--------------|
|   |                                | <b>Naproxen</b>       | <b>2-AMN</b> |
| 0.005   | 5.5                            | 81.2                  | 18.6         |
| 0.01  | 19.3                           | 82.3                  | 12.2         |
| 0.02  | 23.1                           | 80.7                  | 19.1         |

**Reaction conditions:** MNP,  $10.7 \times 10^{-2}$  kmol/m<sup>3</sup>; TBAHS, 0.010 kmol/m<sup>3</sup>; H<sub>2</sub>O<sub>2</sub>, 0.250 kmol/m<sup>3</sup>; MEK, up to  $5 \times 10^{-6}$  m<sup>3</sup> total volume; temperature, 298 K; agitation, 16.6 Hz; time, 6 hours.

#### 4.8.3. TBAHS Concentration Effect

To optimize the concentration of TBAHS, the reactions were carried out at 298K, using different TBAHS concentration in the range of 0.005 to 0.021 kmol/m<sup>3</sup>. The results of the TBAHS concentration effect are presented in Table 4.10. The activity as well as selectivity was found to increase with increase in the concentration of TBAHS.

**Table 4.10.** Oxidation of 2-MNP: effect of TBAHS concentration

| <b>TBAHS,<br/>kmol/m<sup>3</sup></b> | <b>2-MNP Conversion,<br/>%</b> | <b>Selectivity, %</b> |              |
|--------------------------------------|--------------------------------|-----------------------|--------------|
|                                      |                                | <b>Naproxen</b>       | <b>2-AMN</b> |
| 0.005                                | 15.2                           | 60.1                  | 36.2         |
| 0.010                                | 19.3                           | 82.3                  | 12.2         |
| 0.021                                | 21.6                           | 85.3                  | 14.0         |

**Reaction conditions:** MNP,  $10.7 \times 10^{-2}$  kmol/m<sup>3</sup>; Na<sub>2</sub>WO<sub>4</sub>.2H<sub>2</sub>O, 0.010 kmol/m<sup>3</sup>; H<sub>2</sub>O<sub>2</sub>, 0.250 kmol/m<sup>3</sup>; MEK, up to  $5 \times 10^{-6}$  m<sup>3</sup> total volume; temperature, 298 K; agitation, 16.6 Hz; time, 6 hours

#### 4.8.4. H<sub>2</sub>O<sub>2</sub> Concentration Effect

The effect of concentration of H<sub>2</sub>O<sub>2</sub> on the conversion of 2-MNP and selectivity to *dl*-naproxen was studied in the concentration range 0.12 to 0.5 kmol/m<sup>3</sup>. It was observed that the conversion of 2-MNP increases with increase in the concentration of H<sub>2</sub>O<sub>2</sub>, while the selectivity to naproxen remains unaffected, as shown in Table 4.11.

**Table 4.11.** Oxidation of 2-MNP: effect of H<sub>2</sub>O<sub>2</sub> concentration

| H <sub>2</sub> O <sub>2</sub> , kmol/m <sup>3</sup> | 2-MNP Conversion,<br>% | Selectivity, % |       |
|---|------------------------|----------------|-------|
|   |                        | Naproxen       | 2-AMN |
| 0.12  | 10.8                   | 78.3           | 14.2  |
| 0.25  | 19.3                   | 82.3           | 12.2  |
| 0.5   | 24.1                   | 80.5           | 18.2  |

**Reaction conditions:** MNP, 10.7 X 10<sup>-2</sup> kmol/m<sup>3</sup>; Na<sub>2</sub>WO<sub>4</sub>.2H<sub>2</sub>O, 0.010 kmol/m<sup>3</sup>; TBAHS, 0.010 kmol/m<sup>3</sup>; MEK, up to 5X10<sup>-6</sup> m<sup>3</sup> total volume; temperature, 298 K; agitation, 16.6 Hz; time, 6 hours.

#### 4.8.5. 2-MNP Concentration Effect

The effect of 2-MNP concentration on the conversion and product selectivity was studied over a range of 2-MNP concentration of 0.05- 0.22 kmol/m<sup>3</sup> at the temperature of 298 K. Increase in the rate of reaction was observed with the increase in 2-MNP concentration (7.86x10<sup>-7</sup> to 1.93x10<sup>-6</sup> kmol/m<sup>3</sup>/s) with marginal increase in the selectivity to naproxen. The results are shown in Table 4.12.

**Table 4.12.** Oxidation of 2-MNP: effect of MNP concentration

| MNP, kmol/m <sup>3</sup> | 2-MNP Conversion,<br>% | Selectivity, % |       |
|--------------------------|------------------------|----------------|-------|
|                          |                        | Naproxen       | 2-AMN |
| 0.05                     | 28.3                   | 70.6           | 26.5  |
| 0.107                    | 19.3                   | 82.3           | 13.6  |
| 0.22                     | 15.8                   | 84.3           | 15.1  |

**Reaction conditions:** Na<sub>2</sub>WO<sub>4</sub>.2H<sub>2</sub>O, 0.010 kmol/m<sup>3</sup>; TBAHS, 0.010 kmol/m<sup>3</sup>; H<sub>2</sub>O<sub>2</sub>, 0.250 kmol/m<sup>3</sup>; MEK, up to 5X10<sup>-6</sup> m<sup>3</sup> total volume; temperature, 298 K; agitation, 16.6 Hz; time, 6 hours.

#### 4.8.6. Effect of Temperature

The effect of temperature on both 2-MNP conversion and product selectivities in oxidation of 2-MNP was studied in the temperature range of 273 – 308 K and the results are presented in the Table- 4.13. It was found that the conversion of 2-MNP increases from 6 to 15.8 % with increase in the temperature from 273 – 308 K. However, the selectivity to the carboxylic acid, *dl*-naproxen is decreased from 85.6 to 60.8%, but the selectivity of 2-acetyl-6-methoxynaphthalene increased with increasing reaction temperature. The result clearly indicates that although the 2-MNP conversion is increased significantly with increasing temperature, but at the same time the selectivity to naproxen is decreased.

In the concentration variation studies, best results were obtained at a substrate concentration of 0.107 kmol/m<sup>3</sup>, a catalyst concentration of 0.01 kmol/m<sup>3</sup>, and the oxidant: substrate ratio of 1.5

**Table 4.13.** Oxidation of 2-MNP : Effect of temperature

| Temperature, K | 2-MNP Conversion,<br>% | Selectivity, % |       |
|----------------|------------------------|----------------|-------|
|                |                        | Naproxen       | 2-AMN |
| 273            | 6.0                    | 85.6           | 14.5  |
| 298            | 19.3                   | 82.3           | 13.6  |
| 308            | 23.8                   | 70.8           | 28.7  |

**Reaction conditions:** MNP,  $10.7 \times 10^{-2}$  kmol/m<sup>3</sup>; Na<sub>2</sub>WO<sub>4</sub>·2H<sub>2</sub>O, 0.010 kmol/m<sup>3</sup>; TBAHS, 0.010 kmol/m<sup>3</sup>; H<sub>2</sub>O<sub>2</sub>, 0.250 kmol/m<sup>3</sup>; agitation, 16.6 Hz; time, 6 hours.

#### 4.9. Conclusions

Hydroformylation of MVN using homogeneous Rh complex catalysts with dppe as ligand has been studied with the objective of exploring it as the key step in naproxen synthesis. Hydroformylation of MVN followed by oxidation of Hydroformylation product 2-MNP provides an economical and environmentally benign catalytic route for the synthesis of naproxen. Hydroformylation of MVN using Rh(CO)<sub>2</sub>(acac) as a catalyst showed the following trends:

1. Among the Rh complexes screened  $\text{Rh}(\text{CO})_2(\text{acac})$  was found to be the best catalyst for Hydroformylation of MVN
2. Bidentate ligands like dppe, dppp, dppe etc was found to give very high selectivity to branched isomers.
3. Polarity of the solvents was found to have significant effect on the catalytic activity and selectivity; MVN has very less solubility in non-polar solvents. Increase in catalytic activity was observed with increasing polarity of solvents.

Kinetics of Hydroformylation of MVN was studied using  $\text{Rh}(\text{CO})_2(\text{acac})$  as catalyst and dppe as ligand in the temperature range of 353-373 K. Five different rate models were considered and an appropriate rate model was suggested for this reaction. Kinetic study of Hydroformylation of MVN revealed that the reaction was first order with respect to catalyst, substrate and  $\text{H}_2$  concentration. The rate Vs partial pressure of CO showed a substrate-inhibited kinetics at higher CO partial pressure. Activation energies for *iso* and *n*-aldehyde were evaluated as 13.24 and 31.02 kcal/mol.

2-MNP, the hydroformylation product was oxidized to *dl*-naproxen with high yields, using the  $\text{Na}_2\text{WO}_4$ - tetrabutyl ammonium hydrogen sulphate (TBAHS) catalyst system and  $\text{H}_2\text{O}_2$  oxidant. In the present study, oxidation of 2-MNP was studied using  $\text{Na}_2\text{WO}_4$ - TBAHS catalyst system and green oxidant like  $\text{H}_2\text{O}_2$ . The 2-MNP thus obtained could be oxidized under mild conditions in a facile manner using the sodium tungstate- TBAHS catalyst system, and hydrogen peroxide, to yield the racemic naproxen with high selectivity. The present study elucidates the potential application of the hydroformylation-oxidation route for production of naproxen.

## Nomenclature

|                |   |
|----------------|---|
| A              | Concentration of hydrogen, kmol/m <sup>3</sup>  |
| B              | Concentration of carbon monoxide, kmol/m <sup>3</sup>                                     |
| C              | Concentration of catalyst, kmol/m <sup>3</sup>  |
| D              | Concentration of camphene, kmol/m <sup>3</sup>  |
| H              | Henry constant defined by equation 4.4  |
| $k_1, k_2$     | Intrinsic rate constants, m <sup>3</sup> /kmol  |
| $k_2$          | Constant in Eq. 4.9 m <sup>3</sup> /kmol  |
| P <sub>f</sub> | Final pressure MPa  |
| P <sub>i</sub> | Initial pressure MPa  |
| R              | Universal gas constant, kJ/kmol/K   |
| r              | Rate of hydroformylation, kmol/m <sup>3</sup> /s.   |
| $R'_{Ai}$      | Experimental rates, kmol/m <sup>3</sup> /s  |
| $R_{Ai}$       | Predicted rates, kmol/m <sup>3</sup> /s   |
| R <sub>i</sub> | Reaction rate for the hydroformylation step (kmol/m <sup>3</sup> /s)                      |
| t              | Reaction time, h.   |
| T              | Temperature, K  |
| V <sub>g</sub> | Gas volume, m <sup>3</sup>  |
| V <sub>L</sub> | Total liquid volume, m <sup>3</sup>   |
| X <sub>a</sub> | Solubility of gas of the solute gas at pressure P <sub>f</sub> , kmol/m <sup>3</sup> /MPa |
| Φ              | Parameter defined by Eq-4.8   |



## References

---

1. P.J. Harrington, Lodewijk E., *Org. Process Res. Dev.* 1 (1997), 72.
2. P.M. Akbarali, R.K.K Vijaya, R.S. Gani, S. Krishna, S. Venkatraman, M. Mahalinga, US 7084299 2006.
3. S. Jayasree, A. Seayad, R.V. Chaudhari, *Org. Lett.* 2, (2000) 203.
4. V. Elango, M.A. Murphy, B.L. Smith, K.G. Davenport, G.N. Mott, G.L. Moss, US 4981995 1991
5. I.T. Harrison, B.Lewis, P. Nelson, W. Rooks, A. Roszkowski, A. Tomolonis, J.H. Fried, *J. Med. Chem.* 13 (1970), 203.
6. C. Giordano, G. Castaldi, S. Cavicchioli, M. Villa, *Tetrahedron* 45 (1989) 4243.
7. T. Ohta, H. Takaya, M. Kitamura, K. Nagai, R. J. Noyori, *Org. Chem.* 52 (1987) 3174.
8. J. Crosby, *Tetrahedron* 47 (1991) 4789.
9. J. K. Stille, H. Su, P. Brechot, G. Parinello, L. S. Hegedus, *Organometallics*, 10 (1991) 1183. (b) J. E. Babin, G. T. Whiteker, WO 9303839 1993
10. V.S. Nair, S.P. Mathew, R. V. Chaudhari *J. Mol. Catal. A: Chemical*, 143 (1999) 99.
11. Inmaculada del R y'o, Oscar Pa`mies , Piet W.N.M. van Leeuwen, Carmen Claver, J. *Organomet. Chem.* 608 (2000) 115
12. B. El Ali, J. Tijani, M. Fettouhi, M. El-Faer, A. Al-Arfaj, *App. Catal. A: General* 283 (2005) 185.
13. T. Fuchikami, I. Ojima, *J. Am. Chem. Soc.* 104 (1982) 3527.
14. B. A. Barner, J. J. Kurland, WO 9714669, (1997)
15. G. Strukul, Kluwer, Dordrecht (1992)
16. R. Curci, J.O. Edwards, Kluwer, Dordrecht (1992)
17. D. F. Furria, G. Modena, *Rev. Chem. Intermed.* 6 (1985) 51.
18. Y.S. Varshavskii, T.G. Cherkasova, *Russ. J. Inorg. Chem.* 12 (1967) 899.
19. Y. S. Varshavskii, T. G. Cherkasova, *Russ. J. Inorg. Chem.* 12 (1967) 899
20. J. Chatt, L. M. Venanzi, *J. Chem. Soc. A: Chem* (1957) 4735
21. D. Evans, J. Osborn, G. Wilkinson, *J. Chem. Soc. A: Chem* (1968) 3133
22. R. Lazzaroni, A. Raffaelli, R. Settambolo, S. Bertozzi, G. Vitulli *J. Mol. Catal.* 60 (1989) 1.

- 
23. G. Parrinello, J. K. Stille, *J. Am. Chem. Soc.* 109 (1987) 7122.
  24. R. M. Deshpande, B. M. Bhanage, S. S. Divekar, S. Kanagasabapathy and R. V. Chaudhari, *Ind. Eng. Chem. Res* 1998, 37, 2391
  25. R. V. Chaudhari, R. V. Gholap, G. Emig, H. Hofmann, *Can. J. Chem.* 65 (1987) 744.
  26. R. M. Deshpande, R. V. Chaudhari *Ind. Eng. Chem. Res.* 27 (1988) 1996.
  27. R. Lazzaroni, A. Raffaelli, R. Seitambolo, S. Bertozzi, G. Vitulli *J. Mol. Catal.* 60 (1989) 1.
  28. Piet W. N. M. Van Leeuwen, C. P. Casey, G. T. Whiteker in *Rhodium Catalyzed Hydroformylation*, Kluwer Academic Publishers Chapter 4, pp. 83.
  29. A. Castellanos-Páez, S. Castellón, C. Claver, P. W. N. M. van Leeuwen, W. G. J. de Lange, *Organometallics* 17 (1998) 2543.
  30. R. Lazzaroni, A. Raffaelli, R. Settambolo, S. Bertozzi and G. Vitulli, *J. Mol. Catal.*, 60 (1989) 1.
  31. R.A. Sheldon, I.W.C.E. Arends, A. Dijkman, *Catalysis Today* 57 (2000) 157.
  32. B. M. Choudary, B. Bharathi, C. Venkat Reddy, M. Lakshmi Kantam, *J. Chem. Soc. Perkin. Trans.*, 1 (2002) 2069.
  33. B. F. Sels, D. E. De Vos, P. A. Jacobs, *Angew. Chem. Chem. Int. Ed.*, 44 (2005) 310.
  34. D. Hoegaerts, B.F. Sels, D. E. de Vos, F. Verpoort, P. A. Jacobs, *Catal. Today* 60 (2000) 209.
  35. B. F. Sels, D. E. De Vos, P. A. Jacobs, *J. Am. Chem. Soc.*, 123 (2001) 8350.
  36. B. Sels, D. De Vos, M. Buntinx, F. De Ric Pierard, A. Kirsch-DeMesmaeker, P. Jacobs, *Nature* 400 (1999) 855.
  37. K. Sato, M. Aoki, M. Ogawa, T. Hashimoto, R. Noyori, *J. Org. Chem.* 61 (1996) 8310.
  38. B. A. Barner, J. J. Kurland, US 5739385 (1998).

## Chapter 5

# Hydroformylation of Vinyl Acetate Monomer As a Potential Route for the Synthesis of Hydroxy Propionic Acids

Hydroformylation of Vinyl acetate monomer (VAM) using homogeneous  $\text{Co}_2(\text{CO})_8$  as a catalyst followed by oxidation of the products, 2-acetoxy propanal (2-ACPAL) and 3-acetoxy propanal (3-ACPAL), which after hydrolysis gives 2- and 3-hydroxy propionic acids (HPA) has been studied as an alternative route for the synthesis of 2- and 3-hydroxy propionic acids. The feasibility of the VAM hydroformylation route for hydroxypropionic acids has been demonstrated, and a detailed study has been reported on the key hydroformylation step. The role of the catalyst, solvents and the effect of reaction conditions on the reaction rate and regioselectivity of the products have been investigated. Using  $\text{Co}_2(\text{CO})_8$  as a catalyst, ~98% selectivity to acetoxy propanals (ACPALS) has been achieved. A possible mechanism to explain the variation in regio-selectivity with  $\text{Co}_2(\text{CO})_8$  as catalyst has also been discussed. Kinetics of the hydroformylation step has been investigated and a rate equation proposed. The second step in the proposed route, i.e. oxidation of ACPALS to acetoxy propionic acids (ACPAs), has been studied using supported cobalt catalyst and molecular oxygen as the oxidant in a non-acidic medium with >95% conversion of ACPALS and >98% selectivity to ACPAs. Kinetics of the liquid phase oxidation of 2-ACPAL has been investigated and a rate equation proposed. The third step in the proposed route is hydrolysis of ACPAs to hydroxy propionic acids (HPAs) has been studied using solid acid catalysts, the best performance for the hydrolysis step with >90% selectivity to HPAs was observed. This study would be valuable in developing a new environmentally benign route for HPAs synthesis.

## 5.1. Introduction

2-hydroxy propionic acid (2-HPA) and 3-hydroxy propionic acid (3-HPA) known for almost 2000 years have been produced for only a century on an industrial scale<sup>1</sup>. 2-HPA, more popularly known as lactic acid, is important commercially in baking industry, cheese industry, pharmaceutical industry, cosmetic industry and shows assorted applications in dyeing wool and to make plasticizers for resin.<sup>2</sup> 2-HPA has become increasingly important especially in the polymer industry and as a preservative and stabilizer in fat reduced food products. Polylactide polymers have recently been synthesized from 2-HPA, for their further application in the synthesis of biodegradable polymers, which has been the first among the commercial applications of 2-HPA in the manufacture of this important class of polymers. 3-HPA has a wide range of applications in polymer industry for the synthesis of different acrylic polymers, acrylic esters, polyesters and in food industry.<sup>3,4</sup>

There are two commercial methods for the production of 2-HPA, a) fermentation of molasses, and b) Hydrocyanation of acetaldehyde followed by the hydrolysis of cyanohydrin produced. Both commercial processes produce racemic 2-HPA, of which the resolution is carried out separately since only L-2-HPA is useful in polylactide synthesis. Fermentation of molasses is the preferred and most common route, owing to cheap availability of molasses from sugar production. The fermentation is achieved on industrial scale in stirred tank bioreactors with low productivities. 2-HPA is separated from the lactate salts by addition of sulfuric acid and subsequent separation of the emerging gypsum. The gypsum has no further use and is an environmental threat to dispose off. Hydrocyanation of acetaldehyde and the subsequent hydrolysis of the cyanohydrin employ toxic HCN for cyanohydrin and the corrosive sulfuric acid for hydrolysis, which eventually leads to generation of stoichiometric amounts of salts. Thus, a need for a clean, atom efficient and environmentally compatible alternative route exists even today for the synthesis of 2-HPA. The current 3-HPA synthesis involves the biocatalytic route starting from glycerol or glucose, which also suffers from low reaction rates, high dilution and high process cost.

A novel catalytic route starting from vinyl acetate (which is industrially produced in large volumes from ethylene) has been proposed for 2-HPA. The first report describing

2-HPA synthesis by a three steps route *via* VAM appeared in 1978, in which VAM was hydroformylated to yield 2-acetoxy propanal using Rh(COD)(PPh<sub>3</sub>)<sub>2</sub> as a catalyst at 373K and 3.33 MPa synthesis gas pressure.<sup>5</sup> The intermediate aldehyde was then oxidized using cobalt or manganese catalysts with 0.2 MPa air pressure to yield 2-acetoxy propionic acid (2-ACPA) that was hydrolyzed to 2-HPA in 75% yield using acidic catalysts such as TsOH or H<sub>2</sub>SO<sub>4</sub>. The major drawback in this is the use of acetic acid as a solvent in hydroformylation and the oxidation steps, which reduces the chemo-selectivity of 2-ACPAL in hydroformylation step besides being corrosive. In another report, hydrocarbonylation of VAM to yield 2-ACPA using Pd-complex catalysts (373-473K, 0.6-6.9 MPa CO) was reported using [(allyl)PdCl<sub>2</sub>]<sub>2</sub> or Pd(OAc)<sub>2</sub>/ PPh<sub>3</sub> as a catalyst to achieve 96% conversion and 67% selectivity along with VAM hydrolysis products such as acetaldehyde and acetic acid.<sup>3</sup> During hydrocarbonylation reaction, hydrolysis of VAM is a predominant side reaction especially at higher ligand (PPh<sub>3</sub>/Pd ratio > 20) and water concentrations (> 0.9 wt%). A process for *dl*-2-HPA via alkoxy carbonylation of VAM to achieve methyl-2-acetoxypropionate using Pd, Rh and Ni catalysts at 373K and 6.9 MPa CO pressure; PdCl<sub>2</sub>(PPh<sub>3</sub>)<sub>2</sub> being the most effective catalyst, giving the maximum yield (81.6%) of methyl-2-acetoxypropionate, whereas Rh and Ni catalysts were less active for alkoxy carbonylation. Methoxy carbonylation of VAM to yield methyl-2-acetoxypropionate in 62% yield with very low catalytic activity using palladium catalysts in presence of a base such as pyridine or pyridine derivatives was reported at severe operating conditions (373-423K, 15-25 MPa.)<sup>4</sup>, but the route from carbonylation of VAM has major drawbacks like low selectivity, difficulty in catalyst-product separation, and requirement of severe reaction conditions.

Boroley et al<sup>6</sup> have reported hydroformylation of VAM using Co<sub>2</sub>(CO)<sub>8</sub> as catalyst with high chemo selectivity to aldehydes. ~ 50% selectivity to normal aldehyde was achieved, where as previous literature report claim < 95 % regioselectivity to branch aldehyde using Rh as catalyst. Thus, the hydroformylation of VAM followed by oxidation of corresponding products provide an economic and environmentally benign catalytic route for the synthesis of precursors (2- and 3-ACPAs), which can be easily converted to 2-and 3- HPAs by hydrolysis, but clearly requires further improvement in the catalyst performance in all the three steps and environmental compatibility. Specific

literature on the understanding of parameters influencing the performance of these steps is also limited demanding further efforts to innovate new catalysts and optimize reaction conditions.

Hydroformylation of VAM is the key step in the synthesis of HPAs. The literature on hydroformylation of VAM shows that, the  $\text{Co}_2(\text{CO})_8$  catalyzed hydroformylation of VAM gives lower catalytic activity and also poor selectivity to ACPALs due to severe reaction conditions (373-423K, 15-25 MPa). However, cobalt catalysts are economical compared to the rhodium catalysts, and therefore, the  $\text{Co}_2(\text{CO})_8$  catalyzed VAM hydroformylation deserves a detailed investigation of the catalysis and reaction kinetics, which was the motivation of the present work.

In this chapter, a detailed study on the three-step hydroformylation-oxidation-hydrolysis route for the synthesis of 2- and 3- HPAs (Scheme 5.1) is investigated. Based on the results of these studies, a detailed kinetic analysis of the hydroformylation step is presented and a rate equation is proposed. In the second step, mixture of 2- and 3-HPAs was oxidized to 2- and 3-ACPAs with high yields using Co/C carbon as catalyst and air as an oxidant. In the third step, hydrolysis of the ACPAs was carried out using solid acid catalyst at mild reaction condition in high yields to 2- and 3-HPA. This study would be valuable in developing an environmentally benign route for the synthesis of HPAs.

## **5.2. Experimental**

### **5.2.1. Materials**

Cobalt (II) acetate, Cobalt (II) chloride,  $\text{Co}(\text{CH}_3\text{COO})_2 \cdot 4\text{H}_2\text{O}$ , and  $\text{RhCl}_3 \cdot x\text{H}_2\text{O}$ ; the ligands- phosphine, diphosphine, acetylacetonate (acac) etc were procured from Aldrich, USA or Fluka, Switzerland and used without further purification. The solvents toluene, chlorobenzene, MEK, NMP, ethyl acetate, methanol, ethanol, DMF were procured from SD Fine Chemicals, India or E-Merck-India and used after fresh distillation, drying and argon flushing. CO of 99.9 % purity (Matheson, USA) and  $\text{H}_2$  of 99 % purity (Industrial Oxygen Company, India) were used as received without further purification.  $\text{Co}_2(\text{CO})_8$  (Dicobalt octacarbonyl) was prepared in the laboratory by high pressure-high temperature technique described in section 5.2.4. Synthesis gas mixture with a CO: $\text{H}_2$  ratio of 1 was prepared in a reservoir and used for hydroformylation reactions.

### 5.2.2. General Experimental Procedure

All the hydroformylation reactions were carried out in a 50 ml Parr Autoclave made of stainless steel material (SS-316; maximum pressure capacity of 20.7 MPa at 548 K), having gas inlet, outlet, intermediate sampling valve, temperature controlled heating ( $\pm 1$  K) and variable agitation speed (0 - 33.3 Hz). As a safety precaution, a rupture disc (gold faced), which can withstand a maximum pressure of 20.7 MPa, was attached to the reactor. For experiments with  $\leq 7$  MPa pressure, gas was fed through a constant pressure regulator attached to the synthesis gas reservoir while for high pressure experiments, the reactor pressure was maintained by intermittent gas supply from the synthesis gas reservoir (at 1:1 ration of CO:H<sub>2</sub>), after every drop of  $\sim 0.2$  MPa reactor pressure. Synthesis gas reservoir was always maintained at a minimum 1.5 MPa higher than the reactor pressure. The reaction set-up used in the present study is shown in the Figure 5.1. Ice water-cooled condensers were used for intermediate sampling. For Co<sub>2</sub>(CO)<sub>8</sub>-catalyzed hydroformylation, maintaining synthesis gas atmosphere is very critical due to instability of Co<sub>2</sub>(CO)<sub>8</sub> at lower pressures.<sup>6</sup> In typical cobalt catalyzed hydroformylation experiment, the known quantities of the substrate, catalyst, and the solvent were charged into the autoclave. The contents were immediately flushed thrice with synthesis gas. The reactor was pressurized to  $\sim 2$  MPa synthesis gas, the solution was saturated by keeping agitation speed of  $\sim 16.6$  Hz for 2-3 minutes and then heating was started at a constant  $\sim 1.66$  Hz stirring. After attaining the desired temperature, the synthesis gas was made up to the required pressure from the reservoir and the reaction was initiated by increasing the agitation speed to 20 Hz. The pressure drop in the reservoir vessel was recorded by means of a pressure transducer (precision-  $\pm 0.0067$  MPa) as a function of time. Intermediate liquid samples were also taken at regular intervals of time. Unless otherwise mentioned, all the reactions were run till the synthesis gas absorption nearly stopped. The autoclave was thoroughly cooled to  $< 293$  K, synthesis gas was vented off, the reactor was flushed thrice with nitrogen and the reaction mixture removed. After every reaction, the reactor was cleaned thoroughly and a wash with 10 % HNO<sub>3</sub> was given to ensure the total removal of the metal particles. For solvent screening study, the VAM concentration and the total volume of the charge were kept constant. The analysis of the liquid samples was

carried out using GC to examine the product distribution pattern quantitatively. Details of GC analysis are given in the following section.

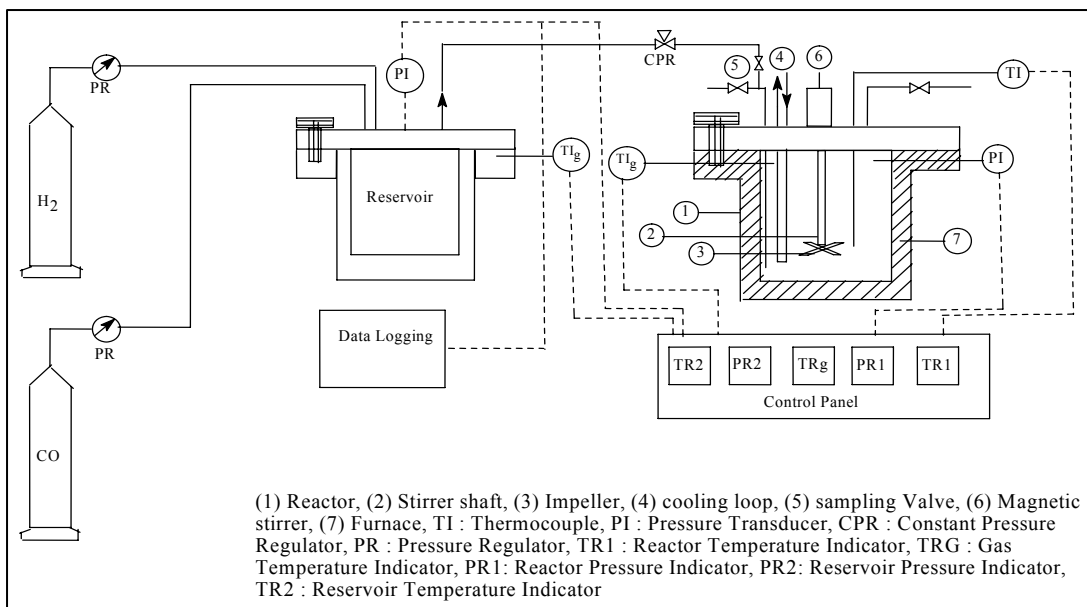


**Figure 5.1.** A schematic of the reactor setup for hydroformylation of VAM

### 5.2.3. Catalyst Recycle Procedure

After completion of a typical hydroformylation reaction, 10 ml of distilled water was added to the reactor through the intermediate addition device at 1.4MPa pressure under continuous agitation. The contents were further stirred under pressure for 15 minutes. After this, the gas was vented off. The reactor contents consisted of two distinctly separate layers- an aqueous layer and an organic layer. The organic phase consisting of the catalyst was recycled and the aqueous phase containing products were analyzed for the quantification of products. VAM was freshly added for the recycle experiments.

### 5.2.4. Synthesis of $\text{Co}_2(\text{CO})_8$

The synthesis of  $\text{Co}_2(\text{CO})_8$  was carried out in a 50 ml Parr Autoclave made of Hastelloy C-276, (Rating -maximum pressure 20.7 MPa at 548K) having facilities for gas inlet, outlet, intermediate sampling, temperature controlled heating and variable agitation



speed (0–33.3 Hz). As a safety precaution, a rupture disc (gold faced), with a capacity to withstand a maximum pressure of 20.7 MPa was fitted to the reactor.

Generally, the pressures required for  $\text{Co}_2(\text{CO})_8$  synthesis are in the range of 15.2–16.6 MPa at temperatures in the range of 463–473K. In view of the non-availability of gas-cylinders of such high pressures, we used a different technique to boost up the pressure. After charging the cobalt precursor ( $\text{CoCl}_2 \cdot 6\text{H}_2\text{O}$ ), and solvent to the reactor, the reactor was chilled down to 0–3 °C. At this low temperature, the reactor was pressurized to ~ 11.2 MPa with synthesis gas at a constant agitation of 20 Hz. The reactor was allowed to attain the room temperature and then heated to the desired temperature at constant stirring of 8 Hz. The reaction was started by increasing the stirring speed to 20 Hz. Due to large temperature gradient of ~ 463K, while attaining the temperature of 468K, the pressure increased to ~ 16.5 MPa. Even at this temperature and pressure, an induction period of ~ 20–40 minutes was observed. The induction period was found to vary with the  $\text{CO}:\text{H}_2$  ratio of the synthesis gas. All the reactions were conducted till the gas absorption stopped. After cooling the reactor to ~ 280–285K, it was depressurized slowly, flushed thrice with argon and the liquid contents were poured into a 100 ml beaker. The black particles obtained (if any) were weighed and discarded. The solvent was removed by purging argon through the reaction crude following which, shining dark-red crystals of  $\text{Co}_2(\text{CO})_8$  were obtained. These were immediately transferred into a high-pressure container under CO atmosphere. The Infra-red analysis (Figure 5.2) of the  $\text{Co}_2(\text{CO})_8$  prepared was found to be consistent with the reported spectra with a characteristic absorption band at  $1857 \text{ cm}^{-1} (\nu_{\text{CO}})$ .  $\text{Co}_2(\text{CO})_8$  is a red-violet colored, highly unstable compound soluble in organic solvents. Under ambient conditions, it decomposes to  $\text{Co}_4(\text{CO})_{12}$  and higher nuclearity clusters of Co. At slightly higher temperatures (~ 305K), it releases CO almost instantaneously. It has been reported<sup>7</sup> have reported that decomposition of  $\text{Co}_2(\text{CO})_8$  is an inverse second order with respect to CO concentration. Thus, to avoid decomposition of  $\text{Co}_2(\text{CO})_8$  to  $\text{Co}_4(\text{CO})_{12}$  (which is an irreversible reaction) it must be stored under positive CO pressures and at low temperatures (~ 273K).

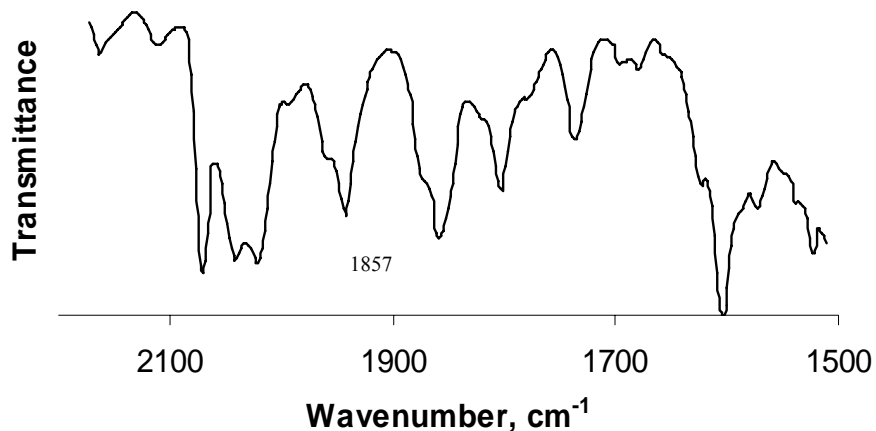


**Figure 5.2.** FTIR spectra of  $\text{Co}_2(\text{CO})_8$

### 5.2.5. Preparation of 3-acetoxy Propanal (3-ACPAL)

3-ACPAL required for analysis was prepared according to a procedure described by Ballard and co-workers<sup>8</sup>. Glacial acetic acid and acrolein in a mole ratio of 4.5:1 were mixed and heated in a glass-lined reactor for four hours at 402K. The mixture was then subjected to fractional distillation.

3-ACPAL is highly unstable and decomposes rapidly to acrolein and acetic acid. Acrolein, being an  $\alpha$ ,  $\beta$ -unsaturated aldehyde where a double bond and a carbonyl group are in conjugation, is more stable and so 3-ACPAL shows a tendency to decompose. So purification of 3-ACPAL through distillation was futile, as the purity of the distillate didn't exceed 80 %. Attempts to purify 3-ACPAL with column chromatography were also unsuccessful as it was decomposed on TLC plate as well as on the silica in a column. Therefore, the ~80 % pure 3-ACPAL was used as a standard by subtracting the quantities of acrolein and acetic acid with the help of pre-calibration of acrolein and acetic acid.

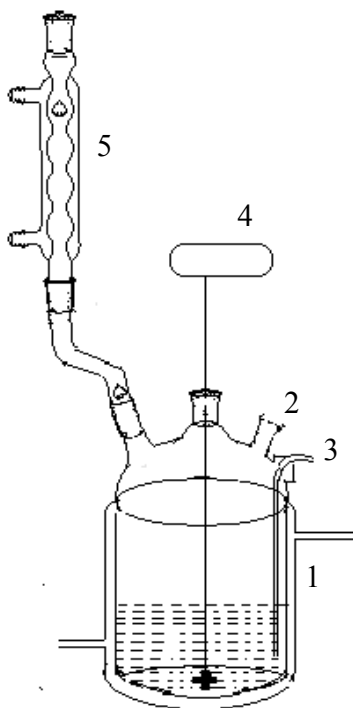
### 5.2.6. Preparation of 2-acetoxy Propanal (2-ACPAL)

2-ACPAL was prepared by hydroformylation of VAM using the conventional  $\text{Rh}(\text{CO})_2(\text{acac})$  as catalyst and  $\text{PPh}_3$  as ligand. The hydroformylation of VAM gave high regioselectivity (>98%) to 2-ACPAL. This reaction was carried out in a stainless steel Parr autoclave of 2-liter capacity, at 5.5MPa syngas pressure and at 373 K for 6 hours.

The product was separated by using vacuum distillation and nitrogen purging to get pure 2-ACPAL. The analysis was carried out using GC and found to get 97.3% purity of 2-ACPAL, which was then taken for the further studies.

### 5.2.7. Oxidation Experiments

Oxidation of ACPALs was carried out in a 50 ml jacketed glass reactor equipped with gas inlet sparger, condenser, thermo well and sampling port. Desired amounts of reaction mixture and catalyst were added to the reactor. The stirring was provided by using an overhead stirrer equipped with digital indicator for stirring speed measurement. A constant reaction temperature was maintained using a thermostat. The typical glass reactor setup used for the reaction is as shown in the Figure 5.3.

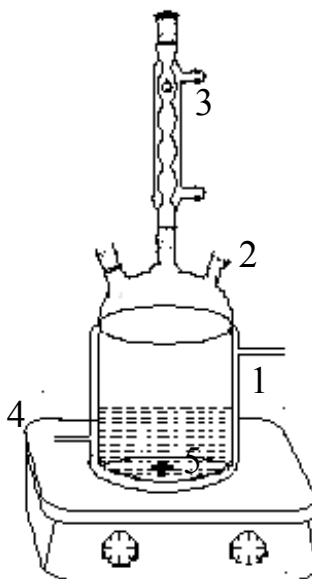


(1) Jacketed glass reactor (2) Sampling port (3) Gas Spurger (4) Overhead stirrer (5) Condenser

**Figure 5.3.** A schematic of reaction set-up for oxidation experiments

### 5.2.8. Hydrolysis Experiments

Hydrolysis of ACPAs was carried out in a 50 ml jacketed glass reactor equipped with thermo well, condenser, sampling port. The stirring was done by using magnetic stirrer as shown in the Figure 5.4. Desired amounts of ACPAs, water, and catalyst were added to the reactor and stirred at 353K for required time using a magnetic stirrer.



(1) jacketed glass reactor (2) Sampling port (3) Condenser (4) Magnetic stirrer (5) Magnetic needle

**Figure 5.4.** A schematic of reaction set-up for hydrolysis experiments

### 5.2.9. Analytical Methods

IR spectra were obtained using a Bio-rad FTS 175C spectrometer in transmission mode using KBr pellets as well as liquid cells. GC-MS analysis was carried out for identification of products on an Agilent GC of 6890N series equipped with 5973N Mass Selective Detector. Liquid reaction samples were analyzed on a Hewlett Packard 6890 Series GC controlled by the HP-Chemstation software and equipped with an auto sampler unit, by using a HP-1 capillary column (30 m x 30  $\mu\text{m}$  x 0.25  $\mu\text{m}$  film thickness with a stationary phase of polymethyl siloxane). The quantitative analysis was obtained by

constructing calibration curve in the range of concentrations studied. The conversion, chemo- and regio-selectivities of aldehydes and alcohols were calculated using the following formulae; and the results are discussed in terms of conversion, selectivity, turn over number (TON), turn over frequency (TOF), which are calculated as given below.

$$\text{Conversion, (\%)} = \frac{\text{Initial concentration of VAM} - \text{Final concentration of VAM}}{\text{Initial concentration of VAM}} \times 100$$

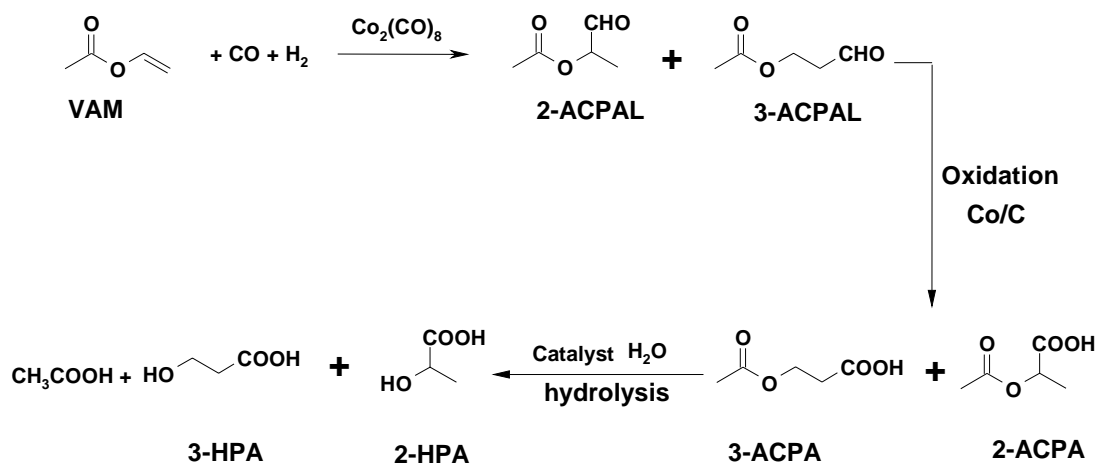
$$\text{Selectivity, (\%)} = \frac{\text{Number of moles a product formed}}{\text{Number of moles VAM converted}} \times 100$$

$$\text{TON} = \frac{\text{Number of moles of hydroformylation products formed}}{\text{Number of moles of catalyst}}$$

$$\text{TOF, (h}^{-1}\text{)} = \frac{\text{Number of moles of hydroformylation products formed}}{\text{Number of moles of catalyst} \times \text{time in hours}}$$

### 5.3. Results and Discussion

Hydroformylation-oxidation-hydrolysis route to HPAs involves the following reaction steps (Scheme 5.1): (1) Hydroformylation of VAM to the regio-isomers 2-ACPAL and 3-ACPAL, (2) Oxidation of the mixture of 2- and 3-ACPAL to 2- and 3-ACPA respectively, using molecular oxygen as the oxidant. (3) Hydrolysis of mixture of 2- and 3- ACPAs to 2- and 3-HPAs respectively. Tailoring the regioselectivity in hydroformylation step is the most important issue, and hence, hydroformylation step in this route is the key step, since the regioselectivity obtained in this step decides the overall yields of the 2- and 3-HPAs at the end of the process.



**Scheme 5.1.** Synthesis of hydroxy propionic acid

The important objectives of the work presented in this chapter are:

1. Evaluation of hydroformylation-oxidation-hydrolysis as an alternative route for selective synthesis of racemic 2-and3-HPA.
2. Hydroformylation of VAM;  $\text{Co}_2(\text{CO})_8$  as catalyst for achieving high regioselectivity to linear-aldehyde (3-ACPAL) and detailed kinetic investigation of VAM hydroformylation as the key step in the present study.
3. Screening of catalysts and optimization of reaction conditions for the oxidation of 2- and 3-ACPAL for achieving high yields of corresponding carboxylic acids. Also the detailed kinetic investigation of oxidation of 2-ACPAL to 2-HPA using molecular oxygen as oxidant.
4. Screening of catalysts and optimization of reaction conditions for the hydrolysis of 2- and 3-ACPA for achieving high yields of corresponding carboxylic acids.

These objectives have been achieved in the present study with detailed experimentation, and the results obtained are presented below in three separate sections Hydroformylation of VAM, oxidation of ACPALs and hydrolysis of ACPAs.

### 5.3.1 Hydroformylation Experiments

#### 5.3.1.1 Preliminary Experiments

The hydroformylation of VAM was studied as the key step in the synthesis of HPAs with the focus on understanding the activity of  $\text{Co}_2(\text{CO})_8$  catalyst, selectivity to ACPALs and reaction kinetics. It was essential to assess product distribution and material

balance in a few initial experiments. A typical concentration-time profile for VAM hydroformylation at 393K temperature and 5.51 MPa pressure of synthesis gas is as shown in Figure 5.5. Almost complete conversion of VAM was achieved in 3 hours and the material balance of CO or H<sub>2</sub> and VAM consumed was in good agreement with total amount of products formed. In the range of the conditions investigated, the major products formed were 2- and 3-ACPALs, while byproducts like acrolein and acetic acid were found in trace quantity (<2% on the basis of VAM consumed).

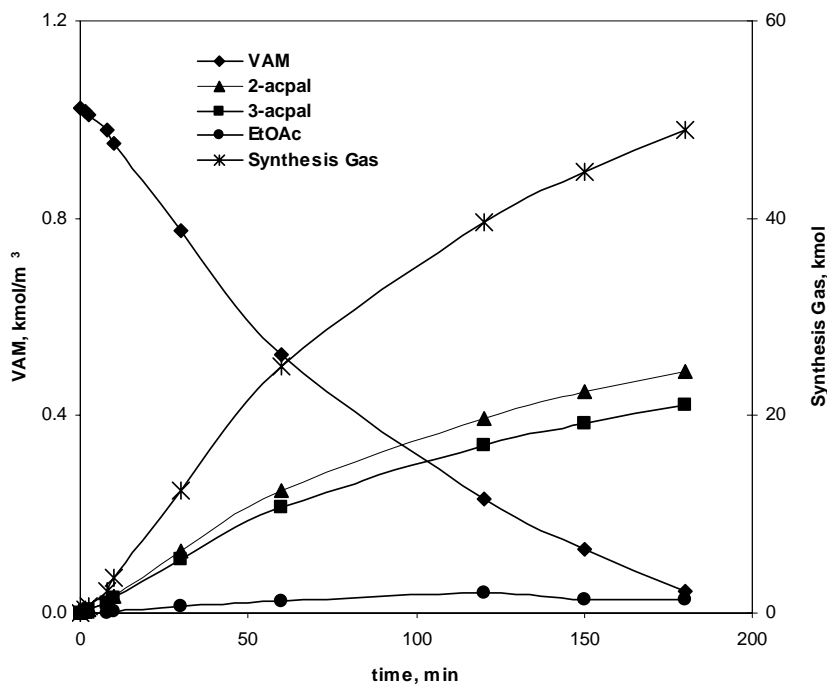


**Figure 5.5.** Concentration time profile of hydroformylation of VAM

**Reaction Conditions:** Co<sub>2</sub>(CO)<sub>8</sub>, 3.3X 10<sup>-4</sup> kmol/m<sup>3</sup>; VAM, 1.02 kmol/m<sup>3</sup>; temperature, 393K; agitation speed, 16.6 Hz, synthesis gas, 5.51 MPa; Solvent, Toluene; up to 2.5 X 10<sup>-2</sup> m<sup>3</sup> total volume

### 5.3.1.1.1 Effect of Synthesis Gas Pressure

The effect of synthesis gas pressure on the rate of hydroformylation of VAM was studied at a constant VAM concentration of 1.05 kmol/m<sup>3</sup> and a Co<sub>2</sub>(CO)<sub>8</sub> concentration of 5 × 10<sup>-4</sup> kmol/m<sup>3</sup> at the temperature of 393K. The results are shown in Figure 5.6. The conversion of VAM was found to increase with increase in total pressure of synthesis gas. An increase in the total synthesis gas pressure is expected to increase the effective concentration of the active catalytic species, i.e. HCo(CO)<sub>4</sub>, thereby increasing the rate of

hydroformylation. The n/iso ratio was found to increase marginally with increase in total pressure.

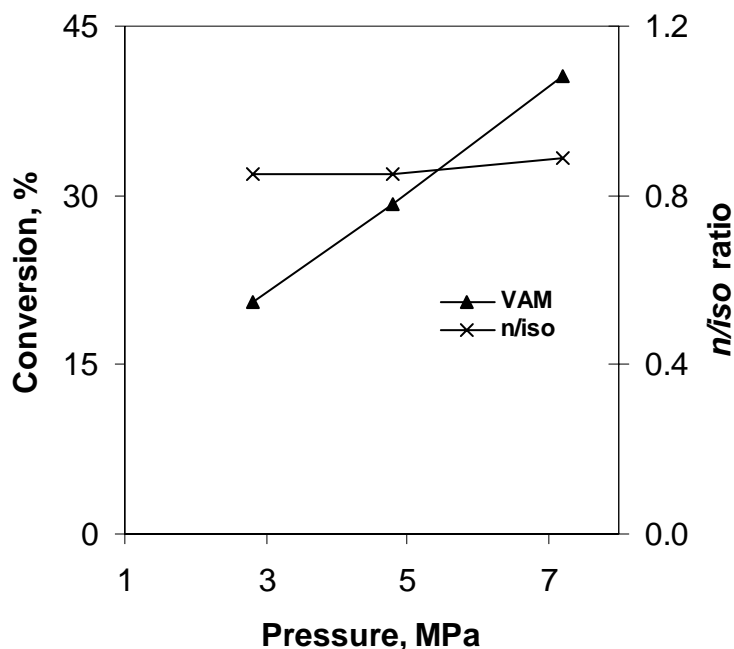


**Figure 5.6.** Effect synthesis gas pressure on conversion of VAM and selectivity to aldehydes

**Reaction Conditions:**  $\text{Co}_2(\text{CO})_8$ ,  $3.3 \times 10^{-4} \text{ kmol/m}^3$ ; VAM,  $1.05 \text{ kmol/m}^3$ ; temperature, 393K; agitation speed, 16.6 Hz; Solvent, Toluene; up to  $2.5 \times 10^{-2} \text{ m}^3$  total volume

#### 5.3.1.1.2 Effect of Temperature

The effect of temperature on the  $\text{Co}_2(\text{CO})_8$  catalyzed hydroformylation of VAM was investigated in the range of 353-393K by keeping other parameters constant. The rate of reaction was found to increase with temperature, upto 373K. Beyond this temperature, the reaction was found to proceed rapidly till the first 20 minutes of reaction time, and then stopped abruptly, and the absorption of synthesis gas ceased completely. A probable reason for the decomposition of the catalyst at higher temperature is the rate of absorption of synthesis gas for reaction being more than the rate of dissolution of synthesis gas into the reaction medium, thus causing the reaction to go into mass transfer limitation, thereby starving the sensitive  $\text{Co}_2(\text{CO})_8$  catalyst of CO. The reaction was very slow at 353K. When the reactions were carried out for longer time, formation of byproducts was



observed. Also, 3-ACPAL was decomposed to some extent, forming acetic acid and acrolein, thus leading to lower *n/iso* ratio. Acetic acid formed in the reaction at 353K, deactivated the catalyst by precipitating pink colored Co(OAc)<sub>2</sub>.

From the temperature effect experiments, the optimum range of temperatures was found to be 373 to 393K. It was observed that at 393K temperature, 50.1 % conversion of VAM with 96.2 % selectivity to aldehydes was obtained with an *n/iso* ratio of 0.85 (Table 5.1; entry 5).

**Table 5.1.** Hydroformylation of VAM: Effect of Temperature

| Sr | Reaction Time | Temp,<br>K | Conversion<br>% | Rate X 10 <sup>-4</sup><br>kmol/m <sup>3</sup> /s | Selectivity,% |        | <i>n/iso</i><br>ratio |
|----|---------------|------------|-----------------|---|---------------|--------|-----------------------|
|    | Min           |            |                 |   | Ald           | others |                       |
| 1  | 60            | 353        | 13.9            | 0.39  | 90.3          | 9.7    | 0.95                  |
| 2  | 60            | 363        | 25.3            | 0.72  | 92.1          | 7.9    | 0.92                  |
| 3  | 60            | 373        | 43.4            | 1.23  | 95.2          | 4.8    | 0.81                  |
| 4  | 60            | 383        | 50.2            | 1.42  | 95.9          | 4.1    | 0.86                  |
| 5  | 60            | 393        | 56.9            | 1.61  | 96.2          | 3.8    | 0.85                  |

**Reaction Conditions:** Co<sub>2</sub>(CO)<sub>8</sub>, 2.5X 10<sup>-4</sup> kmol/m<sup>3</sup>; VAM, 1.05 kmol/m<sup>3</sup>; agitation speed, 16.6 Hz, synthesis gas, 5.51 MPa; Solvent, Toluene; up to 2.5 X 10<sup>-2</sup> m<sup>3</sup> total volume

### 5.3.1.1.3 Screening of Solvents

It is well known that solvent plays a very important role in tailoring activity and selectivity in hydroformylation reaction. Cobalt catalyzed hydroformylation of VAM is a sensitive reaction, and shows considerable change in the activity-selectivity of the reaction on slight variation in the catalyst environment. With the aim to study the effect of solvents on hydroformylation of VAM, screening of halogenated and non-halogenated solvents was carried out. The results are presented in the Table 5.2.

The screening of solvents was carried out by keeping all reaction parameters constant. No reaction occurred in coordinating solvents such as dimethyl formamide, dimethyl acetamide, and acetonitrile. The final solution after these reactions was purple or green instead of usual saffron-red, which may be because of the coordination of the solvents with cobalt, forbidding the possibility of formation of the active hydrido carbonyl species. When the reaction was carried out in neat VAM, (solvent-less

conditions) (entry 1 Table 5.2), no reaction was observed. The reaction was very slow and could not proceed beyond 30 to 35% of VAM conversion (entry 2 and 3). When the reactions were carried out in hexane and cyclohexane, which are most commonly used solvents for the hydroformylation of olefins, the chemo-selectivity to aldehydes was >90%; but the regio-selectivity to 3-ACPAL was low. The solvents toluene and benzene were found to be effective for hydroformylation of VAM, in terms of activity as well as selectivity. In case of hydroformylation of VAM using toluene as solvent, >88% conversion of VAM and the selectivity to 2-ACPAL and 3-ACPAL was found to be 54.2 and 45.8 % respectively (entry 5), making the aldehyde selectivity 100%. Similar results were observed with benzene as solvent (entry 4). Halogenated solvents resulted in high reaction rates and high regioselectivity to 3-ACPAL (entries 6, 7), however, halogenated solvents are not preferred, especially for synthesis of bulk commodities, due to corrosion problems and environmental reasons. Thus from the screening of the solvents it is observed that toluene is the best solvent with high rates and high selectivity to 3-ACPAL.

**Table 5.2.** Screening of solvents

| Sr. | Solvents    | Conversion<br>, % | Rate X 10 <sup>-4</sup> ,<br>kmol/m <sup>3</sup> /s | Aldehyde Selectivity,<br>% |         | n/iso<br>ratio |
|-----|-------------|-------------------|---|----------------------------|---------|----------------|
|     |             |                   |   | 2-ACPAL                    | 3-ACPAL |                |
| 1   | VAM         | 0                 | 0.00  | 0                          | 0       | 0.00           |
| 2   | Hexane      | 28.3              | 0.80  | 70.1                       | 29.9    | 0.43           |
| 3   | Cyclohexane | 32.4              | 0.92  | 72.4                       | 27.6    | 0.38           |
| 4   | Benzene     | 86.4              | 2.45  | 52.1                       | 47.9    | 0.92           |
| 5   | Toluene     | 88.2              | 2.50  | 54.2                       | 45.8    | 0.85           |
| 6   | MCB         | 96.1              | 2.72  | 47.6                       | 52.4    | 1.10           |
| 7   | DCB         | 97.5              | 2.76  | 48.3                       | 51.7    | 1.07           |

**Reaction Conditions:** Co<sub>2</sub>(CO)<sub>8</sub>, 3.3X 10<sup>-4</sup> kmol/m<sup>3</sup>; VAM, 1.05 kmol/m<sup>3</sup>; temperature, 393K; agitation speed, 16.6 Hz, synthesis gas, 5.51 MPa; Solvent, up to 2.5 X 10<sup>-2</sup> m<sup>3</sup> total volume

#### 5.3.1.1.4. Catalyst Recycle Study

The high solubility of product ACPALs in water was helpful for effective separation of cobalt catalyst from the organic reaction mixture. The general method employed for catalyst separation was addition of water to the organic mixture and extracting out the ACPALs and unreacted VAM into the aqueous phase by stirring under synthesis gas pressure of 1.37 MPa. Synthesis gas pressure was found to be essential to save the catalyst from formation of cobalt-aqua complex.<sup>9</sup> The catalyst was recycled 5 times without loss of activity. The result of the catalyst recycle study is as shown in the Figure 5.7. Thus, the catalyst recycles and catalyst product separation was established

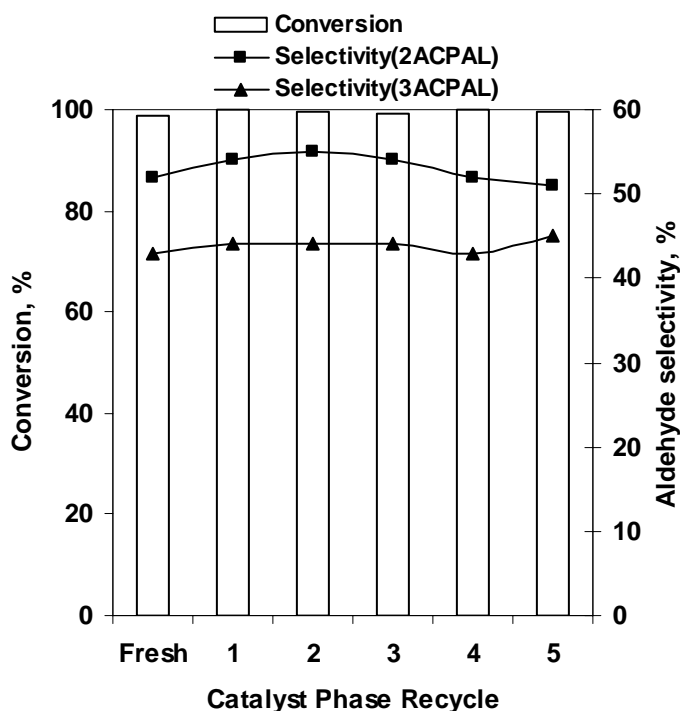


**Figure 5.7.** Hydroformylation of VAM: Study of catalyst recycle

**Reaction Conditions:**  $\text{Co}_2(\text{CO})_8$ ,  $3.3 \times 10^{-4} \text{ kmol/m}^3$ ; VAM,  $1.05 \text{ kmol/m}^3$ ; temperature, 393K; agitation speed, 16.6 Hz, synthesis gas, 5.51 MPa; Solvent, Toluene; up to  $2.5 \times 10^{-2} \text{ m}^3$  total volume

## **5.4. Kinetics of Hydroformylation of VAM**

A detailed kinetic investigation has been carried out for the  $\text{Co}_2(\text{CO})_8$  catalyzed hydroformylation of VAM in this chapter. There is no previous report on the intrinsic kinetics of hydroformylation of VAM using  $\text{Co}_2(\text{CO})_8$  as a catalyst. The knowledge of kinetics and development of rate equations is also important in understanding the mechanistic features of complex catalytic reactions. Such a study would be useful considering the industrial importance of this reaction in synthesis of HPAs. The effect of  $\text{Co}_2(\text{CO})_8$  concentration, VAM concentration and partial pressures of CO and  $\text{H}_2$  on initial rate of hydroformylation of VAM has been investigated in the temperature range of 373 - 393K.

### **5.4.1. Evaluation of Kinetic Regime**

#### **5.4.1.1. Effect of Agitation Speed**

For the study of intrinsic kinetics, it is essential that the reaction operate in the kinetic regime and not under the condition where mass transfer is controlling. For that purpose, the effect of agitation speed on the rate of reaction was studied. The results are presented in Figure 5.8. The rate was found to be independent of the agitation speed beyond 13.33 Hz, which clearly indicates that the reaction is in kinetic regime. Therefore, all the reactions for kinetic studies were carried out at an agitation speed of 20 Hz to ensure that the reaction occurred in the kinetic regime.

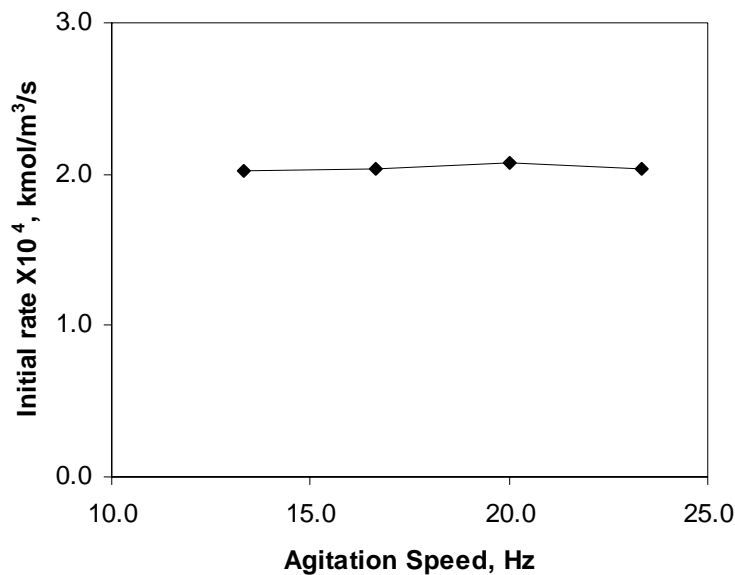


**Figure 5.8.** A plot of rate of hydroformylation of VAM vs. agitation speed  
**Reaction Conditions:**  $\text{Co}_2(\text{CO})_8$ ,  $3.3 \times 10^{-4} \text{ kmol/m}^3$ ; VAM,  $1.05 \text{ kmol/m}^3$ ; temperature, 393K; synthesis gas, 5.51 MPa; Solvent, Toluene; up to  $2.5 \times 10^{-2} \text{ m}^3$  total volume

#### 5.4.1.2 Solubility of $\text{H}_2$ and CO in Solvent

For interpretation of kinetic data, knowledge of the concentration of the gaseous reactants in the reaction medium is essential. The solubility of CO and  $\text{H}_2$  in toluene was determined experimentally at 373, 383 and 393K, by using a method due to Chaudhari and coworkers.<sup>10</sup> The solubility of  $\text{H}_2$  and CO is measured in  $6.0 \times 10^{-4} \text{ m}^3$  capacity stirred autoclave supplied by Parr Instrument Company, USA, designed for 25 MPa pressure. The equipment was provided with automatic temperature control and a pressure recording system. A pressure transducer having a precision of  $\pm 1 \text{ kPa}$  was used to measure the autoclave pressure.

In a typical experiment for the measurement of solubility of  $\text{H}_2$  and CO, a known volume of solvent was introduced into the autoclave and the contents were heated to a desired temperature. After a steady temperature reading was attained, the void space in the reactor was carefully flushed with a solute gas and pressurised to the level required. The contents were then stirred for about ten minutes to equilibrate the liquid phase with the solute gas. The change in the pressure in the autoclave was recorded on-line as a

function of time till it remained constant, indicating saturation of the liquid phase. From the initial and final pressure readings, the solubility was calculated in mole fraction as

$$X_a = \frac{(P_i - P_f)V_g M_s}{RTV_L \rho_s} \quad 5.1$$

Where,  $X_a$  represents the mole fraction of the solute gas in the liquid phase at the partial pressure of the solute gas prevailing at  $P_f$ ,  $P_i$  and  $P_f$  are the initial and final pressure readings in the autoclave,  $V_g$  and  $V_L$  are the volumes of the gas and liquid phases, respectively,  $R$  is the gas constant,  $T$  is the temperature,  $M_s$  is the molecular weight of the solvent and  $\rho_s$  is the molar density of the liquid. The Henry's law constant,  $H$  was calculated as

$$H = \frac{P_f}{X_a} \quad 5.2$$

The results are presented as Henry's law constant in Table 5.3

**Table 5.3.** Henry's law constant

| Temperature<br>K | $H_A$ for $H_2$<br>kmol/ m <sup>3</sup> /MPa | $H_A$ for CO<br>kmol/ m <sup>3</sup> /MPa |
|------------------|--|---|
| 373              | 22.25  | 10.22                                     |
| 363              | 23.50  | 10.60                                     |
| 353              | 24.60  | 10.90                                     |

#### 5.4.1.3 Mass Transfer Effects

The analysis of overall rate of reaction for two-phase (gas-liquid) catalytic reactions is given by Ramachandran et al<sup>11</sup>. The following criteria described by Ramachandran and Chaudhari<sup>20</sup> were used to check the significance of various mass-transfer effects.

### 5.4.1.3.1 Gas-liquid Mass Transfer Effect

The significance of gas-liquid mass transfer resistance was analyzed by comparing the initial rate of reaction and maximum possible rate of gas-liquid mass transfer. The gas-liquid mass transfer resistance is negligible if a factor  $\alpha_I$ , defined as follows, is less than 0.1 for the experimental conditions used.

$$\alpha_{1,A} = \frac{R_{\text{exp}}}{k_L a_B C_{A,aq.}} \quad 5.3$$

$$\alpha_{1,B} = \frac{R_{\text{exp}}}{k_L a_B C_{B,aq.}} \quad 5.4$$

Where,  $R_{\text{exp}}$  is the observed rate of hydroformylation ( $\text{kmol/m}^3$ ),  $k_L a_B$  the gas-liquid mass transfer coefficient and  $C_A$  and  $C_B$  represent the saturation solubility of reacting gases *i.e.*  $\text{H}_2$  and  $\text{CO}$  in equilibrium with the gas phase concentration at the reaction temperature ( $\text{kmol/m}^3$ ). The gas-liquid mass transfer coefficient ( $k_L a_B$ ) used in above equations was estimated by using a correlation (Equation 5.3) proposed by Chaudhari and coworkers<sup>12</sup> for a reactor similar to that used in this work for agitation speed of 1200 rpm.

$$k_L a_B = 1.48 \times 10^{-3} (N)^{2.18} \times (V_g / V_L)^{1.88} \times (d_I / d_T)^{2.1} \times (h_1 / h_2)^{1.16} \quad 5.5$$

The terms involved in above equation are described in Table-5.4 along with the respective values obtained from the reactor and charge used in the present case.

**Table 5.5.** Parameters used for  $k_{LA_B}$  calculations

| Parameter | Description                                | Value                |
|-----------|--|----------------------|
| $V_g$     | Gas volume ( $m^3$ )                       | $4.5 \times 10^{-5}$ |
| N         | Agitation Speed (Hz)                       | 20                   |
| $V_L$     | Liquid volume ( $m^3$ )                    | $2.5 \times 10^{-5}$ |
| $d_I$     | Impeller diameter (m)                      | $1.6 \times 10^{-2}$ |
| $d_T$     | Tank diameter (m)                          | $4.0 \times 10^{-2}$ |
| $h_1$     | Height of the impeller from the bottom (m) | $1.1 \times 10^{-2}$ |
| $h_2$     | Liquid height (m)                          | $2.1 \times 10^{-2}$ |

The  $k_{LA_B}$  value for 1200 rpm (20 Hz) was evaluated as  $0.22 \text{ s}^{-1}$ .

The equilibrium solubilities for the gases given in Table 5.3 were used. The factor  $\alpha_I$  was calculated (taking  $R_{\text{exp}}$  as  $2.02 \times 10^{-4}$  i.e. highest) for both hydrogen and carbon monoxide and found to be  $2.17 \times 10^{-2}$  and  $9.79 \times 10^{-3}$ , respectively. Since the values of  $\alpha_I$  are very much less than 0.1 for both the gaseous reactants, gas-liquid mass transfer resistance can be assumed to be negligible.

#### 5.4.2 Initial Rate Data

The kinetics of the hydroformylation of VAM using  $\text{CO}_2(\text{CO})_8$  as catalyst was investigated in the range of conditions shown in Table 5.6 as per the procedure described earlier .



**Table 5.6.** Range of conditions used for the kinetic studies

| <b>Parameter</b>                              | <b>Value</b>                             |
|---|--|
| Catalyst concentration (kmol/m <sup>3</sup> ) | 2.5x10 <sup>-5</sup> -1x10 <sup>-5</sup> |
| Concentration of VAM (kmol/m <sup>3</sup> )   | 0.51- 3.05                               |
| Partial pressure of hydrogen (MPa)            | 1.04 - 2.07                              |
| Partial pressure of carbon monoxide (MPa)     | 0.34-2.74                                |
| Temperature (K)                               | 373 - 393                                |
| Solvent                                       | Toluene                                  |
| Agitation speed (Hz)                          | 16.6-20.0                                |
| Reaction volume (m <sup>3</sup> )             | 2.5 × 10 <sup>-5</sup>                   |

The initial rates of hydroformylation were calculated from the plot of aldehyde formation as a function of time. Under the conditions chosen for the kinetic study, no side reactions were found to occur and hence, these data would be representative of the overall hydroformylation of VAM to the corresponding aldehydes. An induction was observed during the reaction. Hence for the calculation of the rate, the data was corrected for the induction period. The results showing the dependence of the rates on different parameters and a kinetic model based on these data are discussed in the following sections.

#### **5.4.2.1 Effect of Co<sub>2</sub>(CO)<sub>8</sub> Concentration**

The effect of Co<sub>2</sub>(CO)<sub>8</sub> concentration on the rate of hydroformylation of VAM was studied in the temperature range of 373-393K, VAM concentration of 1.05 kmol/m<sup>3</sup> and a total pressure of CO+H<sub>2</sub> = 5.51 MPa (CO:H<sub>2</sub> = 1). The results are shown in Figure 5.9. The rate was found to be linearly dependent on the Co<sub>2</sub>(CO)<sub>8</sub> concentration, indicating a first order kinetics. An increase in concentration of Co<sub>2</sub>(CO)<sub>8</sub> causes an increase in the effective concentration of active catalyst, hydrido cobalt carbonyl species, as seen from the mechanism (scheme 5.2), thereby increasing the rate of reaction, and hence a first order dependence is observed.

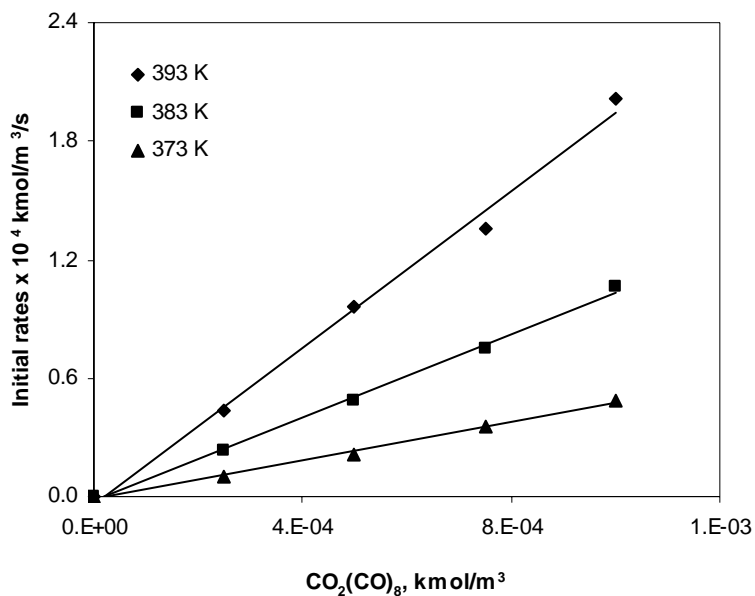


**Figure 5.9.** A plot of Initial rate vs. catalyst concentration in hydroformylation of VAM  
**Reaction Conditions:** VAM, 1.05 kmol/m<sup>3</sup>; temperature, 373- 393K; agitation speed, 16.6 Hz, synthesis gas, 5.51 MPa; Solvent, Toluene; up to 2.5 X 10<sup>-2</sup> m<sup>3</sup> total volume

#### 5.4.2.2 Effect of VAM Concentration

The effect of VAM concentration on the rate of hydroformylation of VAM was investigated in the temperature range of 373-393K. The plot of rate vs. VAM concentration was found to have a linear dependence on VAM in the initial concentration range and at higher substrate concentration; it becomes independent of VAM concentration as shown in Figure 5.10. This could be due to the formation of diolefinic species in equilibrium. Such observation has been reported in kinetics of hydroformylation of olefins using homogeneous catalysts<sup>13</sup> as well as heterogeneous<sup>14</sup> and biphasic<sup>15</sup> catalysts.

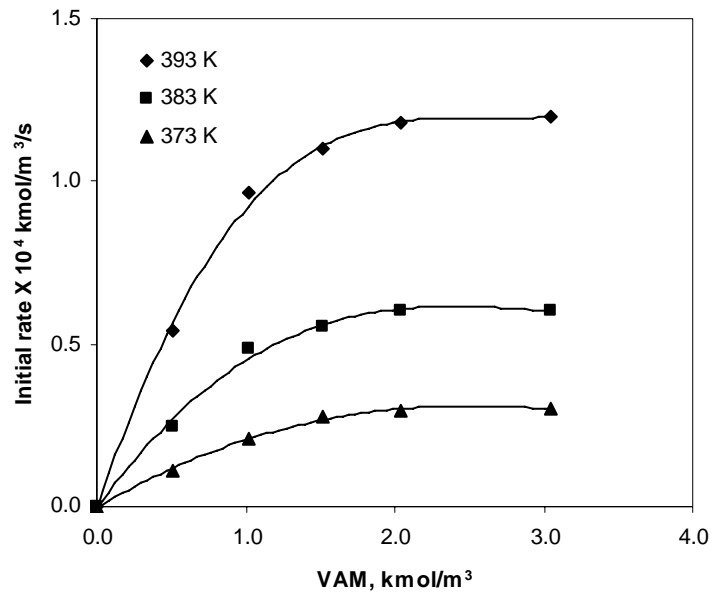


**Figure 5.10.** A plot of Initial rate vs. VAM concentration effect in the hydroformylation of VAM

**Reaction Conditions:**  $\text{Co}_2(\text{CO})_8$ ,  $2.3 \times 10^{-4} \text{ kmol/m}^3$ ; temperature, 373-393K; agitation speed, 16.6 Hz, synthesis gas, 5.51 MPa; Solvent, Toluene; up to  $2.5 \times 10^{-2} \text{ m}^3$  total volume

#### 5.4.2.3 Effect of Partial Pressure of Hydrogen

The effect of partial pressure of  $\text{H}_2$  on the rate of hydroformylation of VAM was investigated at a constant CO partial pressure of 2.75 MPa and the results are shown in Figure 5.11. The rate of reaction was found to have a first order dependence on  $P_{\text{H}_2}$ . As shown in the mechanism, hydrogen preliminarily converts the catalytically inactive  $\text{Co}_2(\text{CO})_8$  into  $\text{HCo}(\text{CO})_4$  which consequently is converted to  $\text{HCo}(\text{CO})_3$ . Also, the alkyl cobalt tri carbonyl species is converted into the aldehydes due to hydrogen. Therefore, it is evident that increase in partial pressure of hydrogen should increase rate of reaction. Hence, with increasing pressure of hydrogen, the rate enhancement is observed.

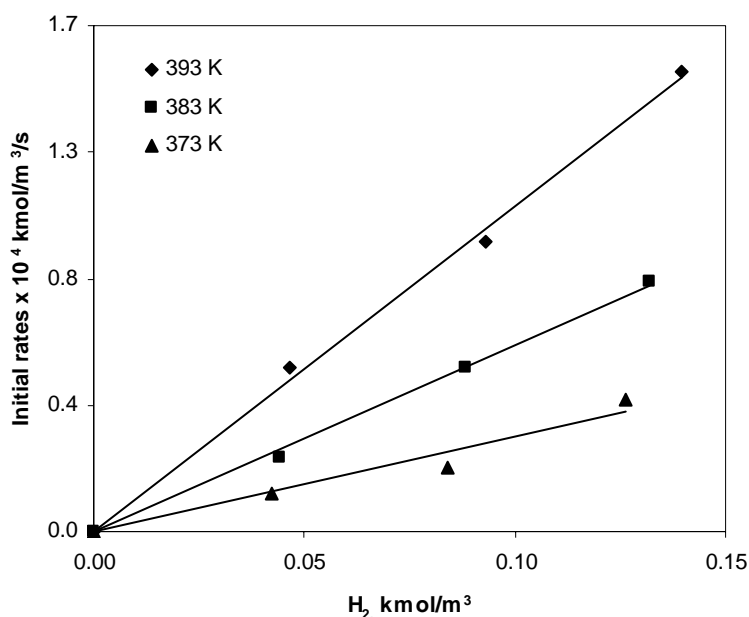


**Figure 5.11.** A plot of rate vs.  $P_{H_2}$  for the hydroformylation of VAM

**Reaction Conditions:**  $Co_2(CO)_8$ ,  $2.3 \times 10^{-4}$  kmol/m<sup>3</sup>; VAM, 1.05 kmol/m<sup>3</sup>; temperature, 393K; agitation speed, 16.6 Hz, Solvent, Toluene; up to  $2.5 \times 10^{-2}$  m<sup>3</sup> total volume

#### 5.4.2.4 Effect of Partial Pressure of Carbon monoxide

The effect of  $P_{CO}$  on the rate of hydroformylation of VAM was studied keeping a constant  $H_2$  partial pressure of 2.75 MPa; the results are shown in Figure 5.12. A plot of rate vs. CO partial pressure passes through maximum. In the initial pressure range, the rate was found to be the first order with  $P_{CO}$  and inversely dependent on  $P_{CO}$  at higher CO pressures. The observed negative effect of  $P_{CO}$  can be readily explained from the proposed mechanism where the CO concentration affects the equilibrium between the 16 electron  $HCo(CO)_3$  species and the 18 electron  $HCo(CO)_4$  species. At very low  $P_{CO}$ , positive effect is observed because of the requirement of certain minimum  $P_{CO}$  for the CO-insertion step. After reaching that minimum  $P_{CO}$  concentration, any further rise in  $P_{CO}$  helps maintaining the  $HCo(CO)_4$  species in preference to the  $HCo(CO)_3$  species, and thereby prohibits olefin insertion.

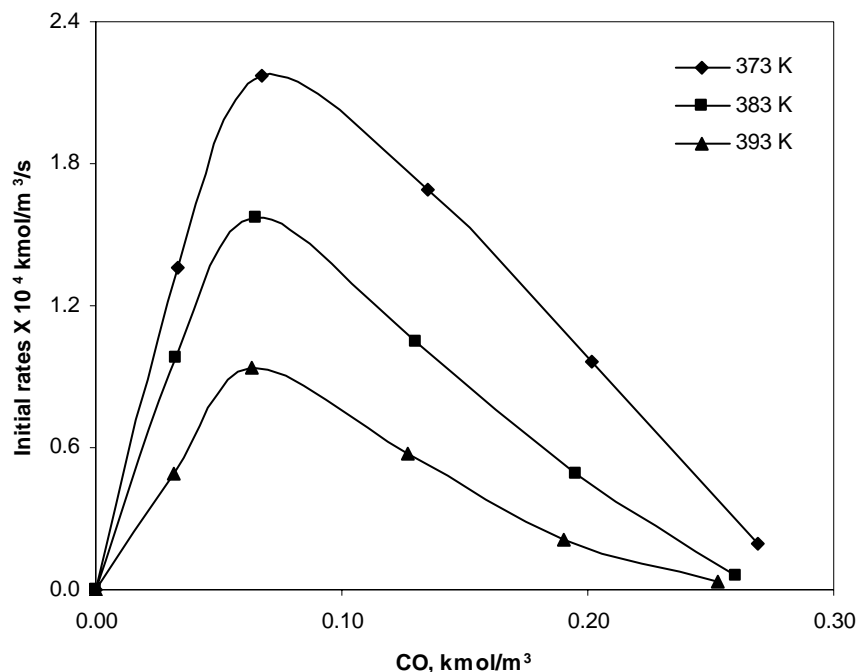


**Figure 5.12.** A plot of rate vs.  $P_{CO}$  for the hydroformylation of VAM.

**Reaction Conditions:**  $Co_2(CO)_8$ ,  $2.3 \times 10^{-4}$  kmol/m<sup>3</sup>; VAM, 1.05 kmol/m<sup>3</sup>; temperature, 373-393K; agitation speed, 16.6 Hz, synthesis gas, 5.51 MPa; Solvent, Toluene; up to  $2.5 \times 10^{-2}$  m<sup>3</sup> total volume

### 5.4.3 Kinetic Models

For the purpose of development of rate models, an empirical approach was followed. Prior to discrimination of rate equations, the rate data was analyzed for the importance of mass transfer resistances. The effect of agitation speed on the rate was investigated at the highest catalyst concentration and at the highest temperature. The rate was found to be independent of the agitation speed, and hence the data were representative of the true kinetics of the reaction. Also the analysis of initial rate data according to the criteria laid down by Ramachandran and Chaudhari<sup>20</sup> confirmed that the gas-liquid ( $\alpha_{gl}$ ) mass transfer resistance was negligible. The initial rate data were hence used to evaluate the intrinsic kinetic parameters.

In order to fit the observed rate data, several rate equations were examined using a nonlinear regression analysis. The results on the kinetic parameters estimated for the

different models are presented in Table 5.6. For this purpose, an optimization program based on Marquardt's method<sup>16</sup> was used. The objective function was chosen as follows;

$$\phi = \sum_{i=1}^n [R_{Ai} - R'_{Ai}]^2 \quad 5.6$$

Where,  $\Phi$  is the objective function to be minimized ( $\Phi_{\min}$ ) representing the sum of the squares of the difference between the observed and predicted rates,  $n$  is the number of experimental data,  $R_{Ai}$  and  $R'_{Ai}$  represent experimental and predicted rates, respectively. The values of rate parameters and  $\Phi_{\min}$ , are presented in Table 5.7.

**Table 5.7.** Rate models examine to fit the data on VAM hydroformylation

| Sr. | Rate Model  | T (K) | $k_1$                 | $K_2$              | $K_3$                  | $\phi_{\min}$          |
|-----|---|-------|-----------------------|--------------------|------------------------|------------------------|
| 1   | $r = \frac{k_1 A^* B^* C D}{(1 + K_2 D)(1 + K_3 B^*)^2}$    | 343   | $3.14 \times 10^{-3}$ | 3.95               | $9.58 \times 10^{-1}$  | $8.76 \times 10^{-12}$ |
|     |   | 353   | $5.92 \times 10^{-3}$ | 4.97               | $9.46 \times 10^{-1}$  | $3.60 \times 10^{-11}$ |
|     |   | 363   | $1.16 \times 10^{-2}$ | 5.90               | $9.24 \times 10^{-1}$  | $1.54 \times 10^{-10}$ |
| 2   | $r = \frac{k_1 A^* B^* C D}{(1 + K_2 D)(1 + K_3 B^*)}$      | 343   | $1.43 \times 10^{-3}$ | $1.76 \times 10^1$ | 2.95                   | $8.12 \times 10^{-12}$ |
|     |   | 353   | $3.27 \times 10^4$    | $4.90 \times 10^8$ | $9.17 \times 10^{-4}$  | $1.20 \times 10^{-9}$  |
|     |   | 363   | 4.49                  | $3.40 \times 10^4$ | $1.82 \times 10^{-2}$  | $5.24 \times 10^{-9}$  |
| 3   | $r = \frac{k_1 A^* B^* C D}{(1 + K_2 D)^2 (1 + K_3 B^*)^2}$ | 343   | $1.51 \times 10^{-2}$ | $7.23 \times 10^1$ | 2.64                   | $1.13 \times 10^{-11}$ |
|     |   | 353   | $2.88 \times 10^{-2}$ | $7.35 \times 10^1$ | 2.61                   | $4.60 \times 10^{-11}$ |
|     |   | 363   | $5.17 \times 10^{-1}$ | $6.95 \times 10^2$ | 2.52                   | $2.06 \times 10^{-10}$ |
| 4   | $r = \frac{k_1 A^* B^* C D}{(1 + K_2 D)(1 + K_3 B^*)^3}$    | 343   | $3.42 \times 10^{-3}$ | 3.98               | 2.72                   | $9.78 \times 10^{-12}$ |
|     |   | 353   | $6.29 \times 10^{-3}$ | 3.93               | 2.64                   | $4.00 \times 10^{-11}$ |
|     |   | 363   | $5.67 \times 10^2$    | 3.91               | $3.65 \times 10^5$     | $2.31 \times 10^{-9}$  |
| 5   | $r = \frac{k_1 A^* B^* C D}{(1 + K_2 D)^3 (1 + K_3 B^*)^3}$ | 343   | $2.52 \times 10^{-3}$ | 1.90               | $5.84 \times 10^{-1}$  | $9.57 \times 10^{-12}$ |
|     |   | 353   | $1.26 \times 10^3$    | $3.82 \times 10^3$ | $-1.47 \times 10^{-1}$ | $6.08 \times 10^{-9}$  |
|     |   | 363   | $9.42 \times 10^{-3}$ | 1.91               | $5.62 \times 10^{-1}$  | $1.68 \times 10^{-10}$ |

Where, A and B represent the concentrations of H<sub>2</sub> and CO in toluene at the gas-liquid interface (kmol/m<sup>3</sup>) respectively. C and D are the concentrations of the catalyst and VAM (kmol/m<sup>3</sup>), respectively.

The discrimination of rate models was done based on the thermodynamic criteria, activation energy and the  $\Phi_{\min}$  values. The rate models II and III were rejected based on

the thermodynamic criteria of inconsistency of equilibrium constant and high activation energy. Model V has rate parameters less than zero (-ve) and hence rejected. In the remaining two models (I and IV), the model IV was rejected based on the higher  $\Phi_{\min}$  values than model I. Therefore, model I (Equation 5.8) was considered to be the best model for representing the kinetics of hydroformylation of VAM using  $\text{Co}_2(\text{CO})_8$  as catalyst.

$$r = \frac{k_1 A^* B^* C D}{(1 + K_2 D)(1 + K_3 B^*)^2} \quad 5.7$$

Where,  $k$  is the intrinsic rate constant ( $\text{m}^9/\text{kmol}^3/\text{s}$ ), A and B represent the concentrations of  $\text{H}_2$  and CO in toluene at the gas-liquid interface ( $\text{kmol}/\text{m}^3$ ) respectively. C and D are the concentrations of the catalyst and VAM ( $\text{kmol}/\text{m}^3$ ), respectively. The rate parameters for Equation 5.8 for all the temperature are presented in Table 5.6 (entry 1). A comparison of the experimental rates with the rates predicted by Equation 5.7 is shown in Figure 5.13, which shows a reasonably good fit of the data. The average deviation in the predicted and observed rates was found to be in the range of  $\pm 3\%$ . The Arrhenius plot showing the effect of temperature on the rate parameters is shown in Figure 5.14, from which the activation energy was evaluated as 67.94 kJ/mol. The dependence of the rate parameters  $K_2$  and  $K_3$  on temperature show opposite trends; however, it is important to note that these parameters may not be representative of a single equilibrium reaction step and are in fact lumped parameters describing observed overall trends.

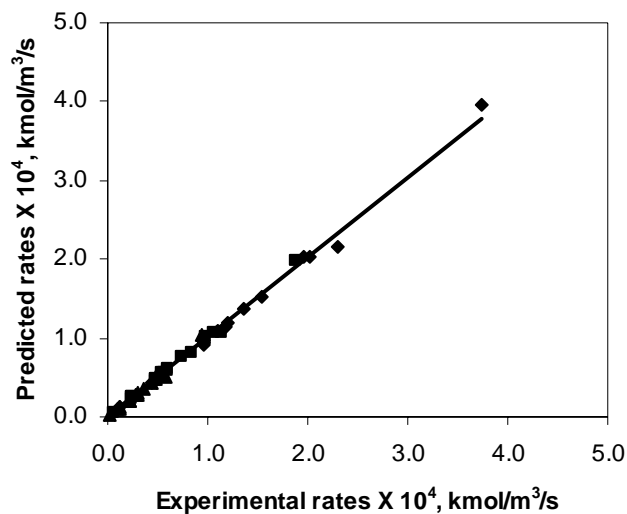


**Figure 5.13.** Comparison of experimental rates and rates predicted using model I

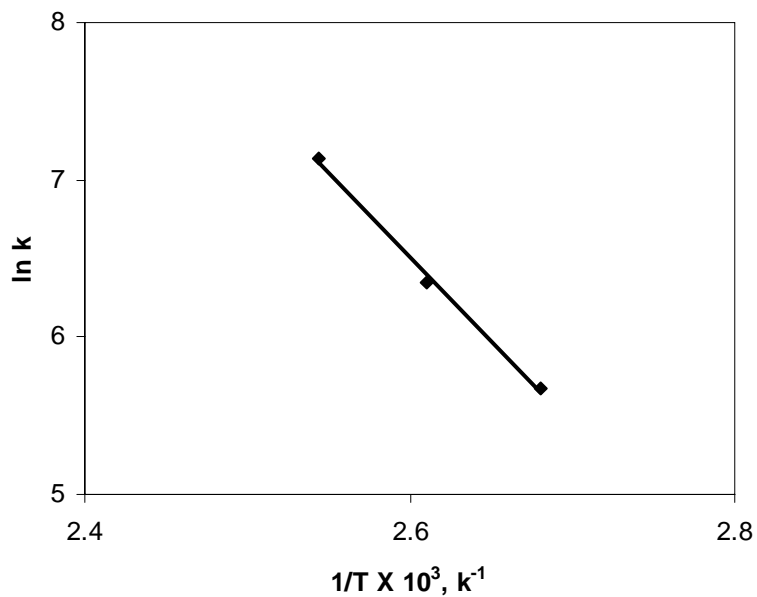


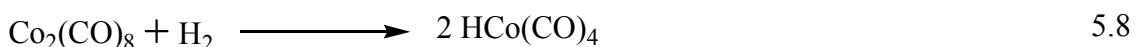
**Figure 5.14.** Temperature dependence of rate constant

### 5.5 Mechanism of Hydroformylation of VAM

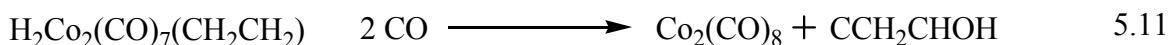
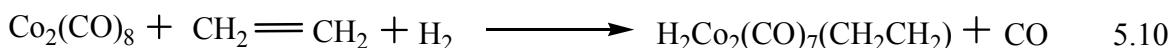
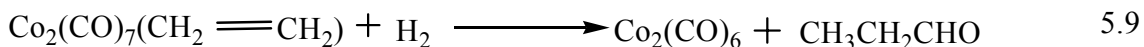
Hydroformylation is one of the most well explored carbonylation reactions in terms of mechanistic aspects. Earlier studies in the cobalt catalyzed hydroformylation of VAM in our laboratory have shown that there is no considerable effect of ligands in



enhancing the rate of reaction, rather, the phosphine ligands cause decomposition of VAM;<sup>17</sup> while a few nitrogen containing ligands actually cause rate retardation and cause undesirable side reactions. Thus, there is no actual role of ligands in the mechanism of cobalt-catalyzed VAM hydroformylation. Although cobalt is one of the earliest discovered hydroformylation catalyst, there has been some debate in the activation of hydrogen by cobalt.<sup>18</sup> The most accepted way of activation is shown below (5.8).



On the basis of kinetic data, two other activation paths have been postulated, one involving a dinuclear olefin complex (Equation 5.9)<sup>19</sup> and the other a dinuclear-dihydrido olefin complex (Equation 5.10)<sup>20</sup>.



These possibilities were ruled out because in the hydroformylation of ethylene with a D<sub>2</sub>/H<sub>2</sub> (1/1) gas mixture propanal-*d*<sub>1</sub> is the primary product.<sup>21</sup> Activation of H<sub>2</sub> by a coordinatively unsaturated acyl-cobalt tricarbonyl has also been proposed.<sup>22</sup> We believe that the activation of hydrogen in the unmodified cobalt catalyzed VAM hydroformylation takes place in dual manner, where the primary activation of H<sub>2</sub> is as shown in equation 5.9, which gives rise to the highly unstable 18 electron HCo(CO)<sub>4</sub>, which reversibly forms the catalytically active 16 electron HCo(CO)<sub>3</sub>, as can be seen in Scheme 5.2. Further, the acyl-cobalt tricarbonyl again activates H<sub>2</sub> to yield a molecule of aldehyde in a manner postulated by Heck and Breslov, giving back the HCo(CO)<sub>3</sub>.

The parametric effects and the effects of concentrations of the catalyst and VAM comply well with the mechanism shown in Scheme 5.2.



TBHP etc in acidic solvents.<sup>24</sup> In the modern chemical industry, the liquid-phase oxidation of aldehydes by molecular oxygen is a very attractive process from an economic and environmental point of view. Several literature references quote oxidation of aldehydes to carboxylic acids using molecular oxygen as oxidant in acidic solvents like acetic acid, peracetic acid, butyric acid etc.<sup>25,26</sup> The use of such acidic solvents implies corrosion and safety hazards, besides the generation of salts, which usually have to be land filled.

Scanty literature is available on the oxidation of ACPALs to ACPAs. These acids on hydrolysis yield the corresponding HPAs, which have wide range of applications in food, pharmaceutical, and polymer industry. Oxidation of 2-ACPAL has been reported by Tinkar and coworkers<sup>27</sup> in acidic solvents like acetic acid with salts of cobalt and manganese as catalysts, in the presence of molecular oxygen as the oxidant. The use of soluble catalysts, which leads to separation problems, and the corrosive acidic solvents, are major shortcomings of this process. Besides this, the isolation and purification of the products are the major issues, mainly because of the applications of the products are in food and pharmaceutical industry.

In this chapter, the detailed study on oxidation of the mixture of 2- and 3-ACPAL has been investigated in a non-acidic solvent like methyl ethyl ketone (MEK), using molecular oxygen as oxidant and 1% Co/C as catalyst with high yield of 2- and 3-HPA. To assess the activity of the Co/C catalyst, a few other catalysts were also screened using the same experimental conditions. The effect of different parameters on conversion of aldehyde and selectivity to corresponding carboxylic acids was investigated to optimize the reaction conditions and parameters. Moreover, to get the detailed understanding of the liquid phase oxidation of ACPALs, oxidation of 2-ACPAL was carried out separately. The kinetics of the 2-ACPAL was carried out using the 1%Co/C as catalyst and air as oxidant in the temperature range of 303 - 343K. The material balance and reproducibility of the experiments was confirmed, by taking a few experiments in which the amounts of 2-ACPAL consumed and the products formed were compared for experiments at high conversions of 2-ACPAL.

### 5.6.1 Oxidation of ACPALs: Screening of Catalysts

Numerous supported transition metal catalysts were screened for liquid phase oxidation of mixtures of 2- and 3- ACPAL to 2 and 3-HPA, the results are presented in Table 5.8. To study the non catalytic oxidation of ACPALs, reaction was carried out without catalyst by purging molecular oxygen as oxidant, but the reaction could not proceed much (entry 1). Among the catalysts screened, 1%Co/C was found to give highest activity and selectivity to corresponding carboxylic acids (entry 7), the other catalysts screened were Ru/C, Pd/C, Pt/C, Fe/C, Cu/C etc (entry 2 - 6). Ru/C was also found to give good activity (entry 6).

**Table 5.8.** Liquid phase oxidation ACPALs: Screening of catalyst

| Sr. | Catalyst      | Conversion, % |         | Selectivity, % |        |
|-----|---------------|---------------|---------|----------------|--------|
|     |               | 2-ACPAL       | 3-ACPAL | 2-ACPA         | 3-ACPA |
| 1   | Non catalytic | 1.86          | 3.96    | 98.36          | 97.60  |
| 2   | 1% Fe/C       | 6.30          | 9.63    | 98.20          | 97.23  |
| 3   | 1% Cu/C       | 9.23          | 10.11   | 95.40          | 98.30  |
| 4   | 1% Pd/C       | 12.82         | 15.69   | 96.50          | 95.30  |
| 5   | 1% Pt/C       | 10.29         | 13.36   | 97.36          | 94.30  |
| 6   | 1% Ru/C       | 14.96         | 17.90   | 97.50          | 98.40  |
| 7   | 1% Co/C       | 25.30         | 33.87   | 98.50          | 96.78  |

**Reaction Conditions:** ACPALS, 2.05 kmol/m<sup>3</sup> (2:3 ACPAL 54:46); ACPALS: Catalyst, 1000:1; temperature, 333K; Agitation speed, 16.6 Hz; Solvent, MEK; Total volume, up to 2.5 X 10<sup>-5</sup> m<sup>3</sup>

### 5.6.2 Screening of Solvents

For the oxidation of aldehydes, several acidic as well as non-acidic solvents were screened and the results are shown in Table 5.9. Among the non-acidic solvents screened methyl ethyl ketone (MEK) was found to give the highest activity and selectivity. Acidic solvents like butyric acid and acetic acid were found to give higher rates than MEK. The reason for not selecting acidic solvents for further detailed study was because they are highly corrosive in nature. MEK was chosen as solvent as it offers advantages as easier separation by distillation, high rate of reaction and non-corrosive in nature.

**Table 5.9.** Liquid phase oxidation ACPALs: Screening of solvents

| Sr. | Solvents        | Conversion, % |         | Selectivity, % |        |
|-----|-----------------|---------------|---------|----------------|--------|
|     |                 | 2 ACPAL       | 3 ACPAL | 2-ACPA         | 3-ACPA |
|     | Toluene         | 2.80          | 5.23    | 98.36          | 97.60  |
| 1   | Cyclohexane     | 4.90          | 7.63    | 97.30          | 96.56  |
| 2   | Dichloromethane | 7.60          | 10.60   | 95.40          | 98.30  |
| 3   | MEK             | 25.60         | 35.92   | 98.50          | 96.78  |
| 4   | Acetic acid     | 39.30         | 57.20   | 98.20          | 97.23  |
| 5   | Propionic acid  | 33.10         | 46.59   | 97.50          | 98.40  |
| 6   | Butyric acid    | 32.60         | 47.90   | 96.90          | 95.60  |
| 7   | Isobutyric acid | 33.62         | 44.93   | 97.36          | 94.30  |

**Reaction Conditions:** ACPALS, 2.05 kmol/m<sup>3</sup> (2:3ACPAL,54:46); ACPALS : Catalyst 1% Co/C, 1000:1; temperature, 333K; Agitation speed, 16.6 Hz; Oxygen flow rate, 30 ml/min; Solvent, MEK ; Total volume, up to 2.5 X 10<sup>-5</sup> m<sup>3</sup>

### 5.7 Liquid Phase Oxidation of 2-ACPAL

The liquid phase oxidation of 2-ACPAL was investigated in detail to understand the catalysis and kinetics involved, using 1%Co/C as a catalyst and air as the oxidant, in the temperature range of 303 to 343K. From the screening of catalysts for ACPALs, it was observed that Co/C gives highest activity and selectivity for the oxidation of ACPALs. Based on these results, further studies were carried out. The effect of Co loading in Co/C was studied. Marginal difference was observed in the activity of 1%Co/C, 3%Co/C and 5% Co/C (entry 1-3). So for the detailed investigation, 1% Co/C was chosen as catalyst. The effect of catalyst concentration was studied and results are presented in Table 5.10. 2-ACPAL conversion increases with increase in catalyst concentration (entry 4-6). To study the effect of temperature, the reactions were carried out in the temperature range of 303 - 343K (entry 7-9). It was observed that the rate of reaction increase with increase in temperature and without affecting the selectivity to 2-ACPA.

**Table 5.10.** Liquid phase oxidation 2-ACPAL: Preliminary experiments

| Sr | Catalyst | Cobalt concentration X $10^5$ , kmol/m <sup>3</sup> | Conversion, % | Selectivity, % | T.O.N. | T.O.F. |
|----|----------|---|---------------|----------------|--------|--------|
|    | -        |   | 0.4           | 92.1           | 10.2   | 20.3   |
| 1  | 1% Co/C  | 0.85  | 38.9          | 98.9           | 988.0  | 1976.0 |
| 2  | 3% Co/C  | 0.85  | 40.1          | 98.6           | 1017.9 | 2035.9 |
| 3  | 5% Co/C  | 0.85  | 38.1          | 97.9           | 967.2  | 1934.3 |
| 4  | 1% Co/C  | 0.34  | 20.1          | 97.7           | 510.7  | 1021.5 |
| 5  | 1% Co/C  | 1.70  | 56.9          | 99.6           | 1444.4 | 2888.8 |
| 6  | 1% Co/C  | 2.55  | 68.2          | 96.3           | 1732.0 | 3464.0 |
| 7  | 303      | 0.85  | 15.9          | 95.9           | 404.4  | 808.8  |
| 8  | 313      | 0.85  | 23.6          | 99.3           | 599.8  | 1199.7 |
| 9  | 323      | 0.85  | 30.3          | 98.7           | 769.2  | 1538.3 |
| 10 | 333      | 0.85  | 38.9          | 98.9           | 988.0  | 1976.0 |
| 11 | 343      | 0.85  | 60.6          | 94.2           | 1538.3 | 3076.6 |

**Reaction Conditions:** 2-ACPAL, 1.4 kmol/m<sup>3</sup>; ACPALs: catalyst: 100:1; 3 kg/m<sup>3</sup>; temperature, 333K; Agitation speed, 16.6 Hz; Reaction time, 0.5 hours; Oxygen flow rate, 30 ml/min; Solvent, MEK; Total volume, up to 5.5 X 10<sup>-5</sup> m<sup>3</sup>

### 5.7.1. Kinetics of Liquid Phase Oxidation of 2-ACPAL

Kinetics of liquid phase oxidation of 2-ACPAL has been investigated using 1%Co/C as catalyst and molecular oxygen as oxidant. In none of the previous studies, detailed investigation of intrinsic kinetics of liquid phase oxidation of 2-ACPAL has been reported. Considering the industrial importance of this reaction in synthesis of HPAs, such a study would be useful. The effect of catalyst concentration, 2-ACPAL concentration and oxygen partial pressure on initial rate of oxidation of 2-ACPAL has been investigated in the temperature range of 293-343K. The material balance and reproducibility of the experiments were confirmed for kinetic study. For this purpose, few experiments were carried out in which the amount of 2-ACPAL consumed, and 2-ACPA formed were compared for the experiments with high conversion of 2-ACPAL. The typical concentration time profile of oxidation of 2-ACPAL is as show in the Figure 5.15.

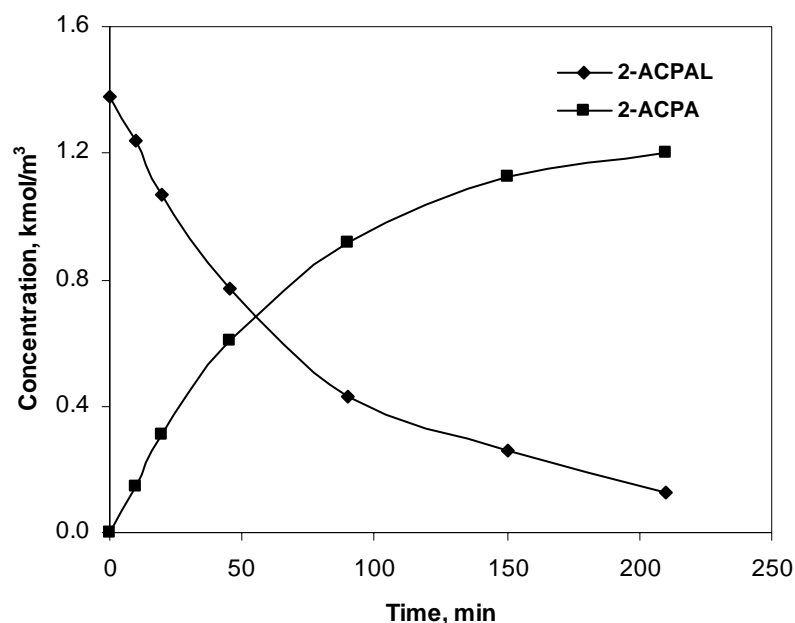


**Figure 5.15.** Concentration time profile for oxidation of 2-ACPAL

**Reaction Conditions:** 2-ACPAL, 1.4 kmol/m<sup>3</sup>; 1% Co/C, 3 kg/m<sup>3</sup>; temperature, 333K; Agitation speed, 16.6 Hz; Oxygen flow rate, 30 ml/min; Solvent, MEK; Total volume, up to 5.5 X 10<sup>-5</sup> m<sup>3</sup>

## 5.7.2 Evaluation of Kinetic Regime

### 5.7.2.1 Effect of Agitation Speed

For the investigation of kinetics, it is essential that the reaction should operate in kinetic regime and not under the condition where mass transfer is controlling. For that purpose, the effect of agitation speed on the rate of reaction was studied and the results are presented in Figure 5.16. The rate was found to be independent of the agitation speed beyond 1000 (16.6 Hz) rpm, which clearly indicates that the reaction is in kinetic regime. Therefore, all the reactions for kinetic studies were carried out at an agitation speed of 1200 rpm (20 Hz) to ensure that the reaction occurred in the kinetic regime. This observation of agitation speed was also supported by criteria's given in chapter-2. The value of  $\alpha_{gl}$ ,  $\alpha_{ls}$  and  $\phi_{exp}$ , which are defined as the ratios of the observed rates to the maximum rates of gas-liquid, liquid-solid and intraparticle mass transfer rates was found

to be  $\alpha_l = 5.32 \times 10^{-4}$   $\alpha_{ls} = 0.031$   $\phi_{\text{exp}} = 1.89 \times 10^{-3}$  respectively, which are less than 1, implies the reaction is in kinetic regime.

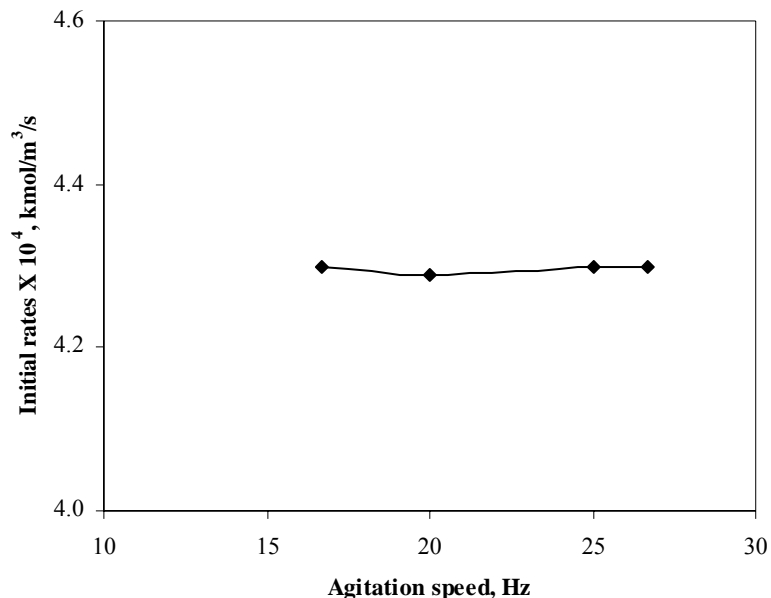


**Figure 5.16.** Effect of agitation speed on the rate of oxidation of 2-ACPAL

**Reaction Conditions:** 2-ACPAL, 1.4 kmol/m<sup>3</sup>; 1% Co/C, 3 kg/m<sup>3</sup>; temperature, 333K; Oxygen flow rate, 30 ml/min; Solvent, MEK; Total volume, up to 5.5 X 10<sup>-5</sup> m<sup>3</sup>

### 5.7.2.2 Effect of Oxygen Flow Rate

To study the effect of oxygen flow rate on the rate of the oxidation, reaction was studied in the range of oxygen flow rate 10 – 70 ml/min. There was a marked improvement in the rate of reaction when the flow rate is very less but it was observed that there is no effect of oxygen flow rate on the rate of reaction in the studied range. The results are as shown in the Figure 5.17.



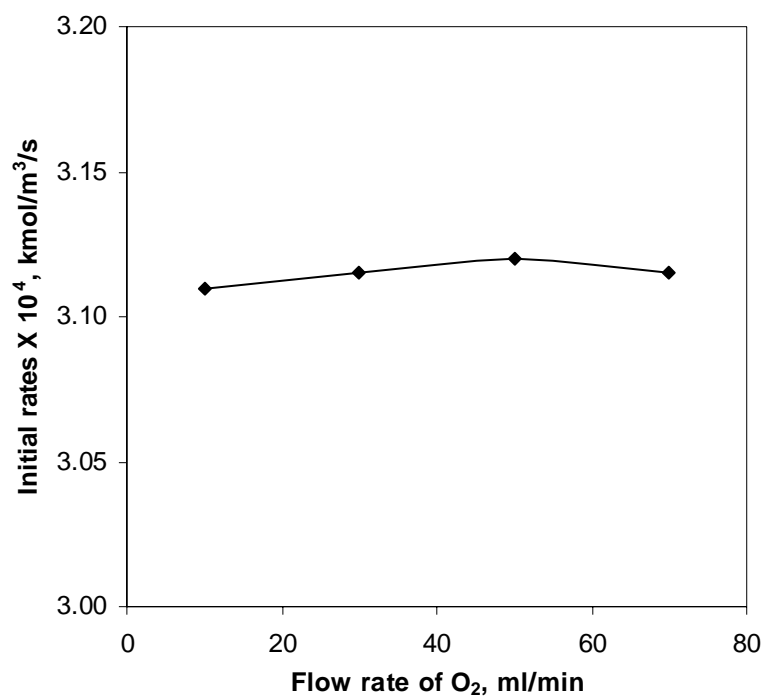


**Figure 5.17.** Effect Oxygen Flow rate on rate of 2-ACPAL oxidation

**Reaction Conditions:** 2-ACPAL, 1.4 kmol/m<sup>3</sup>; 1% Co/C, 3 kg/m<sup>3</sup>; temperature, 333K; Agitation speed, 16.6 Hz; Solvent, MEK; Total volume, up to 5.5 X 10<sup>-5</sup> m<sup>3</sup>

### 5.7.3. Initial Rate Data

The kinetics of the liquid phase oxidation of 2-ACPAL using 1%Co/C as catalyst and molecular oxygen as oxidant was investigated in the range of conditions shown in Table 5.11.

**Table 5.11.** Range of conditions used for the kinetic studies

| Paramter  | Value                                    |
|---|--|
| Catalyst concentration (kg/m <sup>3</sup> )         | 2.5x10 <sup>-5</sup> -1x10 <sup>-5</sup> |
| Concentration of 2-ACPAL (kmol/m <sup>3</sup> )     | 0.51- 3.05                               |
| O <sub>2</sub> concentration (kmol/m <sup>3</sup> ) | 0.5-5                                    |
| Temperature, (K)                                    | 303-333                                  |
| Solvent   | MEK                                      |
| Reaction volume (m <sup>3</sup> )                   | 5.0 × 10 <sup>-5</sup>                   |

The initial rates of oxidation of 2-ACPAL were calculated from the plot of 2-ACPA formed as a function of time. Under the conditions chosen for the kinetic study, no side reactions were found to occur and hence, these data would be representative of the overall oxidation of 2-ACPAL to 2-ACPA. The results showing the dependence of the rates on different parameters and a kinetic model based on these data are discussed in the following sections.

### 5.7.3.1 Effect of Catalyst Concentration

The effect of catalyst concentration, on the rate of oxidation of 2-ACPAL was studied in the temperature range of 303-333K. The results are shown in Figure 5.18. The rate was found to be linearly dependent on the 1% Co/C loading, indicating a first order kinetics.

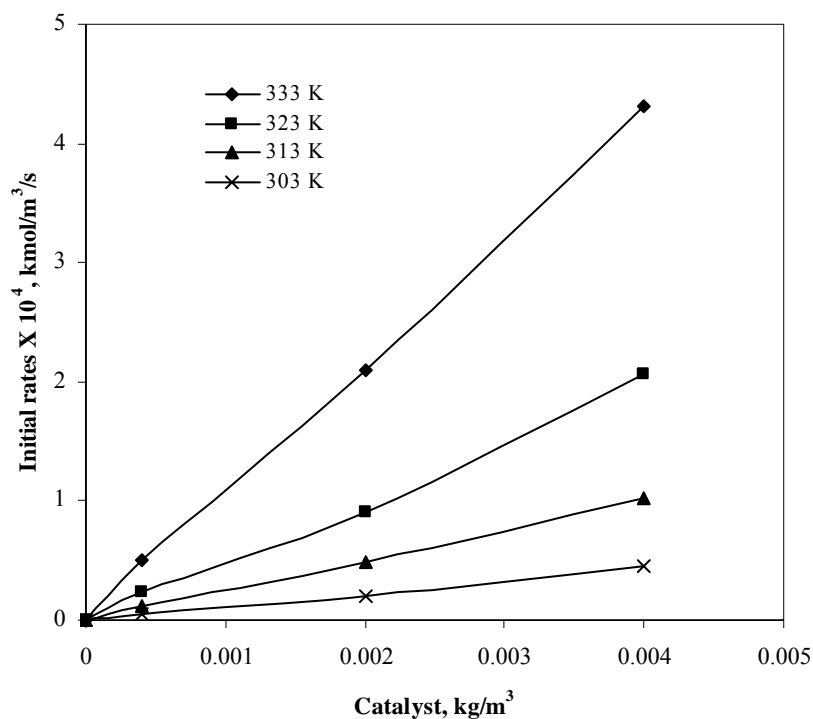


**Figure 5.18.** Effect of catalyst concentration on rate of 2-ACPAL oxidation

**Reaction Conditions:** 2-ACPAL, 1.4 kmol/m<sup>3</sup>; temperature, 303-333K; Agitation speed, 16.6 Hz; Oxygen flow rate, 30 ml/min; Solvent, MEK; Total volume, up to 5.0 X 10<sup>-5</sup> m<sup>3</sup>

### 5.7.3.2 Effect of 2-ACPAL Concentration

The effect of 2-ACPAL concentration on the rate of oxidation of 2-ACPAL was investigated in the temperature range of 303-333K and the results are shown in the Figure 5.19. The plot of rate vs. 2-ACPAL concentration was found to have a linear dependence on 2-ACPAL in the initial concentration range and at higher substrate concentration; it becomes independent of the substrate concentration.

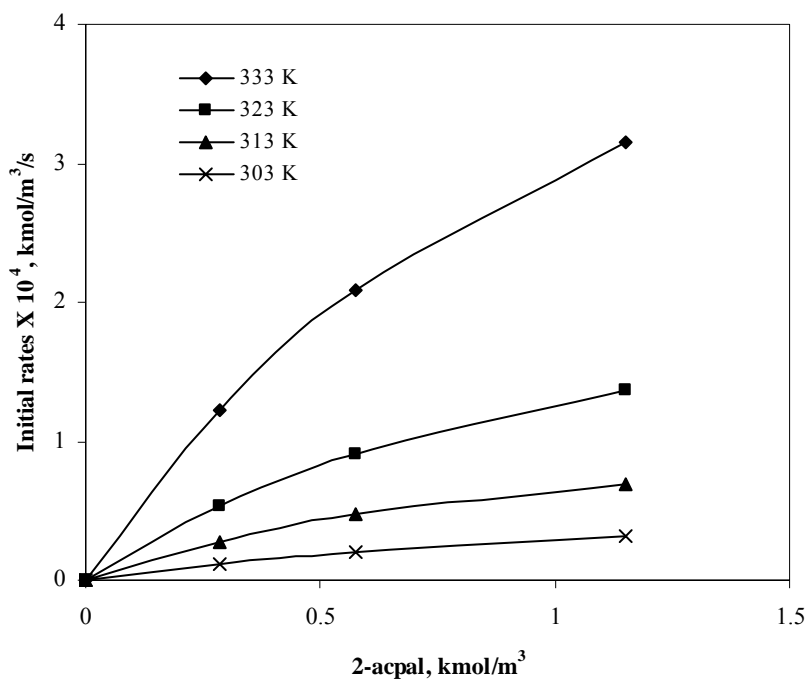


**Figure 5.19.** Effect of 2-ACPAL concentration on rate of 2-ACPAL oxidation

**Reaction Conditions:** 1% Co/C, 3 kg/m<sup>3</sup>; temperature, 303-333K; Agitation speed, 16.6 Hz; Oxygen flow rate, 30 ml/min; Solvent, MEK; Total volume, up to 5.0 X 10<sup>-5</sup> m<sup>3</sup>

### 5.7.3.3 Effect of Oxygen Partial Pressure

The oxygen partial pressure was varied in order to study its effect on rate of the reaction in the temperature range of 293-323K. It was observed that there was marginal increase in the rate of the reaction initially but it was independent of oxygen partial pressure at higher partial pressure of oxygen. The results are as shown in the Figure 5.20.

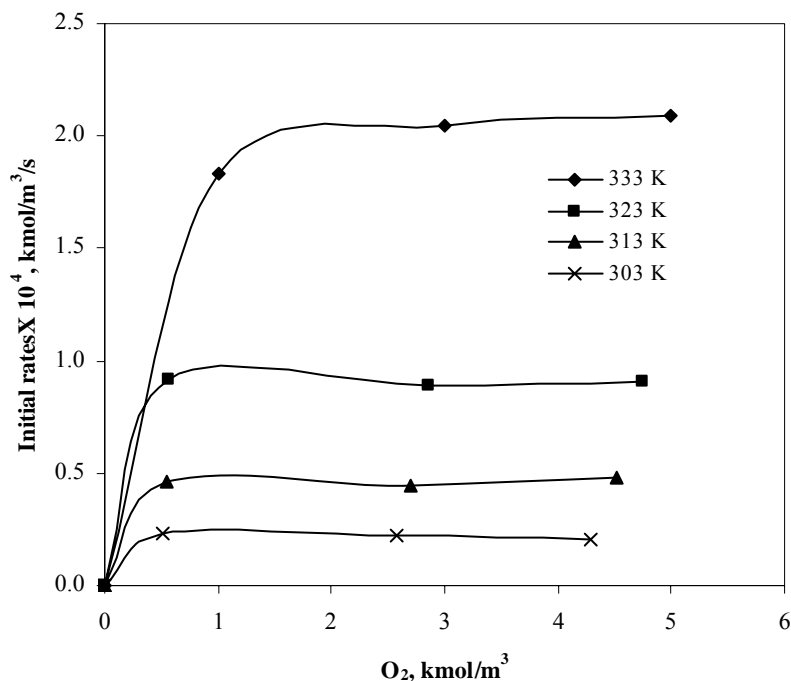


**Figure 5.20.** Effect of  $P_{O_2}$  on rate of 2-ACPAL oxidation

**Reaction Conditions:** 2-ACPAL, 1.4 kmol/m<sup>3</sup>; 1% Co/C, 3 kg/m<sup>3</sup>; temperature, 303-333K; Agitation speed, 16.6 Hz; Oxygen flow rate, 30 ml/min; Solvent, MEK; Total volume, up to 5.0 X 10<sup>-5</sup> m<sup>3</sup>

#### 5.7.4. Kinetic Models

For the purpose of development of rate models, an empirical approach was followed as described in the section 5.4.3. Prior to discrimination of rate equations, the rate data were analyzed for the importance of mass transfer resistances. The effect of agitation speed on the rate was investigated at the highest catalyst concentration and at highest temperature. The rate was found to be independent of the agitation speed, and hence the data were representative of the true kinetics of the reaction. Also the gas-liquid ( $\alpha_{gl}$ ), gas-liquid-solid ( $\alpha_{gls}$ ), mass transfer resistance were found to be negligible.

**Table 5.12.** Rate models examine to fit the data on liquid phase oxidation of 2-ACPAL

| Sr. | Rate Model                                       | T<br>(K) | k <sub>1</sub>        | K <sub>2</sub>       | K <sub>3</sub>        | ϕ <sub>min</sub>       |
|-----|--|----------|-----------------------|----------------------|-----------------------|------------------------|
| 1   | $r = \frac{k_1 EFG^*}{(1+K_2 E)(1+K_3 G^*)}$     | 303      | 3.14×10 <sup>-3</sup> | 3.95                 | 9.58×10 <sup>-1</sup> | 8.76×10 <sup>-10</sup> |
|     |  | 313      | 5.92×10 <sup>-3</sup> | 4.97                 | 9.46×10 <sup>-1</sup> | 3.60×10 <sup>-10</sup> |
|     |  | 323      | 1.16×10 <sup>-2</sup> | 5.90                 | 9.24×10 <sup>-1</sup> | 1.54×10 <sup>-10</sup> |
|     |  | 333      | 1.91×10 <sup>-2</sup> | 7.90                 | 8.12×10 <sup>-1</sup> | 1.54×10 <sup>-10</sup> |
| 2   | $r = \frac{k_1 EFG^*}{(1+K_2 E)(1+K_3 G^*)^2}$   | 303      | 1.43×10 <sup>-3</sup> | 1.76×10 <sup>1</sup> | 2.95                  | 8.12×10 <sup>-9</sup>  |
|     |  | 313      | 3.27×10 <sup>4</sup>  | 4.90×10 <sup>8</sup> | 9.17×10 <sup>-4</sup> | 1.20×10 <sup>-9</sup>  |
|     |  | 323      | 4.49                  | 3.40×10 <sup>4</sup> | 1.82×10 <sup>-2</sup> | 5.24×10 <sup>-9</sup>  |
|     |  | 333      | 5.67×10 <sup>2</sup>  | 3.82×10 <sup>3</sup> | 3.65×10 <sup>5</sup>  | 2.06×10 <sup>-9</sup>  |
| 3   | $r = \frac{k_1 EFG^*}{(1+K_2 E)^2(1+K_3 G^*)^2}$ | 303      | 1.51×10 <sup>-2</sup> | 7.23×10 <sup>1</sup> | 2.64                  | 1.13×10 <sup>-8</sup>  |
|     |  | 313      | 2.88×10 <sup>-2</sup> | 7.35×10 <sup>1</sup> | 2.61                  | 4.60×10 <sup>-9</sup>  |
|     |  | 323      | 5.17×10 <sup>-1</sup> | 6.95×10 <sup>2</sup> | 2.52                  | 2.06×10 <sup>-9</sup>  |
|     |  | 333      | 9.42×10 <sup>-3</sup> | 1.91                 | 5.62×10 <sup>-1</sup> | 2.31×10 <sup>-7</sup>  |
| 4   | $r = \frac{k_1 EFG^*}{(1+K_2 E)^2(1+K_3 G^*)^3}$ | 303      | 3.42×10 <sup>-3</sup> | 3.98                 | 2.72                  | 9.78×10 <sup>-10</sup> |
|     |  | 313      | 6.29×10 <sup>-3</sup> | 3.93                 | 2.64                  | 4.00×10 <sup>-9</sup>  |
|     |  | 323      | 5.67×10 <sup>2</sup>  | 3.91                 | 3.65×10 <sup>5</sup>  | 2.31×10 <sup>-7</sup>  |
|     |  | 333      | 3.14×10 <sup>-3</sup> | 3.95                 | 9.58×10 <sup>-1</sup> | 1.54×10 <sup>-10</sup> |
| 5   | $r = \frac{k_1 EFG^*}{(1+K_2 E)^3(1+K_3 G^*)^3}$ | 303      | 2.52×10 <sup>-3</sup> | 1.90                 | 5.84×10 <sup>-1</sup> | 9.57×10 <sup>-9</sup>  |
|     |  | 313      | 1.26×10 <sup>3</sup>  | 3.82                 | 1.47×10 <sup>-1</sup> | 6.08×10 <sup>-8</sup>  |
|     |  | 323      | 9.42×10 <sup>-3</sup> | 1.91                 | 5.62×10 <sup>-1</sup> | 1.68×10 <sup>-8</sup>  |
|     |  | 333      | 3.27×10 <sup>4</sup>  | 4.90×10 <sup>8</sup> | 9.17×10 <sup>-4</sup> | 1.13×10 <sup>-8</sup>  |

Where, G represent the concentrations of O<sub>2</sub> in MEK at the gas-liquid interface (kmol/m<sup>3</sup>) respectively. E and F are the concentrations of the 2-ACPAL (kmol/m<sup>3</sup>), and catalyst (kg/m<sup>3</sup>), respectively.

The discrimination of rate models was done based on the thermodynamic criteria, activation energy and the Φ<sub>min</sub> values. The rate models II and III were rejected based on the thermodynamic criteria of inconsistency of equilibrium constant and high activation

energy. In models I, IV and V, the model IV and V were discriminated based on the higher  $\Phi_{\min}$  values than model I. Therefore, model I (Equation 5.12) was considered the best model for representing the kinetics of liquid phase oxidation of 2-ACPAL using 1%Co/C catalyst.

$$r = \frac{k_1 EFG^*}{(1 + K_2 E)(1 + K_3 G^*)} \quad 5.12$$

Where,  $k$  is the intrinsic rate constant ( $\text{m}^9/\text{kmol}^3/\text{s}$ ),  $G$  represent the concentrations of  $\text{O}_2$  in MEK at the gas-liquid interface ( $\text{kmol}/\text{m}^3$ ).  $E$  and  $F$  are the concentrations of the 2-ACPAL ( $\text{kmol}/\text{m}^3$ ), and catalyst ( $\text{kg}/\text{m}^3$ ), respectively. The rate parameters for Equation 4.12 for all the temperature are presented in Table 5.12 (entry 1). A comparison of the experimental rates with the rates predicted by Equation 5.22 is shown in Figure 5.21, which shows a reasonably good fit of the data. The average deviation in the predicted and observed rates was found to be in the range of  $\pm 4\%$ . The Arrhenius plot showing the effect of temperature on the rate parameters is shown in Figure 5.22, from which the activation energy was evaluated as 68.9 kJ/mol. The dependence of the rate parameters  $K_2$  and  $K_3$  on temperature show similar trends; however, it is important to note that these parameters may not be representative of a single equilibrium reaction step and are in fact lumped parameters describing observed overall trends.

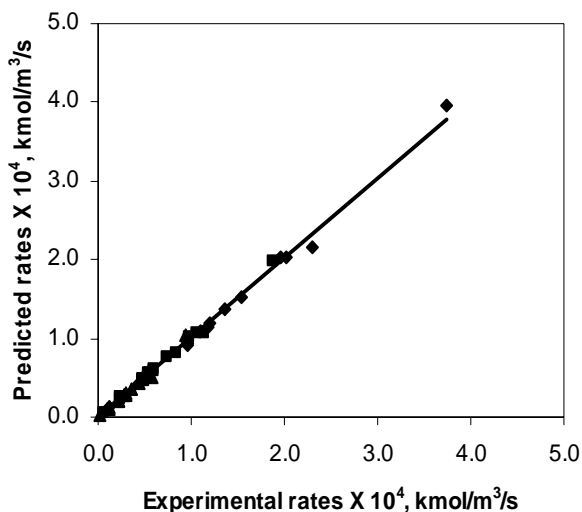


**Figure 5.21.** Comparison of experimental rates and rates predicted using model I

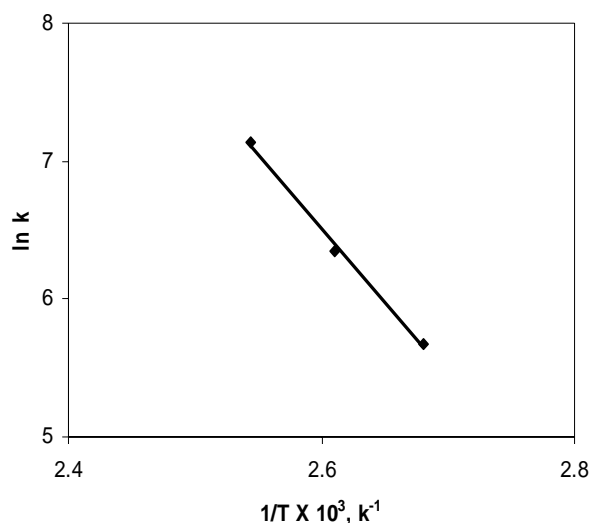
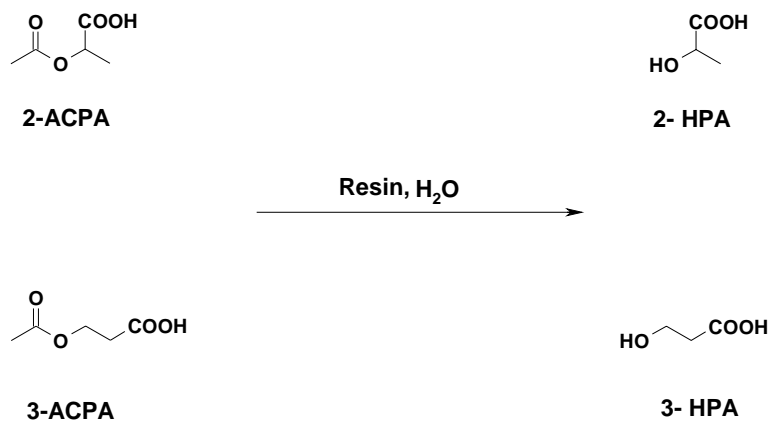


**Figure 5.22.** Temperature dependence of rate constant

### 5.8 Hydrolysis of Acetoxy Propionic Acids

Conventional reagent based hydrolysis requires corrosive mineral acids or bases. In view of the environmental hazards and waste generation from these reagents, they are considered as a last choice from process point of view. Many solid acids like zeolites, oxides, mixed oxides including heteropoly acids, ion-exchanged resins and phosphates<sup>28</sup> etc. are environmentally benign and effective substitutes for such reagents. Cation exchange resin catalysts have been used for several years in several reactions including hydrolysis / esterification reactions.<sup>29</sup> Ion exchange material may be broadly defined as an insoluble matrix containing labile ions capable of exchanging with ions in the surrounding medium without major physical change in its structure.<sup>30</sup> Typical cation exchange resin catalysts are sulphonic acids fixed to a polymer carrier, such as polystyrene cross-linked with divinylbenzene (DVB). Several such resins are commercially available, which include Amberlyst resins (e.g. Amberlyst-15, Amberlite IR-120 etc.) In the present study, to complete the synthesis of HPAs via VAM hydroformylation, Amberlite IR-120 resin was found to be the best hydrolysis catalyst.



**Scheme 5.3.** General scheme for hydrolysis of acetoxy propionic acids

For hydrolysis experiments, 2-ACPA obtained at the end of oxidation reaction was concentrated by distilling off toluene, and then isolated in mixture form by distillation of the two acids under high vacuum, at low temperature (273K). Hydrolysis of the mixture of acids was carried out at 343K to obtain the respective 2-HPA (Lactic acid), as shown in Scheme 5.3. Water was used as a solvent for the hydrolysis of acids and results are presented in Table 5.13. The solid acid catalysts screened included Zr-P, Filtrol- 24, sulphated Zirconia, Amberlite IR 120. (entry1-4). Amberlite IR-120 resin was found to give highest activity for the hydrolysis of the ACPAs (entry 3). The reactions were carried out at 343K for 300 minutes in a batch mode. Acetic acid in the stoichiometric amount of the 2-HPA formed during the reaction, which helps to proceed in the reaction in forward reaction. Similarly, mixture of 2-ACPA and 3-ACPA was hydrolyzed under the similar conditions (entry 6) and found to give selectively 2-HPA (Lactic acid). Amberlite IR-120 resin was filtered out and recycled for reaction without loss of activity (entry 5).



**Table 5.13.** Hydrolysis of ACPAs

| Sr. | Catalyst           | Type of acidity (B or L) | CE C, meq /g | Surface Area, m <sup>2</sup> /g | Conversion, % |        | Selectivity, % |       |
|-----|--------------------|--------------------------|--------------|---------------------------------|---------------|--------|----------------|-------|
|     |                    |                          |              |                                 | 2-ACPA        | 3-ACPA | 2-HPA          | 3-HPA |
| 1   | Zr-P               | B and L                  | ND           | 120                             | 22.9          | -      | 90.3           | -     |
| 2   | Filtrol- 24        | Mainly B                 | 0.3          | 350                             | 35.6          | -      | 88.5           | -     |
| 3   | sulphated Zirconia | B and L                  | ND           | 100                             | 40.2          | -      | 92.6           | -     |
| 4   | Amberlite IR 120   | Mainly B                 | 4.9          | 55                              | 90.5          | -      | 95.1           | -     |
| 5*  | Amberlite IR 120   | Mainly B                 | 4.9          | 55                              | 85.9          | -      | 96.3           | -     |
| 6   | Amberlite IR 120   | Mainly B                 | 4.9          | 55                              | 88.6          | 85.3   | 97.8           | 96.4  |

**B- Brönsted; L-Lewis; CEC- Cation Exchange Capacity**

**Reaction Conditions:** ACPA, 2.05 kmol/m<sup>3</sup> (2:3-ACPA, 54:46); Catalyst, 0.1g; temperature, 343K; Agitation speed, 12 Hz; Solvent, water; Total volume, up to 2.5X 10<sup>-5</sup> m<sup>3</sup>

## 5.9. Conclusions

The VAM hydroformylation-oxidation-hydrolysis route for the synthesis of 2 and 3-HPA is an excellent alternative for the conventional multistep synthesis procedure. A detailed investigation of this route has been carried out in this chapter. Unlike the conventional Rh catalyst, the cobalt carbonyl catalyst yield the linear aldehyde isomers along with the branched aldehyde. The kinetics of CO<sub>2</sub>CO<sub>8</sub> catalyzed VAM hydroformylation step has been carried out with the objective of exploring the key step in synthesis of HPAs. Kinetic study of hydroformylation of VAM revealed that the reaction was first order with respect to catalyst, and H<sub>2</sub> concentration. The rate versus partial pressure of CO and VAM showed a substrate-inhibited kinetics at higher CO partial pressure. Activation energies for VAM hydroformylation was evaluated as 84.6 kcal/mol.

The oxidation of aldehyde formed in the hydroformylation step has been carried out with the heterogeneous Co/C catalyst and the reusability of the same has been

established by recycle experiments. The detailed parametric and kinetic investigation of oxidation step has been carried out with 2-ACPAL as substrate and air as oxidant. The kinetic of oxidation of 2-ACPAL revealed that the reaction was first order with respect to catalyst concentration and 2-ACPAL and oxygen partial pressure shows first order dependence in the initial concentration range, becomes independent at higher concentrations. Both the aldehydes 2- and 3-ACPALs has found to give corresponding acetoxy propionic acids with excellent selectivity at mild reaction conditions.

The acetoxy propionic acid thus obtained were hydrolyzed to corresponding HPAs with different solid acid catalyst including Zirconia and its derivatives and cation exchange resins with  $-\text{SO}_3\text{H}$  groups. The cation exchange resin having bronsted acidic sites were found to be the best with satisfactory reusability, while Lewis acidic zirconia derivatives has been found to be less effective in terms of ACPAs conversion.

The three step involved i.e. VAM hydroformylation- oxidation-hydrolysis were investigated in detail and reaction conditions optimized in order to achieved high conversion of corresponding reactants and selectivity to the desired products in each of the step.

## Nomenclature

|                                 |   |
|---------------------------------|---|
| A                               | Concentration of hydrogen, kmol/m <sup>3</sup>  |
| B                               | Concentration of carbon monoxide, kmol/m <sup>3</sup>                                     |
| C                               | Concentration of catalyst, kmol/m <sup>3</sup>  |
| D                               | Concentration of camphene, kmol/m <sup>3</sup>  |
| H                               | Henry constant defined by equation 4.4  |
| E                               | Concentration of ACPAL, kmol/m <sup>3</sup>   |
| F                               | Concentration of Catalyst, kgl/m <sup>3</sup>   |
| G*                              | Concentration of oxygen, kgl/m <sup>3</sup>   |
| k <sub>1</sub> , k <sub>2</sub> | Intrinsic rate constants, m <sup>3</sup> /kmol  |
| k <sub>2</sub>                  | Constant in Eq. 4.9 m <sup>3</sup> /kmol  |
| P <sub>f</sub>                  | Final pressure MPa  |
| P <sub>i</sub>                  | Initial pressure MPa  |
| R                               | Universal gas constant, kJ/kmol/K   |
| r                               | Rate of hydroformylation, kmol/m <sup>3</sup> /s.   |
| R' <sub>Ai</sub>                | Experimental rates, kmol/m <sup>3</sup> /s  |
| R <sub>Ai</sub>                 | Predicted rates, kmol/m <sup>3</sup> /s   |
| R <sub>i</sub>                  | Reaction rate for the hydroformylation step (kmol/m <sup>3</sup> /s)                      |
| t                               | Reaction time, h.   |
| T                               | Temperature, K  |
| V <sub>g</sub>                  | Gas volume, m <sup>3</sup>  |
| V <sub>L</sub>                  | Total liquid volume, m <sup>3</sup>   |
| X <sub>a</sub>                  | Solubility of gas of the solute gas at pressure P <sub>f</sub> , kmol/m <sup>3</sup> /MPa |
| Φ                               | Parameter defined by Eq-5.6   |

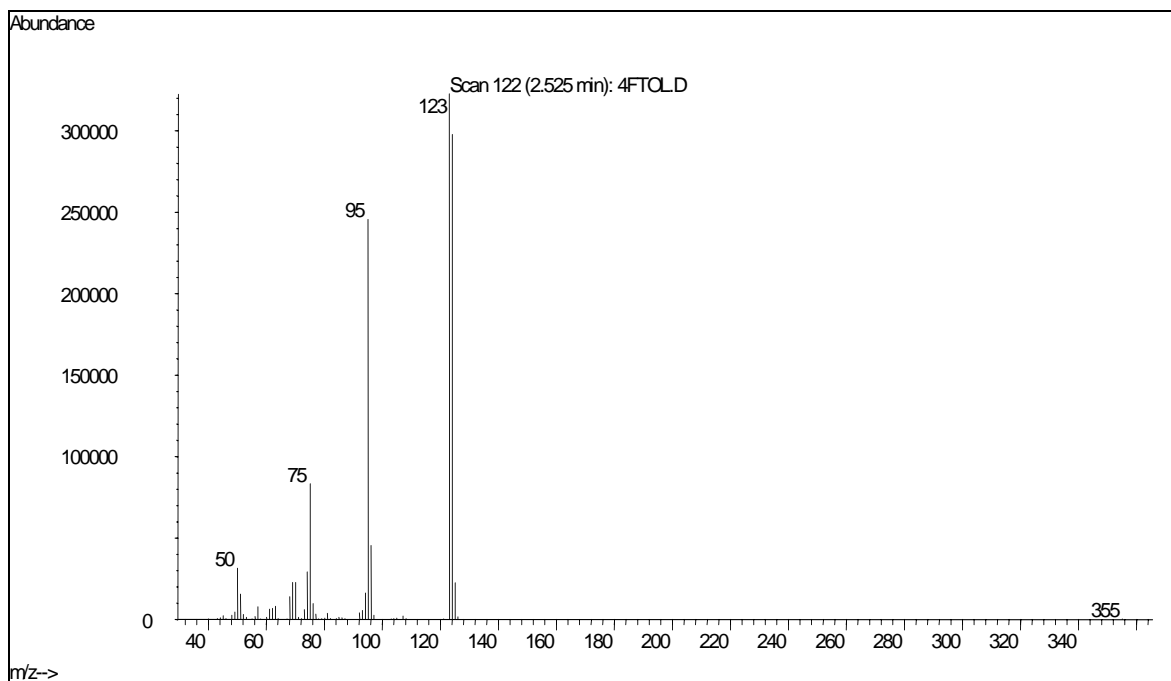
## References

---

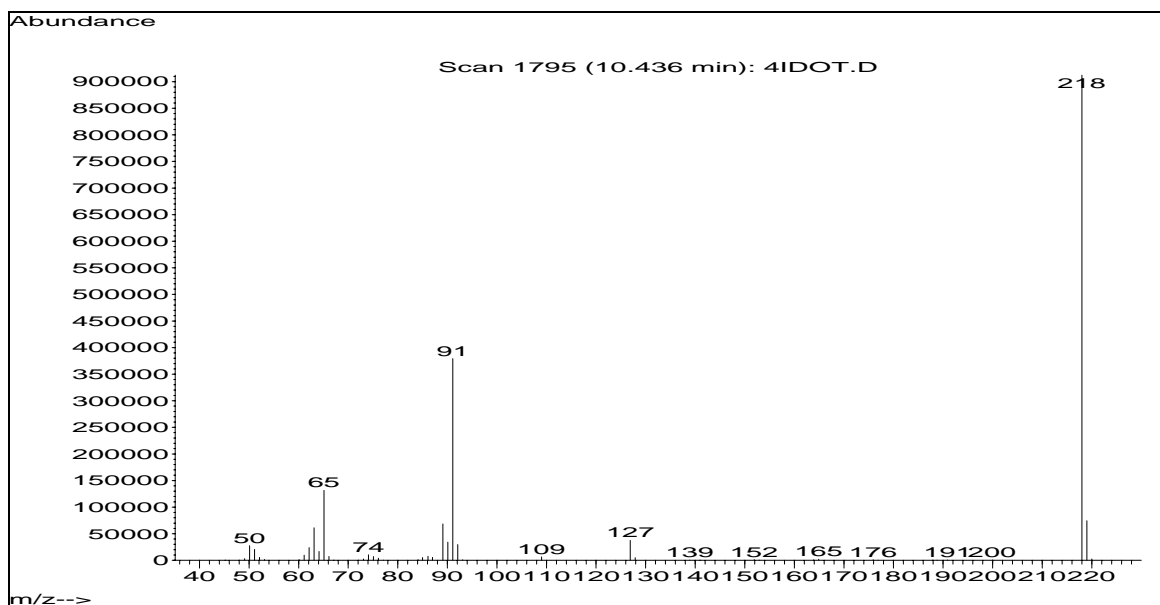
1. F.E. Paulic, *Catal. Rev.* 6 (1972) 49
2. M. Hujanen, Y.-Y. Linko, *Appl. Microbiol. Biotechnol.* 45 (1996) 307.
3. R. Datta, S.-P. Tsai, P. Bonsignore, S-H. Moon, J.R. Frank, *FEMS Microbiol. Rev.* 16 (1995) 221
4. A.Tullo, *Chem. Eng. News* 78 (2000) 44.
5. H. B. Tinkar US4072709 (1978)
6. Y. L. Borole, R. V. Chaudhari *Ind. Eng. Chem. Res.* 44 (2005) 9601
7. A.H.G. Cents, D.W.F. Brillman, G.F. Versteeg *Ind. Eng. Chem. Res.* 43 (2004) 7465
8. S. A. Ballard, US 2638479 (1953).
9. T. Bartik, B. Bartik, B.E. Hanson *J. Mol. Catal.* 85 (1993) 121.
10. R.M. Deshpande, B.M. Bhanage, S.S. Divekar, S.Kanagasabapathy, R.V. Chaudhari, *Ind. Eng. Chem. Res.* 37 (1998) 2391.
11. P.A. Ramachandran, R.V. Chaudhari, *Multiphase Catalytic Reactors* Gordon and Breach, London, (1983).
12. R.V. Chaudhari, R.V. Gholap, G. Emig, H. Hofmann, *Can. J. Chem.* 65 (1987) 744.
13. (a) U. J. Jauregui-Haza, E. P. Fontdevila, P. Kalck, A. M. Wilhelm, H. Delmas, *Catal. Today* 79 (2003) 409. (b) U. J. Jauregui-Haza, O. Diaz-Abin, A. M. Wilhelm, H. Delmas *Ind. Eng. Chem. Res.* 44 (2005) 9636.
14. a) R.M. Deshpande, R.V. Chaudhari, *Ind. Eng. Chem. Res.* 27 (1988) 1996. (b) R.M. Deshpande, R.V. Chaudhari, R.V. *J. Catal.* 115 (1989) 326.
15. A.H.G. Cents, D.W.F. Brillman, G.F. Versteeg *Ind. Eng. Chem. Res.* 43 (2004) 7465.
16. D.W.J. Marquardt, *Soc. Ind. Appl. Math.* 11 (1963) 431.
17. Y. L. Borole, R. V. Chaudhari *Ind. Eng. Chem. Res.* 44 (2005) 9601.
18. P. Pino, A. Major, F. Spindler, R. Tannenbaum, G. Bor, I.J. Horváth, *J. Organomet. Chem.* 411(1991) 65.
19. A.R. Martin, *Chem. Ind. (London)* (1954) 1536.
20. M. Niwa, M. Yamaguchi, *Shokubai*, 3 (1961) 264.
21. P. Pino, F. Oldani F G. Consigho, *J. Organomet. Chem.* 250 (1983) 491.
22. R.F. Heck, D.S.Breslow, *J. Am. Chem. Soc.*, 83 (1961) 4023.

- 
23. R.A. Sheldon , R.S. Downing *App. Catal. A: General* 189 (1999) 163–183
  24. J-K Choi, Y-K Chang, S. Y. Hong *Tetrahedron Lett.* 29 (1988) 1967.
  25. S. Mukhopadhyay *Org. Proc. Res. Dev.* 3 (1999) 365
  26. P. Fristrup, L. B. Johansen, C. H. Christensen *Chem. Commun.* (2008) 2750.
  27. H. B. Tinkar US4072709 (1978).
  28. K. Tanabe, W. F. Hoelderich, *Appl. Catal. A: Gen.* 181 (1999) 399.
  29. S. J. Sonheiemer, N. J. Bruce, C. A. Fyfe, *JMS-Rev. Macromol. Chem. Phys.* C26 (1986) 353.
  30. M. Streat, “Ion Exchange for Industry”, Ellis Horwood, Chichester (1988)

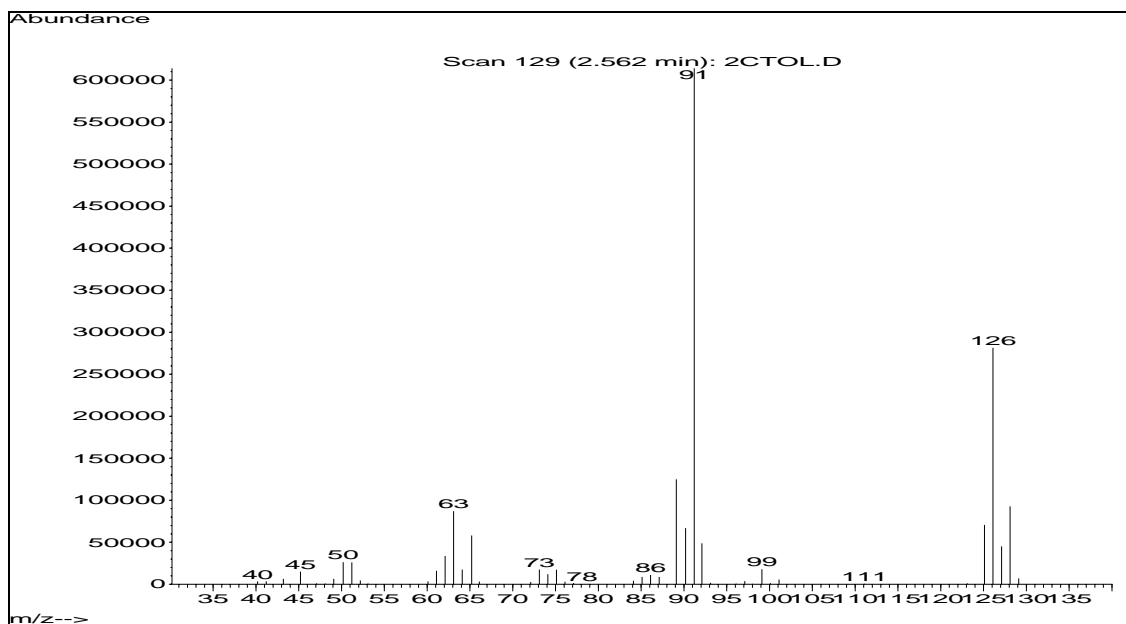
# Appendix-I



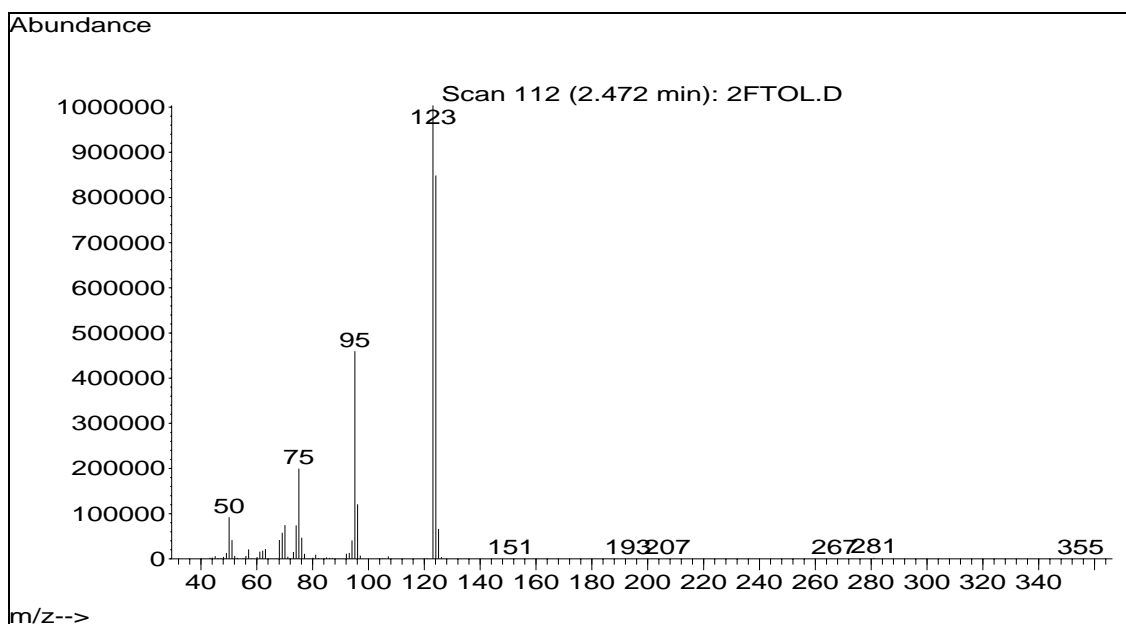
GC-MS Spectrum of 4-fluorobenzaldehyde (70 eV, EI)



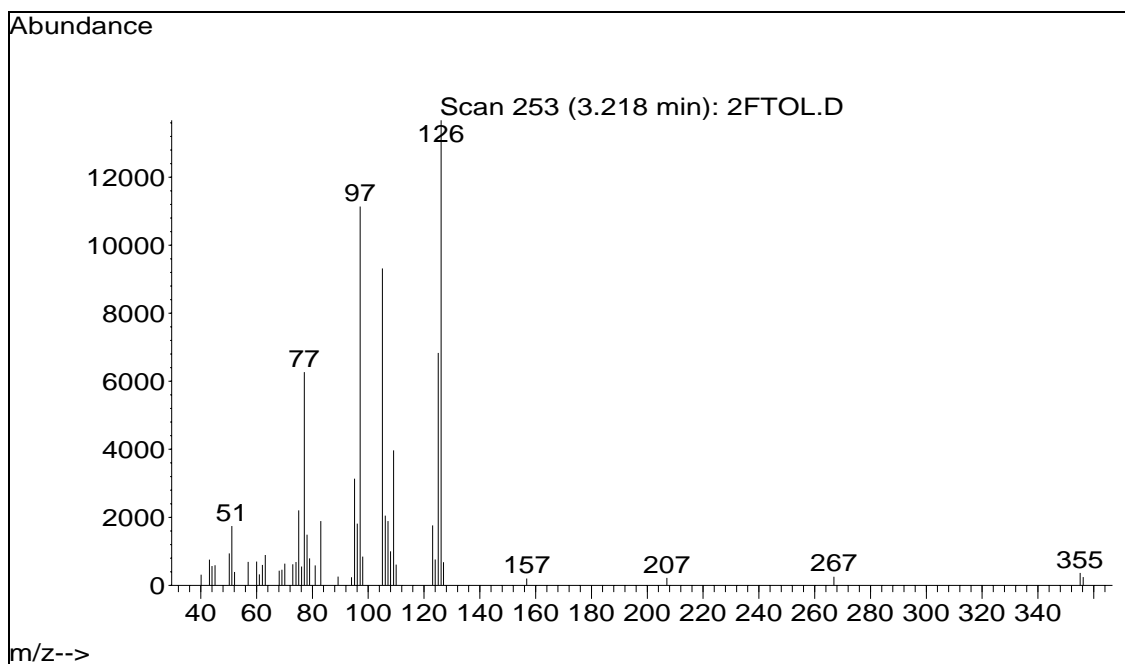
GC-MS Spectrum of 4-iodobenzaldehyde (70 eV, EI)



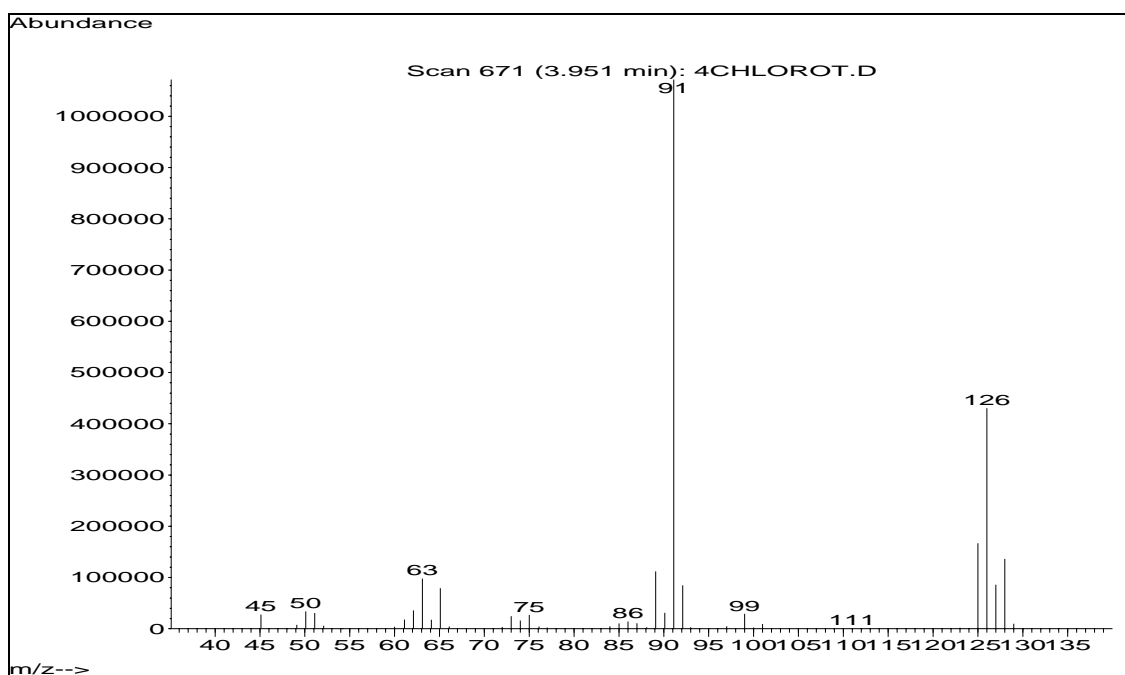
**GC-MS Spectrum of 2-chlorobenzaldehyde (70 eV, EI)**



**GC-MS Spectrum of 2-fluorobenzaldehyde (70 eV, EI)**

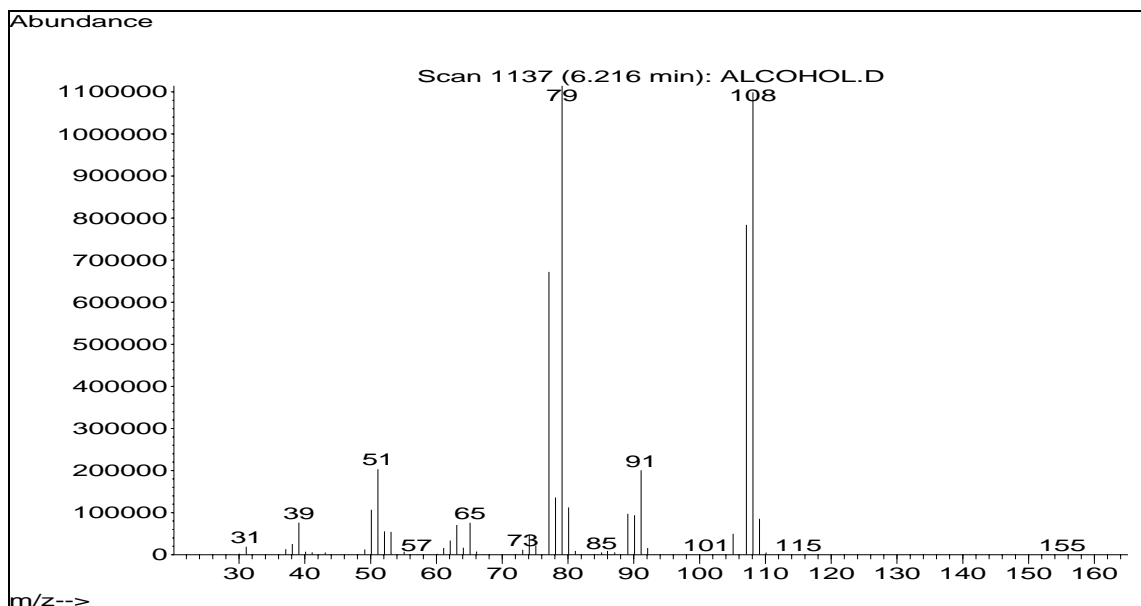


**GC-MS Spectrum of 4-fluorobenzyl alcohol (70 eV, EI)**

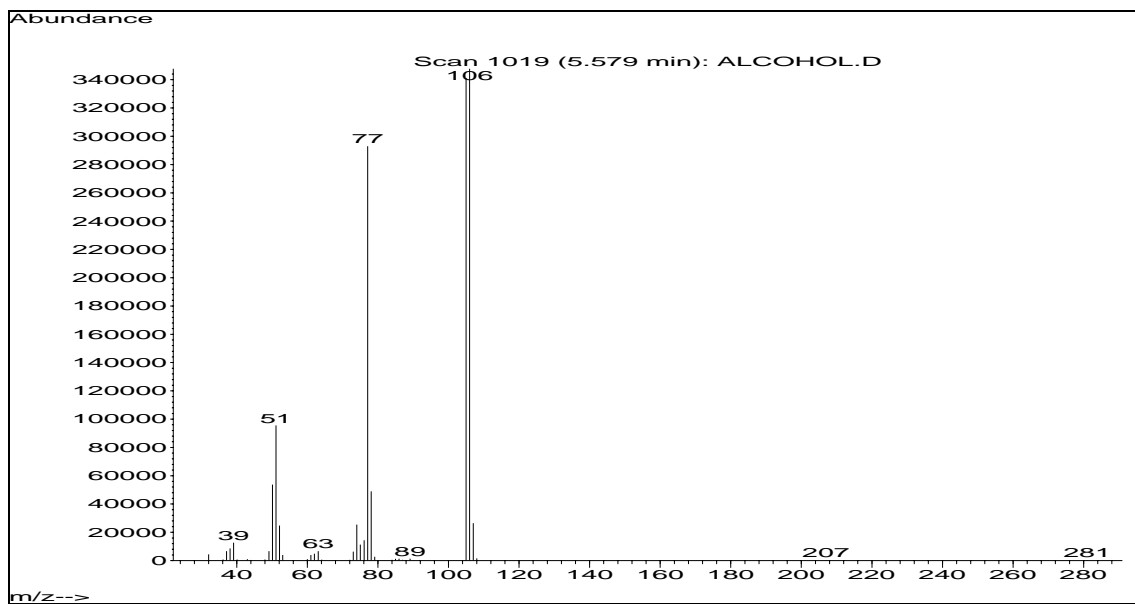


**GC-MS Spectrum of 4-chlorobenzaldehyde (70 eV, EI)**

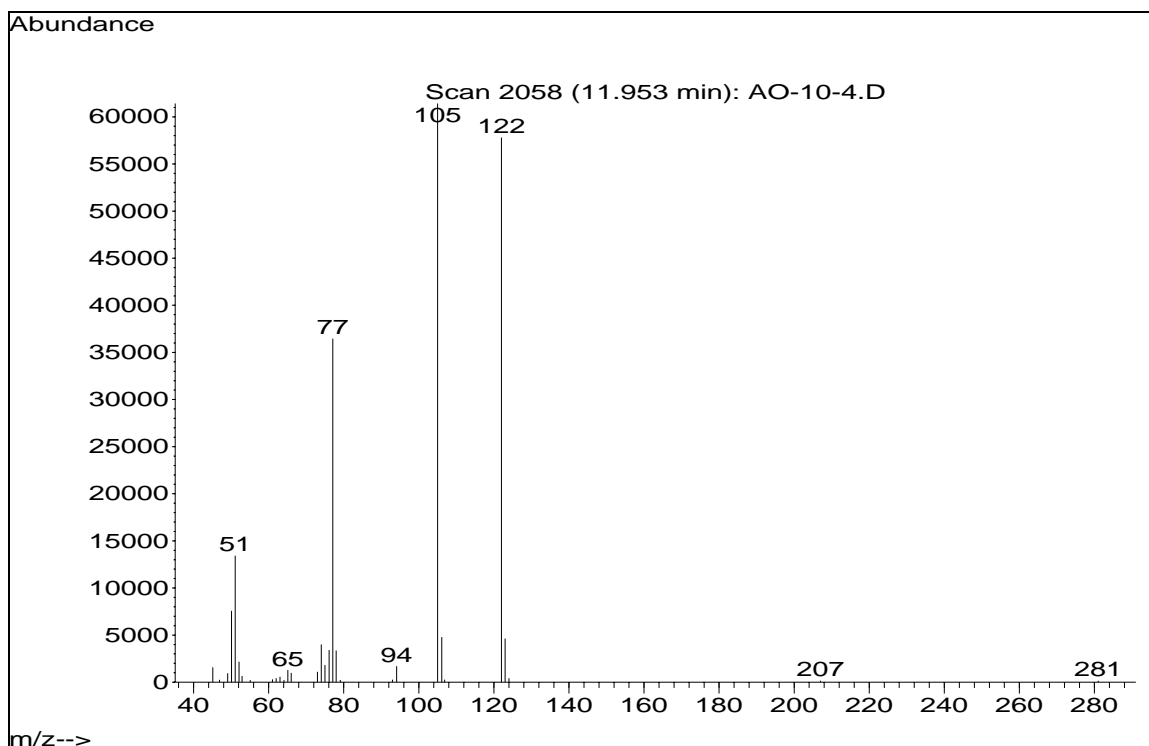




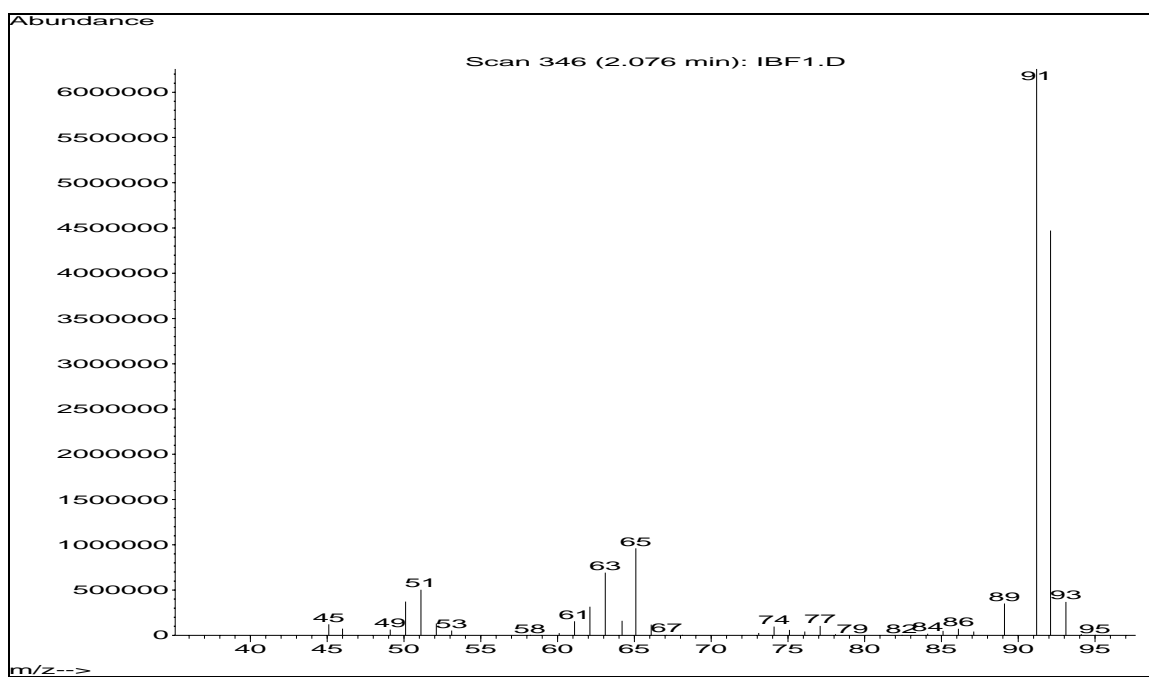
GC-MS Spectrum of benzyl alcohol (70 eV, EI)



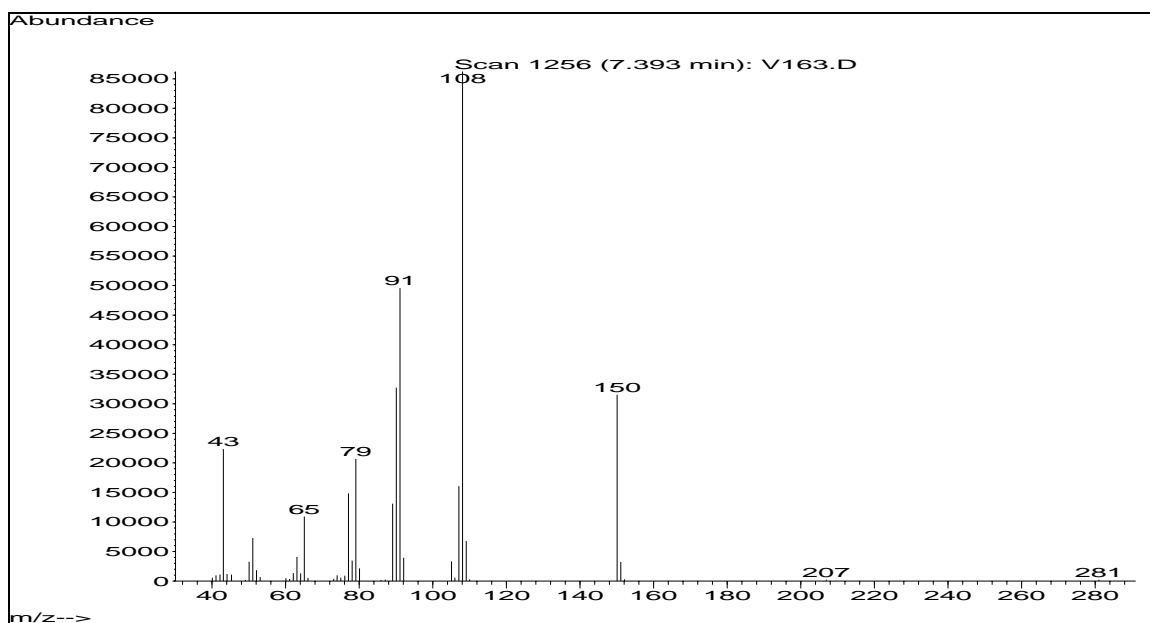
GC-MS Spectrum of benzaldehyde (70 eV, EI)



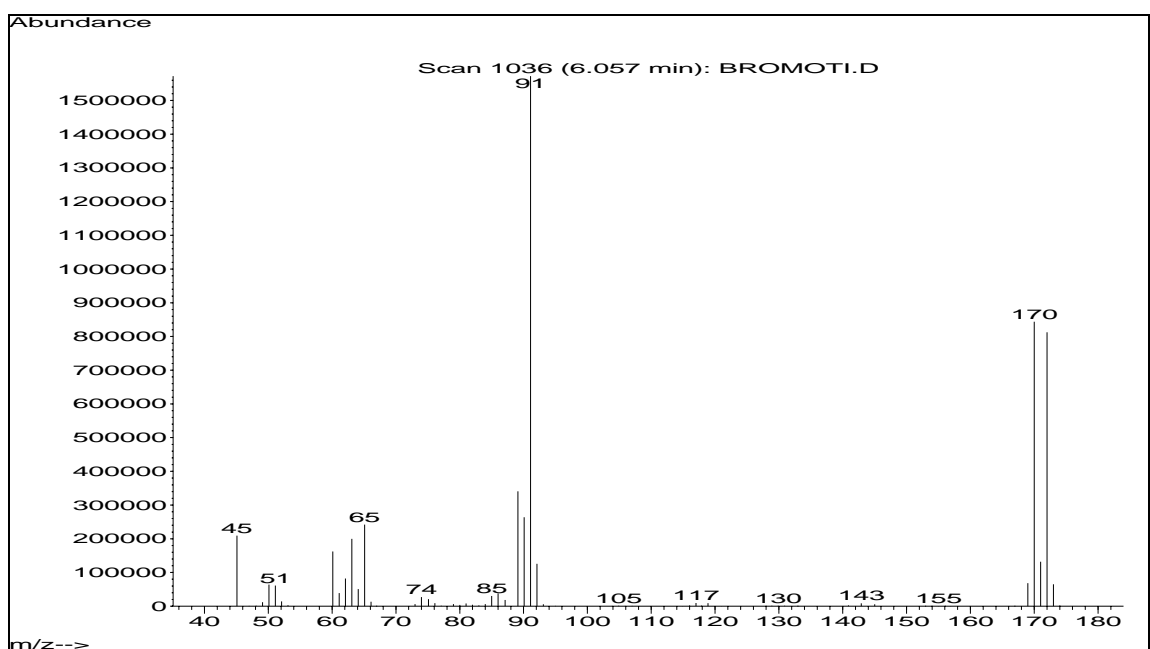
**GC-MS Spectrum of benzoic acid (70 eV, EI)**



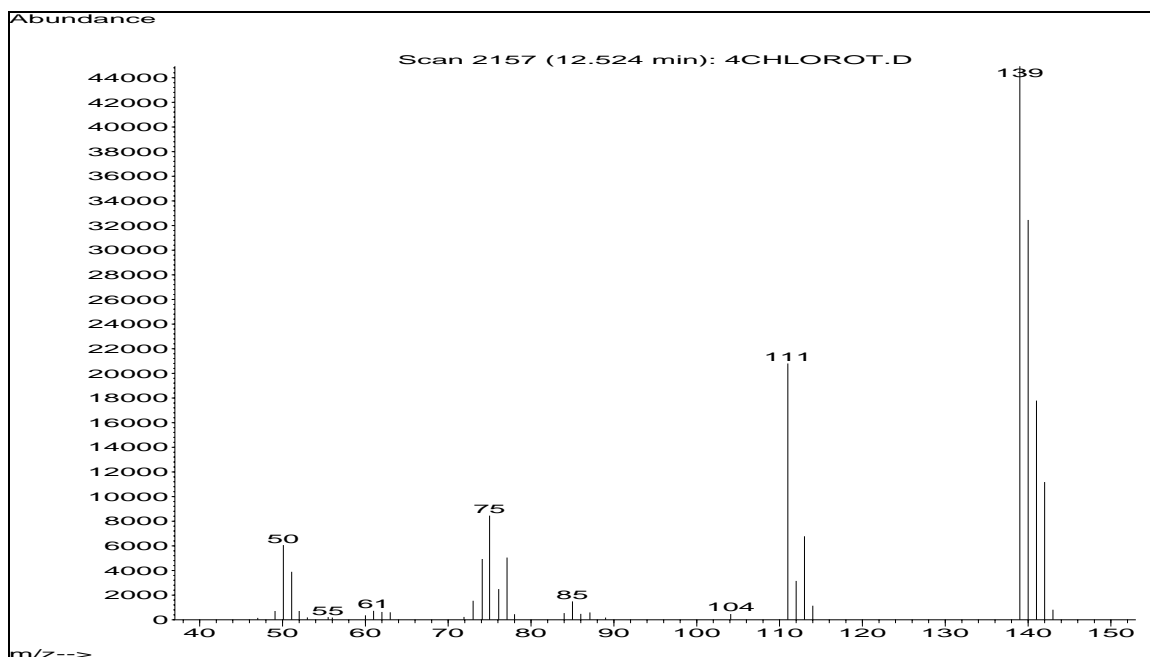
**GC-MS Spectrum of toluene (70 eV, EI)**



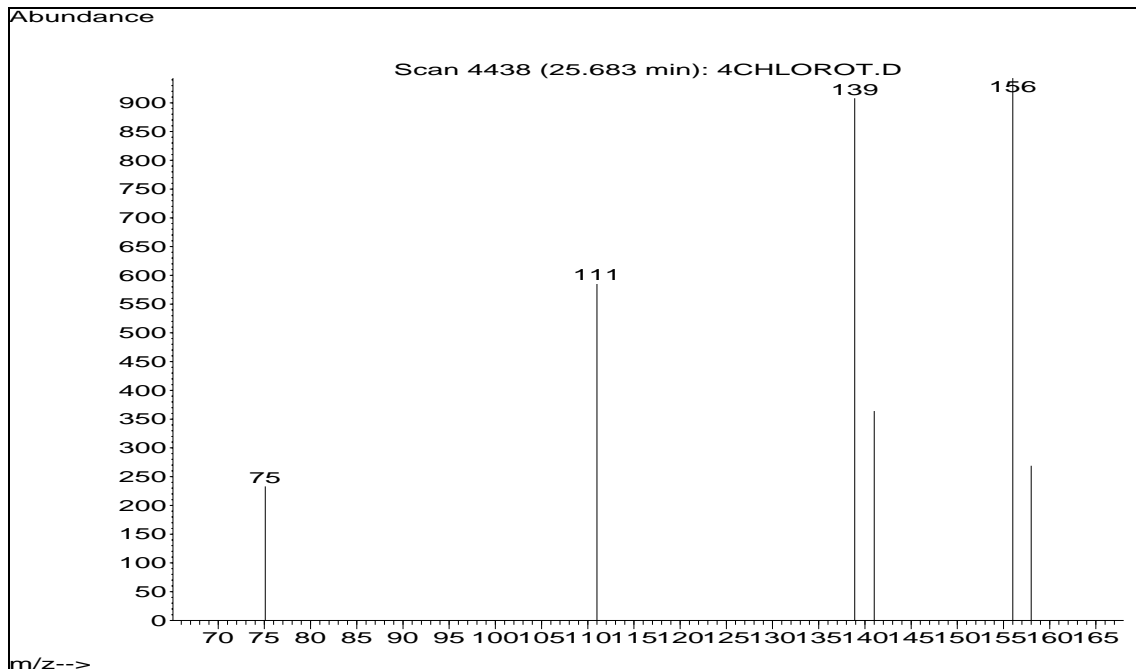
**GC-MS Spectrum of benzyl acetate (70 eV, EI)**



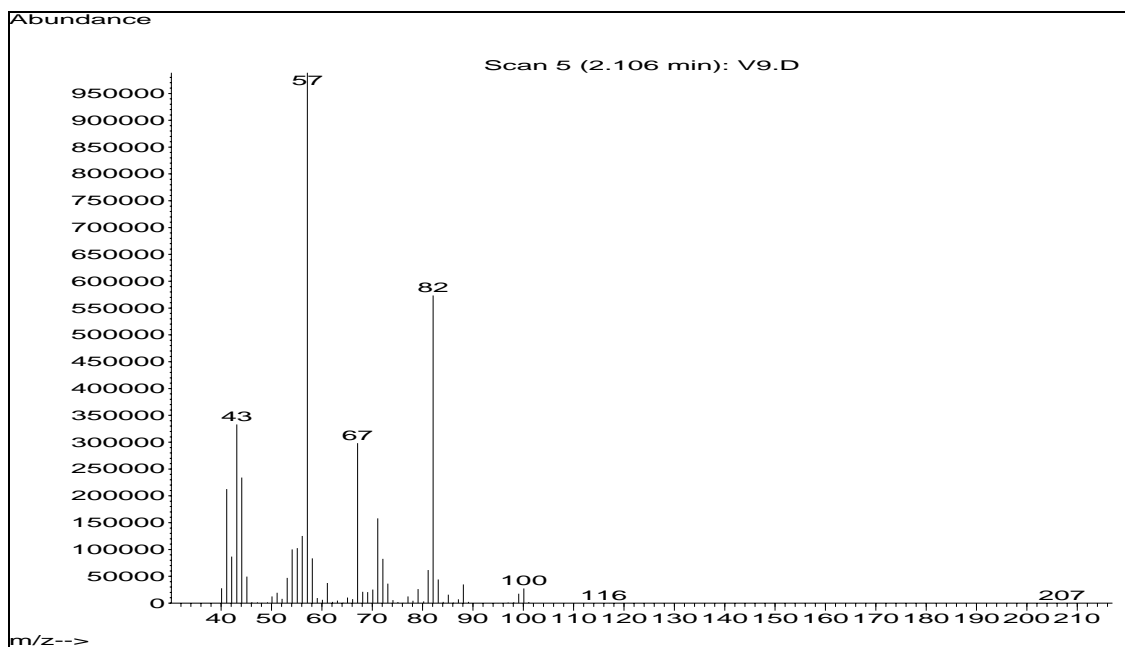
**GC-MS Spectrum of 4-bromobenzaldehyde (70 eV, EI)**



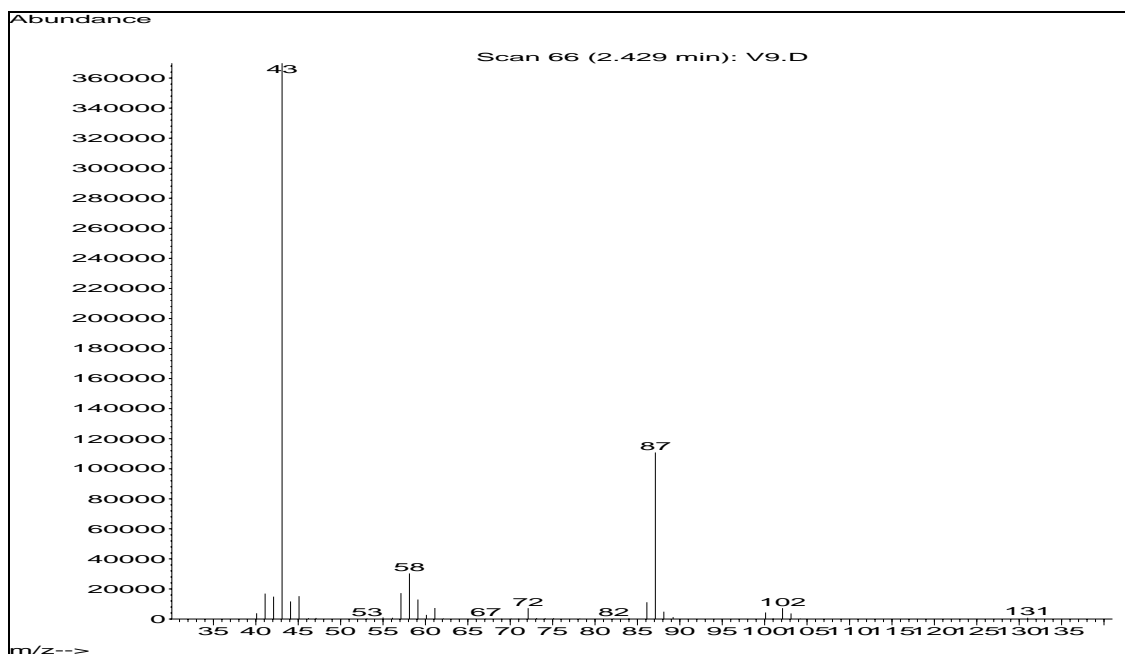
**GC-MS Spectrum of 4-chlorobenzyl alcohol (70 eV, EI)**



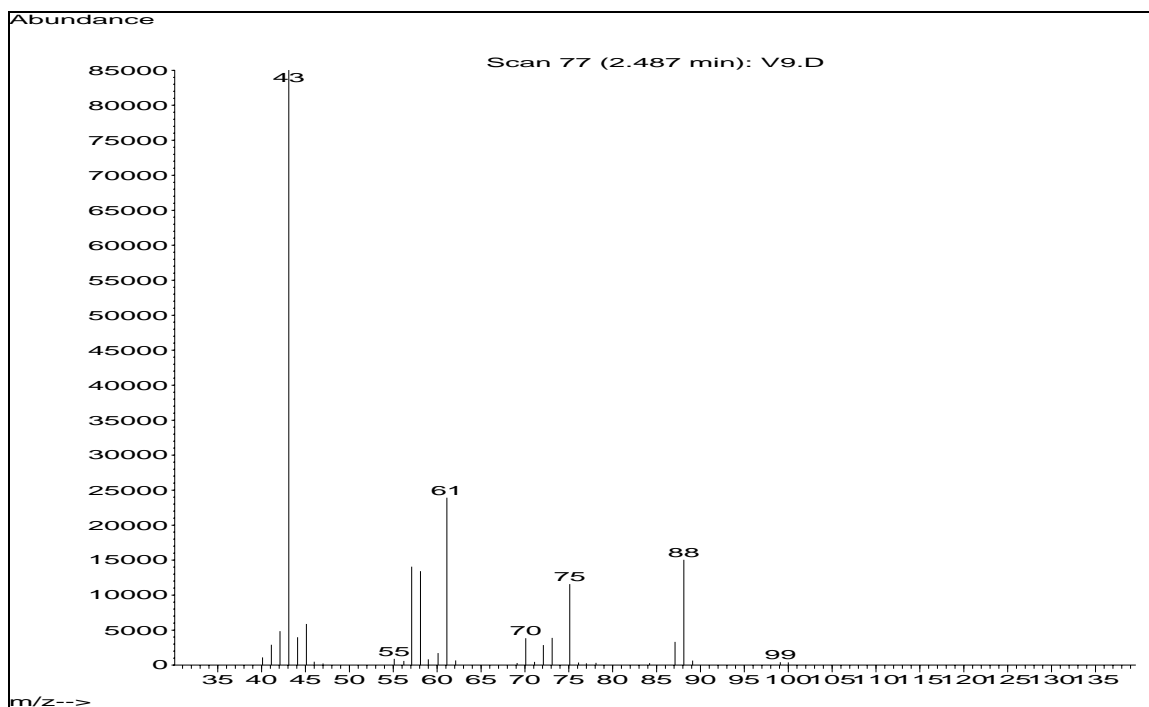
**GC-MS Spectrum of 4-chlorobenzoic acid (70 eV, EI)**



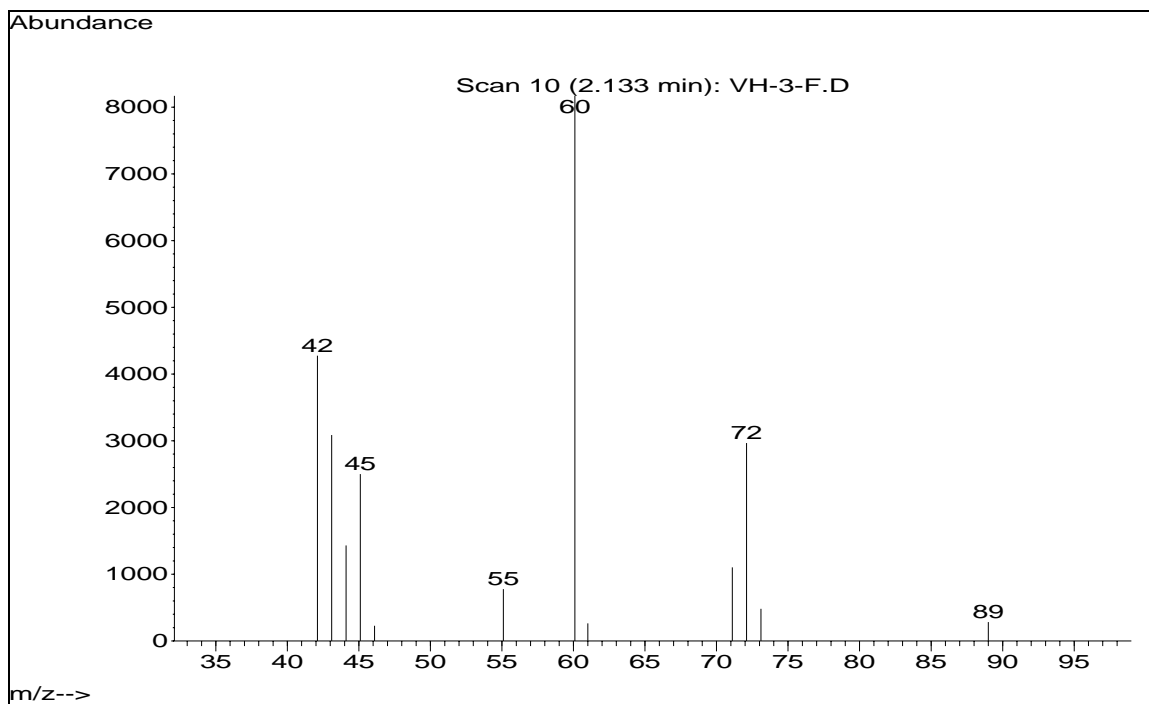
GC-MS Spectrum of 3-acpa (70 eV, EI)



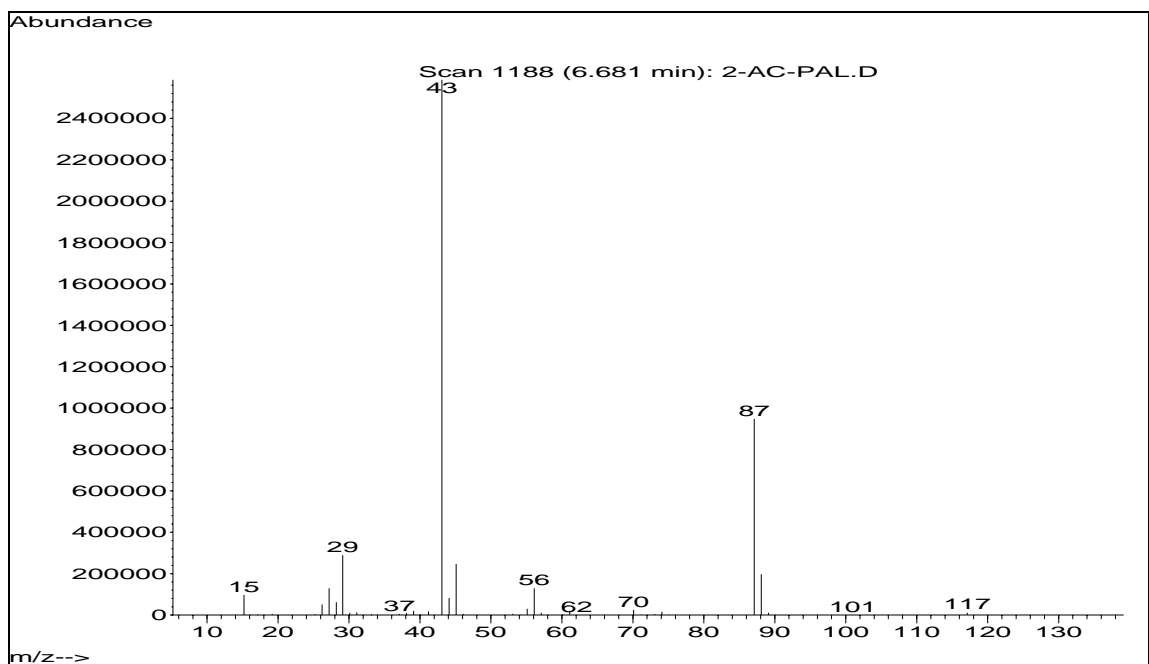
GC-MS Spectrum of 2-acpa (70 eV, EI)



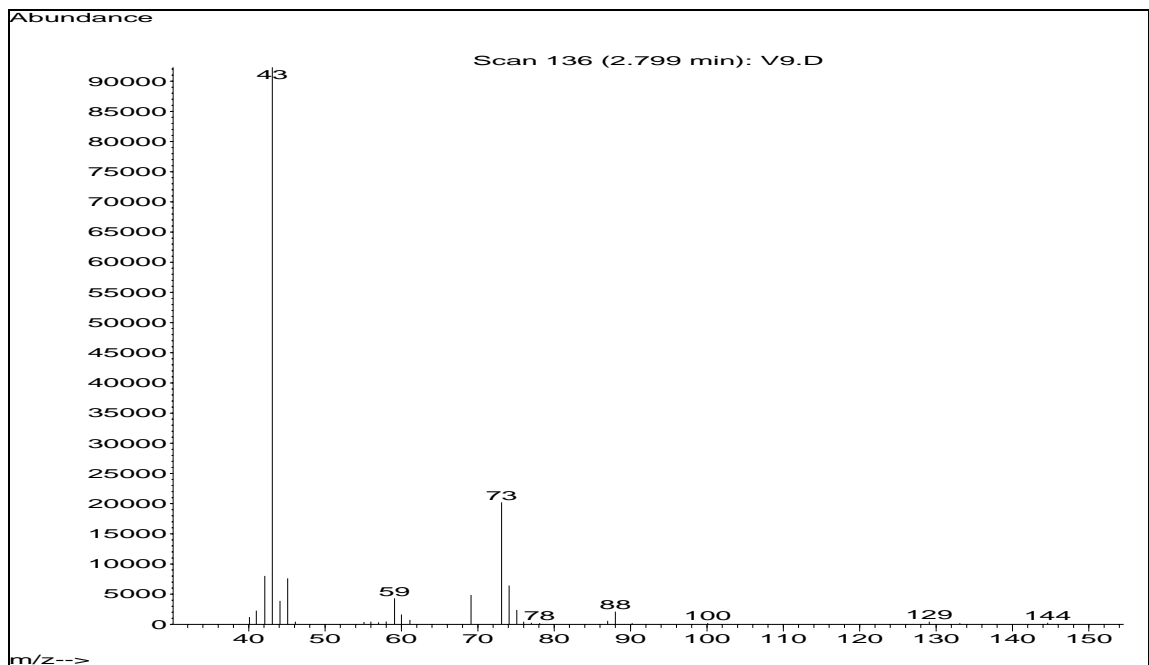
GC-MS Spectrum of 2-hpa (70 eV, EI)



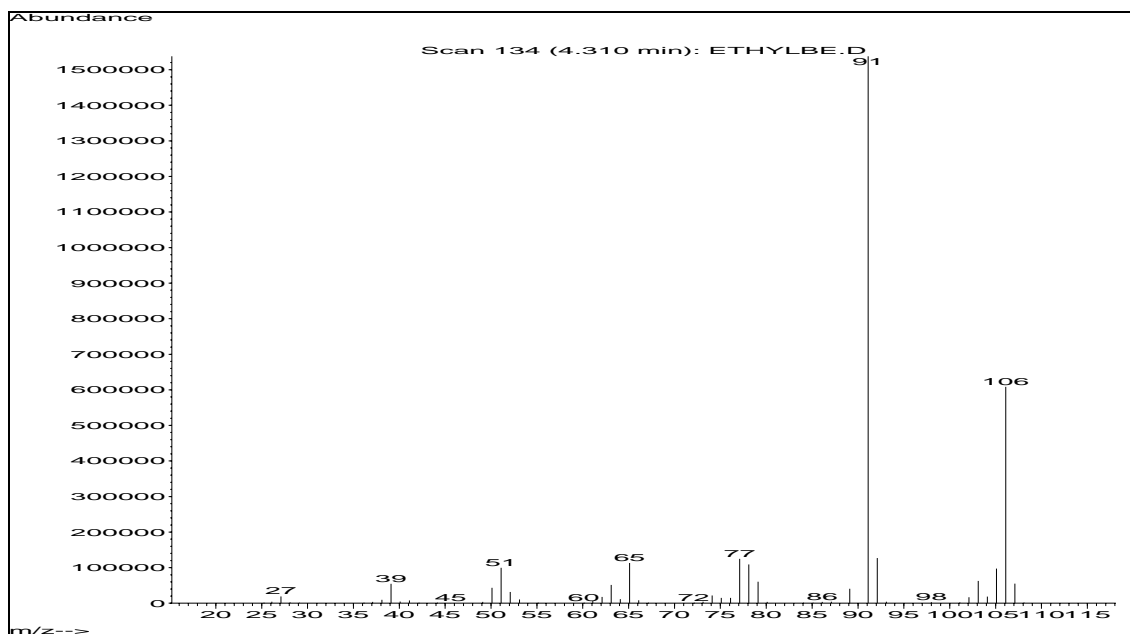
GC-MS Spectrum of 3-hpa (70 eV, EI)



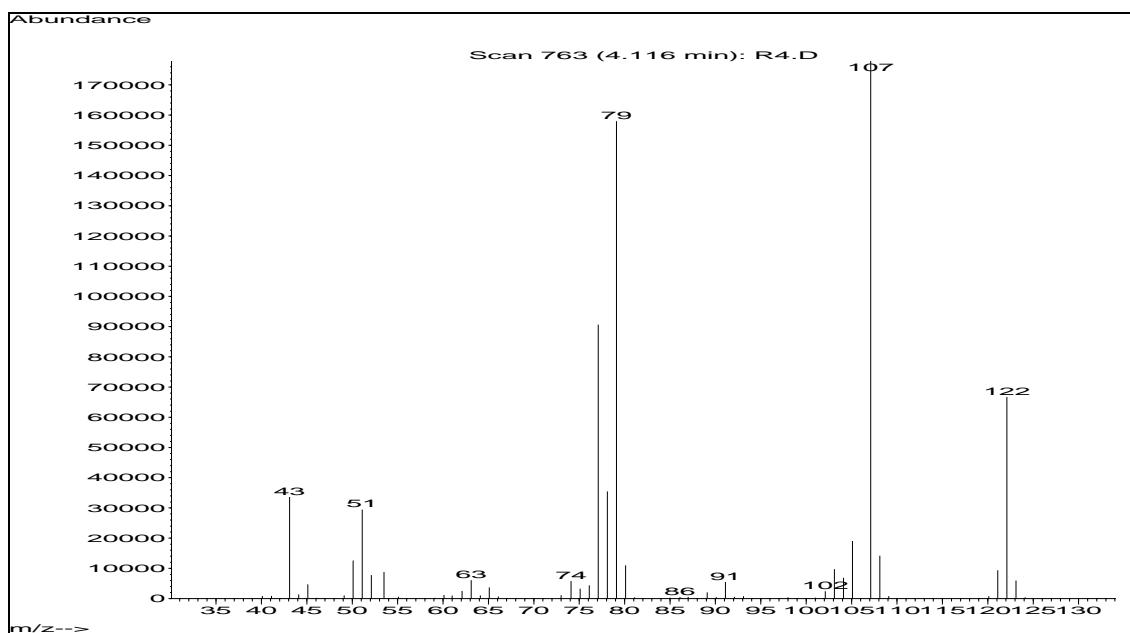
GC-MS Spectrum of 2acpal (70 eV, EI)



GC-MS Spectrum of 3-acpa (70 eV, EI)

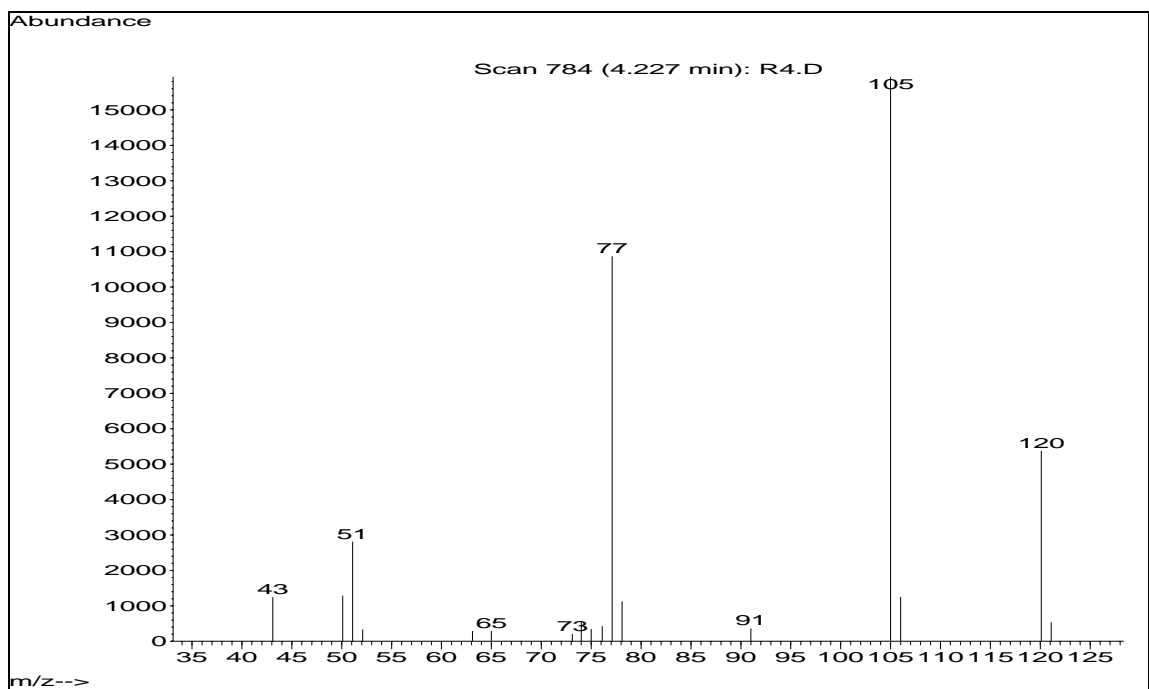


**GC-MS Spectrum of ethylbenzene (70 eV, EI)**

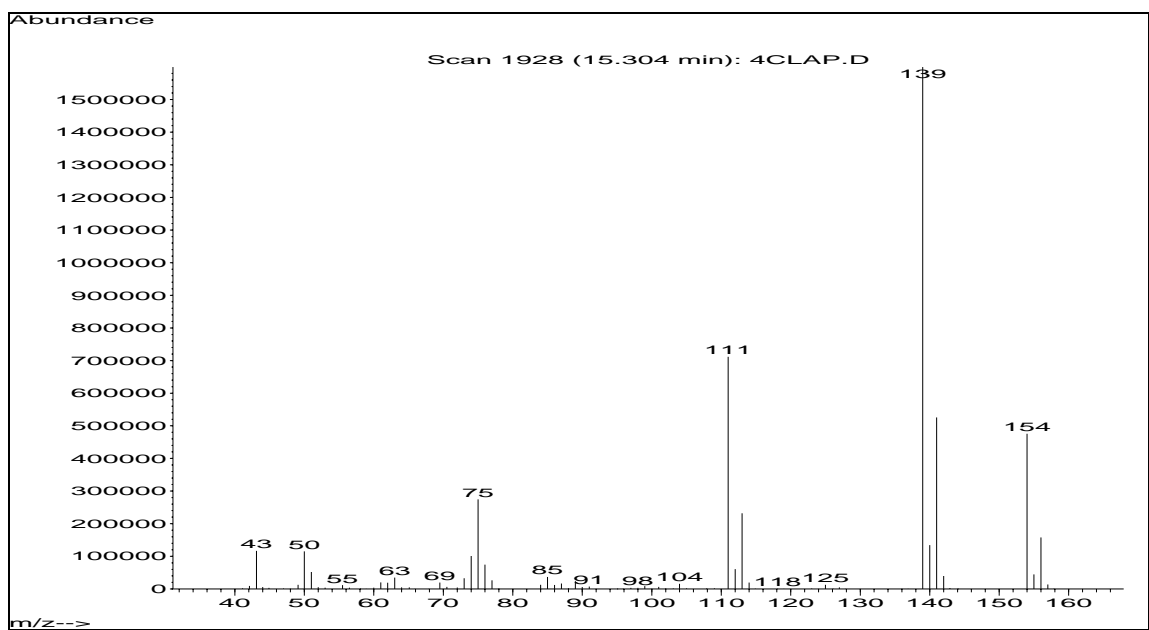


**GC-MS Spectrum of 1-phenylethanol (70 eV, EI)**

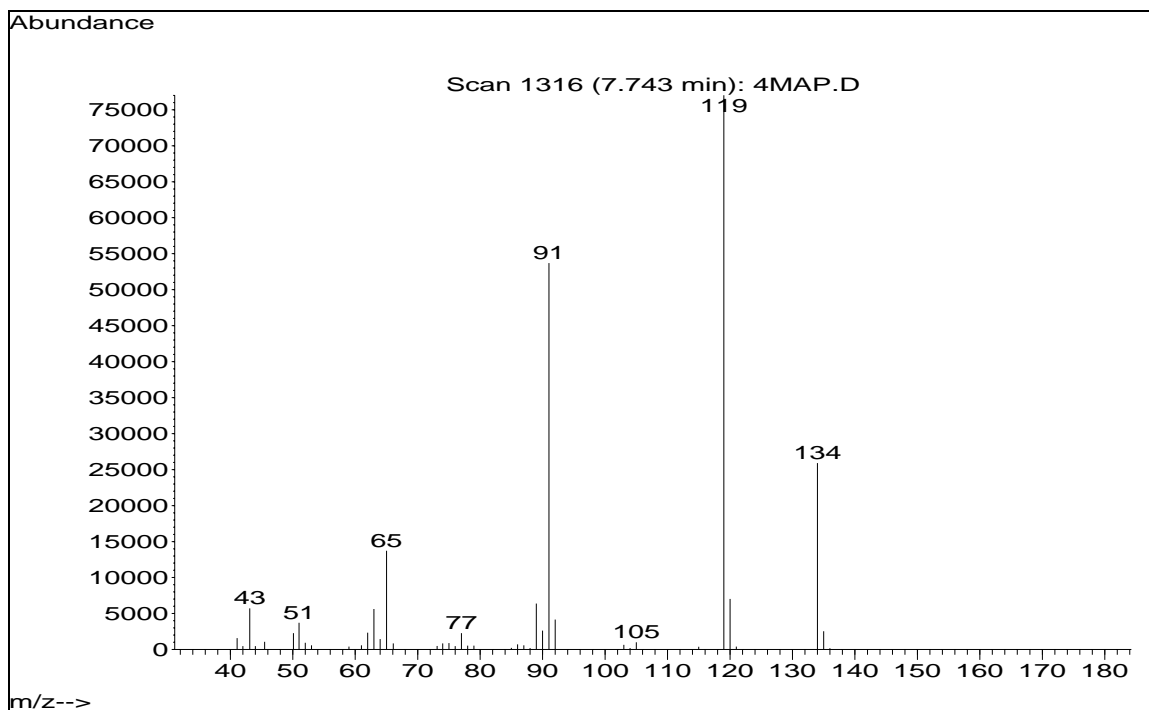




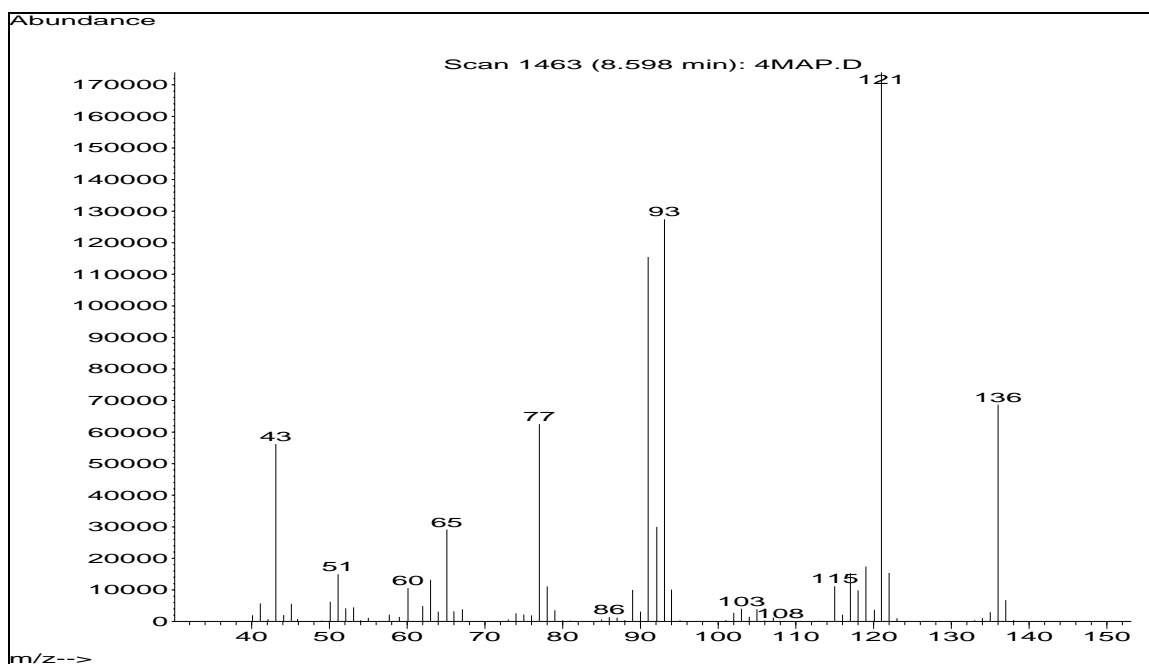
**GC-MS Spectrum of acetophenone (70 eV, EI)**



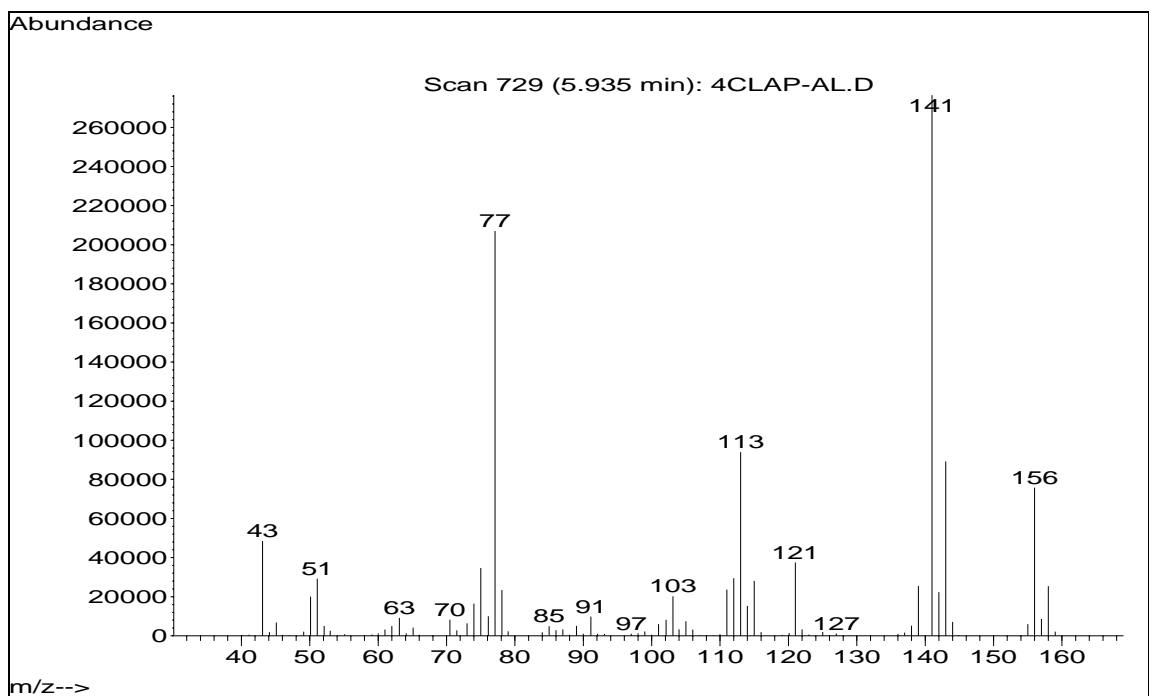
**GC-MS Spectrum of 4-chloro acetophenone (70 eV, EI)**



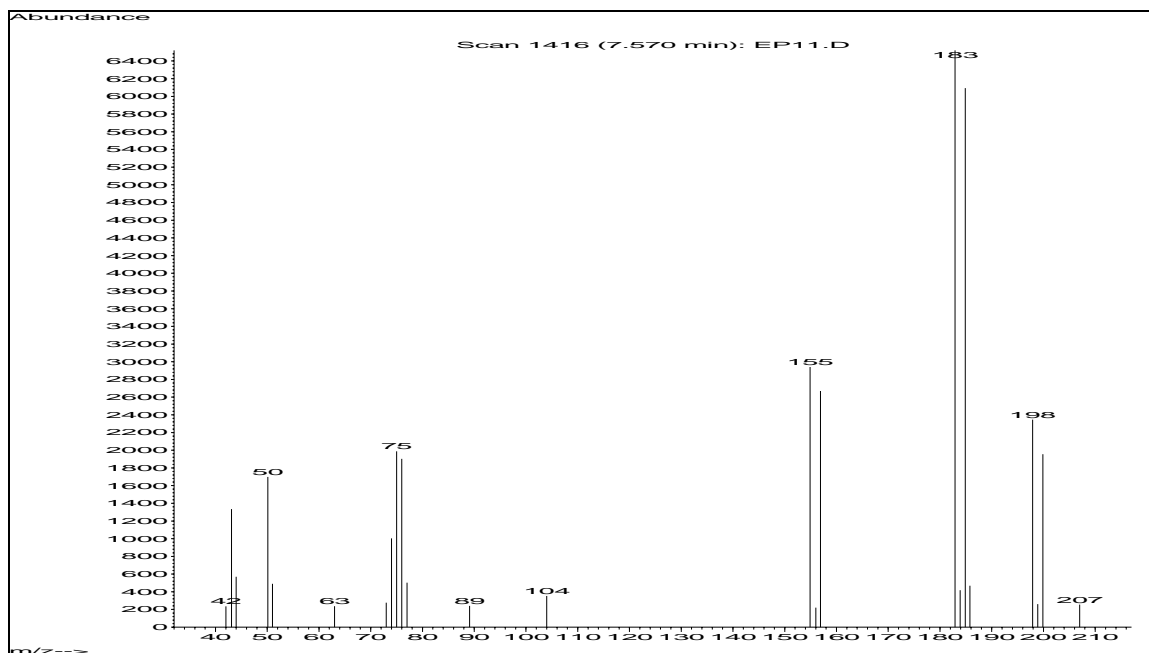
**GC-MS Spectrum of 4-methyl acetophenone (70 eV, EI)**



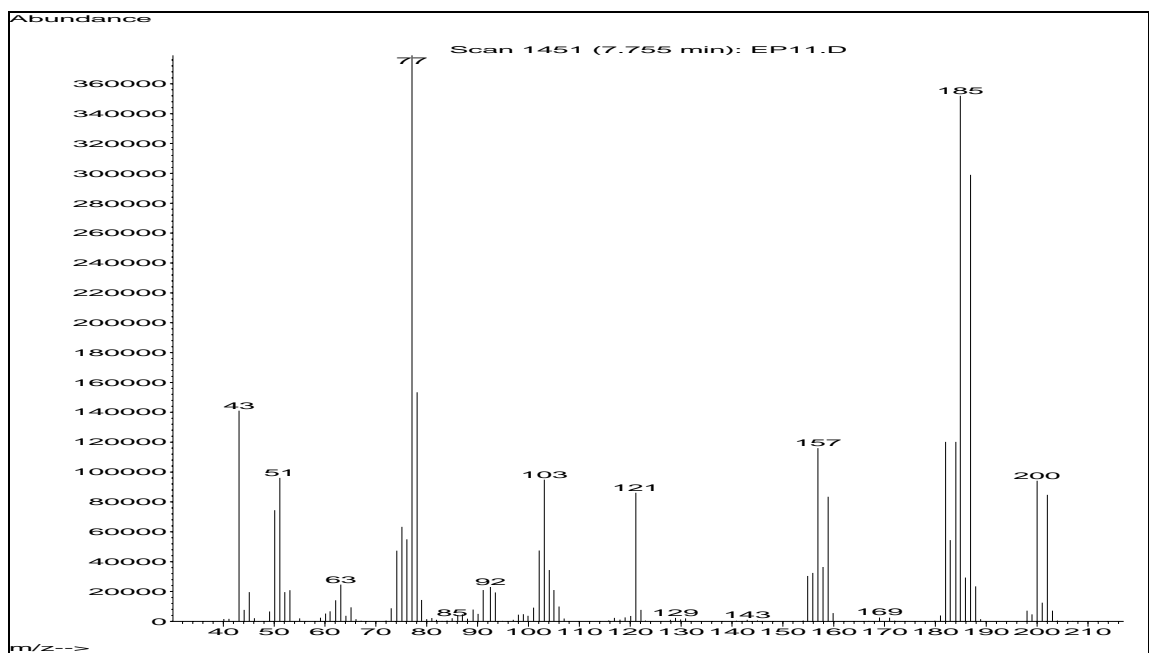
**GC-MS Spectrum of 4-methyl (phenylethanol) (70 eV, EI)**



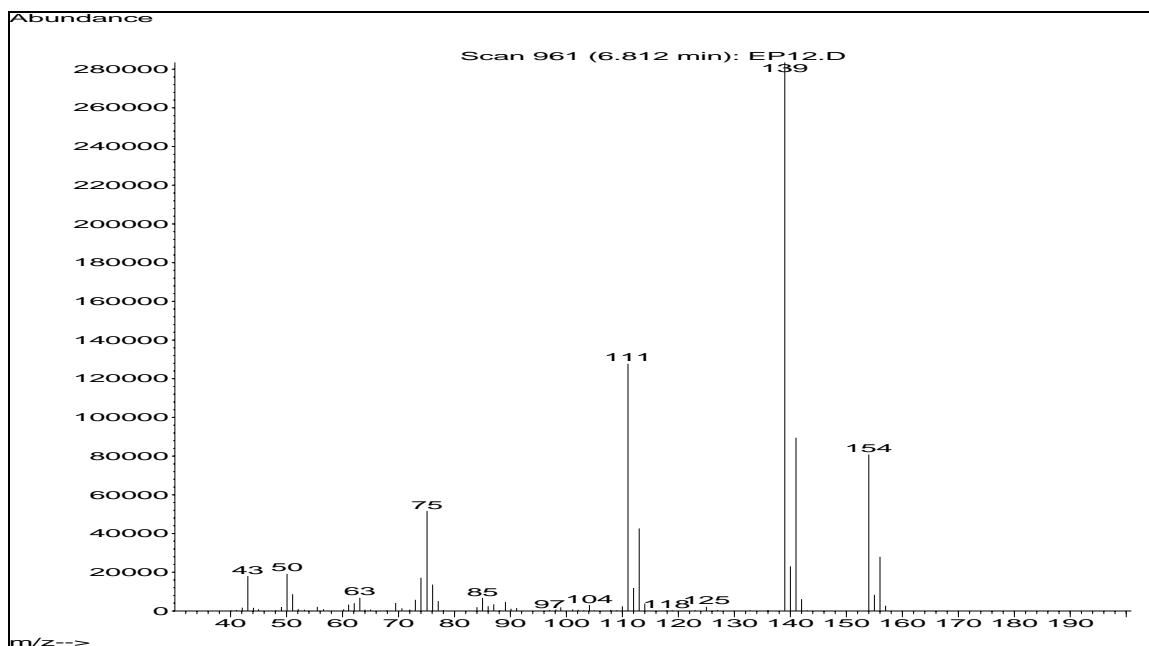
**GC-MS Spectrum of 4-chloro (phenylethanol) (70 eV, EI)**



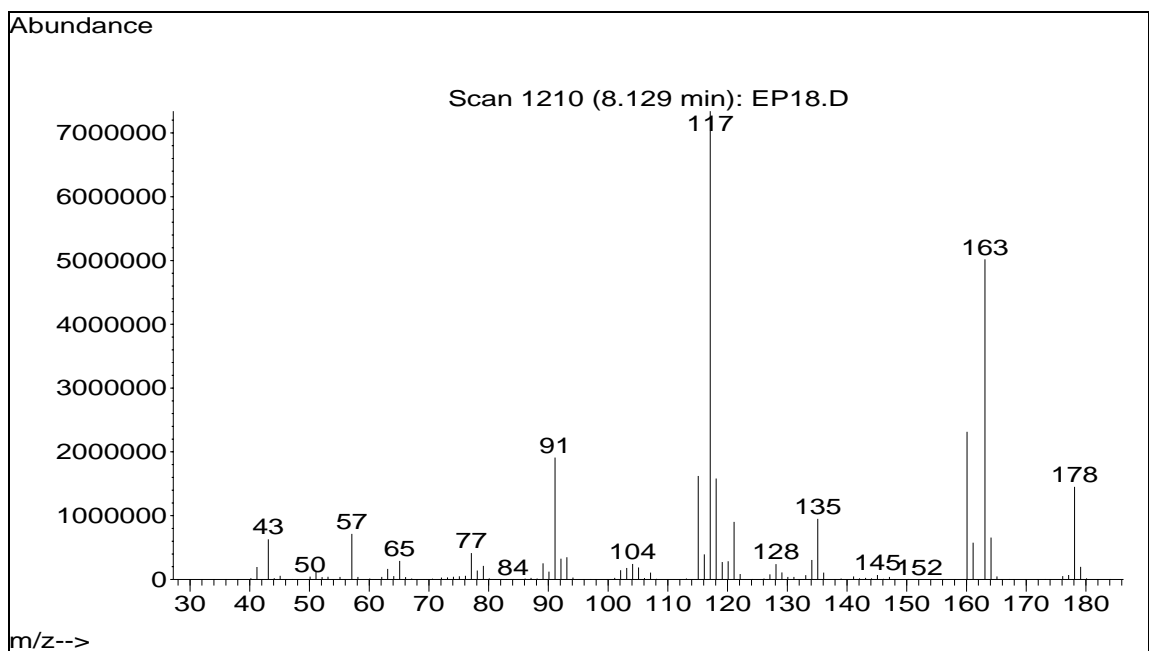
**GC-MS Spectrum of 4-bromoacetophenone (70 eV, EI)**



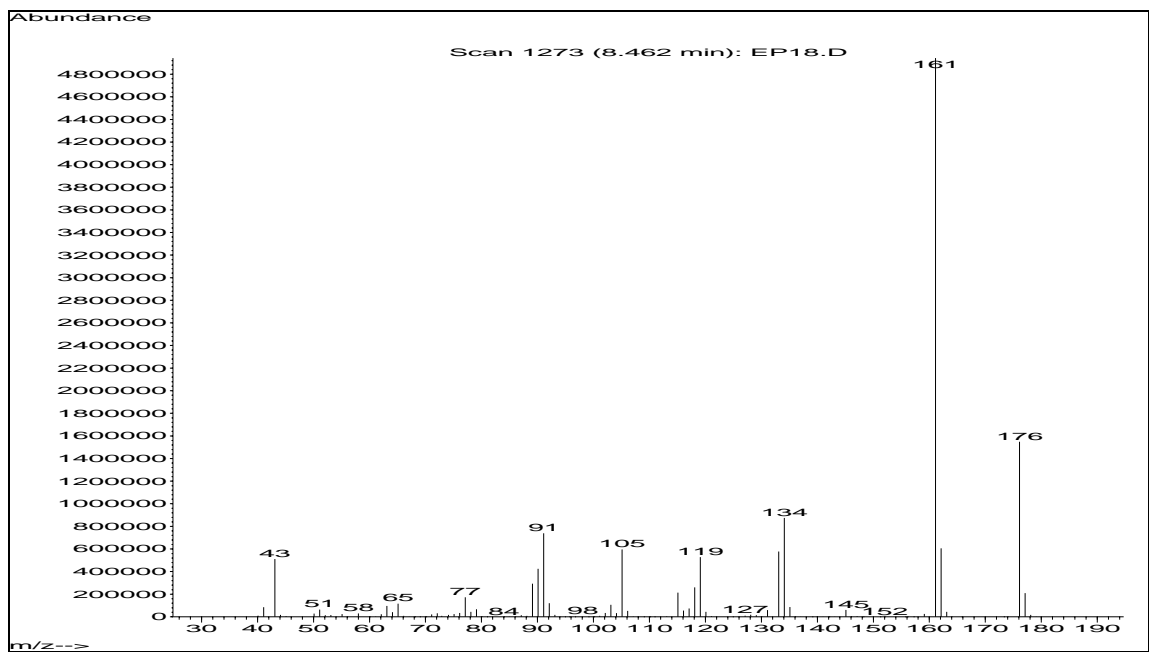
**GC-MS Spectrum of 4-bromo (phenylethanol) (70 eV, EI)**



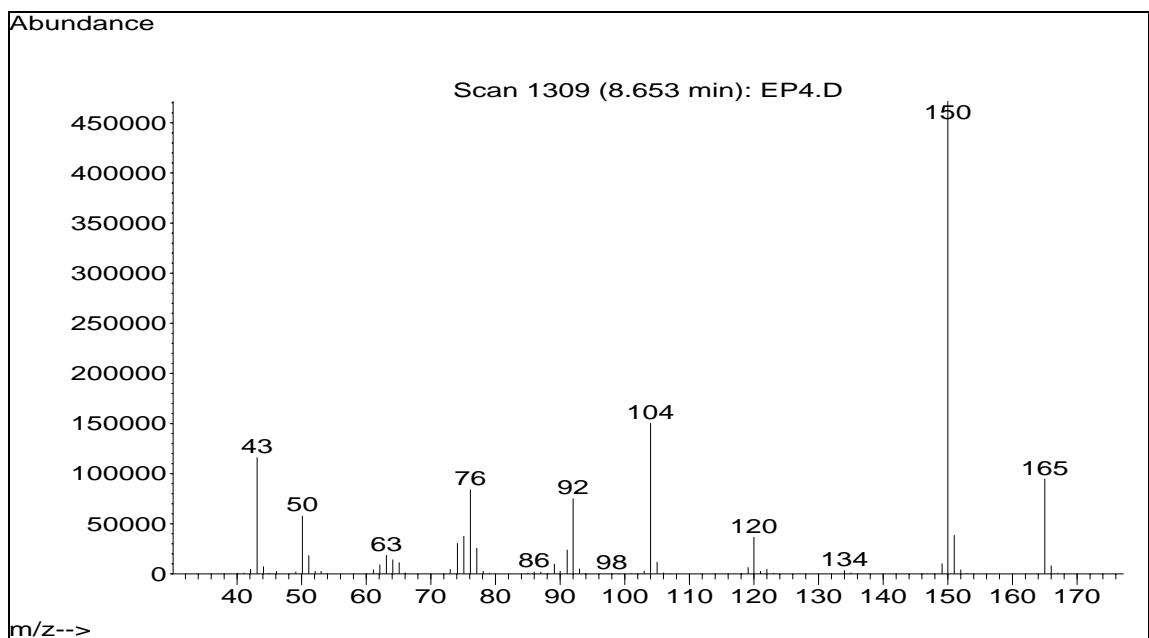
**GC-MS Spectrum of 4-chloroacetophenone (70 eV, EI)**



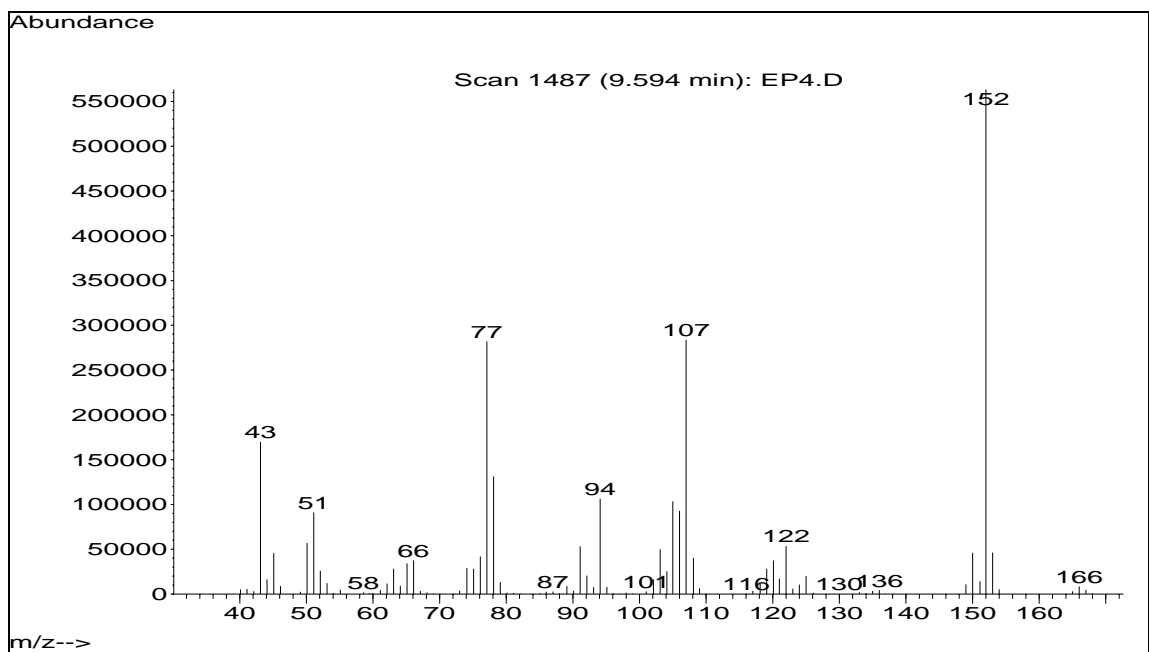
**GC-MS Spectrum of 4-isobutyl phenylethanol (70 eV, EI)**



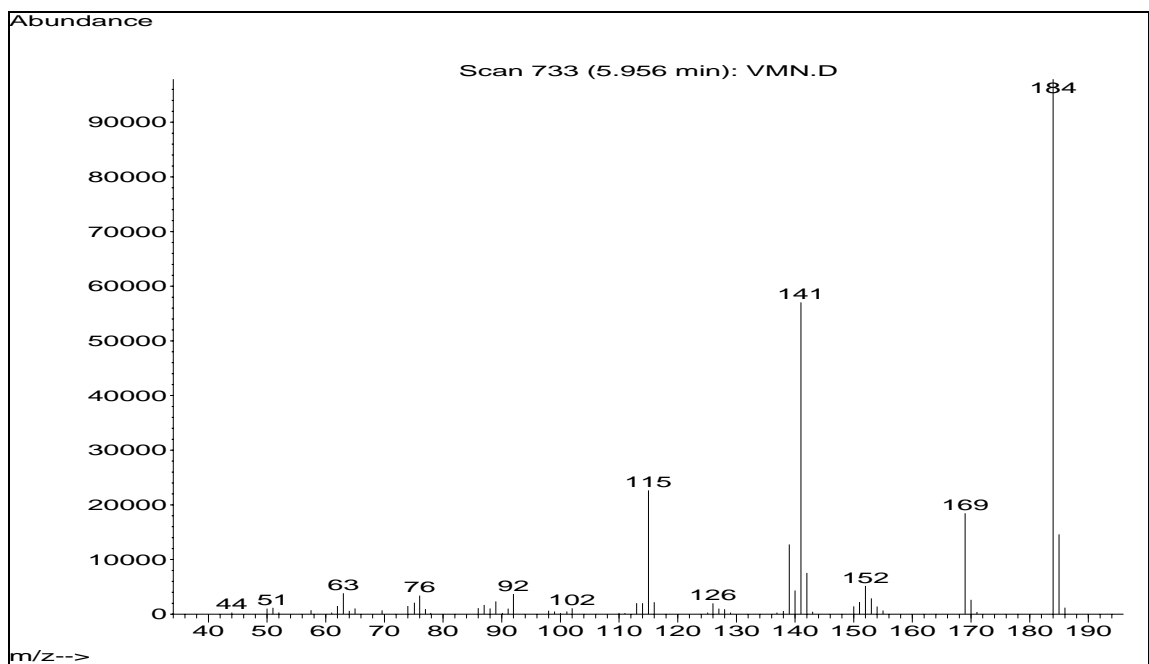
**GC-MS Spectrum of 4-isobutyl acetophenone (70 eV, EI)**



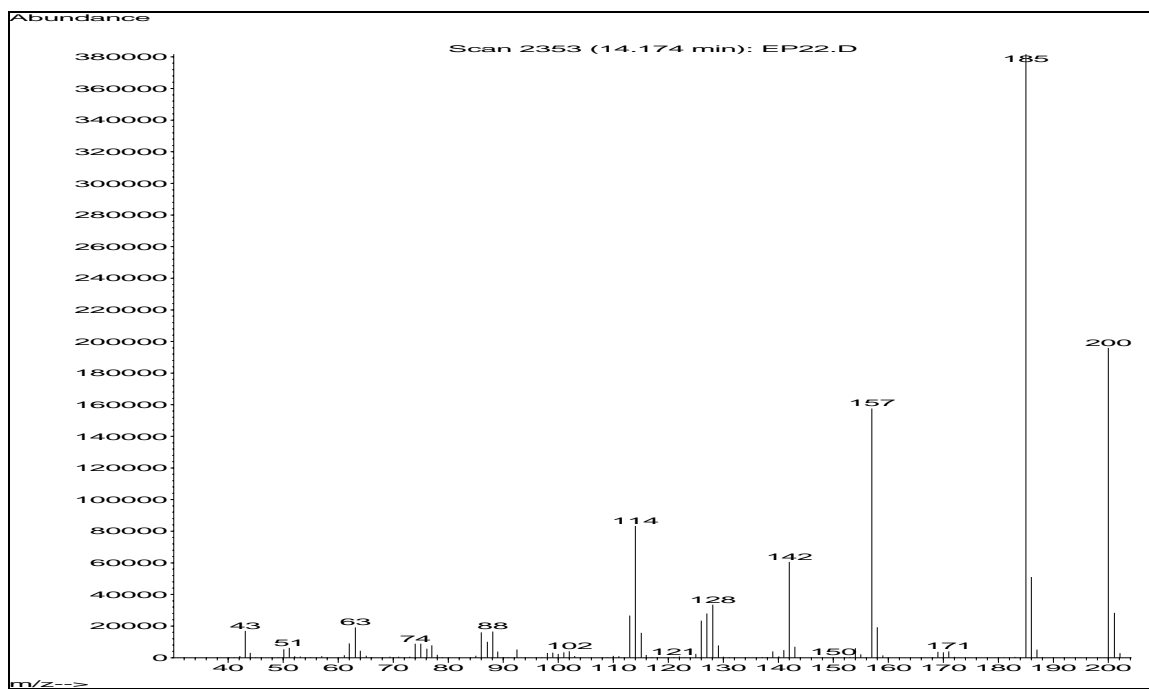
**GC-MS Spectrum of 4-nitro acetophenone (70 eV, EI)**



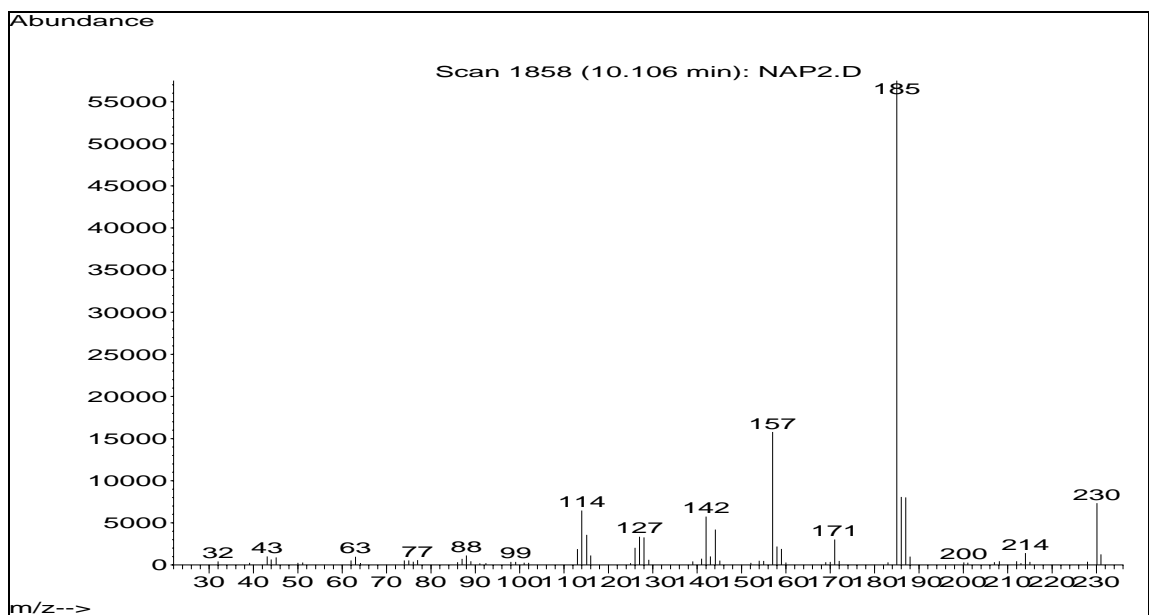
**GC-MS Spectrum of 4-nitro phenylethanol (70 eV, EI)**



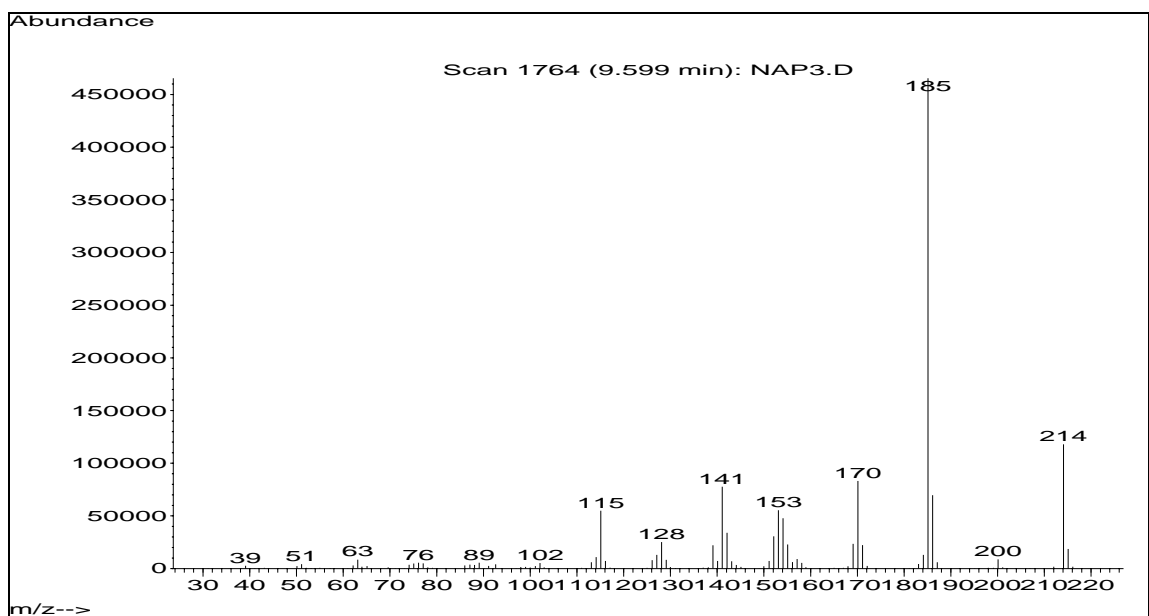
**GC-MS Spectrum of MVN (70 eV, EI)**



**GC-MS Spectrum of 2-acetyl-6-methoxynaphthalene (70 eV, EI)**

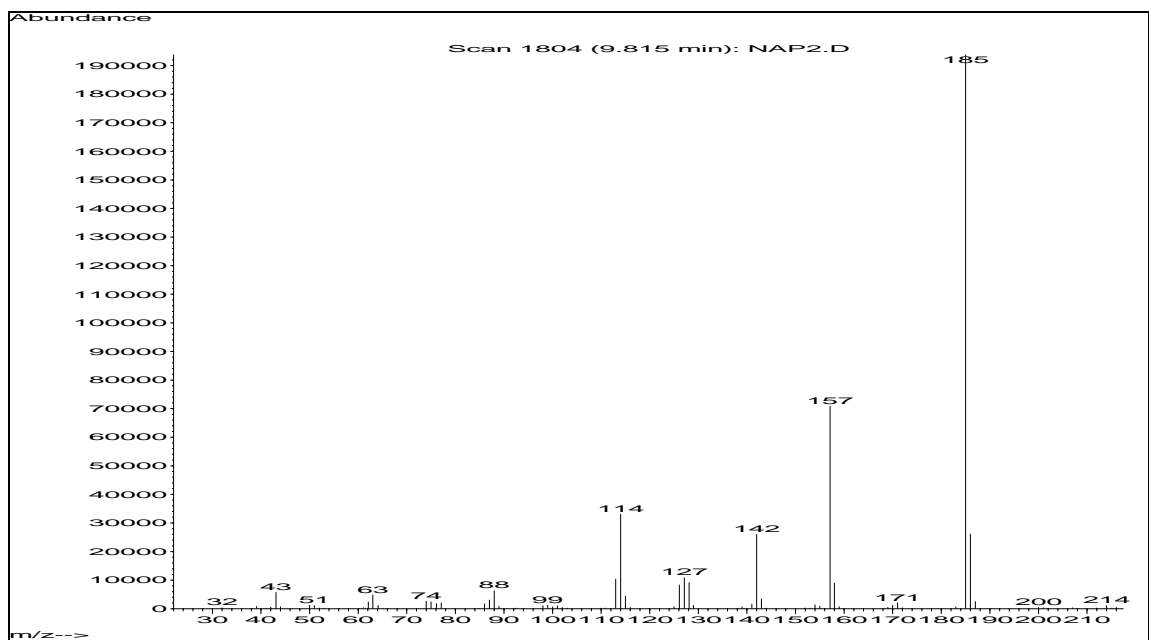


GC-MS Spectrum of *dl*-naproxen (70 eV, EI)



GC-MS Spectrum of 2-MNP (70 eV, EI)





**GC-MS Spectrum of 3-MNP (70 eV, EI)**

## Appendix-II

### List of abbreviations

|             |   |  |
|-------------|---|--|
| %C          | : | % Conversion                                 |
| AAS         | : | Atomic absorption spectroscopy               |
| B.P.        | : | Boiling Point                                |
| M.P.        | : | Melting point                                |
| Conc.       | : | Concentration                                |
| C-T         | : | Concentration-time                           |
| DMF         | : | N,N-Dimethylformamide                        |
| DMSO        | : | N,N-Dimethylsulfoxide                        |
| DPPE        | : | 1,2- <i>bis</i> (diphenyl phosphino) ethane  |
| DPPP        | : | 1,2- <i>bis</i> (diphenyl phosphino) propane |
| e.g.        | : | For example                                  |
| HPLC        | : | High Performance Liquid Chromatography       |
| GC          | : | Gas Chromatography                           |
| i. e.       | : | That is                                      |
| IR          | : | Infra Red Spectroscopy                       |
| MEK         | : | Methyl ethyl ketone                          |
| n-          | : | Normal                                       |
| iso-        | : | Branched                                     |
| NMP         | : | N-methyl-2-pyrrolidinone                     |
| NMR         | : | Nuclear Magnetic Resonance Spectroscopy      |
| RPM         | : | Rotation per minute                          |
| T           | : | Temperature (K)                              |
| TBA         | : | <i>Tert</i> butyl alcohol                    |
| SEM         | : | Scanning electron Spectroscopy               |
| TEM         | : | Transmission Electron Microscopy             |
| XRD         | : | X-Ray Diffraction Spectroscopy               |
| TOF         | : | Turn Over Frequency                          |
| TON         | : | Turn Over Number                             |
| TPP         | : | Tri Phenyl Phosphine                         |
| UV-Vis      | : | Ultraviolet-Visible                          |
| V           | : | Volume                                       |
| <i>viz.</i> | : | Namely                                       |
| w.r.t.      | : | With respect to                              |

## List of Publication / Conference / Symposium

### INTERNATIONAL PUBLICATIONS

- ≈ Environmentally benign catalytic hydroformylation-Oxidation route for Naproxen synthesis **K.B. Rajurkar**, S. S. Tonde, M.R. Didgikar, S.S. Joshi and R. V. Chaudhari, *Ind.Eng. Chem. Res.*, 46, 2, 2007, 8480
- ≈ Kinetics of liquid phase oxidation of toluene to benzaldehyde using Mn based catalyst system, **K.B. Rajurkar**, V.H.Rane, and R.V. Chaudhari, *Ind. Eng. Chem. Res* (To be communicated)
- ≈ VAM hydroformylation: Alternative route for the synthesis of hydroxy propionic acids, **K. B. Rajurkar**, Y.L.Borole, S.S. Tonde and R.V. Chaudhari, (*Under preparation*)
- ≈ Hydroformylation of 1-decene in aqueous biphasic medium using Rh-Sulfoxantphos catalyst: Activity Selectivity and Kinetic study N. S. Pagar, **K.B. Rajurkar**, R. M. Deshpande and R. V. Chaudhari, *Applied Catalysis A: General* (communicated)
- ≈ Kinetics of hydroformylation of 1-decene using carbon supported ossified HRhCO(TPPTS)<sub>3</sub> rhodium catalyst N.S. Pagar, **K.B. Rajurkar**, R. M. Deshpande and R. V. Chaudhari communicated *Industrial Engineering and Chemical Research* (Communicated)
- ≈ Hydroformylation of camphene using rhodium-phosphite complex catalyst: activity and selectivity and kinetic study N. S. Pagar, **K.B. Rajurkar**, R. M. Deshpande and R. V. Chaudhari *Journal of Molecular Catalysis A: Chemical* (Communicated)
- ≈ Selective Oxidation of ethylbenzene using hydrotalcite like compounds and TBHP as oxidant **K. B. Rajurkar**, N.D. Kuilkarni, M.R. Didgikar, S.S. Joshi and R.V. Chaudhari (*Under preparation*)
- ≈ Synthesis of Lactic Acid via Catalytic Carbonylation of Vinyl Acetate S. S. Tonde, **K. B. Rajurkar**, R. V. Chaudhari, *Ind. Eng. Chem. Res.* (*To be communicated*)

### PATENTS

- ≈ An improved process for liquid phase oxidation of toluene to benzaldehyde  
US Patent, R. V. Chaudhari, **K.B. Rajurkar**, S.S. Tonde and V. H. Rane, **US7411099 B2**
- ≈ A process for preparation hydroxy carboxylic acids  
US Patent, R. V. Chaudhari, **K.B. Rajurkar**, S.S. Tonde and Y. L. Borole, Pub. No. 20070213558

### International Conferences

- ≈ Environmental Benign Catalytic Hydroformylation Oxidation Route For The Synthesis of Naproxen, **K.B.Rajurkar**, S.S. tonde, M.R. Didgikar, and R.V. Chaudhari
- ≈ Selective Liquid Phase Oxidation Of Toluene To Benzaldehyde” **K. B. Rajurkar**, V.H. Rane and R.V. Chaudhari, CAMURE-6 and ISMR-5, Jan 2007

- ≈ Kinetics of methoxy carbonylation of amines using lead compounds, M.R. Didgikar, **K.B. Rajurkar**, and S.S. Joshi CAMURE-6 and ISMR-5, Jan 2007
- ≈ Selective Liquid Phase Oxidation of Ethyl Benzene to acetophenone Using Cu-Resin a catalyst **K. B. Rajurkar** and R.V. Chaudhari International conference on drug delivery and nanotechnology, Nanded, India, January 2008
- ≈ Selective Liquid Phase Oxidation of Ethyl Benzene Using Hydrotalcite Like Compound **K. B. Rajurkar**, N.D. Kulkarni, and R.V. Chaudhari, APOGEE-2K7 conference at BITS-Pilani, India, March 2007

#### **National Conferences**

- ≈ Liquid Phase Oxidation of p-Cresol to p-Hydroxy Benzaldehyde, **K.B. Rajurkar**, M.R. Didgikar, S.S. Joshi and R.V. Chaudhari, NCFCE-2007 IIT Guwahati, December 07
- ≈ Kinetics of liquid phase oxidation of benzyl alcohol to benzaldehyde, **K.B. Rajurkar** M.R. Didgikar, , and S.S. Joshi NCFCE-2007 IIT Guwahati, December 07
- ≈ Kinetics of methoxy carbonylation of amines using DBTO as catalyst, M.R. Didgikar, **K.B. Rajurkar**, and S.S. Joshi NCFCE-2007 IIT Guwahati, December 07
- ≈ Selective liquid phase oxidation of glucose to gluconic acid **K.B. Rajurkar** and R.V. Chaudhari NCFCE-2007 IIT Guwahati, December 07
- ≈ Selective Liquid Phase Oxidation Of Ethyl Benzene Using Hydrotalcite Like Compounds **K.B. Rajurkar** and R.V. Chaudhari at APOGEE-2K7 conference at BITS-Pilani, India, March 2007